Evaluation of TiO2 exposure impact on adult and vulnerable brains

Clémence Disdier

NNT : 2016SACLS097

THESE DE DOCTORAT
DE L'UNIVERSITE PARIS-SACLAY,
préparée à l'université Paris sud

ECOLE DOCTORALE N° 569
Innovation thérapeutique : du fondamental à l'appliqué

Toxicologie

Présentée au
Commissariat à l'Energie Atomique et aux Energies Alternatives
CEA Saclay

par

Clémence DISDIER, Pharm D

EVALUATION OF THE EFFECTS OF TIO_2 NANOPARTICLES EXPOSURE ON THE ADULT AND VULNERABLE BRAINS

Soutenue le 11 Avril 2016

Jury :

KERDINE-RÖMER Saadia	Professeur (UMR-S 996, Université Paris Sud)	Présidente du jury
BAEZA Armelle	Professeur (CNRS UMR8251, Université Paris Diderot)	Rapporteur
GUILLOUZO André	Professeur (INSERM, U620, Université Rennes I)	Rapporteur
FATTAL Elias	Professeur (UMR CNRS 8612, Université Paris Sud)	Examinateur
GHERSI-EGEA Jean–François	Docteur (INSERM U1028, CNRS UMR5292, Lyon)	Examinateur
MABONDZO Aloïse	Docteur (CEA Saclay, DRF, Institut de Biologie et de Technologie, Service de Pharmacologie et d'Immunoanalyse)	Directeur de thèse

Titre :

Evaluation de l'effet de l'exposition aux nanoparticules de dioxyde de titane sur le cerveau adulte et vulnérable.

Mots clés :

Nanoparticules de dioxyde de titane ; barrière hémato-encéphalique ; neuro-inflammation, transporteurs ABC.

Résumé :

La présence croissante de nanoparticules (NPs) dans les produits de la vie quotidienne (alimentation, médicaments, cosmétiques, textiles…) soulève de sérieuses inquiétudes quant à leurs potentiels effets nocifs pour la santé humaine. Les NPs de dioxyde de titane (TiO_2) sont produites à l'échelle industrielle et peuvent déjà être trouvées dans plusieurs produits commerciaux tels que les peintures, les cosmétiques ou dans les systèmes de décontamination de l'eau ou de l'air. Dans le passé, les NPs de TiO_2 étaient considérées comme inertes, mais, très récemment, l'Agence Internationale pour la Recherche sur le Cancer les a classées comme possiblement cancérogènes (groupe 2B) pour l'homme. De nombreuses études *in vitro* et *in vivo* ont démontré la potentielle neuro-toxicité des NPs de TiO_2, mais très peu d'études se sont concentrées plus spécifiquement sur la barrière hémato-encéphalique (BHE), protégeant le cerveau. Aujourd'hui, en dépit des avancées constatées, la bio-cinétique et la bio-accumulation des NPs de TiO_2 ainsi que les conséquences sur la physiologie de la barrière hémato-encéphalique (BHE) *in vivo* restent très peu documentées. De plus, dans l'évaluation du risque lié à l'exposition aux NPs, des facteurs de risque tel que l'âge ont jusqu'ici été quasiment ignorés. Dans ce contexte, l'objectif de ce projet est donc d'évaluer chez le rat adulte et âgé, l'impact d'une exposition aux NPs de TiO_2 sur les fonctions de la BHE et sur le métabolisme cérébral. Nos résultats ont montré que les NPs de TiO_2 s'accumulent dans certains organes et tissus (principalement dans les poumons, la rate et le foie) et ne sont pas distribuées au système nerveux central (SNC) que ce soit après injection intra-veineuse (IV) ou après une inhalation subaiguë à un nano-aérosol de TiO_2. Après administration IV, une interaction directe entre NPs et les cellules endothéliales microvasculaires conduit à des altérations fonctionnelles au niveau de la BHE. Malgré l'absence de translocation vers le SNC, la bio-persistance du titane dans les organes périphériques semble être la cause de modulations de perméabilité de la BHE et d'une inflammation cérébrale. L'implication de médiateurs circulants faisant le lien entre la bio-persistance de titane dans les organes périphériques et les modulations observées au niveau cérébral a été démontré en utilisant un modèle *in vitro* de BHE. Une réponse exacerbée en termes de neuro-inflammation et de modulation de perméabilité de la BHE établit la vulnérabilité du cerveau âgé à la toxicité des NPs inhalées. Ces résultats ont démontré que malgré l'absence de translocation cérébrale, l'exposition aux NPs de TiO_2 induit des altérations fonctionnelles de la BHE et une neuro-inflammation qui pourraient conduire à des troubles neurologiques. L'identification des médiateurs et la description des effets neurotoxiques restent encore à préciser.

université PARIS-SACLAY | ÉCOLE DOCTORALE Innovation thérapeutique : du fondamental à l'appliqué

Title:

Evaluation of the effect of titanium dioxide nanoparticles exposure on adult and vulnerable brains

Keywords :

Titanium dioxide nanoparticles, blood-brain barrier, neuro inflammation, ABC transporters.

Abstract :

The overwhelming presence of nanoparticles (NPs) in products including foods, medications, cosmetics, or textiles raises serious concerns about their potential harmful effects on human health. In the wide diversity of NPs, titanium dioxide (TiO_2) NPs are among those produced on a large industrial scale and can already be found in several commercial products such as paints, cosmetics or in environmental decontamination systems. In the past, TiO_2 NPs was considered inert, but, very recently, the International Agency for Research in Cancer (IARC) has classified TiO_2 as possibly carcinogenic (group 2B) to human beings. Numerous *in vitro* and *in vivo* studies have shown the potential neuro-toxicity of TiO_2 NPs, but very few studies focus on the central nervous system (CNS), Nowadays, notwithstanding the reported advances, the biokinetic and bioaccumulation ofTiO_2 NPs and the consequences on the physiology of the blood-brain barrier (BBB) *in vivo* are unknown. In addition, NPs effect on susceptible population such as the elderly have been mostly ignored. In this context, the target of the present studies is to evaluate the *in vivo* impact of exposure to NPs on the BBB physiology and brain inflammation which could promote neurotoxicity in young adults and aging. Our results have shown that TiO_2 NPs bioaccumulate in organs and tissues (lungs, spleen and liver especially) and don't translocate to the brain either after IV or subacute inhalation exposure. In IV administration case, the direct interaction between NPs and brain endothelial cells induces BBB functional alterations. Despite the lack of CNS translocation, the biopersistence of titanium in peripheral organs may be indirectly the cause of BBB permeability alteration and brain inflammation. The involvement of circulating mediators linking titanium biopersitence in peripheral organs and brain impact has been demonstrated using an *in vitro* BBB model. An exacerbated response in term of neuro-inflammation and BBB permeability modulation has established the vulnerability of the aging brain to inhaled NPs toxicity. Taken together, our findings demonstrated that despite lack of brain translocation, exposure to TiO_2 NPs induce BBB physiology alteration and neuro-inflammation that may lead to CNS disorders. Thereafter, identification of mediators and description of the neurotoxic effects may complete the assessment of the impact of TiO_2 NPs exposure on the brain.

Aknowledgements

Je souhaite remercier l'ensemble des membres du jury, Professeur Armelle Baeza, Professeur Elias Fatal, Docteur Jean-François Gheri-Egea, Professeur André Guillouzo, Professeur Saadia Kerdine-Römer, pour avoir accepté de juger ce travail.

Un grand MERCI au Docteur Aloïse Mabondzo pour l'opportunité qui m'a été offerte de stage puis de thèse au sein de son équipe et pour la confiance qu'il m'a accordée pour mener à bien ce projet. Merci de m'avoir guidée, encouragée, conseillée.

Je tiens également à remercier les docteurs Christophe Créminon et Christophe Junot, respectivement chef du Service d'Immuno-analyse (SPI) et chef du laboratoire d'Etude du Métabolisme du Médicament (LEMM) pour m'avoir accueillie au sein de ce service.

L'étude par inhalation de nanoparticules de dioxyde de titane repose sur une collaboration entre le CEA et l'INRS. Mes plus sincères remerciements vont au Docteur Monique Chalansonnet. Merci pour l'implication dans le projet NanoTransBrain et pour l'accueil à Nancy. Je tiens également à remercier le docteur Jérôme Devoy pour la mise en œuvre des précieux dosages de titane et l'ensemble des équipes techniques de l'INRS qui ont permis de concrétiser ce projet.

J'adresse mes plus sincères remerciements au docteur Emilie Brun, pour sa participation dans ce projet, ces conseils scientifiques et ces quelques heures passées au microscope à regarder des nanoparticules de titane sous toutes les coutures.

Merci à toute l'équipe de Pharmacologie Neurovasculaire, plus communément les PCEL. Merci aux anciens, aux nouveaux, ceux qui sont partis vers de nouveaux horizons et ceux qui restent, pour cette ambiance sympathique dans laquelle j'ai travaillé plus de trois ans. Merci à tous pour les débats scientifiques, les coups de main à la paillasse mais aussi pour les discussions plus personnelles, les pique-niques et les restos. Le labo étant la résidence principale du thésard pendant trois ans, je suis ravie d'avoir partagé cette colocation avec vous tous. Je remercie donc Anne-Cécile Guyot pour le soutien en salle de culture, Emilie Jaumain pour toutes ces heures passées à l'animalerie, mes camarades doctorants et post doctorants de choc, Charlotte Leuxe, Ricardo Soares, Gabriella Ullio, Gwenaëlle Le Roux, sans oublier Minh Tuan Do, Gael Noyalet, Jerôme Telliet et Anne Cosnefroy. Je remercie et je souhaite la bienvenue à Susie Barbeau. Merci pour la participation technique sur ces derniers mois de thèse et bon courage pour toutes les PCR qu'il te reste à faire. Je laisse ma place à regret et espère que tu sauras faire

vivre ce projet. J'espère que nos vies personnelles et peut être professionnelles nous permettront tous de nous recroiser dans un avenir proche. Merci à vous tous pour votre contribution au livre des citations, certaines sont inoubliables.

Merci au Docteur Hervé Volland pour avoir été le premier à avoir écouté mon projet et à m'encourager en me permettant de rencontrer les équipes du CEA.

Merci à l'ensemble des collègues du SPI que je ne citerai pas tous ici.

Je passe ensuite une dédicace spéciale à tous ces doctorants que j'ai croisé pendant ces trois ans, au SPI, au sein de l'équipe Ibithèse, lors de formations diverses ou dans ma vie personnelle, à tous ces « bébés » chercheurs qui consacreront leurs carrières à faire avancer la science.

Enfin, ces remerciements vont à mes parents, frère et sœur et à l'ensemble de ma famille pour avoir été à mes côtés et pour leur soutien et leurs encouragements tout au long de mon cursus.

Dissemination

The results obtained in this work have been presented in international congresses and are subject of several articles:

The method development for TiO_2 nanoparticles mineralization and quantification is the subject of a publication in Journal of Analytical Chemistry under the title:
"Mineralization of TiO_2 nanoparticles for the determination of titanium in rat tissues"
Liste of authors: Devoy J, Brun E, Cosnefroy A, **Disdier C**, Melczer M, Antoine G, Chalansonnet M, Mabondzo A.
doi: 10.7868/S0044450216040046

Results concerning intravenous administration study is subject of an article published in Particle and Fibre Toxicology in September 2015 under the title:
"*Tissue biodistribution of intravenously administrated titanium dioxide nanoparticles revealed blood-brain barrier clearance and brain inflammation in rat.*"
Liste of authors: **Disdier C**, Devoy J, Cosnefroy A, Chalansonnet M, Herlin-Boime N, Brun E, Lund A, Mabondzo A.
Part Fibre Toxicol. 2015 Sep 4;12:27. doi: 10.1186/s12989-015-0102-8.

These results were also presented as a poster at the 50th Congress of the European Societies of Toxicology in September 2014 in Edinburgh, UK and at the French association for toxicology research symposium in June 2014 in Paris, France.

Results of the biokinetics study after inhalation of TiO_2 NPs aerosol are the subject of an article submitted to Nanotoxicology in February 26th, 2016 under the title:
"*Biopersistence and Translocation to Extrapulmonary Organs of Titanium Dioxide Nanoparticles after Subacute Inhalation Exposure to Aerosol in Adult and Elderly Rats."*
Liste of authors: **Disdier C**, Gaté L, Cosnier F, Gagnaire F Devoy J, Saba W, Brun E, Chanlansonnet M, Mabondzo A.

Results of biokinetic comparison after intravenous administration and subacute aerosol inhalation of TiO_2 nanoparticles have been presented at the SOT (Society of Toxicology) 54th meeting in March 2015 in San Diego, USA.

Results on the impact of TiO_2 nano-aerosol exposure on the blood brain barrier functions and brain inflammation in adults and aging rats are subject to an article submitted to Particle and Fibre Toxicology on February 26th under the title:

"Brain Inflammation and Blood Brain Barrier Dysfunction after Subacute Inhalation Exposure to Titanium Dioxide Nano-aerosol in Aging Rats."

List of authors: **Disdier C**, Chanlansonnet M, Gagnaire F, Barbeau S, Gaté L, Cosnier F, Devoy J, Saba W, Lund A, Brun E, Mabondzo A.

List of figures

Figure 1: Length scale showing the sizes of nanomaterials in comparison to various biological components.

Figure 2: Increase reactive surface as a function of particle diameter, specific cases of atmospheric NPs.

Figure 3: Number of products containing nanomaterials on the market since 2005.

Figure 4: Composition of nanomaterials in commercial products.

Figure 5: Major industrial fields using nanomaterials for consumer products.

Figure 6: Crystal structure of the two main forms of titanium dioxide, anatase and rutile.

Figure 7: Variables and physicochemical parameters that need to be take into account during nanotoxicology studies.

Figure 8: Possible exposure routes for current and future nanomaterial applications.

Figure 9: Cells of the respiratory epithelium.

Figure 10: Schematic view of the structure of a pulmonary alveoli and its environment.

Figure 11: Digestive tube mucosa structure.

Figure 12: Actors at the intestinal barrier.

Figure 13: Schematic representation of the skin layers.

Figure 14: The five epidermal layers.

Figure 15: Penetration pathways of topically applied substances through the skin.

Figure 16: Biokinetics of nano-sized particles.

Figure 17: Brain vascularization.

Figure 18: Schematic representation of the cerebral microvasculature at the Virchow-Robin space.

Figure 19: Schematic representation of the BBB and it different component cells.

Figure 20: Tight junctions and associated proteins between the BBB endothelial cells.

Figure 21: Schematic representation of the different transport at the BBB.

Figure 22: Regulation of ABC efflux transporters activity and expression at the BBB level in inflammatory environment.

Figure 23: Trigeminal innervation and vasculature of the nasal respiratory region.

Figure 24: Design of the single dose intravenous administration study.

Figure 25: Design of the sub-acute inhalation exposure study.

Figure 26: Plasma concentration of atenolol, digoxin and prazosin steady state.

Figure 27: Evolution of brain /plasma ratio over time of infusion.

Figure 28: Luminex bead-based Multiplex assay principle.

Figure 29: Schematic representation of the *in vitro* BBB model.

Figure 30: Schematic representation of sucrose, vinblastine and prazosin passage through brain endothelial cells monolayer.

Figure 31: Effect of 24 hours exposure to TiO_2 NPs on the vinblastine efflux ratio as a function of the concentration of NPs.

Figure 32: mRNA expression of ceramidase ASAH 1, ASAH 2, ACER 2 and ACER 3 in the liver 28 days after IV injection of 1 mg/kg TiO_2 NPs.

Figure 33: mRNA expression of cytokines interleukin 2 (IL2) interleukin 10 (IL10) and Tumor necrosis factor α (TNFα) in the spleen 28 days after IV injection of 1 mg/kg TiO_2 NPs.

Figure 34: translocation to extra-pulmonary pathways hypothesis.

Figure 35: Entry pathways to the CNS after inhalation exposure.

Figure 36: Detection of 5 inflammatory markers in young adults and aging rat sera after subacute inhalation exposure to TiO_2 nano-aerosol.

Figure 37: Impact of exposure to plasma from exposed animals on the *in vitro* BBB model.

Figure 38: Impact of exposure to plasma from aging and young adults exposed animals on the *in vitro* BBB model.

Figure 39: Schematic summary of the early events and indirect long term consequences of TiO_2 NPs exposure on the BBB physiology and on inflammation in the brain.

Figure 40: TEM image of TiO_2 P25 Degussa NPs and size distribution diagram.

Figure 41: SEM spectrum of TiO_2 P25 Degussa NPs.

Figure 42: Dynamic light scattering of TiO_2 P25 Degussa NPs in water suspension.

Figure 43: A: Theoretical X-ray diffraction patterns of anatase and rutile TiO_2 and experimental X-ray diffraction patterns of TiO_2 P25 Degussa NPs.

Figure 44 : Example of calibration curves obtained for the 11 analytes targeted in brain cortexes extract matrix.

List of tables

Table 1: Summary of key properties of materials at nanometric sizes.

Table 2: Studies reporting translocation of TiO_2 NPs to extra-pulmonary organs after intratracheal instillation or inhalation.

Table 3: *In vivo* studies that evidence TiO_2 NPs translocation across the gastro-intestinal tract.

Table 4: Studies that investigated *in vitro* or *in vivo* skin penetration of TiO_2 NPs.

Table 5: *In vivo* studies that investigated the adverse effects of TiO_2 NPs exposure on liver.

Table 6: *In vivo* studies that investigated the adverse effect of TiO_2 NPs on the cardiovascular system.

Table 7: *In vivo* studies: Adverse effects of TiO_2 NPs on the immune system and the spleen.

Table 8: Summary of changes in ABC efflux transporters activity in neurological disorders

Table 9: Distribution of TiO_2 NPS to the central nervous system.

Table 10: *In vitro* investigation on TiO_2 NPs neuro-toxicity.

Table 11: *In vivo* investigation on TiO_2 NPs neuro-toxicity.

Table 12: Chemical reagents, kits and culture media.

Table 13: Sofwares.

Abbreviations

ABC: Adenosine triphosphate Binding Cassette

ABCB1: ATP-binding cassette, sub-family B, member 1

AD: Alzheimer Disease

ATP: Adenosine TriPhosphate

BBB: Blood Brain Barrier

BECs: Brain Endothelial Cells

BET: Brunauer-Emmett-Teller

BCRP: Breast Cancer Resistance Protein

Cldn 5: Claudin 5

CNS: Central Nervous System

CNT: Carbone Nano Tube

CSF: Cerebro-Spinal Fluid

DLS: Dynamic Light Scattering

DNA: Deoxyribo-Nucleic Acid

EDX: Energy dispersive X-ray

EGF: Epidermal Growth Factor

GALT: Gut Associated Lymphoïd Tissue

GFAP: Glial Fibrillary Acid Protein

Glut1: Glucose transporter 1

Hprt 1: Hypoxanthine phosphoribosyltransferase 1

HUVEC: Human Umbilical Vein Endothelial Cell

IARC: International Agency for Research on Cancer

IBA1: Ionized calcium-Binding Adapter molecule 1

ICP-MS: Inductively Coupled Plasma Mass Spectrometry

IFNγ: Interferon γ

Il-1β: Interleukine 1 β

IL6: Interleukine 6

IP10: Interferon gamma-Induced Protein 10

IV: intravenous

$Kp_{brain/plasma}$: Brain Plasma partition coefficient

LC-MS/MS: Liquid Chromatography coupled Mass Spectrometry in tandem

LY: Lucifer yellow

MCP1: Monocyte Chemoattractant Protein 1

MIP2: Macrophage Inflammatory Protein 2

MRPs: Multi-drug Resistance related Proteins

MRI: Magnetic Resonance Imaging

NIOSH: National Institute for Occupational Safety and Health

OECD: Organisation for Economic Co-operation and Development

Ocln: Occludin

P_{app}: Apparent Permeability

PEL: Permissible Exposure Limit

PET: Positron Emission Tomography

PIXE: Particle-Induced X-ray Emission

PBR: Peripheral Benzodiazepine Receptor

P-gp: P-Glycoprotein

RANTES: Regulated on Activation, Normal T cell Expressed and Secreted

RNA: Ribo-Nucleic Acid

ROS: Reactive Oxygen Species

RT-qPCR: Real-Time quantitative Polymerase Chain Reaction

SEM: Scanning Electron Microscopy

SLC: SoLute Carrier family

SLC2a1: Solute carrier family 2 member 1

TEER: Trans Endothelial Electrical Resistance

TEM: Transmission Electron Microscopy

TiO_2 NPs: Titanium dioxide nanoparticles

TNFα: Tumor Necrosis Factor α

TSPO: translocator protein

UV: Ultra-violets

VEGF: Vascular Endothelial Growth Factor

XRD: X-Ray Diffraction

ZO: Zonula Occludens

TABLE OF CONTENTS

CHAPTER I: RATIONAL AND HYPOTHESIS 18

CHAPTER II: BACKGROUND 21

PART I: TITANIUM DIOXIDE (TiO_2) IN THE EMERGING NANO WORD 22
1. General definition of nanoparticles 22
2. Specific scale and properties 23
3. Market status 24
4. TiO_2 nanoparticles 27
4.1 Description 27
4.2. Properties and uses 28
4.2.1. White pigment 28
4.2.2. UV protection 29
4.2.3. Photocatalysis applications 29
4.2.4. Health care applications 30

PART II: TiO_2 NPs EXPOSURE AND HUMAN HEALTH RISK 31
1. Specificity and complexity of nanoparticles risk assessment 31
2. Exposure route and entry pathway in the organism 32
2.1. Exposure route 32
2.2. Translocation and Interaction across physiological barriers 34
2.2.1. The pulmonary barrier 34
2.2.1.1. Pulmonary toxicity 37
2.2.1.2. Translocation across the alveoli barrier 38
2.2.2. The intestinal barrier 40
2.2.2.1. Gastro-intestinal toxicity 43
2.2.2.2. Translocation across the intestine 44
2.2.3. The skin barrier 45
2.2.3.1. Cutaneous toxicity 48
2.2.3.2. Translocation across the skin 48
3. In vivo fate 50
3.1. Biodistribution, accumulation and elimination 50
3.2. Systemic toxic effects 52
3.2.1. Hepatotoxicity 52
3.2.2. Cardiovascular toxicity 54
3.2.3. Spleen toxicity and immune toxicity 56

PART III: TiO_2 NPs IN THE CENTRAL NERVOUS SYSTEM 58
1. The blood brain barrier (BBB) 58
1.1. Physiology of the cerebral vascularization 58
1.2. The neurovascular unit: structure and functions 60

1.2.1. A cooperation of multiple cell types 61
1.2.1.1. Astrocytes 61
1.2.1.2. Pericytes 61
1.2.1.3. Microvascular endothelial cells 62
1.3. A functional barrier 62
1.3.1. Physical barrier 62
1.3.2. Transport and detoxification functions 64
1.3.2.1. ABC transporters 65
1.3.2.2. SLC transporters 68
2. Entry pathway to the CNS 68
2.1. Translocation along the olfactory nerve 68
2.2. Translocation across the BBB 70
2.2.1. *In vitro* data 70
2.2.2. *In vivo* data 70
3. Impact on BBB physiology 72
3.1. Integrity and transport functions 72
3.2. Neuro-vascular inflammation. 73
4. Neuro-toxicity liability after TiO_2 NPs exposure 73
4.1. *In vitro* data 73
4.2. *In vivo* data 73

CHAPTER III: EXPERIMENTAL METHODS 78

1. Acute Intravenous injection exposure study design 79
2. Sub-acute Inhalation exposure study design 81
3. Titanium distribution analysis: ICP-MS 83
4. Blood brain barrier physiology evaluation 83
4.1. Integrity evaluation 84
4.2. Transport function evaluation 85
5. Mediator research 85
5.1. Neurovascular inflammation evaluation 85
5.2. *In vitro* tool 86

CHAPTER IV: RESULTS AND DISCUSSION 89

PART I: INTRAVENOUS ADMINISTRATION STUDY 91
1. Context and introduction 91
2. Major findings and Discussion 92
3. Article 1: Tissue Biodistribution of Intravenously Administrated Titanium Dioxide Nanoparticles Revealed Blood-Brain Barrier Clearance and Brain Inflammation in rat . 99

PART II: INHALATION EXPOSURE STUDY 121
1. Distribution description 121
1.1. Context and introduction 121
1.2. Major findings and Discussion 122
1.3. Article 2: Biopersistence and Translocation to Extrapulmonary Organs of Titanium Dioxide Nanoparticles after Subacute Inhalation Exposure to Aerosol in Adult and Elderly Rats. 125
2. Impact on the central nervous system and the BBB physiology..……...147
2.1. Context and introduction 149
2.2. Major findings and discussion 150
2.3. Article 3: Brain Inflammation and Blood Brain Barrier dysfunction after Sub acute Inhalation Exposure to Titanium Dioxide Nano-aerosol in Aging Rats 154

CONCLUSIONS AND PERSPECTIVES 182

REFERENCES 188

ANNEXES 205
ANNEXE 1: Mineralization of TiO_2 nanoparticles for the determination of titanium in rat tissues 206
ANNEXE 2: TiO_2 NPs caracterization data 214
ANNEXE 3: Bioplex calibration curves 217
ANNEXE 4: MATERIALS 218
ANNEXE 5: RESUME..……221

Chapter I:

RATIONAL AND HYPOTHESIS

The brain controls behavior through sensory input. The brain is the most complex and sensitive biological structure known and despite scientific progress many aspects of brain functioning are still unknown. The brain is well protected by the blood brain barrier (BBB). This gatekeeper protects the brain by excluding, effluxing and metabolizing potential neurotoxic compounds.

Research in our laboratory has highlighted *in vitro* evidence of dysregulation of BBB functions associated with an inflammatory response after exposure to acute and chronic titanium dioxide nanoparticles (TiO_2 NPs) [1]. This study carried out on a primary cell-based BBB model showed that BBB integrity and efflux activities are impaired after exposure to TiO_2 NPs. Interestingly, glucose transporter and insulin receptor expressions are also decreased in brain endothelial cells (BECs) suggesting carbohydrates metabolism impairment. Several pieces of evidences suggest that central nervous system (CNS) glucose transport have a pathophysiologic significance in neurodegenerative disorders [2, 3]. Altogether, permeability alteration, modification of ABC (ATP-Binding Casette) transport activity and altered carbohydrates metabolism at the BBB level may lead to neurotoxic complications. Notwithstanding these *in vitro* findings, concerns have been raised about *in vivo* consequences of interactions between TiO_2 NPs and the BBB.

BBB functional alteration is involved in various diseases affecting the CNS such as neurodegenerative diseases, amyotrophic lateral sclerosis and brain cancer. As example, BBB permeability changes and decrease efflux functions associated with immune cells extravagation have been observed in Parkinson's disease patients [4]. Moreover, several pieces of evidence suggest a link between exposure to NPs and brain diseases. Several facts pointed out the potential neurotoxic effects of NPs. Indeed, exposure to fine and ultra-fine air pollution has been associated with early dysregulated neuro-inflammation and perturbations in the integrity of the BBB in people living in Mexico [5-8]. These detrimental processes likely contribute to progressive neurodegenerative course [9]. Air borne manganese NPs was also associated with deficits in olfactory and motor function among adolescents [10]. In the case of TiO_2 NPs, neuro-inflammation processes have been highlighted both *in vivo* and *in vitro* after exposure [11-13]. These facts suggest that the BBB and neurological functions may be impaired by exposure to TiO_2 NPs.

As the proportion of the aging population is growing, it is critical to understand age-related disorders due to environmental NP exposure. At the BBB level, age related vulnerability has already been established as results of several phenomena leading to BBB dysregulation (decrease of tight junction proteins, changes in the astrocytic endfeet…) [14]. In addition, many brain diseases are closely related to aging. Taken together, we suggest that response to TiO_2 NPs exposure in aging brain may exacerbate BBB dysregulation and brain inflammation and thereby promote neurotoxicity.

Based on this concept, the overall objective of my thesis project is to explore the *in vivo* impact of exposure to TiO_2 NPs on the BBB physiology and brain functions which could promote neurotoxicity.

For better assessment of potential titanium neuro-toxicity we need to describe precisely the biodistribution of TiO_2 NPs and access to the CNS in rats. By so doing, we intended to evaluate the BBB physiology and brain inflammation after exposure to TiO_2 NPs.

The time line of the experiments undertaken was as follows:

First of all, we expose adult rat by intravenous (IV) injection to TiO_2 NPs suspension. The main objective is to describe the biodistribution by escape the absorption step of the kinetic that is to say the potential of the translocation across other physiological barriers such as the alveoli barrier of the lung in the case of inhalation. We intended to focus on the brain distribution. Secondly, this IV study aims to examine potential effects of a blood borne TiO_2 NPs exposure on the BBB physiology. After intravenous injection, the only translocation pathway of the NPs to the CNS is across the BBB. The physiology of the barrier can therefore be impaired by direct interaction between TiO_2 NPs transported by blood and endothelial cells of the BBB.

Second, we focused on the inhalation exposure. The inhalation experiment design follows OCDE guidelines TG 412 for sub-acute exposure. This design aim to mimic workers exposure: 2 periods of 3 hours per day, 5 days a week during 4 weeks. The chosen concentration for exposure was 10 mg/m^3 corresponding to the French OEL (Occupational Exposure Limit) for ultrafine dust including TiO_2 NPs**.**

In the case of inhalation exposure, the distribution to the CNS can occur through several pathways. First if the NPs could translocate across the alveoli barrier of the lungs, the NPs will reach the blood circulation. Under this scenario, we could expect similar biodistribution profile as after IV injection. Another pathway to the CNS is the transport through the olfactory nerve directly to the olfactory bulb bypassing the BBB. This pathway remains debated. The NPs may reach directly the brain parenchyma and induce neurotoxic effects. Choosing this exposure route, the objective is to be representative of real environmental exposure conditions taking into account the absorption steps.

In the last part of this project we expose aging rats and young adult rats to a TiO_2 NPs aerosol. This last step in the project aims to highlight age-related sensibility to NPs toxicity.

Chapter II:

BACKGROUND

Part I: titanium dioxide (TiO_2) in the emerging nano word

1. General definition of nanoparticles

The term "Nanoscience" covers generally the study of existing principles and properties on the nanometer scale (Figure 1) at the level of atoms and molecules.

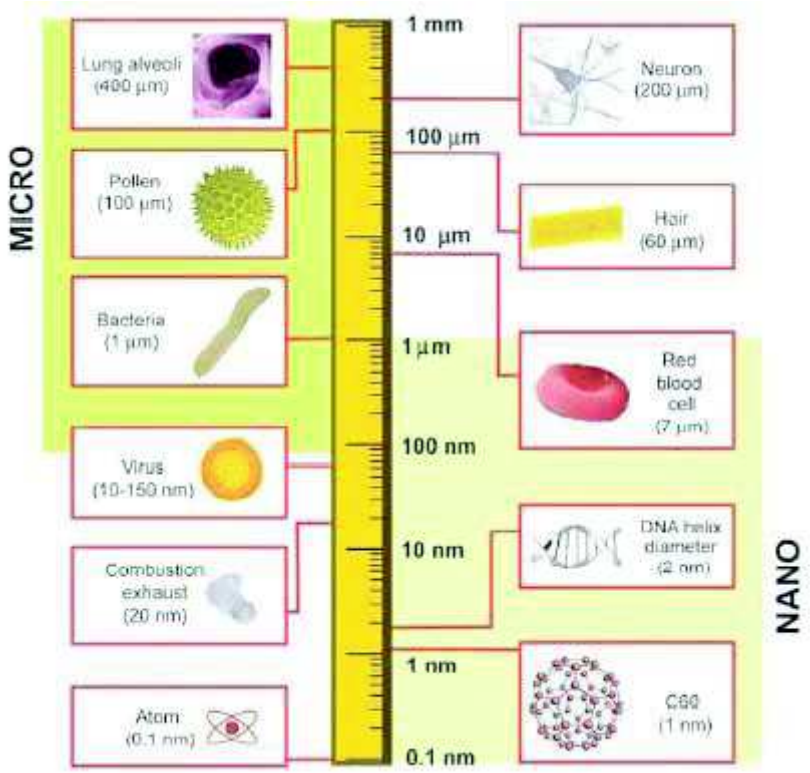

Figure 1: Length scale showing the sizes of nanomaterials in comparison to various biological components (from Buzea *et al.*, 2007) [15].

The aim of nanotechnology is to produce materials with nanometric dimensions, between 1 and 100 nm. These nanomaterials are made of nano-objects and are intentionally produced, unlike the so-called "ultra-fine" particles that are of natural origin. Nanomaterials can be metals, ceramics, polymers or silicates which have specific characteristics compared to the same material at the macroscopic scale (thermal, mechanical, electrical, biological ...). The discovery of these new physical, chemical or biological properties opens new possibilities for applications in many and varied industrial fields.

A nano-object is an entity with at least one of the dimensions in the nanoscale: diameter, length or thickness. Nano-objects can be classified according to their sizes in the three dimensions:

• particles, quantum dots and fullerenes have their three dimensions in the nanometer range (point);
• nanotubes, dendrimers, nanowires, fibers and fibrils have two nanometric dimensions (line);
• thin films have only one nanometric dimension (plan).

A nanoparticle (NP) (or ultra-fine particle) is defined by IUPAC (International Union of Pure and Applied Chemistry) as a nano-object with three dimensions on the nanoscale. These NPs may consist of aggregates of atoms (silver, gold ...) or small molecules (titanium dioxide, silicon dioxide ...).
NPs may have several origins. They may be naturally produced, for example during volcanic eruption, forest fires or due to erosion. The second origin is anthropogenic. These NPs are found in the emissions of pollutants into the atmosphere (emission of diesel engines, cigarette smoke ...) or can be intentionally produced for the purpose of industrial applications. In this study we have been focusing on TiO_2 NPs which are intentionally produced NPs.

2. Specific scale and properties

The small size of NPs allows their physical and chemical properties to differ from those of the same materials on the macroscopic scale. Indeed, the physical and chemical properties of a nanoscale particle don't depend on the particle's nature. For a particle with nanoscale dimensions, the surface effect is much more important. Increasing the number of atoms in the particle surface grants a higher reactivity (Figure 2). It is increased reactivity of these surfaces which confer to the NPs these special properties including optical, mechanical, magnetic, or catalytic [16]. The emergence of new properties when decreasing the particle diameter may also suggest a particular toxicity of NPs [17].

Particle diameter (µm)	Particle no. (cm^{-3})	Particle surface area ($\mu m^2/cm^3$)
5	153,000,000	12,000
20	2,400,000	3,016
250	1,200	240
5,000	0.15	12

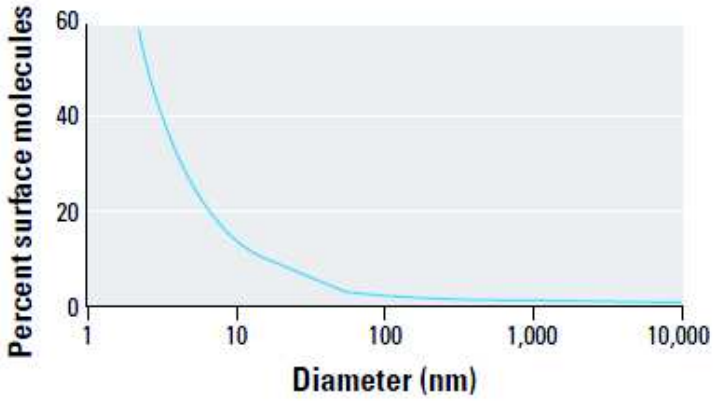

Figure 2: Increase reactive surface as a function of particle diameter, specific cases of atmospheric NPs (adapted from Oberdorster *et al.*, 2005) [16].

Among the outstanding properties of NPs (Table 1), we can point to:

- mechanical properties acquisition: strength increases (e.g. reinforcing materials with carbon nanotubes (CNTs) [18]).

- electrical properties: increase of electrical conductivity (e.g. by adding CNTs to composite matrix of Al_2O_3 [19])or an increase in electrical resistance.

- Optical properties of NPs are also exploited: absorption of ultraviolet light (presence of TiO_2 NPs as ultra-violet filters in sunscreens) or fluorescence property at nanometric sizes.

- Finally, the small size of the NPs confers opportunities for interaction with biological systems (increase biocompatibility, increased permeability for biological barriers ...).

Property	Examples
Catalytic	High catalytic efficiency due to high surface / volume ratio.
Electrical	Increase in the electrical conductivity of the ceramic and magnetic nanocomposites Increase in the electrical resistance of metals
Magnetic	Increased magnetic coercivity, superparamagnetic behavior
Mechanical	Increased hardness and strength metals and alloys, ductility and elasticity of super ceramics
Optical	Spectral shift of the optical absorption and fluorescent properties increase the quantum efficiency of semiconductor crystals
Steric	Increase in selectivity, hollow spheres design for specific drug transport and controlled dispensing
Biological	Increased permeability at biological barriers interface (epithelial barrier ...); increasing biocompatibility

Table 1: Summary of key properties of materials at nanometric sizes.

3. Market status

As a result of these properties, there has been a significant increase in the presence of NPs in many products that are much in use on a daily basis. To describe NPs market, the Woodrow Wilson International Center for Scholars and the Project on Emerging Nanotechnology created the Nanotechnology Consumer Product Inventory in 2005. A recent paper summarized this inventory with various description parameters [20]. This inventory contains products that can be readily purchased by consumers and said to contain nanomaterials by the manufacturer or another source. This means that the number of commercial product is underestimated giving the fact that there is no legislation in Europe or the United States that obligates manufactures to declare nanomaterials compound in their products. Moreover, the market for NPs worldwide represents billions of dollars annually of which 18 billion for the sole pharmaceutical industry.

According to the consumer product inventory, the number of manufactured products containing NPs and marketed globally increased 33 fold between March 2005 and March 2014 from 54 products surveyed in 2011 to 1814 in 2014 (Figure 3).

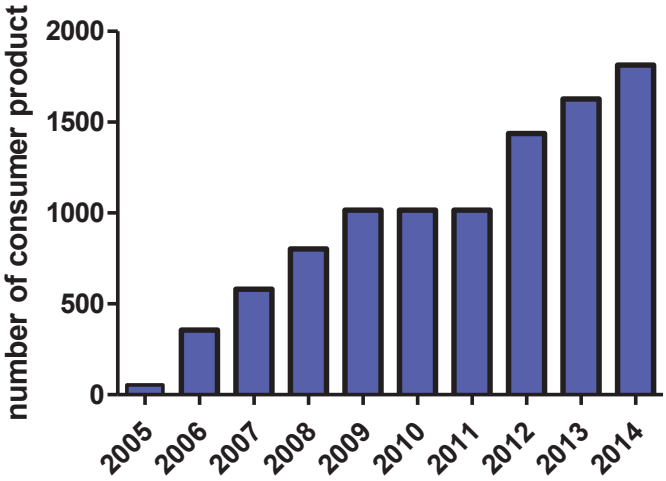

Figure 3: Number of products containing nanomaterials on the market since 2005 (adapted from Vance *et al.*, 2015) [20].

39 different types of nanomaterials were inventoried and metal nanomaterials (silver, titanium, zinc and gold) are the most represented (Figure 4).

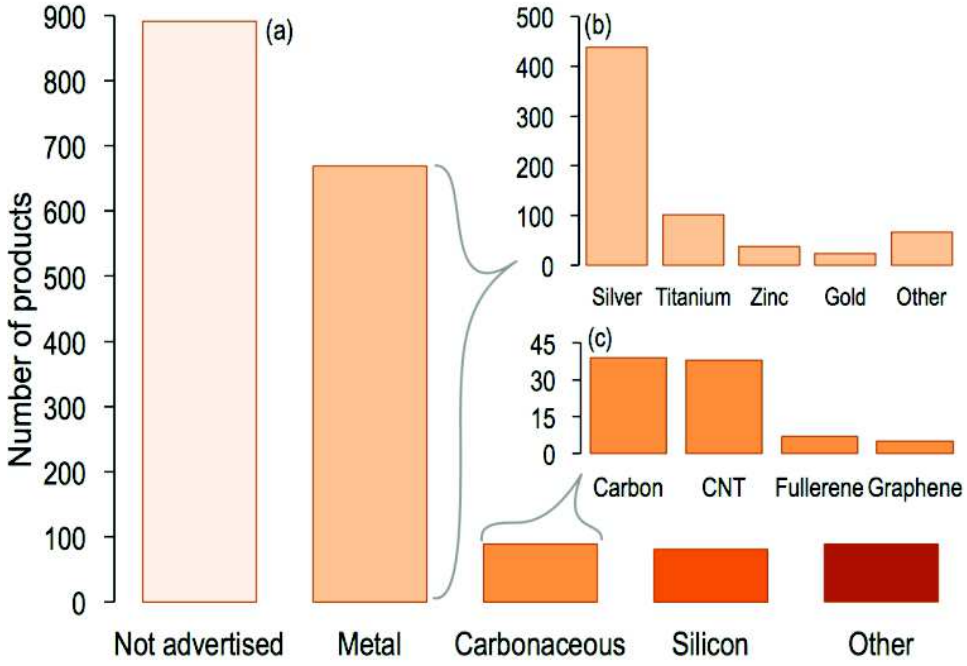

Figure 4: Composition of nanomaterials in commercial products (from Vance *et al.* 2015)[20].

Numerous areas of application are concerned, ranging from cosmetics, optics, textiles and food processing to construction materials, electronics, air or water filtration system. Among consumer products, it is important to note that most of them are listed in the category "health and fitness products" (Figure 5).

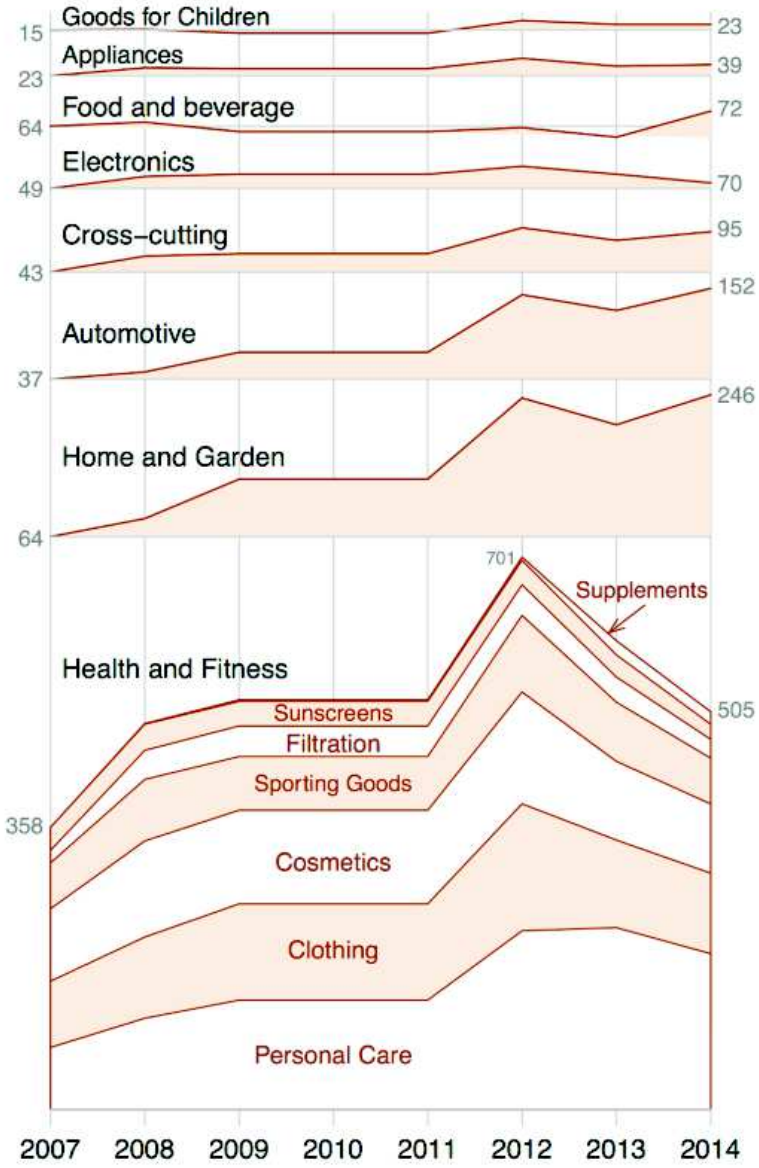

Figure 5: Major industrial fields using nanomaterials for consumer products (From Vance *et al.* 2015)[20].

Moreover, thanks to their special characteristics and their ability to cross biological barriers, NPs are the subject of research for many medical applications including drug vectorization strategies. A special interest is in the field of oncology where some NPs can be used as vectors to target cancer cells specifically, thereby avoiding the major side effects of chemotherapy. Their uses in medical imaging is also booming. And they have also been widely used in allied fields, including cosmetics (e.g. presence of TiO_2 and ZnO_2 in sunscreens).

In France, manufacturers, importers and distributors on the national territory must report annually to the Ministry for the Environment, identification, quantity and uses of nano-materials and professional users. From 100 grams of nanomaterial used, the declaration must be made with the status of the NP produced, imported or distributed. The declaration concerns NPs alone

or in mixture, as well as products that potentially release NPs under normal conditions of use. 670 producers, importers or distributors declared 3409 products in 2012. This corresponds to 280 000 tons of substances with NP status produced in France in 2012 and 220 000 tons of imported substances. A total of 500,000 tons of substances with NP status have been declared and marketed in France[21].

4. TiO_2 nanoparticles

4.1 Description

TiO_2 is a natural mineral that can be found in various crystal phases including rutile, anatase and brookite and also in amorphous form (Figure 6). Main TiO_2 resources are located in Brazil, China, Canada and Australia. The main minerals are ilmenite ($FeTiO_3$, Fe_2O_3) and natural rutile (TiO_2). Global reserves are estimated at 600 Mt of TiO_2 equivalents. Two industrial processes can be used to obtain pure oxide from ilmenite or rutile minerals [22]:

Sulphate Process

Ilmenite ($FeTiO_3$) is treated with concentrated sulfuric acid (H_2SO_4) and the titanium oxygen sulfate ($TiOSO_4$) is selectively extracted and converted into TiO_2.
1. Ilmenite is treated (digested) with an excess of concentrated sulfuric acid at around 100°C. The following reaction takes place:
$FeTiO_3 + 2H_2SO_4 \rightarrow FeSO_4 + TiOSO_4 + 2H_2O$
2. The waste product $FeSO_4$ is removed by crystallization and filtration after cooling to 15°C. The titanium oxygen sulfate is hydrolyzed by heating the remaining solution at 110°C.
$TiOSO_4 + (n+1)\ H_2O \rightarrow TiO_2 \bullet nH_2O + H_2SO_4$
At this stage, sulfuric acid waste and a precipitate gel containing hydrated titanium dioxide are produced.
3. Water is removed at temperatures between 200–300 °C:
$TiO_2 \bullet nH2O \rightarrow TiO_2 + nH_2O$
Depending on the final heating temperature (800−850 °C or 900−930 °C), either anatase or rutile is formed, respectively.

Chloride Process

The chloride process requires at least 70% pure rutile mineral which is a rare form.
1. TiO_2 is reduced with carbon and then oxidized with chlorine.
$TiO_2 + C \rightarrow Ti + CO_2$ $Ti + 2Cl_2 \rightarrow TiCl_4$
2. Liquid $TiCl_4$ is distilled and converted back into TiO_2 at 1200–1700 °C.
$TiCl_4 + O_2 \rightarrow TiO_2 + 2Cl_2$

The sulfate process requires the use of very large volumes of sulfuric acid and produces acid waste. This acid waste is considered toxic for the environment. The chloride process has been favored on financial and environmental grounds since the early 1990s.

The three common phases of TiO_2 are rutile, anatase and brookite. Rutile is the most stable form of TiO_2. Anatase and brookite are stable at normal temperatures but slowly convert to rutile upon heating to temperatures above 550 and 750 °C, respectively. The crystal is formed by repeating identical crystal cell. All three forms of TiO_2 have six co-ordinated titanium atoms in their crystal cells. Both rutile and anatase structures are tetragonal (Figure 6). The anatase crystal cell is more elongated but the atoms in the rutile form occupy less space. This makes the rutile form more stable especially at high temperatures. The stability but also reactivity of TiO_2 depends on this crystal structure, the size and shape of the particles. For example, the crystal's form that has the highest catalytic activity is anatase[23].

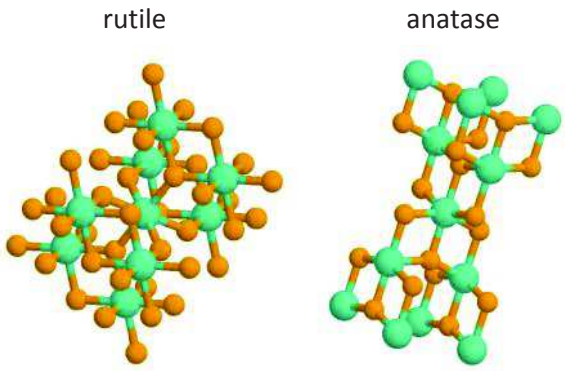

Figure 6: Crystal structure of the two main forms of titanium dioxide, anatase and rutile (from Buzea *et al.*, 2007)[15].

TiO_2 has been used in industries since the early twentieth century. In 2005 the global production of TiO_2 NPs was estimated at 2000 metric tons representing a $70 million market. The production increased to 5000 metric tons in 2010, and it is expected to continue to increase until at least 2025 with greater reliance upon nano-size TiO_2. Indeed, today, because of its interesting properties in nanoparticle form, TiO_2 NPs is one of the most NPs exploited by industry all fields together [20]. In France according to data from mandatory annual declarations, 14 321 436 kg of TiO_2 NPs were produced or imported in 2012.

4.2. Properties and uses

4.2.1. White pigment

Historically, bulk TiO_2 is used as white pigment and opacifier because of its refractive index and whiteness. Therefore, it is a component of paint, plastics, paper and inks. As it is also

odorless and tasteless, it is found as opacifier excipient in many medicines mainly in capsules envelope and tablets coatings. It also enters into the composition of medicinal preparations for dermal application and in many health-care products (tooth paste and cosmetics) where it is noted CI 77891.

TiO_2 is a food dye, E171, which is listed in the Codex Alimentarius (guidelines and codes of practice written by the World Health Organization). It is known to be used in sweet manufacturing and pastry but concerns a very wide range of other food products without official limited dose.

In this application, TiO_2 is used as a bulk material. However the presence of a nanometric fraction among the material cannot be neglected. For example, for food grade TiO_2 (E171) fraction of particles under 100 nm, thus corresponding to the strict definition of NPs has been estimated at 36 % by Weir *et al.* and 5–10 % reported by Peters et al [24, 25].

4.2.2. UV protection

TiO_2 is widely used by the cosmetics industry as a pigment but also as a UV filter, because of its refractive index and its UV absorption properties in its nanometric form. TiO_2 is a mineral UV filter which therefore causes fewer photo-allergic reactions than chemical filters. So then it enters into the composition of almost all sunscreens currently on the market. In addition, the nano form of TiO_2 is more interesting than the micrometric form in sunscreens since the decrease in particle size makes it less opaque and therefore leaves less white marks on the skin after application. TiO_2 as UV filter can be used up to a maximum concentration of 25% of the finished product in France [26].

The UV protection ability of TiO_2 NPs is also exploited as a filter in glass bottle containing UV sensitive products or other specialized glass.

4.2.3. Photocatalysis applications

The anatase crystal phase of TiO_2 has a photocatalytic activity [23, 27, 28]. Under UV light activation, particles degrade organic compounds. It is strongly determined by its crystallinity and particle size. Indeed, the high surface area per mass unit in nano-powder creates a larger catalytic surface for the production of hydroxyl radicals that are strong oxidizing agents. This property is exploited to catalyze pesticides degradation in water treatment systems or catalyze NO_2 from air pollution when introduced in air depollution systems or materials such as for concrete coating. Since thin films are transparent, TiO_2 is also introduced into glass to give self-cleaning and anti-fogging properties [29, 30].

This photocatalysis activity is also active on viruses and bacteria [31]. Pure TiO_2 NPs or TiO_2 NPs doped with other materials such as iron or silver exhibit antimicrobial properties [32, 33]. TiO_2 NPs

composites have been shown to be effective at disinfecting air and surfaces for hospitals [34]. Antimicrobial clothing has also been developed using this property [35].

4.2.4. Health care applications

Many applications TiO_2 NPs are considered in medical fields. Firstly, in the field of composite for bone tissue engineering. TiO_2 NPs in medical implants, orthopedic in particular, could have interesting properties. On the one hand because of the bactericidal action, TiO_2 NPs would prevent post-operation site infections [36]. These properties are exacerbated in the case of TiO_2 nanotubes combined with silver NPs [32, 33]. On the other hand, TiO_2 improves the mechanical properties of orthopedic prostheses (e.g. strength) [37]. Several studies have shown that the presence of TiO_2 NPs as a carrier improves the formation of apatite, a biomaterial widely used in the field of bone repair, bone implants and as a bioactive material [38]. In addition, the presence of TiO_2 NPs in biological implants increases the proliferation and differentiation of cells, thereby increasing the biocompatibility of the implant. Moreover, TiO_2 nano-tubes have been incorporated into bandages in order to enhance blood clotting and prevent bacterial infection [39, 40].
In the oncology field, studies have demonstrated interest of TiO_2 NPs uses in anti-cancer strategies: first because of the photo-killing activity to malignant cells, secondly as a drug delivery system in order to minimize side effects [28, 41]. TiO_2 NPs have also been studied as carrier for other drugs such as anti-epileptic drugs because it improves delivery efficiency, control in doses, prolongs the time of exposure to the drug and reduces toxicity.

TiO_2 NPs have been studied for cell imaging when labelled with fluorescent dye or magnetic contrast agent. Those TiO_2 nano-structures have been usefully used *in vitro* and *in vivo* in fluorescence microscopy and magnetic resonance imaging (MRI).

Other researches have focused on genetic engineering and biological test application for diagnosis improvement.

Finally, TiO_2 NPs mimic the enamel opalescence of human teeth when incorporated in resins and thus constitute an interesting material for dental prosthesis[42-44].

Part II: TiO_2 NPs exposure and human health risk

1. Specificity and complexity of nanoparticles risk assessment

Among acquired NPs properties, interactions with the living still need keen attention. Indeed, specific properties appear with decreasing particle size. Some of these features are of interest in the medical field, in both diagnostic and therapeutic points of view. However, the emergence of these new properties to the state of NPs suggests that knowledge about the safety or harmfulness of these bulk materials may not be applicable to their NPs.

Because of their small size and their high activated surface, interactions with living constituents are facilitated (a NP is 100 000 times smaller than a human cell). NPs therefore become issues in toxicology. Conventional toxicological tests have been used to assess the danger of a substance, conclusions therefore cannot be assumed for their NPs. The most important point in NPs risk assessment is to gain knowledge about the factors and properties which play a major role in promoting their toxicity. These additional specific parameters have been presented in several reviews including : Buzea *et al.* 2007, Oberdorster *et al.* 2005, Borm *et al.* 2006, Donaldson *et al.* 2004, Nel *et al.* 2006, Suh *et al.* 2009, Jones *et al.* 2009, Arora *et al.* 2012 [15-17, 45-49].

These settings are mainly physicochemical characteristics:

- Size
- Distribution in size
- Shape (sphere, needle, cube, tube ...)
- Surface chemistry and reactivity
- Purity
- Crystal structure
- Stability
- Surface Reactivity
- Chemical surface functionalization
- Porosity
- Solubility
- Aggregation and agglomeration

The conventional parameters that still need to be considered are:

- Dose tested
- Exposure time
- Administration route
- Biological target

The complexity of the physicochemical parameters and variables to consider are summarized in the following diagram:

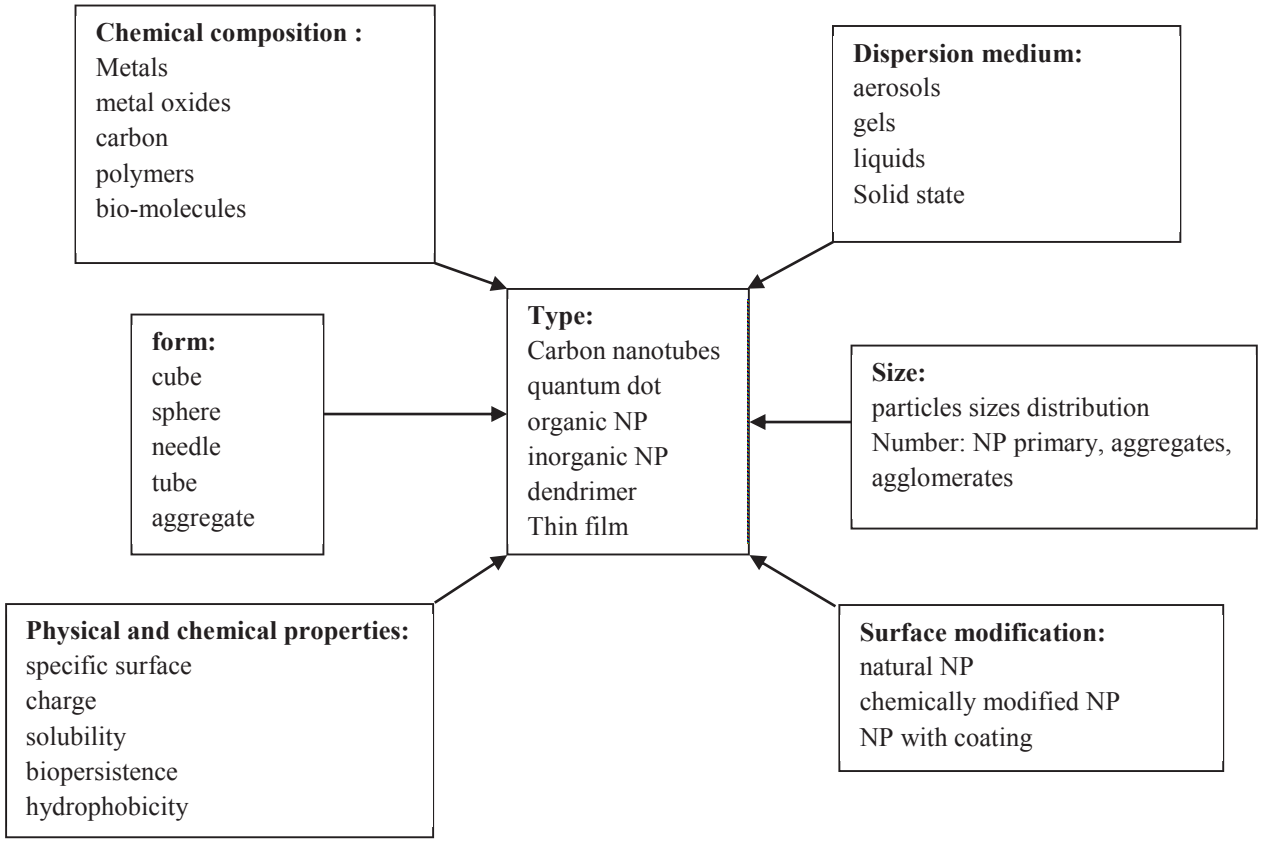

Figure 7: Variables and physicochemical parameters that need to be take into account during nanotoxicology studies (adapted from Ostiguy *et al*., 2010)[50].

2. Exposure route and entry pathway in the organism

2.1. Exposure route

It is very difficult to estimate exposure to the population that may occur during the production of NPs, their handling or their use. In addition, exposure to manufactured NPs can intervene directly through the use of cosmetics, food, textile,... or result indirectly from wear or degradation of nanomaterials and thus from the release NPs present in electronic devices, paints and inks ... (Figure 8). Routes of exposure to NPs are: inhalation of NPs suspended in the air or skin contact, ingestion and injection based on their applications and uses.

Among the exposed population, we see that the workers are the subcategory the most in contact with the NPs in the manufacturing process. In the general population, there is also a particular susceptibility of children, the elderly population [51], pregnant women and diseased people to atmospheric NPs, given their stage of development and exposure [52 53].

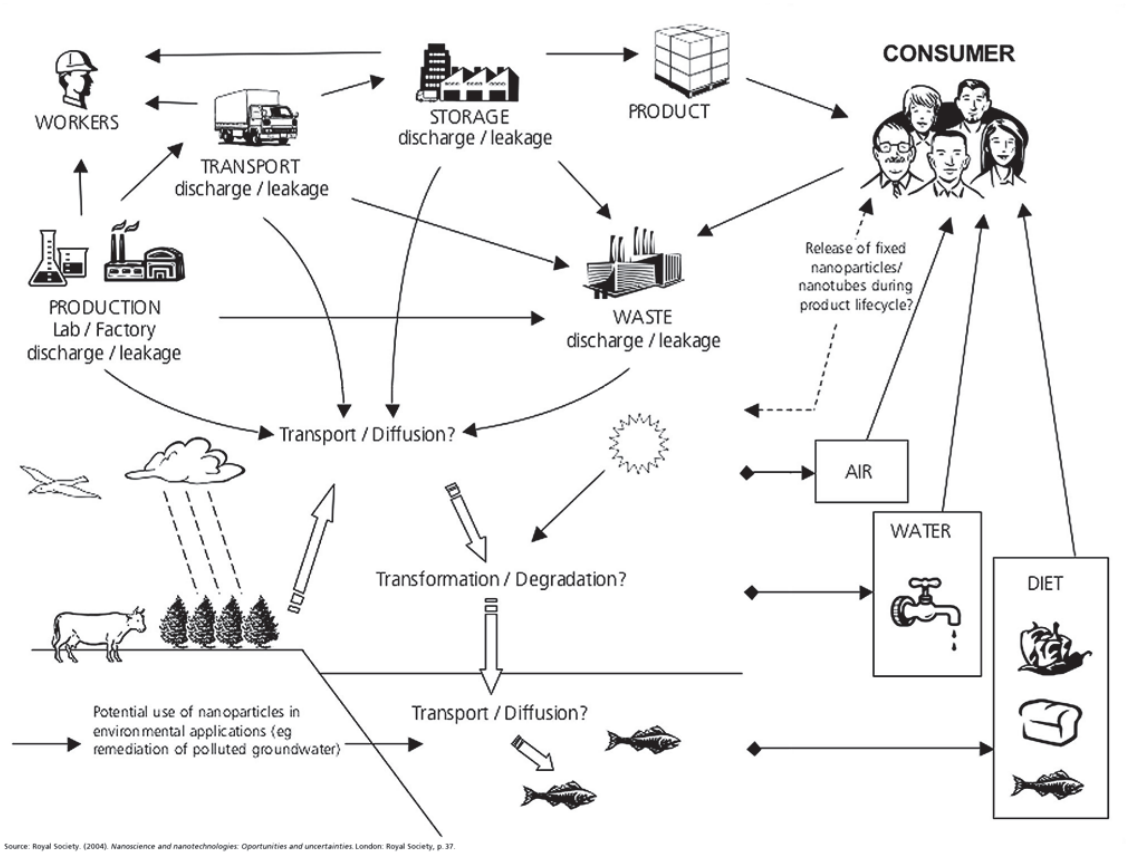

Figure 8: **Possible exposure routes for current and future nanomaterial applications.**

The four routes of exposure to consider in the case of TiO_2 NPs are:

- Skin exposure by application of cosmetic and sunscreen for example
- Ingestion of food containing E171
- Inhalation mainly during the production or handling of TiO_2 powder
- To a lesser extent directly by liberation in the blood in context of biomedical application.

2.2.Translocation and Interaction across physiological barriers

In biology and medicine, the concept of barrier applies to many systems that form an obstacle between two compartments, e.g. skin barrier, gastrointestinal, alveolar-capillary, placenta, testicular, blood-brain, glomerular in kidneys ...

These surfaces represent interfaces between the external environment and the organism or between two internal compartments, playing a critical role in the protection against the intrusion of toxic compounds such as NPs. While the skin acts as a single barrier, transport mechanisms are possible through the gastrointestinal barrier, lung or blood brain barrier. To understand the distribution in the body and the toxicity of NPs (pulmonary toxicity, neurotoxicity or fetal toxicity for example), it is therefore required to study the interactions between these barriers and NPs. A number of studies on rodents have demonstrated that NPs may translocate across physiological barriers such as respiratory and vascular epithelium and may subsequently distribute around the body in various organs and tissues, explaining major concerns as regards their potential specific toxicity.

2.2.1. The pulmonary barrier

The human respiratory system is an exchange surface with the outside environment of 75 to 140 m^2. The respiratory system can be divided into two major parts:

• The upper (mouth, nose, pharynx, larynx) and lower airways (trachea, bronchi, bronchioles) allowing transport of inhaled and exhaled air and inhaled air conditioning.

• The alveoli where gas exchange occurs.

The airways are a relatively robust barrier. The air passages are covered by a pseudostratified epithelium composed of three cell types (Figure 9):

• Epithelial ciliated cells.

• Goblet cells that secrete mucus.

• Basal cells which are located between the basal surfaces of ciliated cells, they are able to replace other cells of the epithelium.

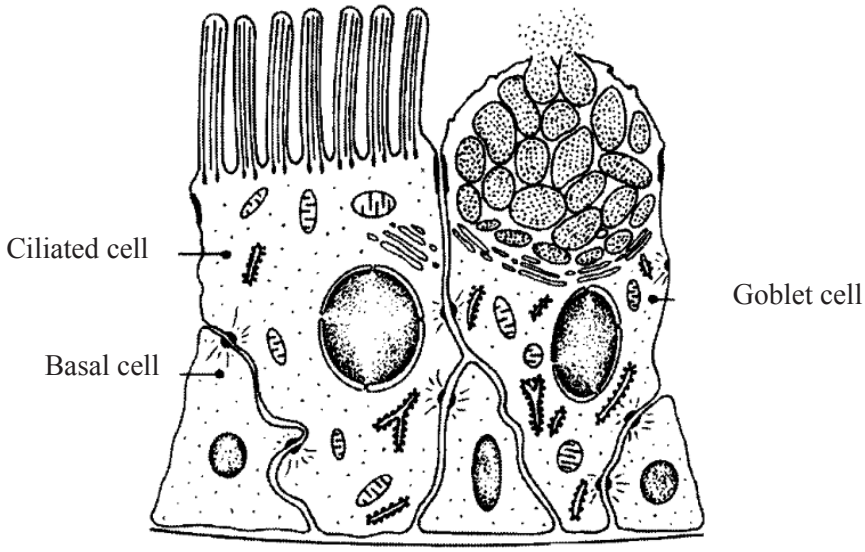

Figure 9: Cells of the respiratory epithelium (available at: https://classconnection.s3.amazonaws.com/445/flashcards/491445/jpg/cells_of_respiratory_epithelium1317806846914.jpg).

The mucocilliary clearance allows evacuation to the trachea of inhaled particles. It corresponds to the combined action of mucus that removes particles and movement of epithelial cilia. Mucus secreted by goblet cells and submucosal glands consists of 2 layers:

- A superficial viscous layer that traps particles and is propelled towards the pharynx.
- A deep fluid layer, that is an aqueous medium adequate for the cilia beats.

Mucus also contains proteins involved in immune reactions. Once in the trachea, the secretions are coughed out or swallowed. Other clearance mechanisms can occur: passing into the blood or lymphatic circulation or phagocytosis by macrophages of the alveoli.

At the bronchioles level, transition zone before the alveoli, the epithelium is slightly different, there are two cell types: epithelial ciliated cells and Clara cells, prismatic cells without cilia easily identifiable by their apical pole-shaped prominent dome of the cubic epithelium.

The cell walls are formed by an epithelium resting on a connective tissue containing a rich network of capillaries (Figure 10). The wall also contains alveolar macrophages that can phagocytose particles. These macrophages are then either transported into the lymph vessels to the hilar lymph nodes, or driven by the alveolar air in the bronchioles, bronchi and trachea, sticky in the mucus and swallowed in the pharynx. This simple squamous epithelium consists of two cell types, type I and II pneumocytes connected by tight junctions. Type I pneumocytes are suitable for gas exchange and represents 90% of the alveolar surface while the type II

pneumocytes secrete a surfactant which forms the mono-layered film lining the alveoli and preventing the collapse of the alveoli when breathing out.

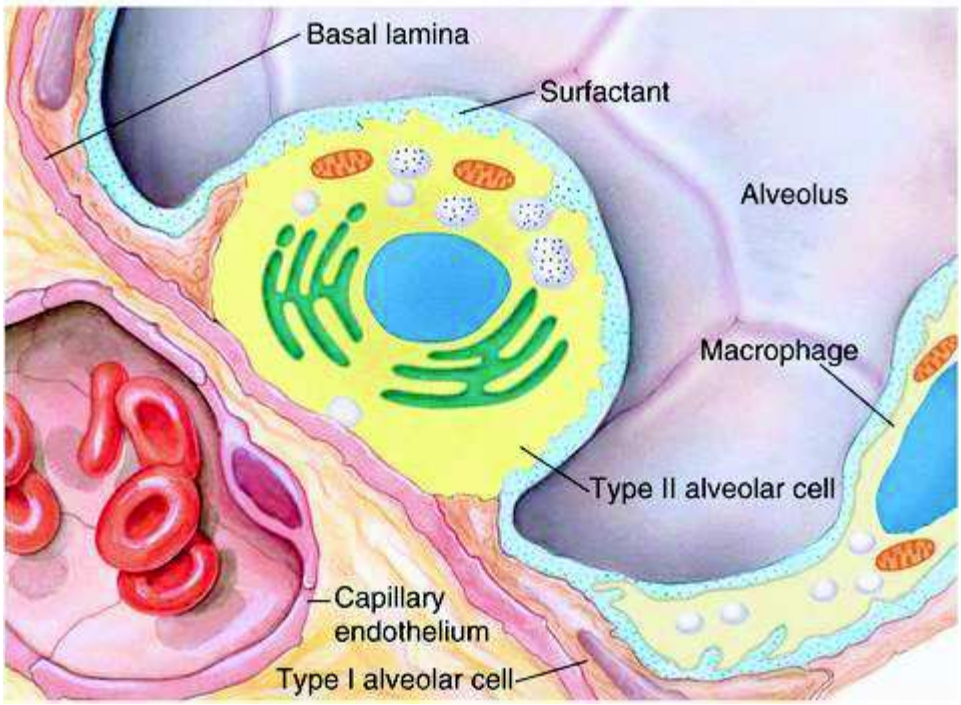

Figure 10: Schematic view of the structure of a pulmonary alveoli and its environment (available at: https://ak47boyz90.files.wordpress.com/2009/08/picture17.jpg?w=510).

The alveolar-capillary barrier also called air-blood barrier is reduced to a thickness of 2.2 microns. It is composed of only four elements:

• The surfactant

• The cytoplasmic sail of a type I pneumocyte

• The single basal membrane resulting from the fusion of the basement membrane of pneumocyte I and the basement membrane of endothelial cell

• The thin cytoplasm of an endothelial cell

It is at this level that haematosis takes place, that is to say, the gas exchange between air and blood. The haematosis is a passive phenomenon that directly results from the presence of appropriate pressure gradients on both sides of the air-blood barrier: oxygen goes from a high partial pressure area (alveolar cavity) to a lower pressure area (plasma) and carbon dioxide takes the opposite direction.

2.2.1.1. Pulmonary toxicity

The respiratory tract is one of the main routes of exposure to NPs. The elimination of these NPs could occur by mucociliary clearance in the conducting airways as well as the alveolar clearance achieved by macrophages in the alveoli. However, there is increasing questioning about the uptake of NPs by different cell populations at the pulmonary level and a possible translocation through the epithelium towards the interstitium and/or the blood stream.

The pulmonary system is an exchange surface with the external environment of 75 to 140 m^2. Airways represent a relatively robust barrier formed by a layer of mucus and a pseudostratified epithelium. The lung is a primary target organ of NPs exposure via inhalation in the occupational setting. The toxic effects of TiO_2 NPs on pulmonary system has raised concerns and in recent years, more and more studies have investigated this lung toxicity. A few epidemiologic studies have surveyed the carcinogenicity of TiO_2 in workers employed in TiO_2 production factories. The results were reviewed by NIOSH in 2005 and reveal elevated risks of lung cancer mortality or morbidity among workers exposed to TiO_2 dust [54]. In 2006, the International Agency for Research on Cancer (IARC) classified pigment-grade TiO_2 in Group 2B as "possibly carcinogenic to human beings".

Toxic effects of NPs in the lungs depend upon their site of deposition and their time of residence in the lungs. The behavior of NPs during their deposition and their clearance from lungs is different from larger particles. The main mechanism for NPs deposition in the lungs is indeed the diffusion while other mechanisms such as inertial impaction gravitational settling, and interception contribute to larger particles deposition [16]. Thus, particles smaller than 10 microns may reach the alveoli while larger particles remain in the airways [55].

Inner surface of the alveoli is formed by a simple squamous epithelium (pneumocytes type I and II) based on a tissue rich in capillaries. Once NPs are internalized in living cells of the alveoli, they may have the ability to pass into the bloodstream. For example, ^{99m}technicium carbon NPs have been observed in the liver of healthy volunteers after inhalation [56]. The eventuality of a translocation to the blood stream from the lungs is also supported by observations of extrapulmonary effects in epidemiological studies (e.g. cardiovascular effects) [57].

Nearly thirty studies have addressed the pulmonary effects induced by TiO_2 NPs during inhalation experiments in rodents [12, 58]. Several routes of exposure have been used, inhalation staying the most relevant for the human exposure (after tracheal instillation, a fraction of the dose can be swallowed and the resulting distribution can be sidestepped with oral route). Toxic effects observed after *in vivo* studies by inhalation or by tracheal instillation of TiO_2 NPs relate primarily the induction of local inflammation characterized by infiltration of neutrophils and macrophages, damage to the epithelium with an increase in permeability and apoptosis [59-71]. After an acute exposition and a recovery period, the inflammation parameter returns to normal levels [72, 73]. Limitations of air flow have also been observed [74].

Toxicogenomic studies provide insight into the mechanisms of toxic actions. Chen *et al.* 2006 [62] have used this method and shown that the morphological and histological changes

in the lungs were associated with changes in the expression of many genes including some involved in cell cycle regulation, apoptosis, cytokines, and the complement cascade. The gene expression of chemokines associated with emphysema and apoptosis of alveolar epithelial cells was increased. Park *et al.* 2009 [61] by the same method have confirmed these observations and also showed the increase of gene expression involved in antigen presentation and induction of chemotaxis of immune cells. Overexpression of genes of acute inflammation and immunity was also confirmed by Halappanavar et al, 2011 [75].

The *in vitro* studies on various cell lines representing different cell types of the lungs correlate with *in vivo* observations and strengthen these mechanisms of action.

- decrease cell viability [76-79].
- increase inflammatory parameters [77, 79-84].
- increase the release of ROS [79, 80, 85, 86]. The MAP kinase pathway may be altered in the presence of ROS. This pathway is involved in the activation of transcription factors including nuclear transcription factor NF-kB which control the expression of numerous genes involved in inflammation. The release of ROS therefore potentially impact the activation of many genes involved in inflammatory response [87].
- induction of apoptosis [79, 84].

For inorganic NPs, mechanisms of action at the cellular level are documented through the toxicogenomic studies. The mechanisms discussed can help understand the emitted hypothesis of a link between exposure to NPs and some human diseases such as asthma or chronic bronchitis. However, the deterioration of lung functions has yet to be directly related to the exposure to NPs.

Raising concerns on NPs lung toxicity have led the NIOSH in 2011 to recommend an exposure limits of 2.4 mg/m^3 for fine and 0.3 mg/m^3 for ultrafine dust including TiO_2 [88]. This literature review pointed a lack of data regarding risk assessment. Therefore, experiments with inhaled NPs are highly relevant means of acquiring sound toxicological data on nanomaterials.

2.2.1.2. Translocation across the alveoli barrier

There is increasing questioning about the uptake of NPs by different cell populations at the pulmonary level and a possible translocation through the epithelium towards the interstitium and/or the blood stream. Despite many studies on the pulmonary toxicity of TiO_2 NPs, information on their ability to cross the lungs blood barrier remains insufficient. Indeed, several *in vivo* inhalation studies have demonstrated that inorganic NPs could cross the lungs blood barrier, be translocated into the bloodstream and be distributed to other organs: Takenaka *et al.* report that after a 6 hour inhalation exposure to silver NPs (4-10 nm), a small amount of particles was recovered in the liver, spleen, brain, heart, and blood of rats 30 minutes after

inhalation [89]; Yu *et al.* observed gold NPs in the heart, liver, pancreas, spleen, kidney, brain and testis in rats exposed to gold NPs by inhalation (majority with a size <35 nm) for 15 days[90]; Geraets *et al.* highlighted translocation to extrapulmonary organs of cerium oxide NPs (5-10 nm) observed 6 hours after the end of exposure [91]and a study by Kwon *et al.* shows that inhalation exposure to fluorescent iron containing magnetic NPs (size 50 nm) for 4 weeks (4 hours/day, 5 days/week) resulted in measurable NP distribution to the liver, spleen, lung, testis and brain in mice [92]. Furthermore, two separate studies report long-term NP biokinetics in secondary target organs over six months after a single short-term iridium NP inhalation [13, 14]. When 15-20 nm iridium NPs were administered by inhalation, iridium could be detected in the brain up to 6 months after exposure [93].

After intratracheal instillation, several studies have highlighted titanium translocation to extrapulmonary organs such as the liver or spleen (Table 2). However this mode of administration is not sufficiently representative of an environmental exposure and certainly overestimates the passage of the lungs blood barrier. After inhalation of NPs TiO_2 in rats, internalization of NPs in the cytoplasm of all cell types of the lung has been observed (epithelial cells, capillary endothelial cells, fibroblasts in the interstitium ...) [94] . However, no studies after inhalation have helped highlight titanium in extrapulmonary organs other than the mediastinal lymph node and connectives tissues.

References	Model	Administration mode	Dose and duration of treatment	Outcome
Shinohara *et al.* ; 2014 [95]	rat	intratracheal instillation	0.375- 6.0 mg/kg	NPs in mediatinal lymph node and small amount of TiO_2 in the liver by 3 days after the administration
Zhang *et al.* ; 2013 [96]	mice	intratracheal instillation	1 mg/kg	small amount of Ti in liver and spleen
Shinohara *et al.*; 2015 [97]	rat	intratracheal instillation	0.375-2.0 mg/kg	Ti in thoracic lymph nodes and small amount in kydneys, spleen and brain
Husain *et al.* ; 2015 [98]	mice	intratracheal instillation	18 or 162 µg/ animal	Ti in blood, heart and liver
Takenaka *et al* ;. 1986 [99]	rat	inhalation	8,6 mg/m^3 for 7hr/day, 5 days/week up to 1 year	NPs in macrophages and in perivascular spaces
Ferin *et al.* ; 1992 [100]	rat	inhalation	23mg/m^3 for 6hr/day, 5 days/week up to 12 weeks	NPs in the interstitium, epithelial cells and alveolar space
Geiser *et al.* ; 2005 [94]	rat	inhalation	0,11mg/m^3 for 1 hr	NPs in connective tissues and capillaries
Muhlfeld *et al.* ; 2007 [101]	rat	inhalation	0,11mg/m^3 for 1 hr	NPs in connective tissues and capillaries
Van Ravenzwaay *et al.* ; 2009 [102]	rat	inhalation	100 and 250 mg/m^3 for 6h/day for 5 days	NPs in mediastinal lymph node
Ma-Hock *et al.* ; 2009 [103]	rat	inhalation	2-50 mg/m^3 6 hr/day for 5 days	NPs in mediastinal lymph node
Landsiedel et al.; 2014[104]	rat	inhalation	2-50 mg/m^3 6 hr/day for 5 days	NPs in mediastinal lymph node

Table 2: Studies reporting translocation of TiO_2 NPs to extra-pulmonary organs after intratracheal instillation or inhalation.

2.2.2. The intestinal barrier

The wall of the whole digestive tract has a complex structure, consisting of four successive coats from the outside inwards: the serosa, muscularis, submucosa and the mucosa (Figure 11).

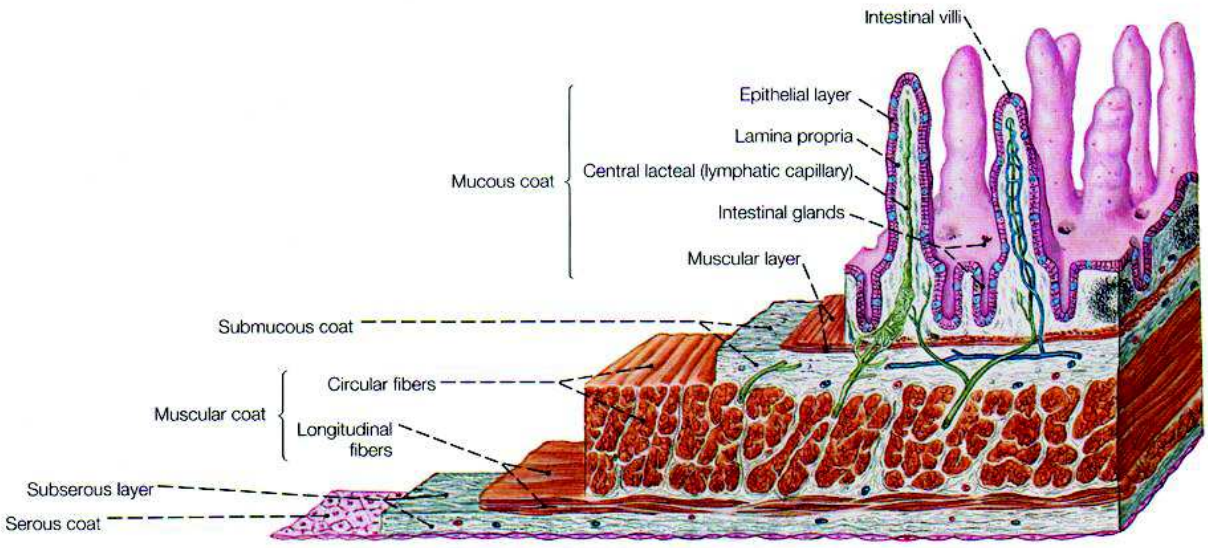

Figure 11: Digestive tube mucosa structure (available at: http://www.corpshumain.ca/en/images/excret_intestin_paroi_(FF)_en.jpg)

The structure of the lining differs substantially from one end to the other of the digestive tract, reflecting differences of activities and functions of each segment of the tract. The mucous membrane is constituted of three layers: the muscular, connective tissue rich in blood and lymph capillaries and the monolayer epithelium formed enterocytes associated with goblet cells that secrete mucus, enterochromaffin cells, endocrine cells and exocrine Paneth cells.

Given the importance of the oral route and the surface of the digestive system, the gastrointestinal barrier is the first surface in contact with xenobiotics. The intestine acts both as a filter to allow the passage of nutrients from the digestive lumen to the blood but also as a barrier opposing the intrusion of toxic microorganisms, viruses present in large quantity in the digestive lumen.

Several parameters allow the digestive system to perform its function as a barrier (Figure 12):

• The peristatic bowel movements that prevent retention and therefore proliferation of microorganisms in the intestine.

• The intestinal flora is essential to the development and differentiation of intestinal epithelial cells. Commensal flora also plays a critical role in the development of the immune system.

• The epithelial barrier consists of a simple columnar epithelium made by brush border enterocytes and goblet cells. The mucus secreted by goblet cells prevents the ingress of microorganisms and toxic substances present in the intestinal lumen. This mucus is divided into two layers: a water-insoluble gel (30 to 450 µm thick) adhering to the mucosa and a water-soluble viscous gel layer covering the so-called stagnant water layer. The gel is made by the polymerization of mucin and forms a physical barrier between the epithelial cells and organisms

or toxic substances present in the intestinal lumen. Epithelial cells also secrete antimicrobial peptides (β defensin for example) which has a lytic effect on bacteria. The actual separation between the body and the external environment is formed by the monolayer of epithelial cells. Epithelial cells are interconnected by complex intercellular junctions. Enterocytes are cylindrical cells with microvilli at their apical side. Junctions connecting the cells ensure the mechanical coherence of the barrier and facilitate communication between enterocytes.

• The immune cells present in the gastrointestinal tract allows the setting of an immune response against the potentially harmful microorganisms while maintaining a tolerance for the commensal flora. GALT (Gut Associated Lympoïd Tissue) is an associated lymphoid tissue in the gastrointestinal mucosa. GALT includes diffuse sites in the mucosa and organized structures such as Peyer's patches, mesenteric lymph nodes, isolated lymphoid follicles or plates crypts. Peyer plates are the primary site for the induction of inflammatory reactions. They are aggregations of lymphoid follicles in the basal lamina of the terminal portion of the ileum. These lymphoid follicles, consisting largely of B and T cells, are separated from the intestinal lumen by special epithelial cells called M cells (for Microfold cells). The high endocytic activity of these M cells makes them particularly suitable for interaction with microorganisms and particulates present in the intestinal lumen.

From the intestinal lumen, the molecules have to cross different layers successively before reaching the blood:

1) the mucus layer

2) epithelial cells: at this level there are several modes of transition: The transcellular passage (passive diffusion through the membrane, passive diffusion through a channel, facilitated diffusion, which requires a carrier but not energy, active transport, endocytosis) or paracellular passage which concerns only small molecules (water, ions and monosaccharides) that diffuse according to their concentration gradient.

3) the basement membrane (7-9 nm) (this is a classic layer that consists of laminins, collagens (predominantly collagen IV), proteoglycans, calcium binding proteins such as fibulin, and various other structural or adhesive proteins)

4) the fenestrated capillary

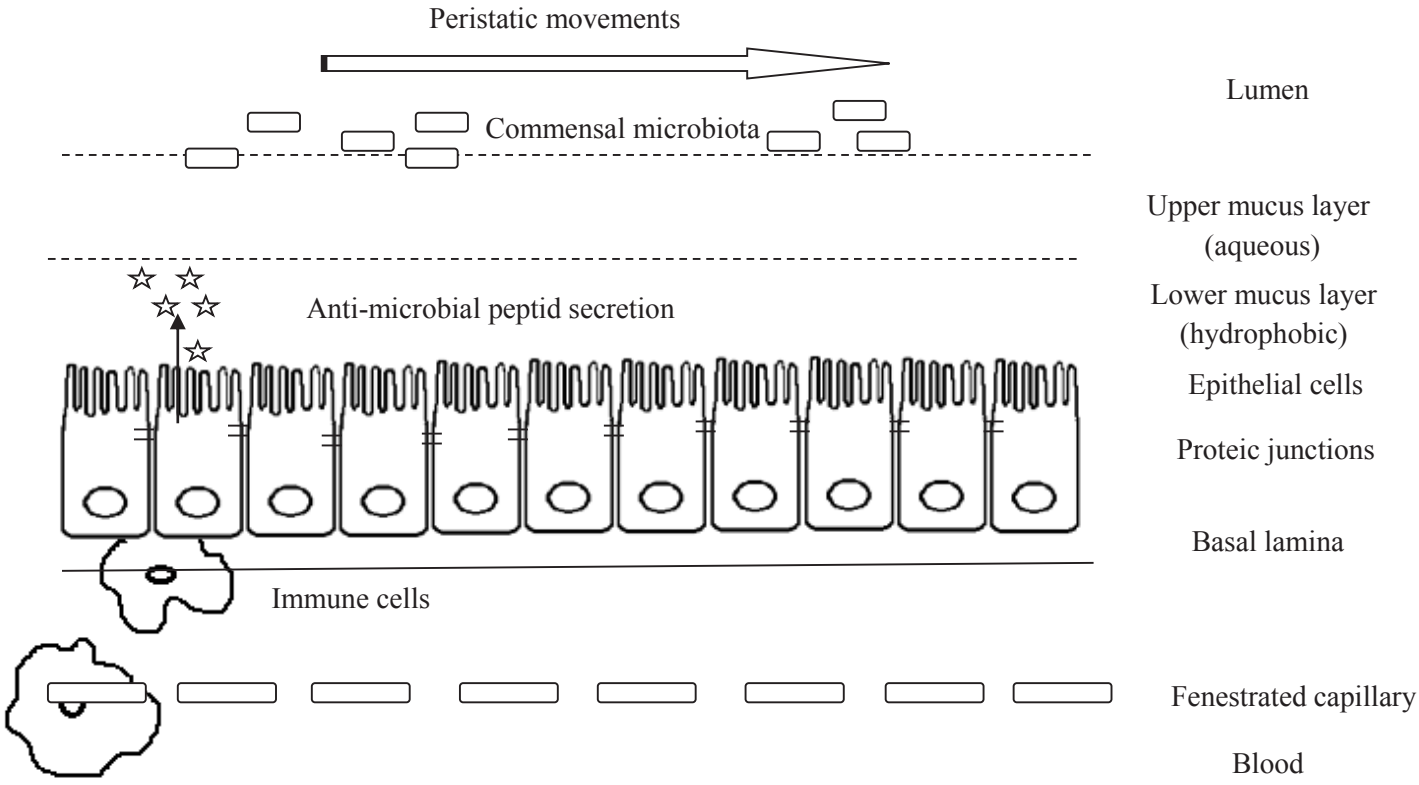

Figure 12: Actors at the intestinal barrier.

2.2.2.1. Gastro-intestinal toxicity

NPs which come into contact with the gastrointestinal barrier may have several origins:
1) NPs directly ingested in food, water, cosmetics (toothpaste and lip balm) or
2) inhaled NPs which take the mucocilliary escalator then pass through the digestive tract after swallowing [105].
Children under 10 years are the most exposed consumers, with an average intake of 1 to 2 mg of TiO_2 per kilogram of body weight per day against 0.2-0.7 mg for other consumers [24].

The study by Wang *et al.* 2007 made possible to show that TiO_2 NPs administered as a single dose could cross the digestive barrier without inducing acute toxic effect in the digestive tract [106]. Sycheva *et al.* 2011 highlighted the genotoxic potential of TiO_2 NPs in mice after oral administration [107]. Despite positive mutagenicity tests *in vitro* [108], no carcinogenic effect of TiO_2 NPs has been detected on the intestinal cells.

Studies of intestinal barrier *in vitro* models using Caco2 cell line have confirmed that NPs TiO_2 were able to cross the intestinal epithelium [109]. The lack of cytotoxicity and the maintenance of

the integrity of the monolayer cell suggest that TiO_2 NPs cross the epithelial layer by transcytosis. This study has also highlighted the accumulation of TiO_2 NPs at the brush border and structural changes of the enterocytes: disappearance of microvilli associated with an increase in intracellular calcium [109]. The increase in intracellular calcium might be the starting point of the disappearance of the microvilli mechanism. Indeed, the microvilli are formed through cytoskeletal proteins. These proteins (e.g. actin) are calcium dependent that is to say, they are rearranged in the event of modulations in intracellular calcium concentration. These changes are not lethal for the enterocytes but alter their functions. A previous study on human colon carcinoma cells (LS-174-t) showed absence of cytotoxicity of TiO_2 NPs on cells from intestinal origin [110]. Another study by Brun *et al.* 2014 compared *in vitro*, *ex vivo* and *in vivo* impact of TiO_2 NPs in gut epithelia [111]. It highlighted increased paracellular permeability associated with deregulation of genes encoding for proteins involved in cell junctions. Recently, Dorier *et al.* have investigated efflux pumps functions of Caco2 barrier after acute exposure to TiO_2 NPs [112]. They have revealed increased regulation of ABC and SLC transporters suggesting increased barrier capacity against xenobiotics. Increased ROS production and dysregulation of redox balance has also been observed.

Observations from *in vitro* studies are not transposed *in vivo*. This likely reflects the rapid turnover of the intestinal epithelium. Chronic exposure over longer periods would therefore be interesting to understand functional consequences *in vivo* and to establish the link with pathological conditions of the gastro-intestinal tract. Indeed, NPs (carbon, calcium, silver, silica ...) have been found in large quantities in the colon of patients affected by Crohn's disease, ulcers or cancers [113]. NPs found in these patients were absent in healthy people. These NPs are considered non-toxic at larger dimensions. Crohn's disease is due to a combination of genetic and environmental factors. These data suggest a link between this disease and a NPs rich diet. A diet low in NPs even seems to reduce the symptoms of Crohn's disease [114, 115]. The suggested mechanism of action is the exacerbation of a local inflammation by NPs which trigger an increase in the permeability barrier observed in the case of a pathology such as Crohn's disease.

2.2.2.2. Translocation across the intestine

Most studies indicate that the majority of ingested NPs is rapidly eliminated in feces: 98% in 48h [16]. In the lumen, the NPs are in contact with a complex mixture of compounds including food, digestive enzymes, bacteria ... The NPs interact with these compounds which helps explain their rapid elimination with the bolus. However, *in vivo* data have showed that some NPs can be translocated to the digestive lumen to the blood, liver ... (Table 3). The translocation might occur through enterocytes monolayer or by interaction with the Peyer's patches cells [116].

The transport mechanisms of NPs through the gastro-intestinal mucosa are still being studied (transcytosis by vesicle carriers ...). Several *in vivo* studies have nonetheless helped to highlight an uptake of NPs across the intestinal barrier [106, 117-119] . Only one *in vivo* study clearly demonstrated this translocation for TiO_2 NPs 25 and 80 nm after gavage in mice [106]. Significant amount of titanium was assayed in the liver, spleen, lungs and kidneys of the treated animals.

In other studies, the translocation is suggested due to observed TiO_2 NPs in lymphoids tissues close to gastro-intestinal epithelium.

Nanoparticles	Models	Outcomes	References
TiO_2 500 nm	12,5 mg/kg during 10 days	accumulation in gut associated lymphoid tissues, lungs and peritoneal tissues	Jania *et al.* ; 1994 [119]
TiO_2 25 and 80 nm rutile TiO2 155 nm anatase	Single gavage to mice 5g/kg, dosage after 2 weeks	NPs in liver, spleen, lungs and kydneys	Wang *et al.* ; 2007 [106]
TiO_2 25 nm P25	oral administration to rat for 13 weeks, 7 days/weeks, 260,4-1041,5 mg/kg	low absoprtion	Cho *et al.*; 2013 [120]
TiO_2 with different size-range and crystal form	oral administration, single or 5 administrations of 2.3 mg/rat	small amount in mesenteric lymph nodes	Geraets *et al.* ; 2014 [121]
TiO_2 6 nm anatase	Oral administration 2-10mg/kg daily for 6 months	Ti in the liver	Hong *et al.*; 2014 [122]
TiO_2 12 nm 95% anatase	single oral gavage 12,5 mg/kg to mice	Ti rich regions in peripheral zone of lymphoid nodules	Brun *et al.* ;2014 [111]
TiO_2 15 nm anatase	Single oral dose 5mg/kg to healthy human volonteers	No evidence of titanium absorption	Jones *et al.;* 2015 [123]

Table 3: *In vivo* studies that evidence TiO_2 NPs translocation across the gastro-intestinal tract.

2.2.3. The skin barrier

The skin is one of the tissues that is the most in contact with the external environment. Its average area is evaluated to 2 m^2. The skin is made of several layers (Figure 13):

- The epidermis
- The dermis
- The hypodermis

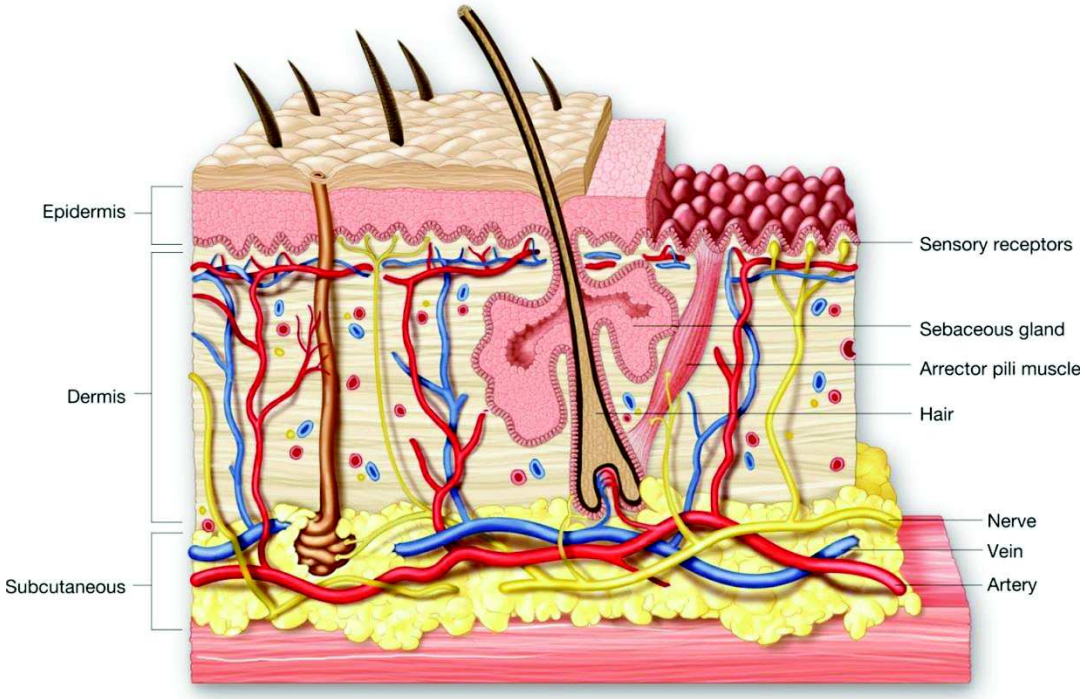

Figure 13: Schematic representation of the skin layers (available at: http://biology-forums.com/gallery/14755_16_09_12_5_57_13_87522080.jpeg).

The hypodermis is a loose connective tissue consisting mainly of adipose cells that store lipids. Adipose cells are grouped into lobules separated by connective tissue. The hypodermis serves as a heat insulator, lipid reserves and mechanical protection.

The dermis is a connective tissue innervated and vascularized. It plays a role of support and nutrition of the epidermis and annexes structures, but is also involved in thermoregulation, wound healing and defense against pathogens due to the presence of immune cells (dendritic cells, macrophages and lymphocytes T). Fibroblasts are the main cell type of the dermis. They synthesize collagen and elastin, which confer mechanical strength and elasticity to the skin. The epidermis is the outermost skin structure. It is a multilayered keratinized and squamous epithelium. Its thickness is about several hundred micrometers, and varies depending on the anatomical areas.

The epidermis consists in more than 90% of epithelial cells called keratinocytes, the other cells corresponding to melanocytes (which synthesize the pigments required for photo-protection), Langerhans cells (dendritic cells providing immune protection) and Merkel Cell (which function as mechanoreceptors). The epidermis consists of five layers of superimposed cells (Figure 14):

• The basal cell layer or stratum basal: layer of columnar or cuboidal cells attached to the dermis by the dermal-epidermal junction. Keratinocytes of the basal layer are the only mitotically active and relatively undifferentiated ones. They ensure the renewal of the epithelial cells of the epidermis.

• The pickle cell layer or stratum spinosum: composed of 5 to 10 foundation of cylindrical cells. "Spines" visible by optical microscopy are actually desmosomes, from which many intermediate filament bundles converge ensuring mechanical intercellular cohesion.

• The granular cell layer or stratum granulosum: consisting of 2 or 3 layers of flattened keratinocytes containing keratohyalin granules in their cytoplasms. These keratinocytes also contain tubulo-vesicular structures called lamellar bodies or keratinosomes. They play a major role in the establishment of the epidermal barrier function by dumping their protein and fat contents by exocytosis in the interface stratum granulosum / stratum corneum leading to the formation of an intercorneocyte cement.

• The stratum lucidum: it is a clear cell layer only found in thick skin. The cells appear flattened with very few organelles.

• The horny layer or stratum corneum: composed of thirty dead keratinocytes layers and anucleated then called corneocytes. The cell organelles and the nucleus have been degraded and cytoplasm transform in a fibrous matrix of keratin and filaggrin. The cytoplasmic membrane is replaced by a rigid and insoluble shell. This layer is highly lipophilic and represents a robust physical barrier.

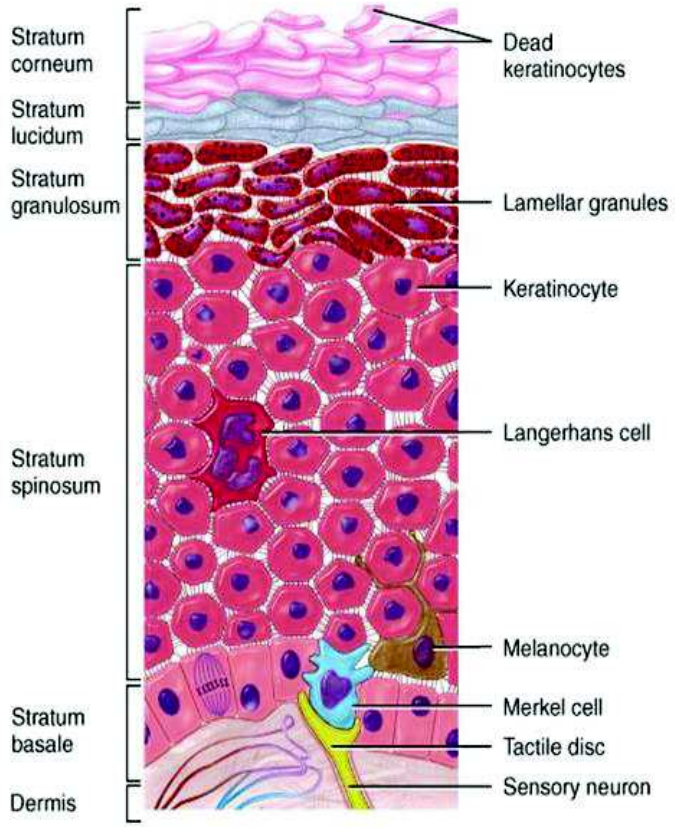

Figure 14: The five epidermal layers (available at: http://spaces.imperial.edu/thomas.morrell/Picture2.jpg).

2.2.3.1. Cutaneous toxicity

The skin has been a source of particular attention given the presence of TiO_2 in sunscreens and other cosmetics. The observed effects are variable depending on the cell type used and the physicochemical parameters of the particles (size, coating ...). *In vitro*, these effects are a decrease of cell proliferation associated with increased production of reactive oxygen species (ROS) and antioxidant depletion. Genotoxicity phenomena related to oxidative stress were also demonstrated on fibroblasts [124, 125]. TiO_2 NPs absorbs UV light and in an aqueous medium and generate free radicals (superoxide, hydroxyl) hydrogen peroxide or singlet oxygen, which can cause oxidative damage to DNA [86, 126]. *In vivo* observations are contradictory: some studies have shown histopathological changes of skin structures without clinical signs in pigs after application for 30 days while other studies have not been able to confirm these results [127, 128]. The influence of co-exposure to TiO_2 NPs and UV light (ultraviolet) has yet to be studied. In addition, the effects on damaged skin, for example in case of burns due to exposure to UVB or aging skin are also unknown. Toxicity data after application on injured skin (wounds, bedsores) are scarce. Studies on longer applications corresponding to the reality wound treatment with wound dressings in humans also need to be conducted.

2.2.3.2. Translocation across the skin

The dermal route is one of the most studied exposure routes due to the massive use of NPs in cosmetic products but also in bandages and textile. The dermis is a tissue rich in blood and lymph vessels, dendritic cells, macrophages and nerve endings. Thus, NPs crossing the stratum corneum and epidermal thickness are potentially available for distribution to secondary organs.

Translocation from a topical administration to the lymphatic system has been shown with soil particles accumulating in patients suffering from podoconiosis [129].

Several studies have investigated the dermal absorption of manufactured TiO_2 NPs. The results are highly variable which is explained probably by the variety of techniques and models used (*in vivo* and *in vitro*). So far, healthy skin is considered to provide an effective barrier, the risk associated with this exposure route is estimated to be relatively low (Table 4). However, some conflicting studies suggest that this path cannot be neglected because NPs can pass through the stratum corneum layer of the epidermis to reach the dermis.

Nanoparticles	Models	Outcomes	References
TiO_2 coated 20 nm; TiO_2 10–15 nm	*In vivo:* 45 mg applied on distinct areas on the forearm of a human volunteer	localization exclusively on the outermost layer of the human stratum corneum	Schulz *et al.*; 2002 [130]
TiO_2 45–150 nm long and 17–35 nm wide	*In vivo*: pig skin biopsies	NPs penetrated into the stratum granulosum *via intercellular space*	Menzel *et al.* ; 2004 [131]
TiO_2 (from commercial sunscreen)	*In vivo*: penetration *via* human foreskin grafts transplanted to immunodeficient mice	NPs were observed having penetrated into the corneocyte layers of stratum corneum	Kertesz *et al.* ; 2005 [132]
TiO_2 coated with silica 30–60 × 10 nm	*In vitro:* porcin skin	No penetration	Gamer *et al.*; 2006 [133]
TiO_2 10-60 nm	*In vitro*: vertical diffusion cells with full-thickness porcine skin	NPs in 5 epidermal layers	Wu *et al.* ; 2009 [128]
TiO_2 10-60 nm	*In vivo* : skin application during 60 days to hairless mices	Distribution to liver ; spleen and lungs	Wu *et al.*; 2009 [128]
Uncoated TiO_2 30-50nm; Coated TiO_2 20-30nm wide 50-150nm long	*In vivo:* application on minipig	No significant penetration through the intact normal epidermis	Sadrieh *et al.* ; 2010 [127]
Uncoated TiO_2 35nm; Coated TiO2 35nm; Coated TiO2 10x50nm	*In vitro:* application on full thickness hair removed micropig skin in diffusion cell	No penetration to dermis or viable epidermis observed	Senzui *et al.* ; 2010 [134]
TiO_2 10-50nm from commercial sunscreen	*In vivo:* application on pig and pig overexposed to UVB light In vitro: intact and UVB damaged pig skin	Minimal transdermal absorption, deeper penetration in UVB damaged skin	Monteiro-Riviere *et al.* ; 2011 [135]
TiO_2 (from commercial sunscreen) 20–30 nm long and 50–150 nm wide	*In vitro* : intact, damaged, irradiated, and damaged/irradiated pigskin	Lack of transdermal diffusion through the intact living skin. Minimal penetration of TiO_2 NPs into epidermal living cellular elements occurs in the case of damaged skin	Miquel-Jeanjean *et al.* ; 2012 [136]
TiO_2 (from commercial sunscreen)	*In vitro:* excised intact and several damaged rat skin, porcin ear skin	distribution into the groove and hair follicles but no migration to viable epidermis and dermis	Kimura *et al.* ; 2012 [137]

Table 4: Studies that investigated *in vitro* or *in vivo* skin penetration of TiO_2 NPs.

Indeed, skin penetration depends on many external (dose, vehicle, protein reactivity ...) and endogenous factors (age of the skin, disease or skin alteration, anatomical site of application ...). Before considering distribution to the blood or lymphatic system, NPs must pass through the stratum corneum and the different layers of the epidermis to reach the dermis, the living part of the skin. Despite its low thickness (of the order of a millimeter), the stratum corneum provides resistance against skin penetration. Through this layer several pathways are possible: between the cells (intercellular) through cells (transcellular) or through hair follicles [17](Figure 15). Theoretically, only low molecular weight materials and in the appropriate formulation (dependent on octanol/water partition coefficient) may penetrate an intact human skin.

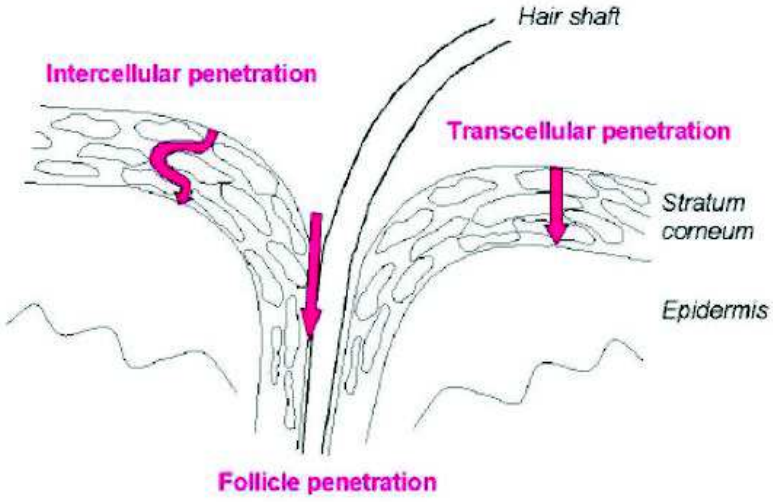

Figure 15: Penetration pathways of topically applied substances through the skin (Borm *et al.*; 2006) [17].

3. *In vivo* fate

3.1. Biodistribution, accumulation and elimination

Exposure to TiO_2 NPs at relevant lower doses should be conducted in order to clearly conclude on the NPs ability to cross a biological barrier. Therefore, results from existing literature suggest that TiO_2 NPs can be absorbed through the lungs and gastro-intestinal tract. After initial absorption through a biological barrier, the blood stream can distribute the TiO_2 NPs to all organs and tissues in the body. In the blood, NPs may interact with plasma proteins and blood cells which can play a critical role in their distribution in the body. The resultant absorption, distribution, metabolism and elimination (ADME) process determines target tissue burden and accumulation ability. This is critical for the systemic adverse health effects evaluation.

In a literature review, Oberdörster *et al.* in 2005 summarized *in vivo* fate of NPs. Some of the channels were confirmed by several *in vivo* studies primarily in rodents such as the passage of the nasal mucosa to the CNS, other channels remain to be studied (Figure 16). In the case of absorption in the blood or direct delivery to the systemic circulation (IV), biokinetics studies showed that TiO_2 NPs can be found in many organs including liver, spleen, kidneys, bone marrow, brain .... The studies of IV injections in rodents have identified the target organs and the fate of NPs in the body. The organs in which NPs are most often found are: liver, lungs and kidneys.

As inorganic NPs, TiO_2 NPs can be cleared by two possible pathways: kidneys/urine or bile/feces. These two separated pathways have been proposed : Xie *et al.* in 2011 followed Ti burden in mice organs for 30 days after intravenous injection of 20 nm rutile-type TiO_2 NPs labeled with CF680 or ^{125}I [138]. They observed accumulation primarily in liver and spleen. The excretion through urine and to a lesser extent through feces was observed suggesting that renal excretion is the main excretion pathway for TiO_2 NPs. Another study by Geraets *et al.* in 2014, concluded, after single or repeated intravenous administration to rats, that elimination of total TiO_2 has a long half-life. In addition, titanium measured in feces and urine was not significantly increased in the exposed group suggesting a long term biopersistence up to 90 days [121]. Elimination in sweat and breast milk has never been investigated for TiO_2 NPs. It seems that because of their small size NPs are less easily eliminated, are retained in the body longer and that they would tend to lead to organ damage, particularly to the liver and kidneys after continuous exposure [106]. Organ accumulation needs to be considered in the context of biomedical application to avoid potential toxicity. Contradictory results underscore the need of further biokinetics studies to understand the distribution, long term persistence and elimination process of TiO_2 NPs.

Route of exposure, physico-chemical characteristics (e.i. size or coating) and doses can affect distribution, metabolism and elimination profile of NPs [139-141].

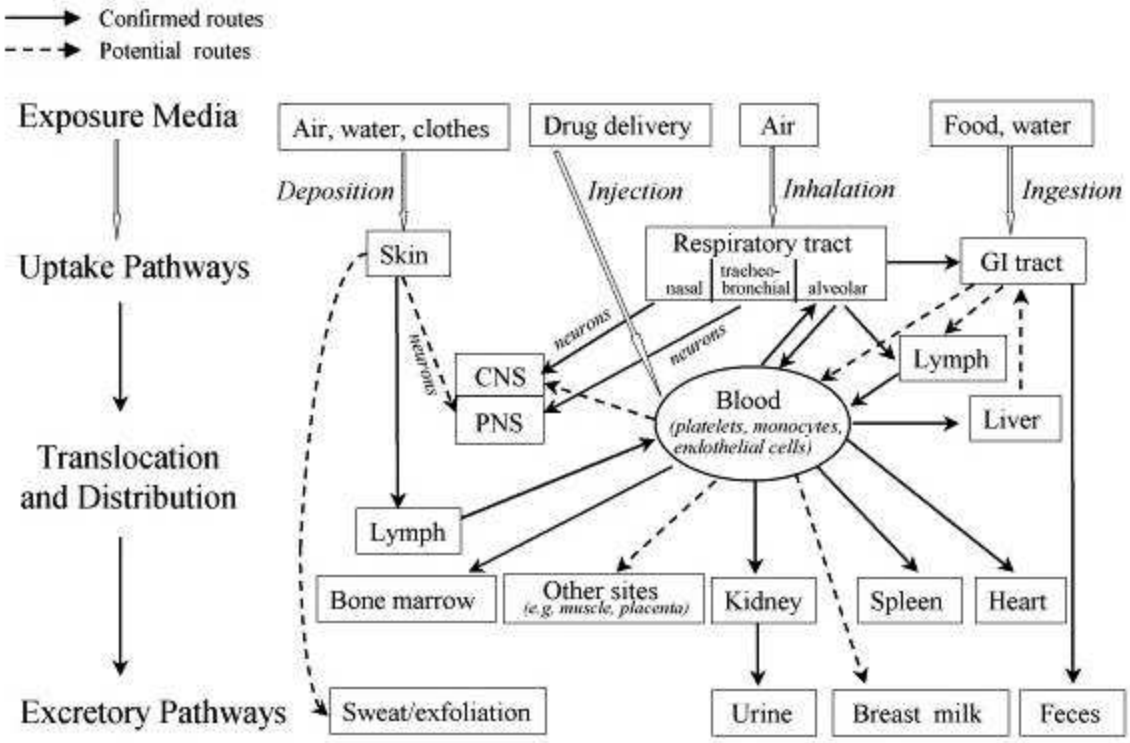

Figure 16: Biokinetics of nano-sized particles (from Oberdörster *et al.;* 2005) [142].

3.2. Systemic toxic effects

3.2.1. Hepatotoxicity

Effects of TiO_2 NPs exposure on liver functions have been studied *in vivo* in rodents following exposure protocol and doses. Whatever the administration route, phenomena such as oxidative stress, modifications in enzymes activities (e.g.: transaminases), inflammation, modulations of serum and urine biomarkers representative of hepatic dysfunction have been observed. Histology examinations of liver tissue also reveal induced apoptosis or fibrosis and impact on liver vascularization. Major outcomes of studies which have investigated the adverse effects of TiO_2 NPs on liver are summarized in Table 5. Liver is the key organ for metabolism processes: energetic metabolism and as a detoxification functions. Indeed the liver is implicated in fat, protein and carbohydrate metabolism but it is also in charge of elimination of endogenous and exogenous toxic compounds. Thus, modifications of liver functions can have serious systemic repercussion.

References	Model	Administration mode	Dose and duration of treatment	Outcome
Wang *et al.*; 2007 [106]	mice	intragastric administration	5g/kg	hydropic degeneration and necrosis
Liang *et al.*; 2009 [143]	rat	intratracheal instillation	0,5-50mg/kg	oxidative stress
Guo *et al.*; 2009 [144]	mice	intraperitoneal injection	200 or 500mg/kg for 5 days	modifications of biochemical liver parameters
Chen *et al.*; 2009 [145]	mice	intraperitoneal injection	324-2592mg/kg	modification of biochemical liver parameters, fibrosis, hydropic degeneration, necrosis, apoptosis
Ma *et al.*; 2009 [146]	mice	intra-abdominal injection	5-150mg/kg for 14 consecutive days	modifications of serum parameters, inflammation, ischemia and vein congestion, apoptosis
Wu *et al.*; 2009 [128]	mice	cutaneous application	24mg of 5% TiO_2 formulation	oxidative stress
Wang *et al.*; 2009 [147]	rat	intra-articular injection	0,2-20mg/kg 4 days	biochemical liver parameters modifications, fatty degeneration, inflammatory cell infiltration
Wang *et al.*; 2010 [148]	rat	intratracheal instillation	0,8-20mg/kg	increased biochemical liver parameters, modifications of urine parameters
Duan *et al. ;* 2010 [149]	mice	intragastric administration	62,5-250mg/kg for 30 consecutive days	blurred hepatocytes, congested vessels, increased biochemical liver parameters
Cui *et al.*; 2010 [150]	mice	intragastric administration	5-50mg/kg for 60 consecutive days	fatty degeneration, necrosis, apoptosis, inflammation, increased transaminases
Bu *et al.*; 2010 [151]	rat	intragastric administration	0,16-1g/kg once a day for 14 consecutive days	modifications of serum and urine parameters
Tang *et al.*; 2011 [152]	rat	intratracheal instillation	0,8-20mg/kg	increased biochemical liver parameters, swollen hepatocytes, congested sinusoids, modification in serum parameters
Nemmar *et al.*; 2011 [153]	rat	intratracheal instillation	1,5mg/kg	increased transaminases, inflammatory cell infiltration
Cui *et al.*; 2011 [154]	mice	intragastric administration	5-50mg/kg for 60 consecutive days	hepatocyte apoptosis, oxydative stress and modification of gene expression involved in metabolism
Umbreit *et al.* ; 2012 [155]	mice	intravenous or subcutaneous injection	i.v.: 56 or 560 mg/kg s.c.: 560 or 5600 mg/kg	macrophages infiltration
Jeon *et al.;* 2013 [156]	mice	intraperitoneal injection	1.5mg/kg daily for 7 days	enhanced activities of liver damage-related enzymes, alterations of defense related enzymes, and histopathological changes
Hong *et al.*; 2014 [122]		Oral administration	2-10 mg/kg daily for 6 months	increases in liver indices, liver dysfunction, infiltration of inflammatory cells, and hepatocyte apoptosis or necrosis

Table 5: *In vivo* studies that investigated the adverse effects of TiO_2 NPs exposure on liver.

3.2.2. Cardiovascular toxicity

In recent years, toxicological as well as epidemiological studies have reported an association between airborne ultra-fine particles pollution and adverse cardiovascular effects [157, 158]. These observations raise concerns about impact of engineered NPs on the cardiovascular system. *In vivo* studies that investigated adverse effects of TiO_2 NPs on the cardiovascular system reported modification of cardiovascular parameter (such as heart rate and systolic blood pressure) and biochemical parameters relevant for heart function evaluation (Table 6). Interestingly, the cardiovascular system and the brain share common triggers and biochemical characteristics, including inflammation, oxidative stress, and hypoxia, an oxygen deficit caused by impaired blood flow. Adverse effect on the cardiovascular system can therefore be an early indication of potential impact on the brain.

References	Model	Administration mode	Dose and duration of treatment	Outcome
Wang *et al.*; 2007 [106]	mice	intragastric administration	5g/kg	increased cardiac injury biomarkers
Chen *et al.* ; 2009 [145]	mice	intraperitoneal injection	324-2592mg/kg	pulmonary thrombosis
Liu *et al.* ; 2009 [159]	mice	intra-abdominal injection	5-150mg/kg for 14 consecutive days	increased cardiac injury biomarkers
Bu *et al.*; 2010 [151]	rat	intragastric administration	0,16-1g/kg once a day for 14 consecutive days	increased cardiac injury biomarkers
Nurkiewicz *et al.* ; 2008 [160]	rat	Inhalation	1,5-20mg/m^3 for 120-720min	impaired spinotrapezious arteriolar endothelium
Nurkiewicz *et al.*; 2009 [161]	rat	Inhalation	1,5-16mg/m^3 for 240-720min	impaired spinotrapezious arteriolar endothelium
LeBlanc *et al.* ; 2009 [162]	rat	Inhalation	6mg/m^3 for 240min	decreased dilatory responsiveness of microvessels in the shoulder muscle and the heart
LeBlanc *et al.* ; 2010 [163]	rat	Inhalation	6mg/m^3 for 240min	impaired coronary arteriolar endothelium dilatation, oxidative stress
Nemmar *et al* ;. 2011 [153]	rat	intratracheal instillation	1,5mg/kg	increased heart rate and systolic blood pressure
Sha *et al* ;. 2013 [164]	rat	intraperitoneal injection	0,5mg/kg	decreased heart rate, pathological changes in heart tissues, increased cardiac injury biomarkers
Wang *et al.* ; 2013 [165]	rat	oral administration	10- 200 mg/kg	increased cardiac injury biomarkers
Savi *et al.* ; 2014 [166]	rat	Intratracheal administration	2mg/kg	Increased cardiac conduction velocity and tissues excitability
Kan *et al.* ; 2014 [167]	rat	Inhalation	6mg/m^3 for 4h	Increased heart rate and diastolic blood pressure
Chen *et al.* ; 2015 [168]	rat	oral administration	2-50 mg/kg for 30 or 90 days	increased cardiac injury biomarkers ; changes in heart rate and blood pressure, cardiac impairment and inflammatory response

Table 6: *In vivo* studies that investigated the adverse effect of TiO_2 NPs on the cardiovascular system.

3.2.3. Spleen toxicity and immune toxicity

Few *in vivo* studies reported adverse effects of TiO_2 NPs exposure on immune system. Evidence of systemic inflammation initiation after exposure was provided after intratracheal or intragastric administration [151, 153, 169]. The spleen is a peripheral lymphoid organs and a key organ of the immune response. Thus, accumulation of TiO_2 NPs, histopathological damage, morphological changes and alterations in immune cell number in spleen observed after exposure can lead to immunological toxicity (Table 7). Altogether, data from the literature suggest that TiO_2 NPs exercise either pro-inflammatory (inappropriate inflammatory response) or immunosuppressive effects (congestion and tissue damage in peripheral lymphoid organs; damage of immune cells activity). Data from *in vivo* and *in vitro* studies underline the ability of TiO_2 NPs to modulate immune system response [170].

References	Model	Administration mode	Dose and duration of treatment	Outcome
Nemmar *et al* ;. 2008 [169]	rat	intratracheal instillation	1,5mg/kg	modulation of blood parameters
Chen *et al* ;. 2009 [145]	mice	intraperitoneal injection	324-2592mg/kg	spleen lesions and neutrophil infiltration
Li *et al.* ; 2010 [171]	mice	intra-abdominal injection	5-150mg/kg for 14 consecutive days	spleen: increased oxidative stress, congestion, lymph nodule proliferation, apoptosis
Liang *et al.*; 2009 [143]	rat	intratracheal instillation	0,5-50mg/kg	oxidative stress
Duan *et al.* ; 2010 [149]	mice	intragastric administration	62,5-250mg/kg for 30 consecutive days	modulation of blood parameters, decreased immunological cells
Bu *et al.* ; 2010 [151]	rat	intragastric administration	0,16-1g/kg once a day for 14 consecutive days	modulation of blood parameters
Rossi *et al.* ; 2010 [63]	mice	Inhalation	10mg/m^3 2hr/day 3day/week for 4 weeks	inflammatory action in spleen
Nemmar *et al.*; 2011 [153]	rat	intratracheal instillation	1,5mg/kg	modulation of blood parameters
Moon *et al.* ; 2011 [172]	mice	intraperitoneal injection	once a day for 7 days	impact on spleen cells including immune cells
Wang *et al.*; 2011 [173]	mice	intragastric administration	5-150mg/kg for30 consecutives days	spleen congestion and lymph nodule proliferation, oxidative stress
Sang *et al.* ; 2012 [174]	mice	intragastric administration ;	2,5-10 mg/kg for 90 days	increases of spleen indices, immune dysfunction, macrophage infiltration, apoptosis, alterations in the expressions genes involved in immune/inflammatory responses, apoptosis, oxidative stress metabolic processes, ion transport, signal transduction, cell proliferation/division, cytoskeleton
Sang *et al.* ; 2013 [175]	mice	intragastric administration	2.5, 5 and 10 mg/kg for 90 days	congestion, white pulp rarely, disperative replication of white pulp and anemia of red pulp
fu *et al.* ; 2014 [176]	rat	intratracheal instillation	0.5, 4, and 32 mg/kg twice a week, for four consecutive weeks	congestion in spleen ; increase lymphocyte proliferation and enhanced natural killer cell activity
Sheng *et al* . ; 2014 [177]	mice	intragastric administration ;	2,5-10 mg/kg for 90 days	Alterations of gene expressions biomarkers of spleen toxicity

Table 7: *In vivo* studies: Adverse effects of TiO_2 NPs on the immune system and the spleen.

Part III: TiO_2 NPs in the central nervous system

The central nervous system (CNS) is certainly the most sensitive system and performs the most critical function in the organism. The brain only represents 2% of body weight but consumes 20% of the oxygen of the organism [13, 178, 179]. Indeed the brain operates in a pure aerobic manner, so it needs constant and considerable inputs of oxygen and glucose. Moreover, the neurons need a constant extra cellular environment. The blood brain barrier (BBB) is a functional barrier that isolates the brain parenchyma from the bloodstream and regulates brain homeostasis. Considering the sensibility and the key functions of BBB, it appears essential to evaluate the potential effects of environmental exposure such as NPs.

1. The blood brain barrier (BBB)

The first experimental evidence for the BBB existence dates back to 1885, when Paul Ehrlich observed that the IV injection of an aqueous dye (Evans blue) stained all organs except the brain and spinal cord. The theory of the existence of such a barrier was subsequently confirmed by Edwin Goldmann who in 1913 observed that the brain and spinal cord were stained in the case of a direct injection into the cerebrospinal fluid but remained intact upon IV injection. The BBB is described throughout the brain with the exception of cerebral-ventricular organs where the capillaries are fenestrated to allow the release and transport of hormones synthesized by the neurohypophysis. Thus highlighted, the BBB is a considerable exchange surface between blood and brain tissue.

1.1.Physiology of the cerebral vascularization

An arterial and venous system drains about 750 ml of blood per minute to ensure brain supplies. The Circle of Willis is located at the base of the brain (Figure 17). These cerebral arteries drain blood at the brain surface before entering the cortex in the Virchow-Robin space (Figure 18). They then branch out to form intracerebral arterioles and capillaries and define parenchymal brain microvaculature [180].

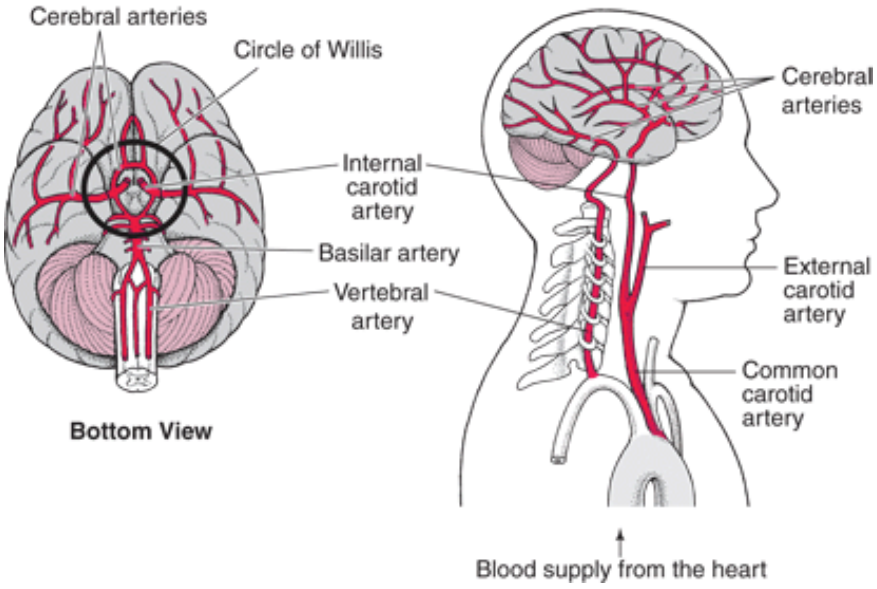

Figure 17: Brain vascularization (available at : http://www.joeniekrofoundation.com/wp-content/uploads/2014/08/NEU_supplying_brain_blood_stroke.gif)

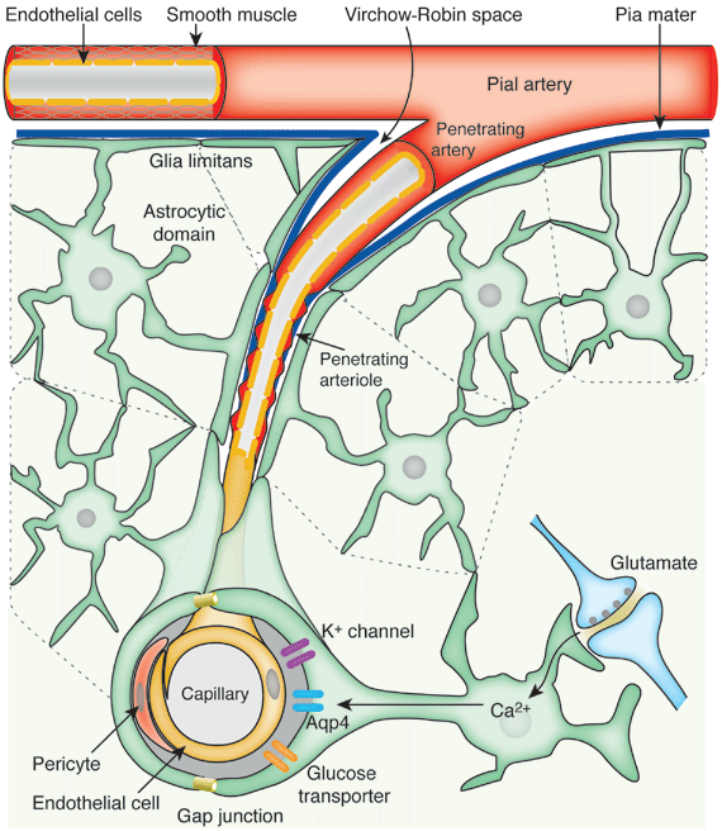

Figure 18: Schematic representation of the cerebral microvasculature at the Virchow-Robin space (from Iadecola *et al.* 2007) [181].

1.2.The neurovascular unit: structure and functions

The structure of the cerebral microvasculature is unique compared to other endothelia. Brain endothelial cells (BECs) and pericytes described further are based on a tick basal lamina which contains the extracellular matrix proteins (collagen IV, heparin sulfate proteoglycans, laminin, fibronectin) [182-184]. The basal lamina of brain endothelium is covered on the other side by astrocytic end feet. Astrocytes are then in intimate contact with microglia and neurons. This polarized structure forms the neurovascular unit (Figure 19). This system associating multiple cells from endothelial to neuronal cells enables proper brain homeostasis and function. The BBB is an essential part of the system providing both physical and functional protections in order to allow proper neurons activity.

The BBB is the cellular structure that separates the brain parenchyma from the bloodstream. Only less than 1% of brain areas is devoid of this structure [185]. This membrane is about 18 m^2 wide in the adult and has several functions [186]: 1) it constantly regulates the extracellular environment. Indeed, it is through it that flows of fluids and ions are regulated. 2) It insures the essential nutrients needs from the blood and allows the elimination of metabolic waste. Thus the BBB protects the brain from any fluctuation composition of the extracellular medium, which is essential to the smooth running of synaptic transmission between neurons. 3) This barrier also prevents the crossing of some toxic chemical or biological (bacteria and viruses) into the CNS.

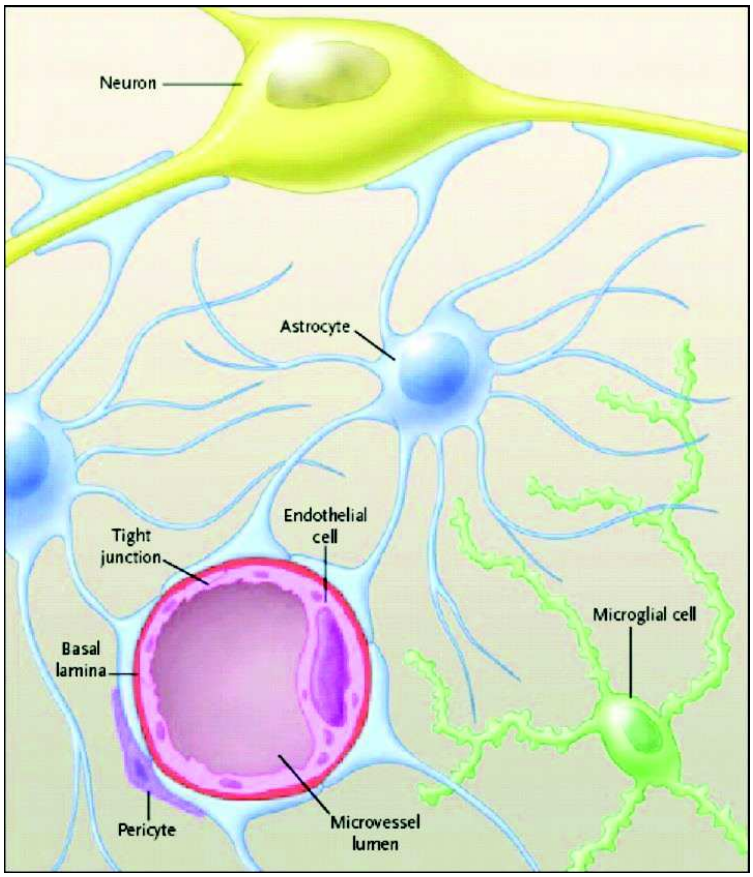

Figure 19: Schematic representation of the BBB and it different component cells (from Bushnell *et al.* 2006) [187].

1.2.1. A cooperation of multiple cell types

The BBB is composed of several cell types: brain endothelial cells (BECs), astrocytes, pericytes and microglial cells (Figure 19). Interactions between all constituents of the BBB are essential for barrier functions.

1.2.1.1.Astrocytes

Astrocytes are the most represented cell class in the BBB. They cover the BECs and pericytes with their extensions named astrocytic end feet. They cover approximately 98% of the cerebral vascular surface. On their other extremity, they are in close contact with neurons. Their particular shape allows them to create an interface between BECs and neurons. Thus they are involved in nutritive function for the neurons or the regulation function of the endothelium permeability. Indeed functions of astrocytes are multiple:

- Communication between neurons and endothelial cells;
- Metabolic support for neurons: a source of energy as glycogen and lactate export [188];
- Regulation of the neurons activities and uptake of neurotransmitter [189];
- Production of trophic factors;
- Regulation of ionic homeostasis;
- Brain tissue healing and regeneration;
- Regulation of the immune response in the CNS [190];
- Regulation the diameter of the cerebral microvasculature [191];
- Induction of characteristics of the BBB and protection of this barrier [184, 186, 192] .

1.2.1.2.Pericytes

Pericytes are located, evenly spaced, along the wall of the capillaries and share a common basal lamina with BECs. Thanks to their contracting ability, pericytes also named vascular smooth muscle cells or myofibroblasts, are involved in local blood flow regulation [193, 194]. These cells play a role in endothelial proliferation and angiogenesis by synthesizing growth factor and basal lamina components [195]. Moreover, they play a crucial role in inflammatory processes [184, 196]. Pericytes are also involved in cellular communication between all cell types constituting the BBB. Indeed, there are, for example junctions between pericytes and BECs allowing the direct exchange of ions and small molecules.

Generally speaking, pericytes allow the maintenance of the BBB structure [182] and have a critical role in the development, maturation and remodeling of blood vessels [197, 198].

1.2.1.3. Microvascular endothelial cells

BECs are the key cell type of the BBB. Unlike classic endothelial cells of peripheral vessels, they have a large cytosolic mitochondrial content, low pinocytosis activity and lack of fenestrations. On the contrary, the presence of protein junctions between neighboring cells form a physical barrier between the blood stream and the brain parenchyma. The monolayer of BECs is based on a thick basal lamina of 20 to 200 nanometers [199]. The basal lamina is composed of extracellular matrix proteins such as collagen IV, heparan sulphate proteoglycans, laminin, fibronectin or elastin [184]. The role of the basal lamina is to insure an anchorage for surrounding cells including endothelial cells.

The BECs are the first cells in contact with the molecules from the bloodstream. The penetration into the brain tissue of these molecules can then be done by transcellular or paracellular pathways.

1.3. A functional barrier

1.3.1. Physical barrier

The physical barrier is due to a very limited paracellular passage (between cells). This limitation is explained by the presence of tight junctions between neighboring BECs (Figure 21). Indeed, the protein junctions are in connection with actin cytoskeletal proteins to form a continuous membrane with very high electrical resistance (1500 to 2000 Ω / cm). These junctions are of three types: tight junctions, adherens junctions and gap junctions.

The attachment between cells and the extracellular matrix is provided by the adherens junctions. These junctions are mediated by homophilic interactions between membrane proteins: cadherins. Cadherins, which are expressed on the surface of the adjacent cells, have extracellular domains which interact together to form a homodimer. On the cytosolic side, cadherins are linked to the actin cytoskeleton via intermediate proteins: catenins and form the primary seal of junctions [200]. Adherens junctions form a continuous belt around the cells thereby maintaining the contiguous cells and strengthening the tight junctions [201].

Tight junctions form a complex protein network at luminal BECs side. The latter are formed of three major proteins: claudins, occludins and molecules of adherens junctions which interact with accessory proteins (including zona occludens or ZO and cingulins). The accessory proteins too are themselves in association with the actin cytoskeleton. These tight junctions make countering the paracellular passage of molecules possible.

Finally, gap junctions mediate the passage of chemical or electrical signals between cells' partners.

This organization of junctions maintains cell polarity by stopping the spread of membrane molecules and limits the penetration of xenobiotic to the brain parenchyma. Indeed, most of the molecular traffic is forced to take a transcellular route.

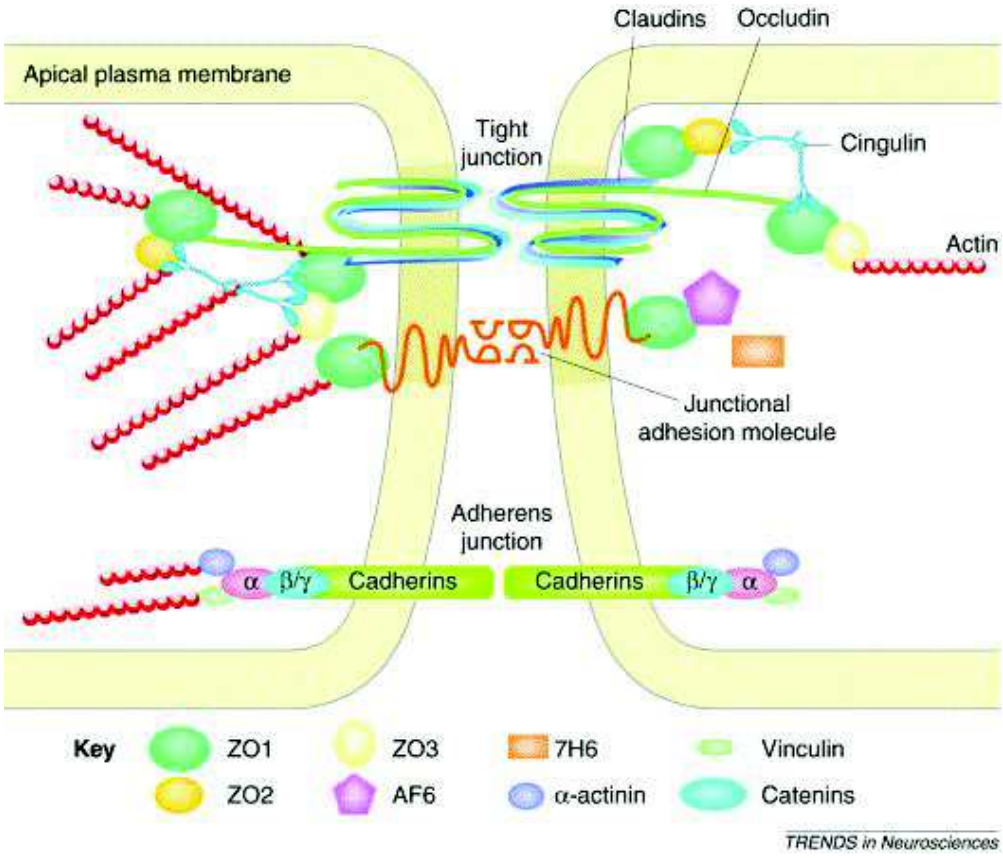

Figure 20: Tight junctions and associated proteins between the BBB endothelial cells (From Huber *et al*. 2001) [202].

These junctions are made permeable, for example in an inflammatory environment to allow the immune cells to enter [203]. Indeed, The BBB integrity is affected by pro-inflammatory mediators (cytokines and chemokines). These mediators can't initiate changes in permeability and adhesions properties of BECs that allow immune cells to infiltrate the CNS. The BEC and the close microglials cells also modulate the immune response in the brain by releasing pro-inflammatory mediators. Inflammation within the CNS and BBB permeability alterations has been associated with chronic neurodegenerative disease including Alzheimer's diseases, multiple sclerosis and Parkinson's disease [204-209]. Many of these changes have been linked to alterations in BBB tight junctions.

The BBB plays a crucial role in maintaining homeostasis by regulating the ion balance of the brain. In fact, brain edema formation after stroke has been linked to the inability of the BBB to maintain necessary ion gradient. Furthermore, alterations in BBB ion homeostasis have been linked with epilepsy [204, 205, 210].

1.3.2. Transport and detoxification functions

The different transport mechanisms to cross the BBB are summarized in figure 21:

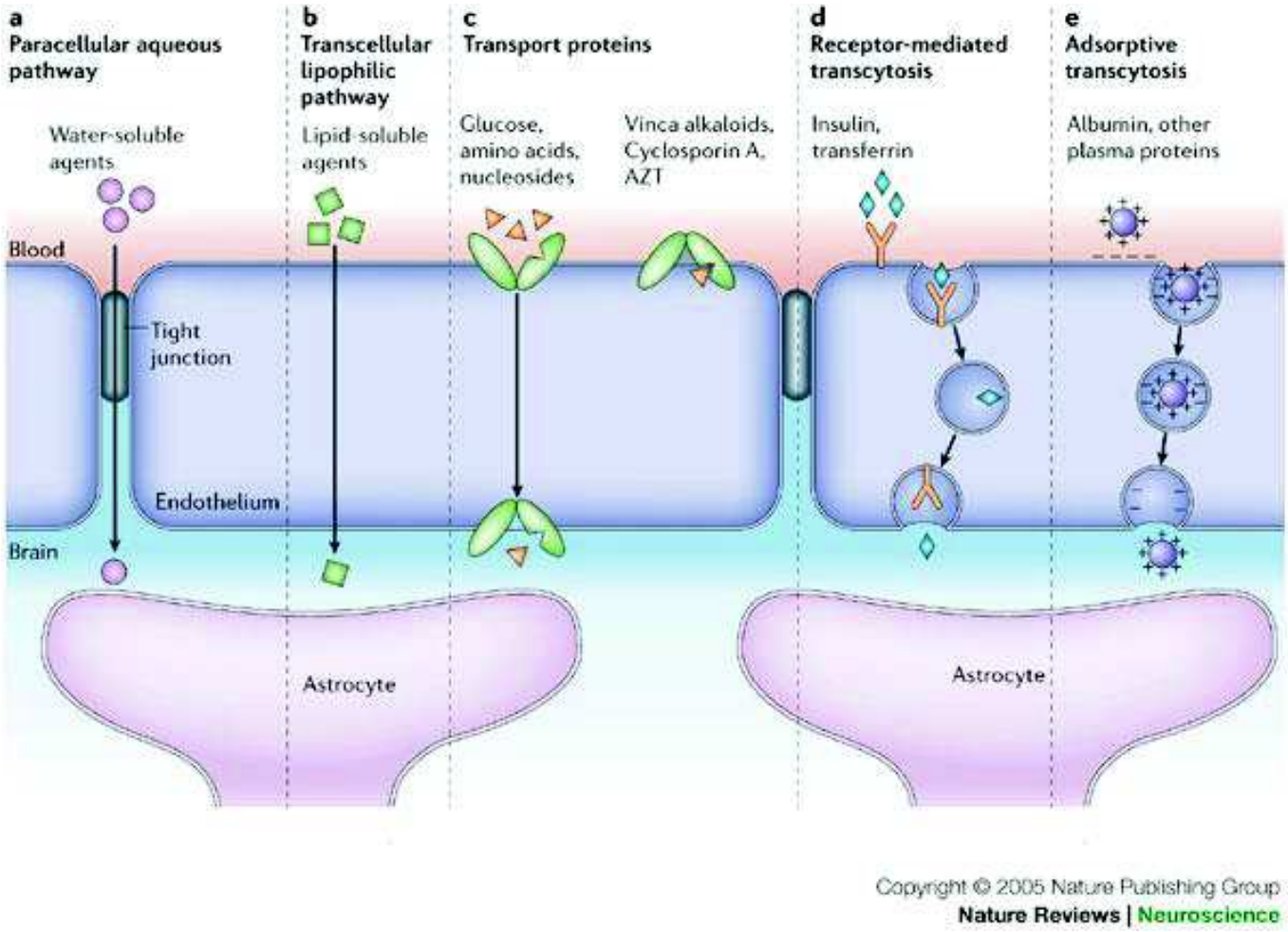

Figure 21: Schematic representation of the different transport at the BBB (From Abbott *et al*., 2006) [192].

Compounds can cross through the cells by several mechanisms:

- passive diffusion for small lipophilic compounds (e.g.: oxygen, ethanol, CO_2 ...)
- passage *via* specific transporters (e.g.: Glut 1 for glucose)
- trancytose mechanisms by adsorption or *via* receptors (eg: several hormones, such as insulin and leptin, use receptor-mediated endocytosis).

In the case of passive diffusion for small lipophilic compounds (e.g.: ethanol or drugs such as barbiturates) and small gaseous molecules (O_2 and CO_2), the transition is made in accordance with the concentration gradient.

At the abluminal and luminal membranes, various transport systems regulate the transcellular traffic. All those polarized transports provide a selective 'transport barrier' in order

to meet the high nutrient and energy demand of the brain and exclude potentially harmful compounds. Indeed, there are several types of transporters through the BBB:

1) Carriers of essential molecules (nutrients, amino acids ...) allowing optimal brain function,

2) Carriers which limit the entry of xenobiotics in the brain. Among them, ABC transporters (Adenosine triphosphate Binding Cassette) play a critical role in preventing neurotoxic molecules from entering the brain. The Solute Carrier family (SLC) is the other important carrier group controlling uptakes and effluxes of nutrients, metabolites and toxins. Altogether, carriers and transporters of the BBB are responsible for the multidrug resistance (MDR) phenomenon. Indeed among xenobiotics whose brain access is limited by ABC and SLC efflux transporters activity, are a large number of CNS drugs therapy.

During various disease states, alterations in the levels or distribution of transporters can be seen. For example, obesity has been linked to an impaired transport of leptin across the BBB [211] or neurodegeneration progression with altered ABC transporters function [212, 213].

1.3.2.1. ABC transporters

ABC transporters are localized at luminal and abluminal membranes of the BECs. They prevent entry of toxic and therapeutic substances in the CNS by active transport process. They bind and hydrolyze ATP to translocate lipid-soluble molecules across brain endothelial cells plasma membrane. There are 48 known ABC transporters present in humans, which are classified into seven families. At the BBB level two efflux transporters have a great significance: The P-glycoprotein (P-gp or ABCB1) and the Breast Cancer Resistance Protein (BCRP or ABCG2). Dauchy *et al.* found that the P-gp and the BCRP were the two main ABC transporters expressed in BECs based on mRNA expressions and protein levels [214]. Among C subfamily of ABC proteins are Multi-drug Resistance related Proteins (MRPs). Some of these efflux pumps have also been shown to contribute to resistance to many CNS drugs.

The P-gp is probably the most studied transporter in the CNS, it is also called ABCB1 or MRP1. P-gp is a functional monomer with two transmembrane domains and two nucleotide-binding domains. It is expressed in multiple cell types in the CNS: predominantly in BECs but also in astrocytes and neurons. The P-gp is localized at the luminal side of BECs and has an extremely wide range of substrates. Among P-gp substrates, there are many therapeutics agents (opioids, antibiotics, immunosuppressant…). P-gp also mediates efflux of endogen compound such as aggregated protein involved in neurodegenerative disorders [213] .

The BCRP is also localized at the luminal membrane of the BECs. Like P-gp, many therapeutic agents are among BCRP substrates (antihistamines and anticancer drugs...).

ABC transporters expressions or activities are regulated in several conditions: oxidative and inflammatory stress environment, pharmacotherapy or toxicant exposure, disease [215-217]. Compromised BBB transport functions is a common feature observed in many CNS diseases.

Several evidences associate this alteration with ABC transporters functions [218]. Changes in ABC transporters observed in CNS diseases context are summarized in Table 8.

Disease	P-gp	BCRP	MRP1	MRP2
Alzheimer's disease	↓	↔	↓	?
Amyotrophic lateral sclerosis	↑	↑	↔	↔
Brain tumors	↓	?	↑	↔
Creutzfeldt-Jakob disease	↓	?	?	?
Depression	↓	?	?	?
Epilepsy	↑	↑	↑	↑
HIV-encephalitis	↔	↑	↑	?
Multiple sclerosis	↓	↔	↔	↔
Parkinson's disease	↓	?	?	?
Schizophrenia	↓	?	?	?
Stroke and ischemic brain injuries	↑	↑	↑	?

Table 8: Summary of changes in ABC efflux transporters activity in neurological disorders (from Qosa *et al.*; 2015) [218].

Regulation of the expression and activity of ABC efflux transporters is complex and involves pre- and/or post-transcriptional modifications. Most of these signaling pathways in brain endothelial cells are activated by surface or nuclear receptors. Examples of signaling pathway involved in inflammatory stress environment are represented in Figure 22. As ABC transporters play a critical role in BBB detoxification function, changes in transporters expression or activity could elicit alteration of the brain protection mechanisms against neurotoxic compounds.

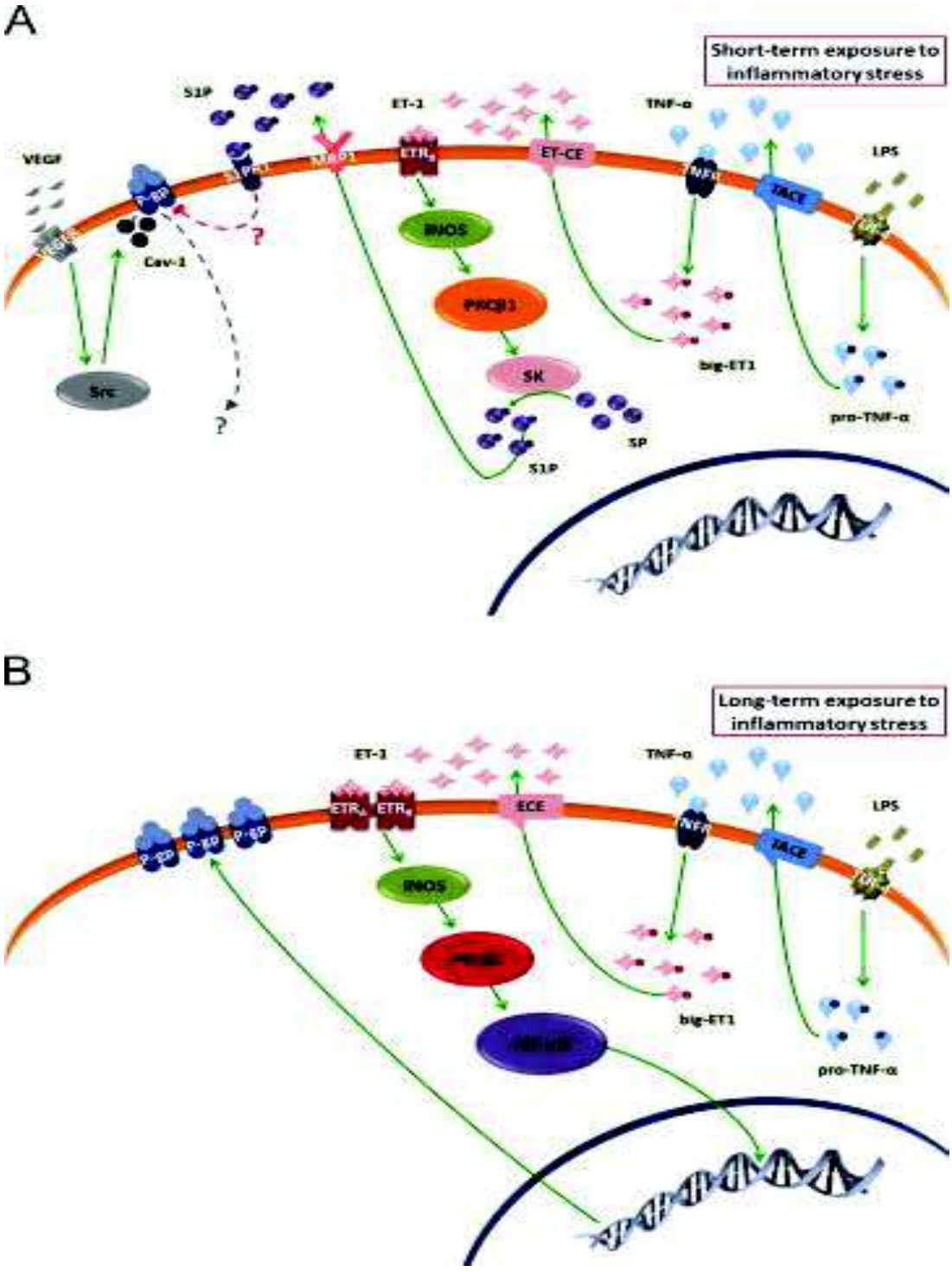

Figure 22: Regulation of ABC efflux transporters activity and expression at the BBB level in inflammatory environment. The P-gp activity is rapidly deregulated after activation of PKCβ1 and Src kinase by ET-1 and VEGF. In prolonged inflammatory context, P-gp is regulated by PKCβ2 and NF-κB pathway. In both pathways, TNF-α or LPS could stimulate ET-1 release. BCRP and MRP1 activity and expression did not change upon short-term exposure to inflammatory stress, only BCRP expression decreased after long-term exposure (from Qosa *et al.*; 2015) [218].

1.3.2.2. SLC transporters

SLC transporters are among a large superfamily including about 300 members organized in 52 families that transport a wide variety of substrates and nutrients into and out of the brain parenchyma. Among this family, facilitative transporters can be found, as well as secondary active transporters, ion channels, primary active transporters and efflux transporters. They are located at both luminal and/or abluminal membranes of BECs. They can be functional as either monomers, homo- or hetero-oligomers.

Some of them, such as Glut1 encoded by SLC2A1 gene, play a critical role in brain supplies. Glut1 is responsible for glucose transport across the BBB, and its deficiency causes low level of glucose in cerebrospinal fluid which may manifest itself in convulsions. Glucose transport operated by Glut1 does not require energy and therefore occurs according to the concentration gradient. Glut1 also impacts the BBB physiology directly. Indeed, Slc2a1+/- mice have been found to have decreased brain glucose uptake but also increased BBB permeability due to lower TJ protein levels [219]. It has been shown that Glut1 and Glut3 are also implicated in neurodegenerative disorders [2]. Reduced glucose transporters in patients with AD leads to impairment of energy metabolism and correlate with neurodegeneration in these patients [220-222]. For example, altered glucose transport leading to glucose hypo-metabolism is associated with tau hyper-phosphorylation and/or neurofibrillary degeneration.

2. Entry pathway to the CNS

In case of inhaled NPs, two separated entry pathway have been hypothesized.

2.1.Translocation along the olfactory nerve

The first pathway concerned only inhaled NPs which at the epithelium of the upper airway level can be translocated by sensitive nerve endings to reach the brain. The human nasal cavity represents an absorptive surface of 160 cm^2 [223] but its primary role is filtering, humidifying and warming inhaled air. First NPs need to cross nasal epithelial barriers. Like the BBB, the nasal epithelium is maintained by tight junctions between adjacent cells but the tightness of this barrier is much lower. Indeed, the nasal barrier which has relatively permeable properties is supposed to be close to the intestinal epithelium. In the case of TiO_2 NPs, several *in vitro* and *in vivo* studies have proved their ability to cross a barrier such as the intestinal barrier (see chapter I part 2).

After nasal administration, the mechanism of translocation from the nasal mucosa to the brain is not fully understood. Two main routes of entry into the brain have been highlighted: 1) the olfactory pathway: the transport occurs along olfactory nerve to the olfactory bulb or 2) the trigeminal pathway: the transport occurs along the trigeminal nerve to the brainstem. These paths connect the nasal mucosa to two entry points from where delivered NPs can disperse to

other CNS areas (Figure 23). The transport along olfactory or trigeminal nerve may occur *via* intracellular or extracellular pathways. Moreover particles may cross the olfactory epithelial barrier by paracellular or transcellular transport to reach the lamina propria. This region is rich in blood and lymphatic vessels. Thus NPs may enter the general blood circulation or reach the cervical lymph nodes of the neck.

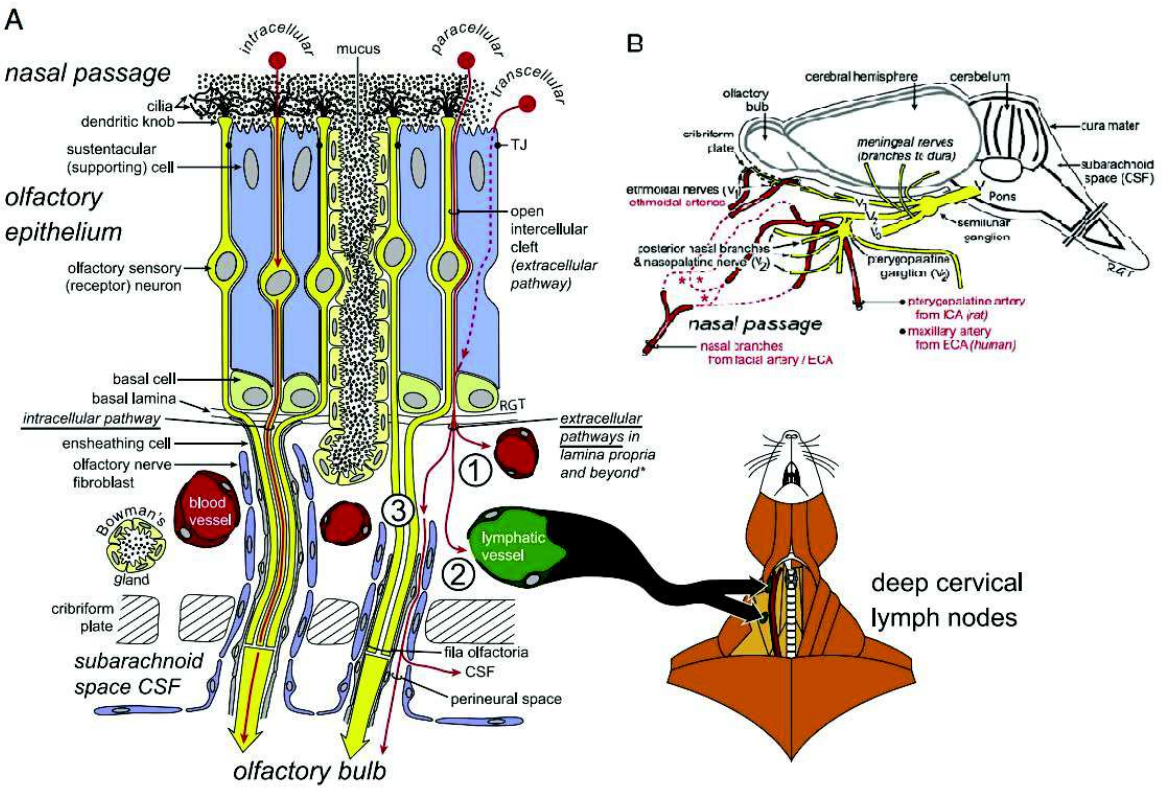

Figure 23: Trigeminal innervation and vasculature of the nasal respiratory region (from Lochhead *et al.*; 2012) [224]

Wang *et al.* have reported translocation of Ti in the olfactory bulb, hippocampus, cerebral cortex, and the cerebellum after nasal instillation in a mouse model (500 µg/mouse; TiO_2 80 nm rutile; daily for 30 days) [225]. The same research group have reported similar findings in a second study (intranasal instillation; 500 µg/mouse; TiO_2 80 nm rutile; daily for 30 days) [226]. Ze *et al.* have also observed translocated Ti in the olfactory bulb of mice after nasal exposure to TiO_2 NPs from 2.5 to 10 mg/kg dose for 90 consecutive days [227]. All these studies suggest a translocation of TiO_2 NPs from nasal mucosa to brain *via* nerve transport. These studies used the intranasal exposure route with high dose rate delivery, which may increase NP translocation *via* the olfactory nerve pathway. The translocation of NPs after inhalation, a more representative mode of exposure has been shown by Oberdörster *et al.* They demonstrated that 6h all-body exposure to ultra-fine ^{13}C NPs can lead to accumulation in the olfactory bulb in rats [228].

Translocation of gold NPs were also observed in rodents [90] and 15-20 nm iridium NPs could be detected in the brain up to 6 months after inhalation exposure [93, 229].

Using this pathway, the NPs bypass the BBB barrier but impact on its physiology can still occur. The NPs are directly distributed to the brain and can interact with glial cells which are involved in structuring and maintaining the barrier properties.

2.2.Translocation across the BBB

The second entry pathway concerns all administration routes that lead to a distribution of NPs through blood circulation. In the case of blood distribution, NPs need to cross the BBB to gain access to the brain parenchyma. This pathway has also been a source of attention in the medical field for new approaches for drug delivery to the CNS. It has been demonstrated that with changes in particular surfaces of NPs, transport across the BBB is facilitated. These NPs can serve as vectors through this barrier for the delivery of therapeutic molecules. However, data concerning the interactions of inorganic NPs at the BBB are scarce.

2.2.1. *In vitro* data

In a previous study, Brun *et al.* determined by TEM (transmission electron microscopy) imaging the localization of TiO_2 NPs in the *in vitro* BBB model after exposure [1]. After 4 hr of exposure mimicking a blood distribution of nanomaterials, a proportion of TiO_2 NPs was observed in large clusters. After a chronic exposure (5 consecutive days), the TiO_2 NPs were packed in cytoplasmic vacuoles. In all three exposure conditions tested, NPs were detected in a far lower proportion in glial cells suggesting that NPs had the ability to cross the physical barrier of endothelial cells.

In a study on human cerebral endothelial cells (HUVEC), internalization of Aeroxide® P25 TiO_2 NPs was observed in small or large endosomes in the cytoplasm or in lysosomes [230]. These observations confirm the uptake of TiO_2 NPs by BECs but are insufficient to conclude about translocation across the barrier.

2.2.2. *In vivo* data

The passage across the BBB from multiple exposure pathways has been demonstrated *in vivo* (Table 9). However translocation of TiO_2 NPs to the brain remains contradictory. Indeed several *in vivo* studies failed to detect titanium in the brain: two studies after IV administration to mice did not detect titanium in the brain [231, 232]. After repeated oral administration of TiO_2 NPs for 13 weeks, Gereats *et al.* also demonstrated insignificant Ti brain content [121]. However in this study, they detected titanium in the brain of exposed animal by IV injection. It is not possible to draw clear conclusions about TiO_2 NPs CNS distribution from those observations.

Undoubtedly, the translocation to the CNS is influenced by several parameters including administration route, size, dosage…

nanoparticles	models	Outcomes	references
TiO_2 25 and 80 nm rutile TiO_2 155 nm anatase	Single gavage to mice. 5 g / kg Dosage after 2 weeks	Increased concentrations of Ti in the brain	Wang *et al.*; 2007 [106]
TiO_2 80 nm rutile	30 days nasal instillation to female mice, 50mg/kg	TiO_2 in the olfactory bulb, hippocampus, cerebral cortex and the cerebellum	Wang *et al.*; 2008 [233]
TiO_2 5 nm anatase	14 days intra peritoneal injections ; 5 ; 10 ; 50 ; 100 and 150mg/kg	Increased concentrations of TiO_2 proportional to the doses	Liu *et al.*; 2009 [159]
TiO_2 25-70 nm anatase	subcutaneous injection in pregnant mice ; 0.1g/animal	TiO_2 in offspring's brain	Takeda *et al.*; 2009[234]
TiO_2 5 nm anatase	14 days intra-abdominal injection to mice; 5 ; 10 ; 50 ; 100 and 150mg/kg	Increased concentrations of TiO_2 proportional to the doses	Ma *et al.*; 2009 [146]
TiO_2 anatase 4 and 10 nm ; rutile 25, 60 and 90 nm, and Degussa P25 21 nm, anatase/rutile	60 days dermal exposure in hairless mice ; 24g of 5% TiO_2 formulation	Increased concentrations of TiO_2 Degussa P25 in the brain	Wu *et al.*; 2009 [128]
TiO_2 5nm anatase	60 days intragastric administration to mice; 5; 10; 50mg/kg/day	Increased concentrations of TiO_2 proportional to the doses	Hu *et al.*; 2010[235]
TiO_2 Degussa P25 21 nm, anatase/rutile	Intraperitoneal injection to pre exposed to LPS male mice; 40mg/kg	Promotion an exaggeration neuroinflammatory responses by enhancing microglial activation in the pre-inflamed brain	Shin *et al.;* 2010 [236]
3 types of Nano TiO_2 rutile	30 days nasal instillation to female mice, 500 g / animal	TiO_2 in cerebral cortex , hyppocampus, cerebellum and striatum	Zhang *et al.;* 2011[226]
TiO_2 5 nm anatase	90 days intransal administration to mice; 2,5; 5 and 10 mg/kg	Increased concentrations of TiO_2 proportional to the doses	Ze *et al.;* 2013 [237]
TiO_2 21 nm	Oral administration, 13 weeks; 260.4 to 1041.5mg/kg/day	Increase Ti brain content	Cho *et al.*; 2013 [120]
TiO_2 10 ; 20 and 200 nm	inhalation	Increase Ti brain content	Liu *et al.*; 2013
TiO_2 with different size-range and crystal form	Intravenous injection or oral administration, single or 5 administrations of 2.3 mg/rat	Detection of small amount in brain	Gereats *et al.*; 2014 [121]

Table 9: Distribution of TiO_2 NPs to the central nervous system.

Overall, much of the available data are inconsistent and sometimes contradictory, since the mechanisms of cell penetration and translocation are still poorly understood. In this respect, it is acknowledged depending on a large number of physical and chemical characteristics of a

given NP (chemical composition, size, surface area…), results may significantly differ and that in most studies, a full characterization is not available. Moreover, there are controversial data on NPs translocation to the brain *via* olfactory nerves.

3. Impact on BBB physiology

In vitro study using HUVEC by Kenzaoui *et al.* has highlighted significant cytotoxicity, reactive oxygen species production, DNA damage and autophagy induction [230]. Several other studies are available concerning other inorganic NPs. For example, *in vitro* BBB model with exposition to silver NPs showed the passage of these NPs by transcytosis across the endothelial cells monolayer and accumulation within cells [238]. Induction of inflammation in brain microcapillaries were also observed after exposure to BECs to gold, silver and copper NPs [239-241]. On the other hand, Chen *et al.* reported a decrease viability of endothelial cells, alteration of mitochondrial function, oxidative stress and impaired proteins junction after exposure to aluminum oxide NPs [242].
Moreover, previous *in vitro* laboratory results suggest that TiO_2 NPs could be responsible for a dysfunction of the BBB [1]. Thus, *in vitro* observations underscore the importance for evaluation of the impact of TiO_2 NPs exposure on BBB functions.
Nowadays, despite evidence of TiO_2 NPs ability to cross the BBB, studies on the *in vivo* impact of NPs on the BBB physiology are scarce.

3.1. Integrity and transport functions

In the BBB model, the permeability for sucrose, a radiolabeled marker was dramatically increased after 4 h of exposure in the apical pole to 100 µg/ml of TiO_2 NPs. The increase of sucrose permeability suggested BBB disruption. 24 h or 5 consecutive days exposure also led to the disruption in the BBB integrity. The decrease in expression of structural components such as occludins, claudin 5 or zonula occludens 1 (ZO1) underscored this alteration of BBB permeability.
Among the altered transport activities, the decrease of P-gp activity of BECs, an efflux pump involved in the detoxification function of the barrier was noticed. These changes were also observed upon exposure of glial cells (in the exposure compartment mimics cerebral paremchyma), whereas BECs were not contacted with the NPs. This suggests a close communication between the two cell types that can influence the functionality of the barrier. At mRNA level, expression of BCRP and other multi-drug resistant proteins (MRP) also decrease revealing an alteration of detoxification function of the BBB. Down regulation in mRNA expressions of other carriers among SLC family were also noticed. Indeed SLC2A1 coding for Glut1 the glucose transporter was dowregulated suggesting altered glucose metabolism. As glucose hypo-metabolism being associated with tau hyper-phosphorylation and/or neurofibrillary degeneration in AD patients, it may promote neurodegeneration in the brain. These permeability changes suggest a decreased detoxification capacity of the barrier followed

by a loss of its integrity. These two phenomena can lead to an accumulation of neurotoxic compounds in the brain and promote neurotoxicity. However, the *in vivo* relevance of these facts remains to be established.

3.2. Neuro-vascular inflammation.

In Brun *et al.* study, the inflammatory profile was also determined. Up-regulations of various cytokines, chemokines and adhesion molecules in the *in vitro* BBB model suggested a severe inflammatory burst at the endothelial and glial cells levels. This *in vitro* observation is in accordance with *in vivo* experiments when animals were exposed intranasaly or by intraperitoneal injection (Table 11).

Induction of neurovascular inflammation has been linked to changes in the permeability of the BBB [243-245] and carrier's activity [216, 246]. Thus, neuro-vascular inflammation may be a critical phenomenon associated with BBB dysregulation. Furthermore, BBB integrity disruption and neurovascular inflammation are common characteristics of CNS diseases including neurodegenerative diseases [247]. Concerns about potential implication in neuro degeneration process, particularly in elderly vulnerable population, can be raised.

4. Neuro-toxicity liability after TiO_2 NPs exposure

4.1. *In vitro* data

In vitro studies about toxicity of TiO_2 NPs on neuronal or glial cells are summarized in Table 10: Cytotoxicity, morphological changes, induction of inflammation and / or oxidative stress are common outcomes that have been highlighted in different *in vitro* models.

4.2. *In vivo* data

Several *in vivo* studies highlighted CNS dysfunctions after exposure to TiO_2 NPs. Outcomes of *in vivo* studies focusing on brain consequences of TiO_2 NPs exposure are summarize in Table 11. A clear evaluation of TiO_2 NPs exposure impact on the CNS is not yet draw because of differences in physiochemical properties of particles, dose, route of administration, animal models or duration of exposure. Despite these discrepancies, it seems clear that TiO_2 NPs can induce neurotoxic effect in the brain. In accordance with *in vitro* data, oxidative stress and inflammatory factors appear to be key response mediators. Histopathological changes such as alteration in neuronal structure, necrosis or inflammatory infiltration have been observed. In term of biological parameters, studies highlighted disturbance of neurotransmitters levels, enzymes activities or trace metal elements in the brain.

Impaired neurobehavioral performance and spatial recognition memory appear as consequences of these cerebral functions modulations.

Several studies have demonstrated the ability of TiO_2 NPs to cross the placenta barrier. The vulnerable fetal brain appears as a target for TiO_2 NPs toxicity. Indeed, alteration of fetus brain development, level of neuro-transmitters as well as oxidative stress have been noted. Postnatal behavioral test also suggest impairments in the brain of offspring when mothers were exposed during pregnancy [234, 248-250].

Based on available literature, there is sufficient evidence underlying potential TiO_2 NPs neurotoxicity. However, before drawing firm conclusions on the TiO_2 NPs neuro-toxicity, distribution to the CNS must be documented. It will be necessary to consider dose parameters, dispersion, route of administration and interaction with other physiological barriers. More generally, data under more realistic exposure condition are needed for risk assessment.

References	Type of NPs	*In vitro* model	Concentration/ dose	Duration of treatment	Outcomes
Long *et al.*; 2006[251]	TiO_2 aeroxide P25	murine BV2 microglia	2,5-120 ppm	1-6 and 18 h	- ROS release - internalization of small clusters - disrupted and swollen mitochondrial lying
Long *et al.*; 2007 [252]	TiO_2 aeroxide P25	murine BV2 microglia Rat; N27 mesencephalic nerons; primary cultures of embryonic striatum	2,5-120 mg/kg	6, 24, 48 or 72 h	- ROS release - apoptosis induction in embryonic stiatum cells - increase ATP in N27 - up regulation of genes involved in apoptosis, death receptor families, calcium signaling, inflammation, cell cycling and oxidative stress - internalization in BV2 and N27 cells
Lai *et al.*; 2008 [253]	anatase <25nm	U87 astrocytoma	0,1-100 µg/ml	up to 72 h	- reduction of cell viability - increase apoptotic cells - cellular morphology changes
Li *et al.*; 2009 [254]	commercial TiO_2 NPs	murine microglia N9 cells	4-125 µg/ml	24 h	- reduction of cell viability - increase apoptotic cells - cellular morphology changes
Liu *et al.*; 2010 [255]	rutile TiO_2 coated by SiO_2; 80-100 nm	Mouse neural stem cells line C17.2	50-250 µg/ml	12, 24, 36, 48, 60, 72 h or 7 days	- internalization in cytoplasm - inhibition of cell proliferation - cell differentiation alteration
Liu *et al.*; 2010 [256]	TiO_2 aeroxide P25	Rat PC12 cells	1-100 µg/ml	6, 12, 24 and 72 h	- reduction of cell viability - increase apoptotic cells - ROS release
Wu *et al.*; 2010 [257]	anatase and rutile; 20 nm	Rat PC12 cells	25-200 µg/ml	24 h	- cytotoxicity - oxidative stress - cell cycle disruption - triggering JNK and p53 mediated signaling pathway
Shin *et al.*; 2010 [236]	TiO_2 aeroxide P25	murine BV2 microglia	25-200 µg/ml	24 h	- enhanced TNFα production -increase NK-κB binding activity
Xue *et al.*; 2012 [258]	20 nm	primary microglial; rat PC12 cells	0,25 and 0,5 mg/ml	24 h and 48 h	- cytotoxicity in PC12 cells after incubation with NPs treated microglia supernatant - microglial activation - release of pro-inflammatory factors
Marquez-Ramirez *et al.*; 2012 [259]	anatase; 40-200 nm	human U373; Rat C6 astrocytoma lines	0-40 mg/cm^2	24, 48 and 96 h	- apoptosis - decrease cell proliferation - morphology and cytoskeleton changes
Valdiglesias *et al.*; 2013 [260]	anatase and rutile; 25 nm	human SHSY5Y neuronal cells	20-150 µg/ml	3, 6, and 24 h	- cell cycle changes - increase apoptotic cells - genotoxicity
Huerta-Garcia *et al.*; 2014 [261]	50 nm	human U373;Rat C6 astrocytoma lines	20 mg/cm^2	2, 4, 6 and 24 h	- oxidative stress - mitochondrial damages - lipid peroxidation
Fujioka *et al.;* 2014 [262]	anatase; 80 nm	Human neuronal stem cells	0,01 -1 mg/ml	7 days	- morphological changes - cell differentiation alteration
Sheng *et al.*; 2015 [263]	anatase; 5 nm	primary cultures hippocampal neurons	5-30 µg/ml	24 h	- decrease cell viability - altered cell ultra-structures - apoptotic rate elevated and disturbance in apoptotic cytokines - elevated cytoplasmic calcium and LDH activity

Table 10: *In vitro* investigation on TiO_2 NPs neuro-toxicity (adapted from Iavicoli *et al.*, 2011; Song *et al.*, 2015 and Czajka *et al.*, 2015) [11, 13, 179]

References	Type of NPs	Model	Administration mode	Dose and duration of treatment	Outcomes
Wang *et al.*; 2007 [106]	TiO_2 25, 80, 155 nm	CD-1 mice	oral	5mg/kg; single dose	- modulation of neurotransmitters levels
Wang *et al.*; 2008 [233]	Rutile TiO_2 80 nm; Anatase TiO_2 155 nm	CD-1 mice	intranasally	500µg; 30 days	- modulation of neurotransmitters levels - oxidative stress
Wang *et al.*; 2008b [225]	Rutile TiO_2 80 nm; Anatase TiO_2 155 nm	CD-1 mice	intranasally	500µg; 30 days	- oxidative stress - morphological changes in hyppocampal neurons - inflammatory response
Shimizu *et al.* 2009 [248]	Anatase TiO_2 25-70 nm	pregnant ICR mice	subcutaneous injection	0,1µg; gestational day 6, 9, 12 and 15	- offsprings: increased gene expressions involved in cell death, oxidative stress, brain development, apoptosis and neurotrnasmitters
Takeda *et al.*; 2009 [234]	Anatase TiO_2 25-70 nm	pregnant Slc:ICR mice	subcutaneous injection	0,1mg; 3, 7, 10 and 14 day postcoitum	- apoptosis
Ma *et al.*; 2010 [264]	Anatase TiO_2 5nm bulk TiO_2 10-15 nm	CD-1 mice	abdominal cavity injection	5-150mg/kg; 14 days	- oxidative stress - inflammatory cells and filamentous shaped neurons
Li *et al.*; 2010 [265]	Anatase TiO_2 3nm	Kunming mice	intra tracheal instillation	13,2mg/kg; once per weeks for 4 weeks	- oxidative stress - inflammatory infiltration and necrosis
Shin *et al.*; 2010 [236]	Rutile TiO_2 ; TiO_2 P25	C57BL/6 mice	intraperitoneal injection	40 mg/kg; single dose	- microglia activation and inflammatory response - oxidative stress
Hougaard *et al.*; 2010 [266]	TiO_2 21 nm	mice	inhalation	42mg/m^3; 1h/day on gestional days 8 to 18	- offsprings: neurobehavioral alterations
Hu *et al.*; 2010 [235]	Anatase TiO_2	CD-1 mice	intragastric	5-50mg/kg; 60 days	- modulation of neurotransmitters levels - modulation in enzymes activity - spacial recognition memory impairment - disturbance of trace elements homeostasis
Takahashi *et al.*; 2010 [249]	Anatase TiO_2 25-70 nm	pregnant Slc:ICR mice	subcutaneous injection	0,1µg; gestational day 6, 9, 12, 15 and 18	- modulation of neurotransmitters levels
Hu *et al.*; 2011 [267]	Anatase TiO_2 6,5 nm	CD-1 mice	intragastric	5-50mg/kg; 60 days	- hippocampal apoptosis - spacial recognition memory impairment - oxidative stress
Gao *et al.*; 2011 [268]	TiO_2 >25 nm	rats	oral exposure of mothers	100mg/kg; from prenatal day 21 to post natal day 2 or form post natal day 2 to 21	- offsprings: alteration of synaptic plasticity in hyppocampus
Zhang *et al.*; 2011 [226]	TiO_2 10-50 nm	mice	intranasally	500µg; 30 days	- neurons morphological changes - disturbance in neurotransmitter levels

Table 11: *In vivo* investigation on TiO_2 NPs neuro-toxicity (adapted from Iavicoli *et al.*, 2012; Song *et al.*, 2015 and Czajka *et al.*, 2015) [12, 13, 179]

References	Type of NPs	Model	Administration mode	Dose and duration of treatment	Outcomes
Ze *et al.*; 2013 [269]	Anatase TiO_2 5-6 nm	CD-1 mice	intranasally	2,5-10mg/kg; 90 days	- hemorrage - oxidative stress - activation of P38-Nrf-2 pathway
Cui *et al.*; 2014 [270]	Anatase TiO_2 50nm	Sprague-Dawley rats	subcutaneous injection	500µl; gestational day 6, 9, 12, 15 and 18	- offsprins: oxidative stress and enhanced the depressive-like behaviors
Ze *et al.*; 2014a [271]	Anatase TiO_2 5-6 nm	CD-1 mice	intranasally	2,5-10mg/kg; 90 days	- hippocampal lesion - alteration in gene and protein expression - spatial recognition impairement
Ze *et al.*; 2014b [227]	Anatase TiO_2 5-6 nm	CD-1 mice	intranasally	2,5-10mg/kg; 90 days	- oxidative stress - overproliferation of glial cells - tissue necrosis -hippocampal cells apoptosis - alterations in gene expression
Ze *et al.*; 2014c [272]	Anatase TiO_2 5-6 nm	CD-1 mice	intranasally	2,5-10mg/kg; 90 days	- hippocampal lesion - overproiferation of glial cells - alteration in expression of genes involved in inflammatory signaling pathway - neuroinflammation - spacial memory impairment
Mohammadipour *et al*. 2014 [250]	Anatase TiO_2 10 nm	pregnant Wistar rats	intragastric	10mg/kg; from gestational day 2 to 21	- offspring: impaired memory and learning; reduced cell proliferation in hyppocampus
Younes *et al.*; 2015 [273]	TiO_2 20-30 nm	rats	intraperitoneal injection	2mg/kg; evary 2 days for 20 days	- alteration of emotional behavior

Table 11 : Continued

Chapter III:

Experimental methods

1. Acute Intravenous injection exposure study design

The design of the acute intravenous (IV) administration study is summarized in figure 24. Fisher F344 Rats were injected in the tail vein with a suspension of TiO_2 P25 Degussa NPs previously characterized in saline buffer (see annexe 2: NPs characterization data). The selected dose was 1 mg / kg. At early end point (6 hours), the effect of a higher dose of TiO_2 NPs, 10 mg / kg was also tested. Principal organs were collected for the titanium distribution analysis from 30 min up to 356 day after exposure. Regarding the brain, earlier collection time points have been added: 5min and 15 min to refine the description of brain distribution. A deep analysis of titanium brain toxicokinetics was assessed by separated the brain microvessels from the brain parenchyma.

The integrity and the BBB transport functions were also evaluated *in vivo* early time points (6 hours and 24 hours) and at 7 days and 28 days later as well as brain inflammation.

The identification of biomarkers responsible of BBB physiology modulation as well as of brain inflammation was carried out. We used the *in vitro* BBB model to demonstrate the concept of circulating mediators responsible for BBB physiology modulations in the absence of titanium detection in the brain.

Figure 24: Design of the single dose intravenous administration study.

2. Sub-acute Inhalation exposure study design

Given the results of experimental studies, occupational or environmental exposures to manufactured NPs or to unintentionally produced ultrafine particles may results in health effects or diseases in human. We assessed biodistribution of TiO_2 NPs in the more representative exhibitions of real human exposure, subacute inhalation.

An inhalation system to expose rat in nose only to nano-aerosols were set up. Young adult (12-13 weeks old) and aging rats (19 months old) were exposed to a well characterized aerosol of TiO_2 NPs in a reproductively manner 6 hours daily (in two periods of three hours), 5 days per week for 4 weeks. These exposures conditions are consistent with the OECD (Organization for Economic Co-operation and Development) guideline TG-412.

As after IV administration, the biodistribution of titanium in major tissues and organs (lungs, liver, spleen, kidneys, and blood) has been described between the end of the inhalation period (day 0) and day 180 (Figure 25). Due to the advanced age of the animals from the elderly group, the last time for organs collection was day 90 after the end of the inhalation period. Distribution in CNS is only described by ICP-MS (Inductively Coupled Plasma Mass Spectrometry) assays in the total brain. BBB physiology and brain inflammation was also assessed.

Figure 25: Design of the sub-acute inhalation exposure study.

3. Titanium distribution analysis: ICP-MS

In order to draw appropriate conclusions about TiO_2 NPs distribution, a quantification method was developed by J. Devoy. A paper describing the development of this method is accepted for publication (see annexe 1).

Prior to ICP-MS assay, samples need an appropriate preparation in order to obtain titanium in the mineral form. Four mineralization methods were compared in term of recovery and quantification limit. Several tissues samples were tested and quantification limits were calculated for each organ matrix. Mineralization with nitric and hydrofluoric acid was selected because it allow to obtain the best recovery and quantification limits (for a TiO_2 NPs suspension, the recovery is 96% and the limit of quantification is 0.9 µg/L). After mineralization, samples added with internal standard and calibration solutions were directly injected for ICP-MS assay.

4. Blood brain barrier physiology evaluation

The study of *in vivo* BBB physiology after exposure to TiO_2 NPs either by IV injection or inhalation was done by calculating the brain to plasma partition coefficients (Kp) of three molecules: Atenolol, digoxin and prazosin. Atenolol does not cross the BBB in normal physiological conditions that make it a paracellular marker to evaluate BBB integrity. Digoxin and Prazosin were selected as substrates of P-gp and BCRP, two main transporters of the BBB. This cocktail of three molecules was administered through osmotic minipumps (Alzet® minipumps) that allow subcutaneous infusion during several hours. Atenolol, digoxin and prazosin were analyzed in plasma and brain homogenates by liquid chromatography coupled with mass spectrometry in tandem (LC-MSMS).
A preliminary experiment demonstrated that after 4 hours of subcutaneous infusion, stables plasma concentrations of these compounds were obtained (Figure 26).

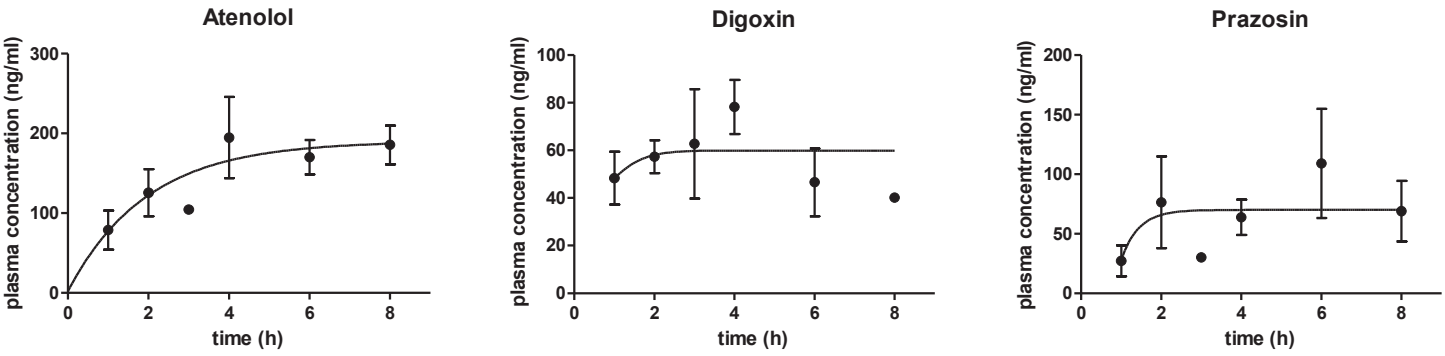

Figure 26: Plasma concentration of atenolol, digoxin and prazosin steady state. Plasma concentration measured after sub cutaneous administration by LC/MSMS. Each data point represent the mean of 3 or 4 animals.

Therefore, the plasma and brain concentration are at the equilibrium. After 4 hours of infusion, brain to plasma Kp can be calculated and are in the extent area of the curve. In the rate area, the Kp represents the blood to brain diffusion, when at the steady state (extent) it allows the evaluation of transporters activities (Figure 27).

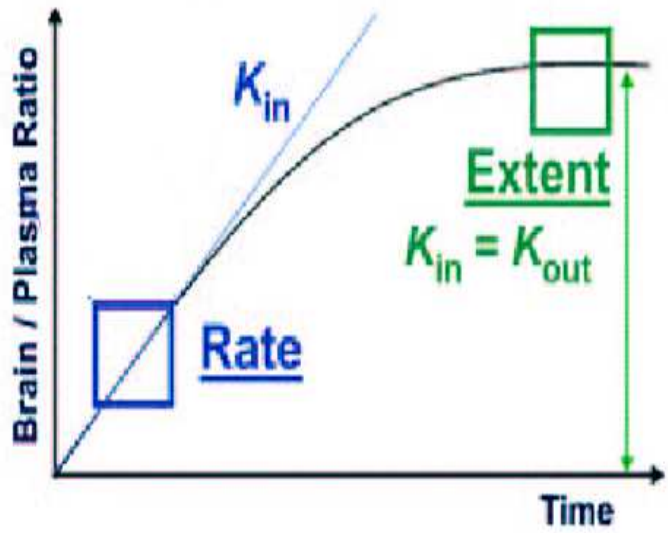

Figure 27: Evolution of brain /plasma ratio over time of infusion.

4.1.Integrity evaluation

In vivo atenolol Kp calculation allow integrity evaluation. An increase in atenolol Kp between controls and exposed rats mean an increase in BBB permeability and inversely a decrease of atenolol Kp means an increase impermeability.

The integrity of the BBB was evaluated by analyzing tight junction proteins expressions. Occludin and claudins are for example key proteins in tight junctions that seal neighboring BECs and limit paracellular diffusion of substances. To evaluate expressions of those proteins at the BBB level, brain endothelial microvessels were isolated and mRNAs expression were measured by real time quantitative polymerase chain reaction (RT-qPCR). Gene expressions were calculated as relative expression: $2^{-\Delta Ct}$, where ΔCt refers to the difference between the threshold cycle of the target gene and hypoxanthine-guanine phosphoribosyltransferase 1 (Hprt1) as a housekeeping gene. Finally, protein expressions were stained by immunohistochemistry on brain slide.

4.2. Transport function evaluation

P-gp and BCRP activities were evaluated throught digoxin and prazosin Kp respectively. An increase of Kp meaning a decrease of the transporter's activity.

The mRNA expressions of P-gp, BCRP but also other transporters at the BBB were evaluated by RT-qPCR in isolated brain endothelial microvessels as described in the previous paragraph.

5. Mediator research

5.1. Neurovascular inflammation evaluation

Two methods were used for cerebral inflammation characterization: 1) Fist on isolated brain microvessels and brain parenchyma fraction, mRNA expressions of several cytokines and chemokines were quantified by RT-qPCR.2) In the inhalation exposure studies this profiling was completed by quantitative analysis of pro-inflammatory mediator using a multiplex approach. This method was applied in brain homogenates but also isolated olfactory bulb homogenates and serum samples. It allows quantification of a panel of proteins (in our case 11 cytokines and chemokines were selected) in one assay and in a limited volume of sample. The principle of multiplex analysis is summarized in Figure 28. Each analytes were quantified based on calibration curved (see annexe 3) than corrected by sample protein concentration.

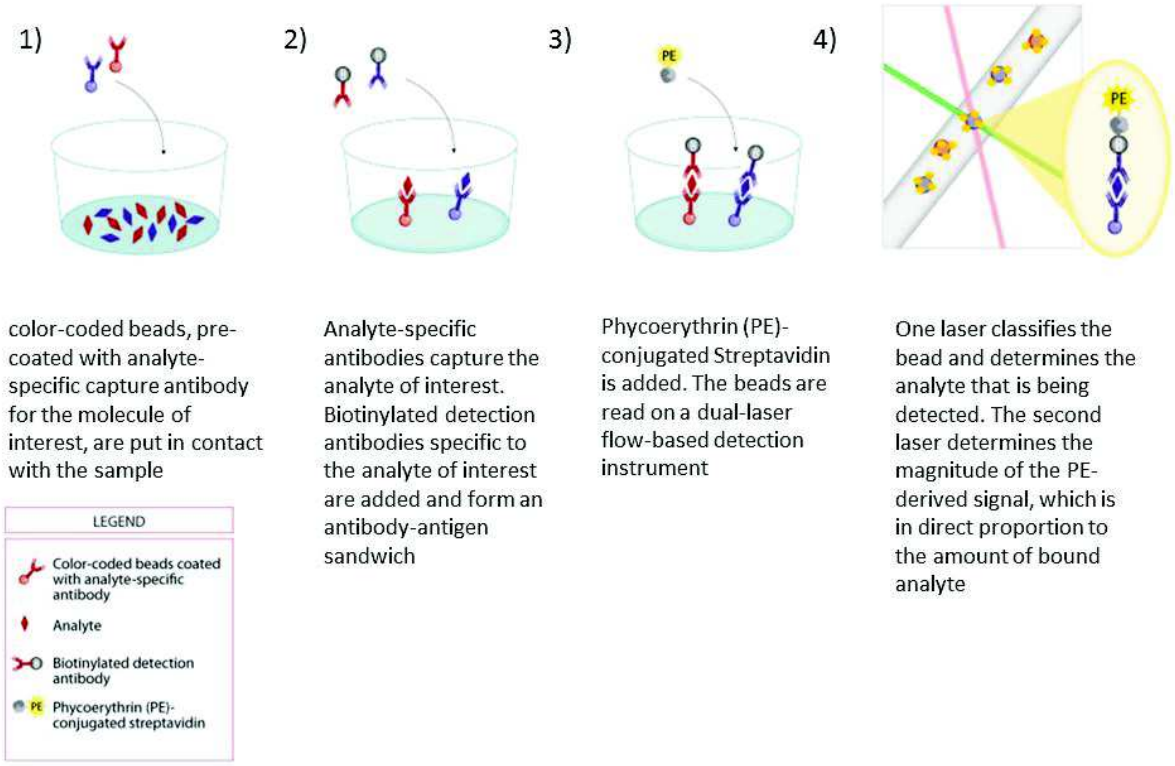

Figure 28: Luminex bead-based Multiplex assay principle (available at www.rndsystems.com/resources/technical/luminex-bead-based-assay-principle).

Il1β was also detected by immunohistochemistry staining on brain slice. These experiments allow the localization of inflammation in different brain areas.

5.2. *In vitro* tool

An *in vitro* approach was used to validate the hypothesis of circulating mediators responsible for modulation of BBB physiology in the absence of brain translocation of NPs and to characterize BECs-NPs direct interaction.

The BBB model used combines two primary cell types in co-culture:

Microvascular endothelial cells were cultured on a semipermeable membrane and glial cells including astrocytes predominantly in the well bottom (Figure 29). The apical pole represents the blood compartment while the basal pole represents the brain compartment. This model reproduces the main features of the BBB *in vivo* [274]:

- Low paracellular permeability
- Presence of tight junctions
- Expression of efflux transporters and pumps

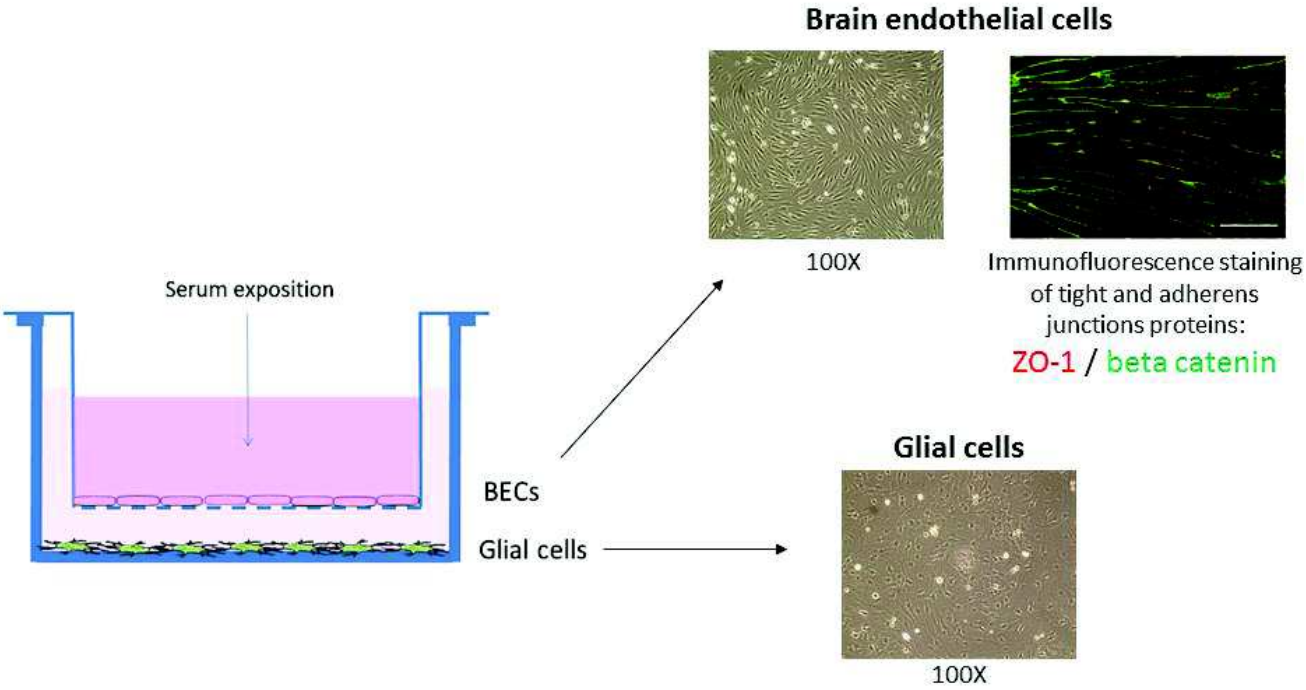

Figure 29: Schematic representation of the *in vitro* BBB model.

A preliminary study allows to determinate the proper sera or plasma dilution to apply in the BBB model during 24 h in order to maintain integrity and transports functions. Then, sera or plasma from control and exposed animals were collected at different time point. *In vivo* modulation of BBB physiology in relation with potential circulating mediators being observed at day 28 after exposure, either after IV injection or after inhalation, we choose sera collected at this same time point for *in vitro* experiments.

Diluted sera or plasma from control and exposed animals were applied in the apical compartment of the model that mimics blood. After 24 h of exposure to sera, we analyzed:

- The potential effect on the BBB integrity by measuring the apparent permeability of the paracellular marker, sucrose (Figure 30).
- The impact on active carriers by measuring the permeability coefficient of P-gp and BCRP substrates. Vinblastine is a molecule which undergoes efflux transport at the BBB in particular by the P-glycoprotein and Prazosin by the BCRP (Figure 28). The impact on active carriers is evaluated based on the ratio of the permeability coefficients measured in the direction A to B (apical to basal) *versus* B to A (basal to apical). The second parameter is a measure of the activity of P-gp and BCRP of endothelial cells.

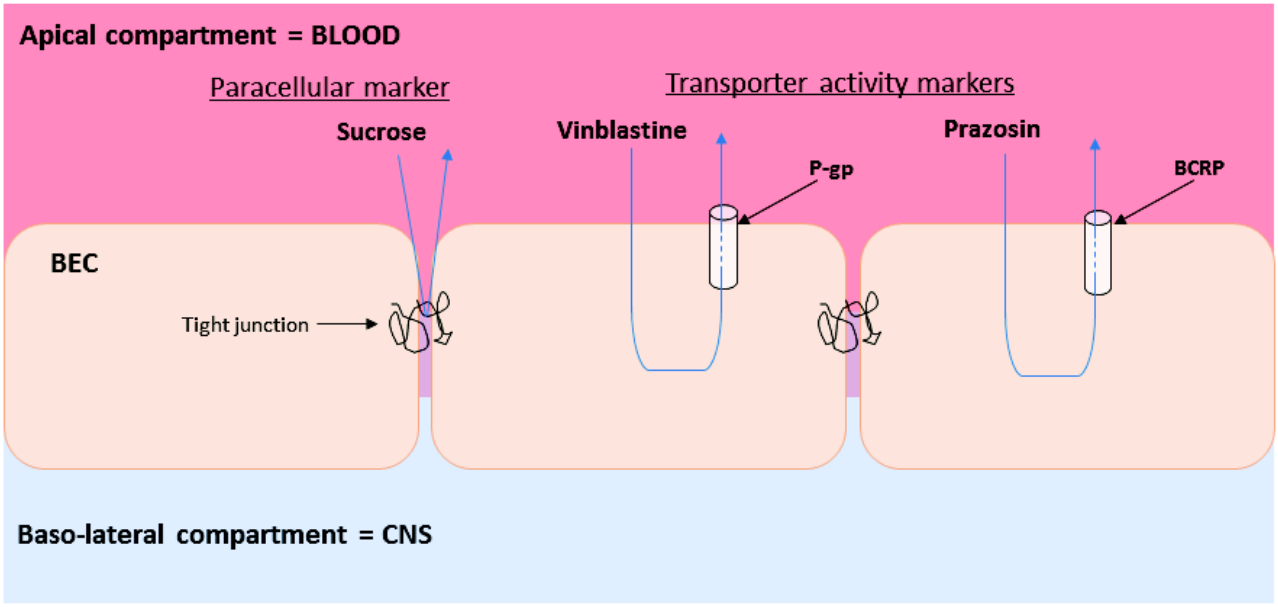

Figure 30: Schematic representation of sucrose, vinblastine and prazosin passage through brain endothelial cells monolayer.

- BECs as well as glial cells were also recovered for cytokines/chemokines and structure proteins mRNA expressions profiling by RT-qPCR.

To study direct interactions between BECs and TiO_2 NPs, NPs powders were suspended in sterile distilled water to achieve a stock suspension at a concentration of 10 mg/mL. This stock suspension was stored at 4 ° C protected from light. The stock suspension was vortexed 5 minutes before using for dilution. Intermediate suspension called 100X was prepared from the stock suspension in sterile distilled water. This 100X suspension was diluted to the hundredth in the endothelial medium to obtain the final concentrations of exposure. Using this dilution method, the percentage of solvent (water) in the endothelial medium is the same whatever the prepared exposure concentration.

During this work, only the exposure *via* the apical compartment corresponding to blood was tested for 24 hours. In this view, the apical media are removed and replaced by 500 µl of endothelial medium containing a selected concentration of NPs. The selected exposure concentrations were in the range from 0.1 to 100 µg/ml. At the end of 24 hours exposure, the permeability and functionality of the barriers were tested as described above.

Chapter IV:

Results and discussion

This section is divided into two parts:

1) Intravenous administration study

This part describes the biokinetics and impact on the brain of IV administered TiO_2 NPs to young adult rats.

2) Inhalation exposure study

This part summarizes the results of biodistribution of TiO_2 NPs in healthy young adults and aging rats after subacute inhalation exposure. Regardless this biodistribution, results of BBB physiology characterization and inflammation assessment were analysed in both age groups.

Part I: Intravenous administration study

1. Context and introduction

The questions which arise from this study relate to the biodistribution and bioaccumulation of blood circulating TiO_2 NPs and to the potential impact on the CNS and more particularly the regulation of the BBB function and brain inflammation.

Despite recent evidences of ability for TiO_2 NPs to cross physiological barrier, distribution to the CNS after IV administration in rodents remain debated. Indeed, Gereats *et al.* described translocation of different sizes TiO_2 NPs to the brain parenchyma 24 hours after the administration [121] whereas three others studies concluded to the lack of translocation after injection of 0.95 mg/kg to 10 mg/kg doses in rats or mice [138, 275, 276]. Therefore, additional investigations are needed to clarify the distribution of TiO_2 NPs to the CNS.
The chosen dose for this study was 1 mg/kg. It was chosen voluntary low compare to published IV studies in rodents [121, 138, 275, 276].
The distribution to major organs is determined from 30 minutes to 356 days after the IV administration in order to provide a wild description of potential elimination and persistence processes. To strengthen analysis of the CNS distribution, early time points is added for brain and blood samples. In addition, the brain endothelial microvessels composing the BBB were isolated from the brain parenchyma to understand the involvement of the BBB in the CNS access. Thanks to a robust ICP-MS method (Devoy *et al.*, accepted paper), small amounts of titanium were measured in the tissues and organs (see annexe 1). Indeed, samples mineralization was optimized to obtained assay with 96% recovery and a limit of quantification down to 0.9 µg/L.
Coupled to the distribution description, the BBB physiology is described. To confirmed previous *in vitro* observations done on a primary rat based cells BBB model several parameters are look at to evaluate BBB functions and neuro-inflammation.

2. Major findings and Discussion

After TiO_2 NPs IV injection, results show a rapid distribution of Ti to tissues with bioaccumulation in liver, lungs, spleen up to one year after IV. In brain, Ti was significantly found during the first 6 hours than cleared. Detailed analysis of CNS distribution highlighted a limited translocation in the brain parenchyma and an internalization of Ti into BECs.

The ICP-MS assays were performed in principal organs but remained limited to highly vascular organs: kidneys liver, spleen, lungs and brain. We observed a long term biopersistence up to one year after administration in several organs including the liver. The distribution to heart has not been investigated. Few studies have shown adverse cardiovascular effects (see Chapter I part II). In heart, the capillaries presents similarities with cerebral microvessels and similar effect on endothelial cells could be observed. Poorly vascularized tissues such as adipose tissue have also not been analyzed. Long term accumulation and toxic effects can occur in these tissue.

To complete this biokinetics study, it would have been interesting to measure titanium in urine and feces to understand the elimination process. This requires isolating animals in metabolism cage for all the duration of the experiment and implementation of specific precautions to avoid samples contamination by environmental titanium. Moreover a complete analysis of the elimination process require collection of a very large number of samples containing small amount of titanium. Small concentration of titanium expected in those samples will likely be under the limit of quantification (i.e. LOQ of 7.4 ng/g in urine). These experiments have therefore not been conducted.

Regarding brain distribution, titanium quantification in the isolated brain microvessels has shown that TiO_2 NPs did not largely cross the BBB. Titanium was detected very quickly after administration (few hours) and rapid clearance from BECs was observed. However, the precise localization of TiO_2 NPs in the BECs and clearance mechanisms remains to be investigated. Previous *in vitro* data suggest that TiO_2 NPs can be internalize by BECs in cytoplasmic vacuoles [1]. Two hypotheses on the clearance mechanisms have been addressed: elimination into the bloodstream or into the CSF. To verify the titanium elimination hypothesis, CSF samples were collected at early time points when the higher titanium concentration where measured in isolated brain microvessels and total brain. The sampled volume being about 10 µl, the ICP-MS assay was not possible. We tried an observation by TEM microscopy but due to the complexity of CSF composition we did not observed NPs. Sample, once deposited on the TEM grids crystallized quickly making impossible the identification of TiO_2 NPs. In addition, titanium concentrations assumed in CSF were extremely low. Finally, since the CSF is fully renewed several times a day, the transitional passage of so low amount of NPs would have been extremely difficult to detect.

The functionality of the barrier has been evaluated according to two parameters:

- Integrity: we observed an overexpression of junction proteins at mRNA and proteins levels at 28 days after administration when titanium was not detected in brain microvessels. These observations at low doses (1 mg/kg) were not associated with

modulation of BBB integrity. However, we demonstrated that high doses (10 mg/kg) induce *in vivo* a breakdown of the BBB.

- Transport functions: we observed a decrease in BCRP transport activity at early time point (6 hours) and a modulation of the mRNA expression of P-gp at late time point (28 days).

The development of Atenolol-Digoxin-Prazosin cocktail was used to evaluate *in vivo* the BBB integrity and transport functions. Integrity and efflux activity was measured by calculating brain/plasma partition. LC-MSMS assays were used to measure brain and plasma concentrations. In blood, drugs such as atenolol, digoxin and prazosin are likely binding to plasmatic proteins. Only the free fraction is substrate of the efflux pumps. It would therefore have had to correct the plasma and brain concentrations through the free fraction to be more representative of the actual pharmacological activity.

In order to go deeper in the analysis of direct interactions between NPs and the BECs cellular machinery that are more than likely to take into account at early time points, we used the *in vitro* BBB model. The purpose of this *in vitro* study was to obtain additional data to better understand and characterize the effects of TiO_2 NPs at the BBB in terms of modulation of integrity and transport functions. After exposure to NPs, the functions of the barriers obtained *in vitro* can be evaluated according to two parameters:

- Impact on the integrity of the BECs monolayer by measuring the sucrose permeability coefficient. Sucrose is a molecule that is not transported and thus cannot pass an undisrupted barrier.
- Impact on carrier' activity by measuring the permeability of vinblastine. Vinblastine is a molecule which undergoes efflux transport at the BBB in particular by P-gp.

By testing a concentration range from 0.001 to 100 µg / mL, we intended to identify a threshold concentration as an effective concentration 50 (EC_{50}). The EC_{50} is the concentration of NPs TiO_2 which induces a variation of 50% of the measured parameter compare to the non-exposed control. An EC_{50} is determined for the integrity parameter (sucrose permeability coefficient) and the transport parameter (efflux ratio of vinblastine).

After exposure for 24 hours to TiO_2 NPs in the apical compartment, the sucrose permeability coefficient increases in a dose-dependent manner. The lowest concentrations tested for this parameter, 0.01 µg/ml to 1 µg/ml did not affect significantly the integrity of the BECs monolayer as the sucrose permeability coefficient remains below the threshold of $8{,}3.10^{-6}$ cm/s. However, the integrity of the barrier is altered at the highest concentration of 100 µg/ml (Additional file 2). Indeed the sucrose permeability after exposure to this concentration is more than 3 times higher than the untreated controls. Previous laboratory study demonstrated that this disruption also results in decreased expression of the structural proteins of the BBB (claudin 5, zonula occludens) [1]. This phenomenon was also observed for longer exposures. These results are supported by the location TiO_2 NPs obtained by TEM. The proportion of TiO_2 NPs internalized in BECs increases with the duration of exposure. In case of repeated exposure,

almost all of the observed TiO_2 NPs were localized within cells, grouped in cytoplasmic vacuoles. Measurements made at intermediate concentrations were used to define a dose response relationship as well as calculate the EC_{50} (Additional file 2). The EC_{50} for sucrose permeability was estimated at 6.16 µg/ml.

After IV administration at low dose, 1mg/kg, we did not observed early alteration of BBB integrity when titanium was detected in brain microvessels (6 hours after IV administration). However, after administration of a higher dose, 10 mg/kg, we observed an increase in atenolol Kp suggesting an alteration of the integrity of the barrier (see additional file 1). Although it is very difficult to correlate blood exposure concentrations and the ones used for *in vitro* experiments on the BBB model, the *in vivo* and *in vitro* observations are consistent. In the scenario of a blood distribution with the possibility of direct interaction between NPs and BECs, our data suggest a disruption of the barrier integrity at higher doses (see additional file 2). This consistency underscore the relevance of the *in vitro* BBB model in nanotoxicology evaluation.

Unfortunately, brain digoxin concentrations being below the limit of quantification by LC-MSMS, the *in vivo* P-gp activity could not be assessed. *In vitro*, the P-gp activity can be evaluated through the efflux ratio of vinblastine. After 24 hours of TiO_2 NPs exposure, the vinblastine efflux ratio is decreased in a dose dependent manner. The lowest concentrations of 0.1 and 1 µg/ml do not induce significant changes in the P-gp activity compared to the untreated controls (Figure 31). The vinblastine efflux ratio was decreased when the concentration of 20 µg/ml of TiO_2 NPs was applied. From the previous results (Additional file 2), at the 100 µg/ml concentration, the integrity of the barrier is disrupted, thus, the P-gp activity no longer has meaning. The EC_{50} for this Pg-p activity parameter was estimated at 0.88 µg/ml. The decrease of vinblastine efflux ratio is notable at concentrations under sucrose EC_{50}. This suggest that at these concentrations, the integrity of the barrier is valid and modification of vinblastine ratio can be interpreted as modifications of P-gp activity.

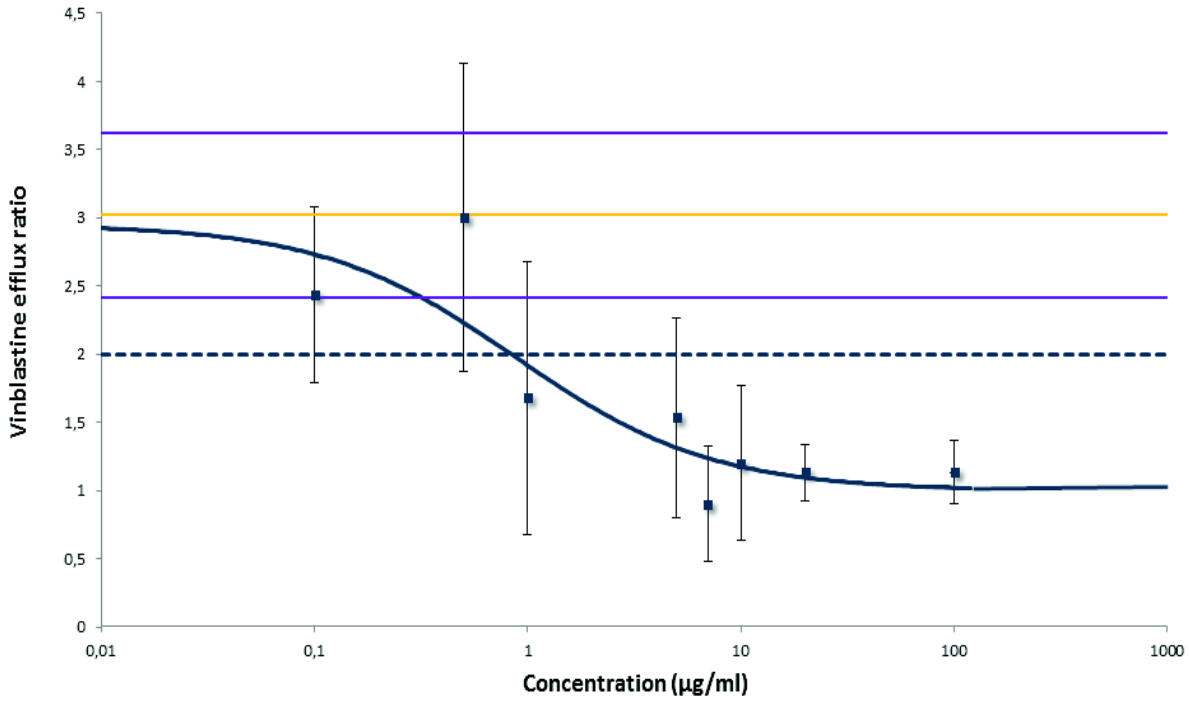

Figure 31: Effect of 24 hours exposure to TiO_2 NPs on the vinblastine efflux ratio as a function of the concentration of NPs. Representation of the average effect of at least 2 experiments, error bars represent the standard deviation. The horizontal dotted line represents the usual limit value of 2 under which the P-gp activity is considered invalid. The zone between two violet lines represents sucrose apparent permeability coefficient for the controls (Mean in yellow).

The *in vivo* P-gp activity was not evaluated after IV administration. Thus, these *in vitro* results suggest that direct interaction between NPs and BECs can impact the P-gp activity. This complete the characterization of transport functions. Altogether, *in vivo* and *in vitro* experiment suggest alteration of BCRP (at 6 hours after IV administration) and P-gp (24 hours after exposure *in vitro*) activities. These rapid modulations of two major ABC transporters activities can have important consequences on CNS protection.

Several hypothesis about mechanisms can raise from these observations:

- Direct interaction between NPs and transporters/involvement of these transporters in NPs transport and clearance
- Interaction with BECs machinery and activation of signaling pathways (e.g. signaling pathways in response to oxidative stress such as P38-Nrf-2 [269])

Our *In vitro* BBB model demonstrated is interest in transport activities evaluation. Here, further investigations are needed to clarify molecular interactions occurring in BECs and the *in vitro* approach may be use in the future.

The BBB has a wide variety of efflux pumps involved in the brain detoxification and cerebral function. These pumps have share substrates and there are substitute mechanisms to maintain brain homeostasis. In this study we focused on P-gp and BCRP, the two major efflux pumps of the BBB. However, it would also have been interesting to assess the functions of other carriers as carriers of energy substrates (e.g. Glut1 and 3 for glucose) which play a major role in supplying the brain.

At late time points in the absence of titanium in the brain were associated with a neuro-vascular inflammation. This neurovascular inflammation was characterized by a profiling the mRNA expression of pro-inflammatory cytokines and chemokines. Only the expression of IL1β was measured at the protein level by immunohistochemistry staining on brain slices.

The neuro-vascular inflammation described *in vivo* is in accordance with previous *in vitro* data on the BBB model [1]. Drawing on the outcomes showing dysfunction of the BBB and neurovascular inflammation in the absence of titanium in the brain, the hypothesis of circulating mediators originating from organs accumulating TiO_2 NPs was assumed. To test this hypothesis, we exposed the *in vitro* BBB model to sera from controls and exposed animals. After 24 hours of exposure mimicking a blood borne exposure, consistent modulations of cytokines and chemokines were noted. The nature of these circulating mediators: inflammatory, metabolic ... needed to be determined.

Circulating metabolites, indicators of systemic and / or tissue inflammation can impact the physiological functions of the BBB. As example, sulphatides, a family of lipid metabolites are involved in many processes in the CNS and may exacerbate the inflammatory response in the brain [277]. Higher blood concentration of ceramides, another family of lipid metabolites has been proposed as biomarkers for early brain changes in AD [278]. Moreover, the crucial role of lipids metabolites is demonstrated by the large number of CNS diseases in which lipid metabolism is altered [279]. This underscores interest to investigate metabolism alteration in blood but also in organs accumulating titanium to understand the indirect effect of the TiO_2 NPs distribution on cerebral functions. In this context, we explored ceramides metabolism pathway in the liver. Ceramidases are enzymes that cleave fatty acids from ceramide, producing sphingosine. mRNA expression of several ceramidases have been analyzed in the liver sampled at 28 days after IV in controls and exposed rats. We highlighted down expression of two ceramidases: the acid ceramidase (ASAH 1) and one isoform of the neutral ceramidase (ACER 3) (Figure 31). These observations suggest that ceramide family species are less catabolized and potentially accumulate in the liver. Once release in the blood, ceramides may promote central effect. Ceramides potentially being circulating mediators linking modulation of BBB physiology and neuro-inflammation, they need to be identified in the liver and in blood.

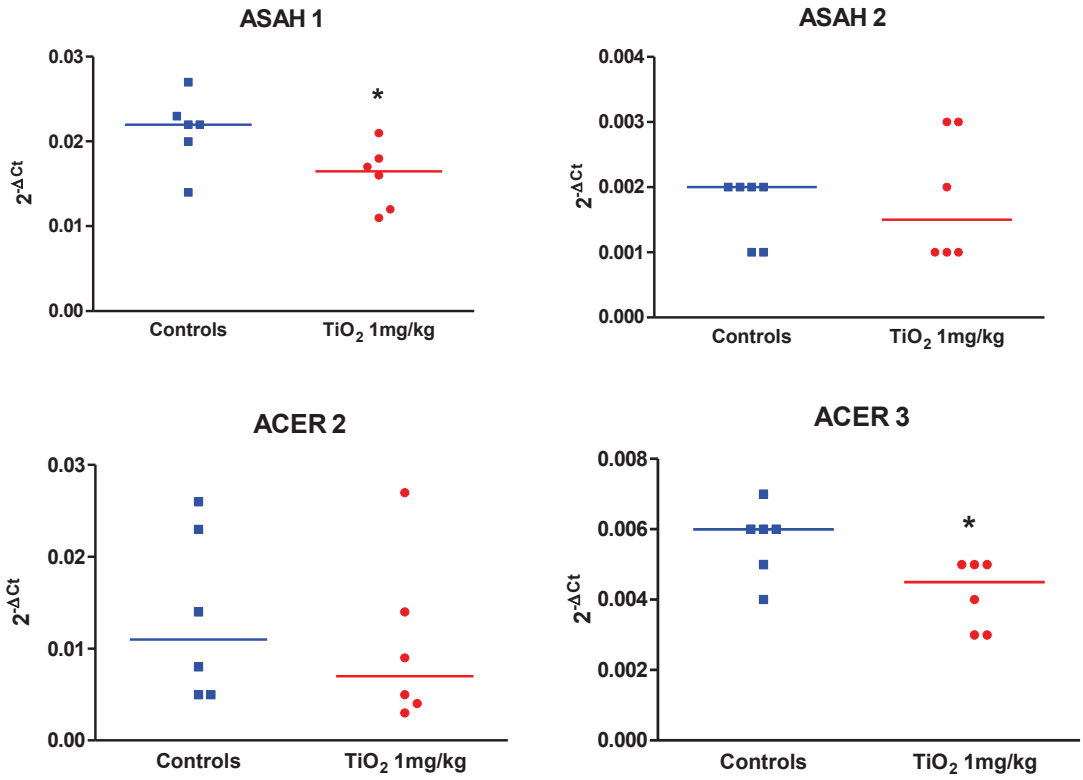

Figure 32: mRNA expression of ceramidases ASAH 1, ASAH 2, ACER 2 and ACER 3 in the liver 28 days after IV injection of 1 mg/kg TiO_2 NPs. RT-qPCR was performed in duplicate for each single liver sample. Relative gene expression values were calculated as $2^{-\Delta CT}$, where ΔCT is the difference between the amplification curve (CT) values for genes of interest and housekeeping genes (beta actin). Results represented as median of n = 6 animals. Statistical comparison was performed by two tailed Mann-Whitney test,* $P < 0.05$.

The spleen is a secondary lymphoid organ which participates in the establishment of systemic inflammatory reaction. Thus we were concerned about potential inflammation in this organ in response to long term titanium accumulation. We explored spleen expression few cytokines and chemokines by RT-qPCR. We noted an increase TNFα expression (P=0.068) (Figure 33). TNFα have already been demonstrated to affect BBB permeability and transport functions [218, 280]. Thus pro-inflammatory mediators such as TNFα can also be propose as mediators linking accumulation of titanium in peripheral organs and effect at the SNC level. Identification in blood will confirm this hypothesis.

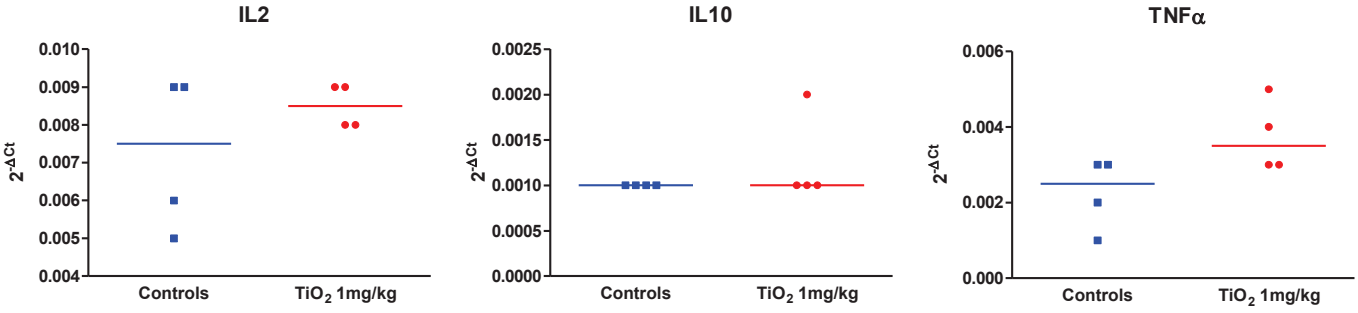

Figure 33: mRNA expression of cytokines interleukin 2 (IL2) interleukin 10 (IL10) and Tumor necrosis factor α (TNFα) in the spleen 28 days after IV injection of 1 mg/kg TiO_2 NPs. RT-qPCR was performed in duplicate for each single spleen sample. Relative gene expression values were calculated as $2^{-\Delta CT}$, where ΔCT is the difference between the amplification curve (CT) values for genes of interest and housekeeping genes (GAPDH). Results represented as of n = 4 animals. Statistical comparison was performed by two tailed Mann-Whitney test.

3. Article 1: Tissue Biodistribution of Intravenously Administrated Titanium Dioxide Nanoparticles Revealed Blood-Brain Barrier Clearance and Brain Inflammation in rat

Disdier et al. Particle and Fibre Toxicology (2015) 12:27
DOI 10.1186/s12989-015-0102-8

PARTICLE AND FIBRE TOXICOLOGY

RESEARCH Open Access

Tissue biodistribution of intravenously administrated titanium dioxide nanoparticles revealed blood-brain barrier clearance and brain inflammation in rat

Clémence Disdier[1], Jérôme Devoy[2], Anne Cosnefroy[1], Monique Chalansonnet[2], Nathalie Herlin-Boime[3], Emilie Brun[4], Amie Lund[5] and Aloïse Mabondzo[1*]

Abstract

Background: Notwithstanding increasing knowledge of titanium dioxide nanoparticles (TiO_2 NPs) passing through biological barriers, their biodistribution to the central nervous system (CNS) and potential effects on blood-brain barrier (BBB) physiology remain poorly characterized.

Methods: Here, we report time-related responses from single-dose intravenous (IV) administration of 1 mg/kg TiO_2 NPs to rats, with particular emphasis on titanium (Ti) quantification in the brain. Ti content in tissues was analyzed using inductively coupled plasma mass spectrometry. Integrity and functionality of the BBB as well as brain inflammation were characterized using a panel of methods including RT-PCR, immuno-histo chemistry and transporter activity evaluation.

Results: Biokinetic analysis revealed Ti biopersistence in liver, lungs and spleen up to one year after TiO_2 NPs administration. A significant increase of Ti in the brain was observed at early end points followed by a subsequent decrease. In-depth analysis of Ti in the total brain demonstrated quantitative Ti uptake and clearance by brain microvasculature endothelial cells (BECs) with minimal translocation in the brain parenchyma. The presence of Ti in the BECs did not affect BBB integrity, despite rapid reversible modulation of breast cancer resistance protein activity. Ti biopersistence in organs such as liver was associated with significant increases of tight junction proteins (claudin-5 and occludin), interleukin 1β (IL-1β), chemokine ligand 1 (CXCL1) and γ inducible protein-10 (IP-10/CXCL10) in BECs and also increased levels of IL-1β in brain parenchyma despite lack of evidence of Ti in the brain. These findings mentioned suggest potential effect of Ti present at a distance from the brain possibly *via* mediators transported by blood. Exposure of an *in vitro* BBB model to sera from TiO_2 NPs-treated animals confirmed the tightness of the BBB and inflammatory responses.

Conclusion: Overall, these findings suggest the clearance of TiO_2 NPs at the BBB with persistent brain inflammation and underscore the role of Ti biopersistence in organs that can exert indirect effects on the CNS dependent on circulating factors.

* Correspondence: aloise.mabondzo@cea.fr
[1]CEA, Direction des Sciences du Vivant, iBiTec-S, Service de Pharmacologie et d'Immunoanalyse, Equipe Pharmacologie Neurovasculaire, 91191 Gif-sur-Yvette, France
Full list of author information is available at the end of the article

Background

Titanium dioxide (TiO_2) nanoparticles (NPs) are the second most frequently used NPs in industry worldwide (http://www.nanotechproject.org). TiO_2 is widely used as a white pigment in paint, ink, plastic, and paper and as food additive, while the nanosized TiO_2 is also used for its photocatalytic activity in self-cleaning materials and for its UV absorption capacity in sunscreen cosmetics [1]. TiO_2 is also used in the composition of dental prosthesis and implant biomaterials. Because of these multiple applications, TiO_2 is massively produced and as nano-sized particles is found in variable proportions in daily life products. For example, for food grade TiO_2 (E171) fraction of particles under 100 nm, thus corresponding to the strict definition of NPs was estimated at 36 % by Weir et al. and 5–10 % reported by Peters et al. [2, 3].

Recent toxicological and pharmacological research on rodents has shown that TiO_2 NPs may translocate across physiological barriers such as respiratory, intestinal and vascular epithelium and therefore reach various organs and tissues including the brain [4–6]. The brain is well protected by the blood brain barrier (BBB), which contains cells of several types: brain endothelial cells (BECs), astrocytes, and pericytes [7–11]. These cells communicate closely to guarantee a physical and functional barrier between the blood and the central nervous system (CNS): tight junctions connecting endothelial cells and many transporters including two major ATP-driven drug efflux pumps, the P-glycoprotein (P-gp) and breast cancer resistant protein (BCRP) [12–14]. This neurovascular unit regulates distribution of xenobiotics to the brain.

Fabian et al. reported a lack of translocation of 20 nm TiO_2 NPs to the brain parenchyma 24 h after intravenous (IV) injection of a dose of 5 mg/kg to rats [15]. These findings are further supported by other studies results in which lack of brain distribution was noticed 6 h following IV administration of 0.95 mg/kg of Degussa P25 TiO_2 NPs to rats [16] and 24 h after administration of a 10 mg/kg dose of rutile TiO_2 NPs to mice [17]. However, Geraets et al. showed the presence of TiO_2 NPs of different sizes and crystalline forms 24 h after a 5 mg/kg IV dose in the brain of rats [18]. While brain translocation of TiO_2 NPs after IV administration remains contradictory, oral and pulmonary exposure in rodents has shown distribution of TiO_2 NPs to the CNS [18, 19]. Disturbance of neurotransmitters and enzymes, oxidative stress and inflammatory response have been described as neurotoxic effects after nasal instillation, intraperitoneal injection, oral administration or prenatal exposure [20–25]. These findings raised the question of the entry of TiO_2 NPs into the brain and of their interactions with the BBB.

Our previous data using an *in vitro* BBB model [26] show that P25 TiO_2 NPs (21.5 nm, 75 – 25 % anatase/rutile) can accumulate in BECs, with very low and limited translocation in the glial cells, hinting at the "physical barrier" role of the BEC epithelium [27]. Overall, these contradictory *in vitro* and *in vivo* findings show that additional investigations are needed to ascertain *in vivo* brain translocation of TiO_2 NPs, interactions between TiO_2 NPs and the BBB, and potential adverse effects in the brain. These are the main subjects of the present study.

We used well-characterized anatase/rutile TiO_2 NPs (P25 aeroxide Degussa) to evaluate *in vivo* biodistribution of TiO_2 NPs, with particular emphasis on *in vivo* interactions with the BBB. We evaluated the biokinetics of TiO_2 NPs from 5 min up to one year after IV administration to adult Fischer rats at a dose of 1 mg/kg. This mode of administration and concentration was chosen for comparison to the contradictory literature. Moreover, IV allows clarify the potential brain translocation under conditions of 100 % systemic bioavailability without impact of NPs transport across other biological barrier that could impact NPs. In addition, the potential effects on BBB physiology and subsequent induction of neuroinflammation markers were analyzed.

Results and discussions

Characterization of titanium dioxide nanoparticles

Morphology and size of TiO_2 NPs in stock suspensions were determined by Transmission Electron Microscopy (TEM). The mean diameter of individual particles was found to be 21.5 ± 7.2 nm (400 counts) (Fig. 1a). Scanning Electron Microscopy (SEM) confirmed spherical morphology of particles and Energy Dispersive X-ray (EDX) analysis on the same images confirmed purity of the product (i.e. only Ti and O are detected indicating the absence of other metal contamination greater than 1 %) (Data not shown). Analysis by X-ray diffraction confirmed the presence of a mixture of 75 % anatase and 25 % rutile crystal phases (Data not shown). The specific surface area, 51 m^2/g, was measured by Brunauer–Emmett–Teller (BET) method and corresponds to 30 nm grain diameter.

Dynamic light scattering (DLS) measurements shows that NPs agglomerate in water and to a larger extent in saline buffer with hydrodynamic diameters of 163.5 ± 12.6 and 520.9 ± 41.7 nm, respectively (Fig. 1b). Those measurements highlight the important tendency of TiO_2 NPs to aggregate/agglomerate as soon as they are in suspension. We choose not to apply other dispersion protocol for *in vivo* experiments as they usually necessitate modifying NPs surface. In addition, the size distribution we obtained is comparable to the one in Fabian, Xie and Geraets's study [15, 17, 18] which would ease data confrontation. Indeed, it is worth noticing that even agglomerated in suspension, NPs form presents a greater

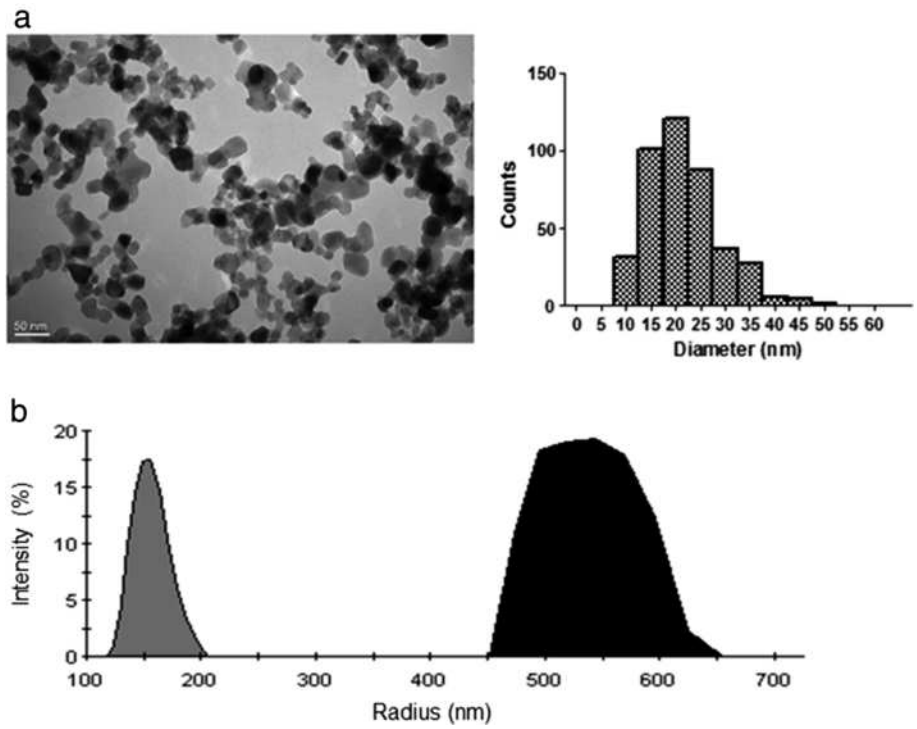

Fig. 1 Characterization of TiO_2 NPs. **a** Representative TEM image of the TiO_2 NPs (magnification 40.000 x) and size distribution histogram. More than 400 NPs were measured randomly on several micrographs. The average diameter was 21.5 nm and the standard deviation 7.2. **b** Size distribution by intensity obtained by DLS for TiO_2 NPs suspended in water (grey) or in saline buffer (black). Vigorous vortexing was the only treatment of the suspensions and measurement conditions were optimized resulting in a fixed lens position at 4.65 mm and a concentration of 25 μg/mL. Mean hydrodynamic radius were 163.5 ± 12.6 and 520.9 ± 41.7 nm for water and saline buffer respectively

reactive surface area that may promote adverse effect compare with the same material particles in micro size scale.

Biodistribution and accumulation studies of titanium dioxide nanoparticles

Ti burdens in organs and tissues after IV administration are shown in Fig. 2. In a previous work, we fully compared four commonly used mineralization methods for TiO_2 NPs and established that one of them involving nitric and hydrofluoric acids, combined to the inductively coupled plasma mass spectrometry (ICP-MS) method allows Ti quantification for NPs in biological samples with limit of quantification (LOQ) from 4.7 to 33.1 ng/g depending on the tissue sample mass available. This method was validated for linearity, repeatability and accuracy. Matrix effects and recoveries were checked and quantification limit was determined, *sine qua none* conditions for providing valuable data (Devoy et al., 2015 accepted paper). Ti burdens in liver, spleen and lungs of the treated group were significantly higher than those of the control group from 30 min to 356 days ($P < 0.001$). The Ti level was higher in the liver than in spleen and lungs. Assays performed one year after TiO_2 NPs administration to rats indicated that Ti burden remained high, suggesting long-term biopersistence and no major elimination from the liver. Indeed, approximately 33 % of the Ti burden at early time points (less than 24 h) remain in the liver one year after IV administration. The Ti burden in kidneys of the treated group was significantly higher from 30 min to 24 h, and then decreased significantly after 7 days after IV administration. Significant levels of Ti were never found in blood (plasma or blood cells) of the treated group, even at early end point (i.e. 5 min).

Our findings confirm previous studies showing that the liver, spleen and lungs appear to be the major organs of accumulation of TiO_2 NPs after IV administration [15–18, 28] in rodents. We estimate that we recover approximately 44 % of the administered dose in the liver, 10 % in lungs and 2 % in spleen 6 h after IV administration. As reported previously, the clearance of TiO_2 NPs from the blood circulation is rapid, so Ti was never detected in plasma or blood cells [15, 28]. The limit of quantification of the ICP-MS method used is about 15 ng/ml for plasma and about 14 ng/g for blood cells.

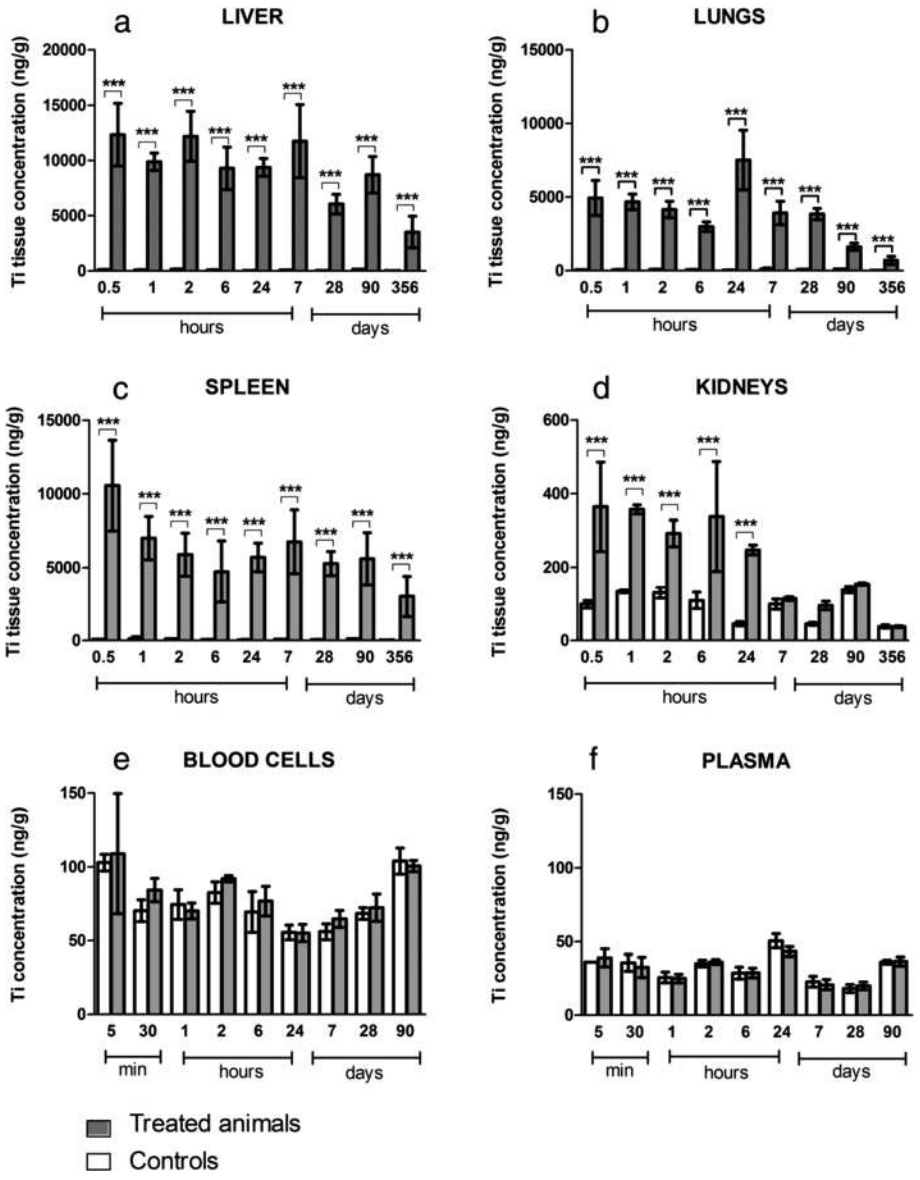

Fig. 2 Tissue distribution of titanium after IV injection of 1 mg/kg TiO_2 NPs in rats. Titanium quantification in liver (**a**); lungs (**b**); spleen (**c**); kidneys (**d**); blood cells (**e**) and plasma (**f**) of treated (*grey*) and control (*white*) animals. Quantification by inductively coupled plasma mass spectrometry (ICP-MS). Each data point represents the mean ± SD of n = 6 animals. Statistical comparison was performed by two-way ANOVA, *$P < 0.05$; **$P < 0.01$; ***$P < 0.001$

In this context a low blood concentration of Ti cannot be ruled out. Driven by the quantification method developed, we then focused on the Ti brain content.

Quantification of titanium dioxide in the brain

IV administration of TiO_2 NPs to rats resulted in trace amount of Ti content in total brain at early end points (Fig. 3). Ti was significantly detected from 5 min (brain Ti concentration was 261.40 ± 28.86 ng/g for the treated group vs. 68.25 ± 6.56 ng/g for the control group, $P < 0.001$) to 6 h (brain Ti concentration was 110.00 ± 25.05 ng/g for the treated group vs. 66.75 ± 7.36 ng/g for the control group, $P < 0.001$) (Fig. 3a). We found a significant decrease in the cerebral tissue Ti concentration after 24 h. Ti content after 24 h in the treated group did not differ significantly from that in the control group. These data are in agreement with the recent study by Geraets et al., who found Ti in rat total brain 24 h after IV administration of 5 mg/kg doses of different TiO_2 NPs whatever their sizes and crystallinity [18]. Shinohara *et al.* also measured traces of Ti in rat total brain 6 h after IV administration of a 0.95 mg/kg dose of P25 Degussa TiO_2 NPs [16]. Fabian et al. did not detect

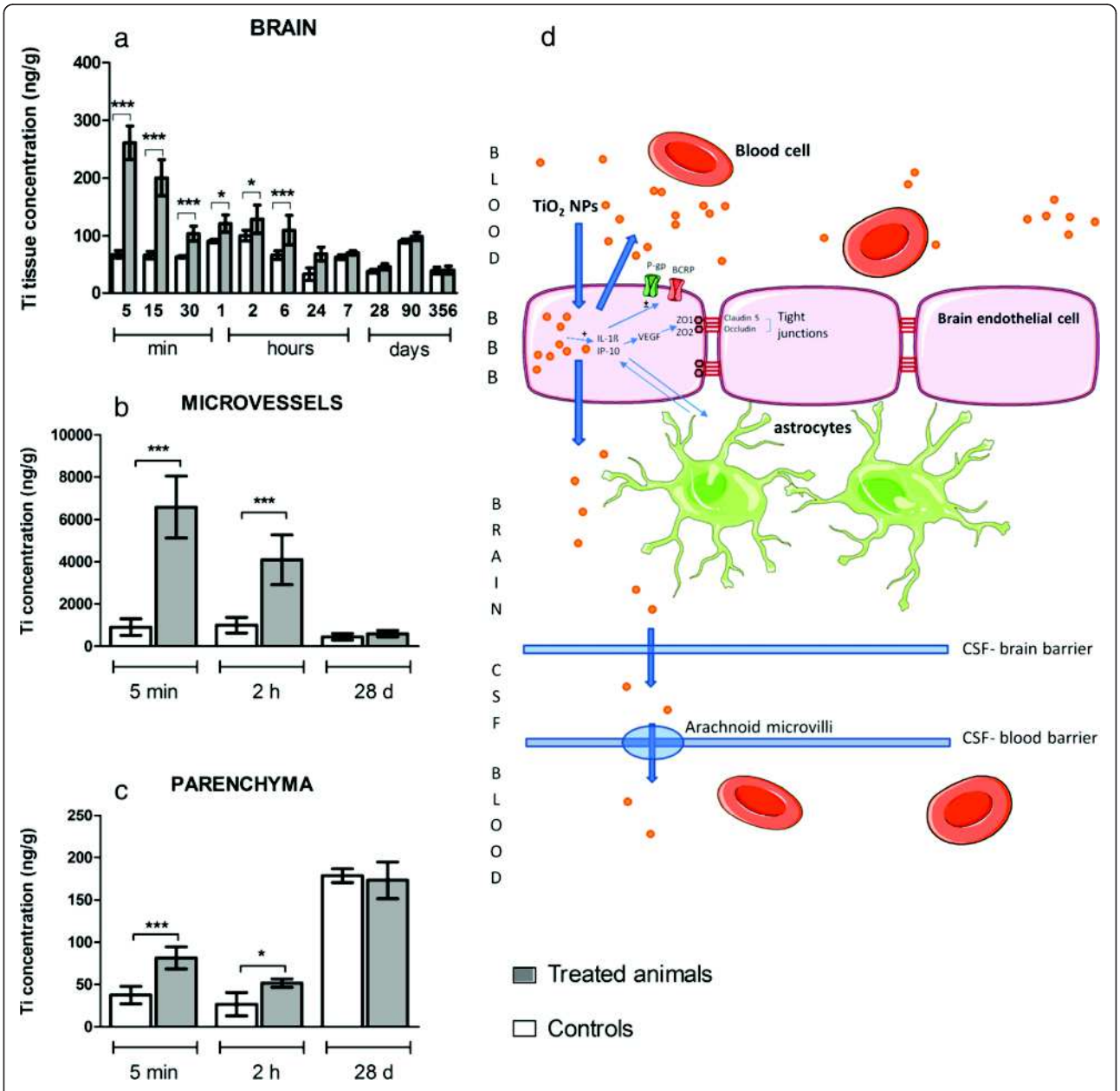

Fig. 3 Titanium quantification in rat brain (**a**), isolated brain microvasculature endothelial cells (**b**) and brain parenchyma (**c**) of treated (*grey*) and control (*white*) animals after IV injection of 1 mg/kg TiO_2 NPs and schematic summary of the events and potential effects on the BBB.. Quantification by inductively coupled plasma mass spectrometry (ICP-MS). Each data point represents the mean ± SD of n = 6 animals. Statistical comparison was performed by two-way ANOVA, $^{*}P < 0.05$; $^{**}P < 0.01$; $^{***}P < 0.001$. Consequences and hypothesis of clearance mechanism of TiO_2 NPs at the BBB (**d**). Transient presence of TiO_2 NPs in brain microvasculature endothelial cells leads to overexpression of cytokines and chemokines (IL-1β and IP-10), which could be linked to the modification of activity or expression of P-gp and BCRP. Integrity of the barrier is not compromised

Ti in the total brain, a result which could be explained by the sensitivity of the analytical inductively coupled plasma atomic emission spectroscopy (ICP-AES) method used.

These observations raise one important question: do TiO_2 NPs cross the BBB and accumulate in the brain parenchyma or remained located in the brain micro vasculature? As a crucial component of the BBB, the BECs and a fraction corresponding to glial and neural cells referred to as the parenchyma fraction were separated, as we described previously [29]. The purity of the resulting BECs was checked after RNA isolation and real-time PCR experiments by measuring the expression of cell-specific marker genes for BECs (CD31 or PECAM) and for glial cells (glial fibrillary acid protein). The purity of isolated BECs was 99.58 ± 0.11 % and of the parenchyma

fraction 98.52 ± 1.17 %. Analysis of Ti content in these two separated fractions highlighted rapid internalization of TiO_2 NPs into BECs (at 5 min after IV Ti concentration in treated group was 6579.33 ± 594.36 ng/g vs 907.16 ± 158.70 ng/g in the control group $P < 0.001$), followed by a significant decrease at 2 h (Fig. 3b). With caution to the background increased in the untreated animals at 28 days, at 5 min and 2 h after IV a significant increase of Ti between controls and treated animals was found in the parenchyma fraction but correspond to a very low amount of Ti (Fig. 3c). At 28 days after IV administration, Ti content in BECs was not different in the control and treated groups as well as in the parenchyma fraction of both same age groups. Notwithstanding the uptake of TiO_2 NPs by the BECs and the very low concentration found in brain parenchyma, our findings suggest that the BBB regulates the uptake and clearance of TiO_2 NPs. This is in line with previous *in vitro* findings from our laboratory that have demonstrated rapid internalization of TiO_2 NPs by BECs [27] wherein NPs have been evidenced in vesicles, suggesting that isolated or aggregated NPs can be exported from the cell *via* exocytosis. *In vivo*, two clearance pathways can be hypothesized: exocytosis back in the blood circulation or transcytosis across BECs to enter the cerebrospinal fluid (Fig. 3d). The mechanism of internalization and clearance of Ti from the BECs thus remain to be determined.

BBB physiology modulations

Here we have shown that there is early clearance of TiO_2 NPs at the BBB and significant biopersistence of Ti in organs (i.e. liver, spleen, etc.) after IV administration of TiO_2 NPs to rats. This raises the question of whether there is a direct or indirect effect of TiO_2 NPs on BBB physiology in terms of BBB integrity, on regulation of proteins involved in brain detoxification, such as P-gp and BCRP, and regulation of neuroinflammation.

BBB integrity

Since alterations in the expression and/or distribution of tight junction proteins are associated with pathophysiological conditions, such as neurological disorders (Alzheimer disease, multiple sclerosis, dementia, epilepsy, etc.) [10, 30–32], we investigated whether the presence or lack of TiO_2 NPs in the BECs after IV administration to rats would compromises BBB integrity or not. Occludin and claudins are key proteins in tight junctions that seal neighboring BECs and limit paracellular diffusion of substances. The expression of claudin-5 and occludin mRNA was determined, as well as the partition coefficient or Kp of atenolol, a known paracellular drug marker [33], which does not cross the BBB in normal physiological condition. The marketed increase of atenolol Kp will reflect the increased in the apparent permeability of atenolol attributed to the BBB disruption.

The expression profiles of the genes encoding claudin-5 and occludin are represented in Fig. 4. In freshly isolated BECs, their mRNA expression levels were not significantly different between control and treated animals at 24 h after IV administration of TiO_2 NPs (Fig. 4a and c). However, notwithstanding the lack of Ti within the brain, the biopersistence of Ti in the other organs revealed an increase of claudin-5 and a slight increase for occludin mRNA expression ($P = 0.057$) in the BECs 28 days after IV administration of TiO_2 NPs (Fig. 4b and d). The up-regulation of tight junction mRNA in BECs correlates with protein expression evidenced by immunofluorescence staining (Figs. 5 and 6). In addition, the brain to plasma concentration ratio (Kp) of atenolol was determined. The atenolol Kp between controls and treated animals remained unchanged (Fig. 7), suggesting lack of BBB breakdown after administration of 1 mg/kg TiO_2 NPs in rats. However, higher doses of TiO_2 NPs (10 mg/kg) induced an increase of atenolol Kp 6 h after IV administration, suggesting compromise of BBB integrity and testifying for the ability of the integrity probe (Additional file 1). These findings on the consequences of exposing the BBB to TiO_2 NPs are in accordance with observations on the *in vitro* BBB model (Additional file 2).

Overall, these data suggest BECs activation at 28 days and a plausible establishment of a BBB repair mechanism after IV administration of TiO_2 NPs (1 mg/kg). This raises the question of the mediators potentially involved in these processes.

Regulation of P-gp and BCRP at the BBB

A number of transport and carrier systems are expressed and polarized on the luminal or abluminal surface of the BECs. Among these systems, Adenosine triphosphate-Binding Cassette (ABC) transporters play a critical role in preventing neurotoxic substances from entering the brain, and in transporting toxic metabolites out of the brain. mRNA expressions as well as transport activities of two major ABC transporters (*Abcb1*/P-gp and *Abcg2*/BCRP) at the BBB were investigated after IV administration of TiO_2 NPs. Data depicted in Fig. 8a and c show no change in *Abcb*1 and *Abcg2* mRNAs at 24 h in the rat BECs, while biopersistence of Ti in organs except brain (28 days) correlated with an increase in *Abcb1* mRNAs but not *Abcg2* mRNAs expression (Fig. 8b, d), suggesting differential P-gp and BCRP transporter regulation mechanisms. The regulation of *Abcb1* mRNAs has been also described in the context of oxidative stress, signaling initiated by Diesel Exhaust Particles for

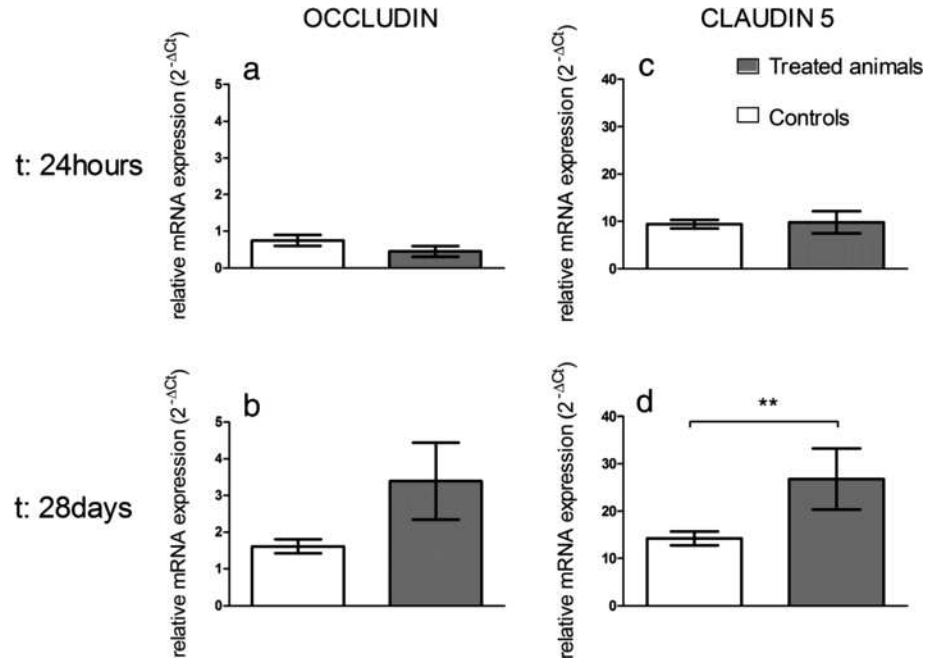

Fig. 4 mRNA expression of tight junction proteins occludin (**a, b**) and claudin 5 (**c, d**) in isolated brain microvasculature endothelial cells 24 h or 28 days after IV injection of 1 mg/kg TiO_2 NPs in rats. RT-qPCR was performed in duplicate for each single brain microvasculature endothelial cells preparation. Each data point represents the mean ± SEM of n = 4 animals. Statistical comparison was performed by two tailed Mann-Whitney test, ** $P < 0.01$. For occludin mRNA expression $P = 0.057$

example, due to the activation of Nicotinamide Adenine Dinucleotide Phosphate-oxidase which produces Reactive Oxygen Species, stimulates Tumor Necrosis Factor - α (TNF-α) release and activate TNF receptor 1 (TNF-R1). In turn, TNF-R1 activates the transcription factor Activator Protein 1 leading to an increase in P-gp expression. Activation of nuclear factor E2-related factor-2, a sensor of oxidative stress, also upregulates P-gp expression at the BBB [34]. To determine whether the increase in mRNA expressions resulted in changes in protein activity, we measured the Kp of digoxin and prazosin as examples of P-gp and BCRP substrates [35–39], respectively. A decrease of transporter activity is indicated by his substrate Kp increase. Functional studies show a rapid down regulation of BCRP activity indicated by a brain increase of prazosin concentration 6 h after exposure to TiO_2 NPs ($Kp_{prazosin} = 0.48 \pm 0.03$ for treated group versus $Kp_{prazosin} = 0.34 \pm 0.03$ for control group), whereas no change in transport activity was observed at 24 h, 7 or 28 days after TiO_2 NP exposure (Fig. 8e). These findings pointed out different signaling processes at the BBB level during early (e.g. direct interaction of TiO_2 NPs with the BBB) and late events (e.g. cytokine signaling) after IV TiO_2 NPs administration to animals. Such regulation has been evidenced when brain capillaries was exposed to low levels of Lipopolysaccharide [34, 40]. We could not correlate the increase in *Abcb1* mRNA expressions 28 days with the P-gp protein transport activity since brain digoxin concentrations were under the quantification limit in both the controls and the treated group, so P-gp activity was not measurable. It is worth noticing that this disturbance of P-gp and BCRP expression or activity was also observed on the *in vitro* cell based BBB model after 24 h exposure to TiO_2 NPs (data not shown). Such disturbance of BCRP or P-gp activities could alter the detoxification function of the BBB. Indeed, P-gp and BCRP have a very wide variety of substrates and modulation of their efflux capacities even low can potentially lead to accumulation of neurotoxics in the brain parenchyma [41].

Neuroinflammation assessment and relation to biopersistence of TiO_2 NPs in organs

Finally, we were concerned about a potential neuroinflammation as such a phenomenon was at stage in our *in vitro* cell based BBB model and described *in vivo* after intraperitoneal injection of TiO_2 NPs [22, 42]. We studied the influence of the short-term presence of Ti in the BECs and the impact of biopersistence of Ti in other organs on CNS inflammation, especially at the BBB and in the brain parenchyma. The presence of Ti in BECs at early end point depicted in Fig. 3b (significant up to 24 h after IV administration) is correlated with a significant increases of interleukin 1β (IL-1β) and chemokine ligand 1 (CXCL1) (Fig. 9). These increases in addition to

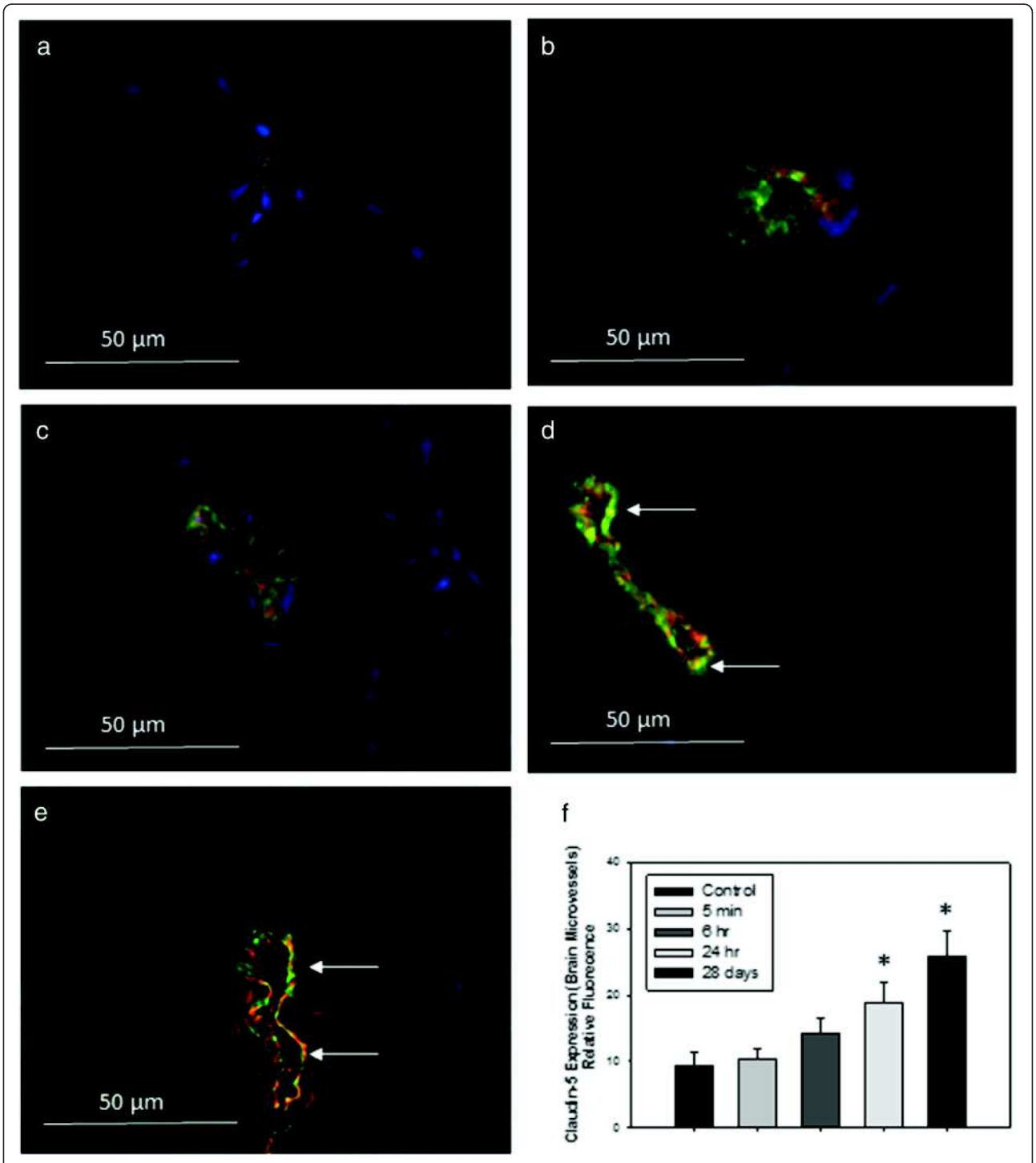

Fig. 5 Representative images of immunofluorescence expression of tight junction protein claudin-5 (*red*) and endothelial cell marker vonWillebrand factor (vWF, *green*) in the cerebral microvasculature of (**a**) control rats, or tissues collected from rats treated with 1 mg/kg TiO_2 (IV) at (**b**) 5 min; (**c**) 6 h; (**d**) 24 h or (**e**) 28 days post-treatment. Yellow fluorescence indicates overlay (co-localization) of claudin-5 and vWF. Arrows indicate areas of increased yellow fluorescence. Graph in (**f**) shows analysis of relative fluorescence of overlay images ± SD. *$P < 0.050$ compared to controls

γ inducible protein-10 (IP-10/CXCL10) are maintained 28 days after IV administration, whereas no Ti was detected in BECs or in the brain parenchyma. In the brain parenchyma, we also noted an increase of interleukin 6 (IL6) expressions at 28 days after IV administration (Fig. 9). First, the persistent brain inflammation evidenced in this study at the brain microvasculature level 28 days after TiO_2 NPs exposure raised the question of

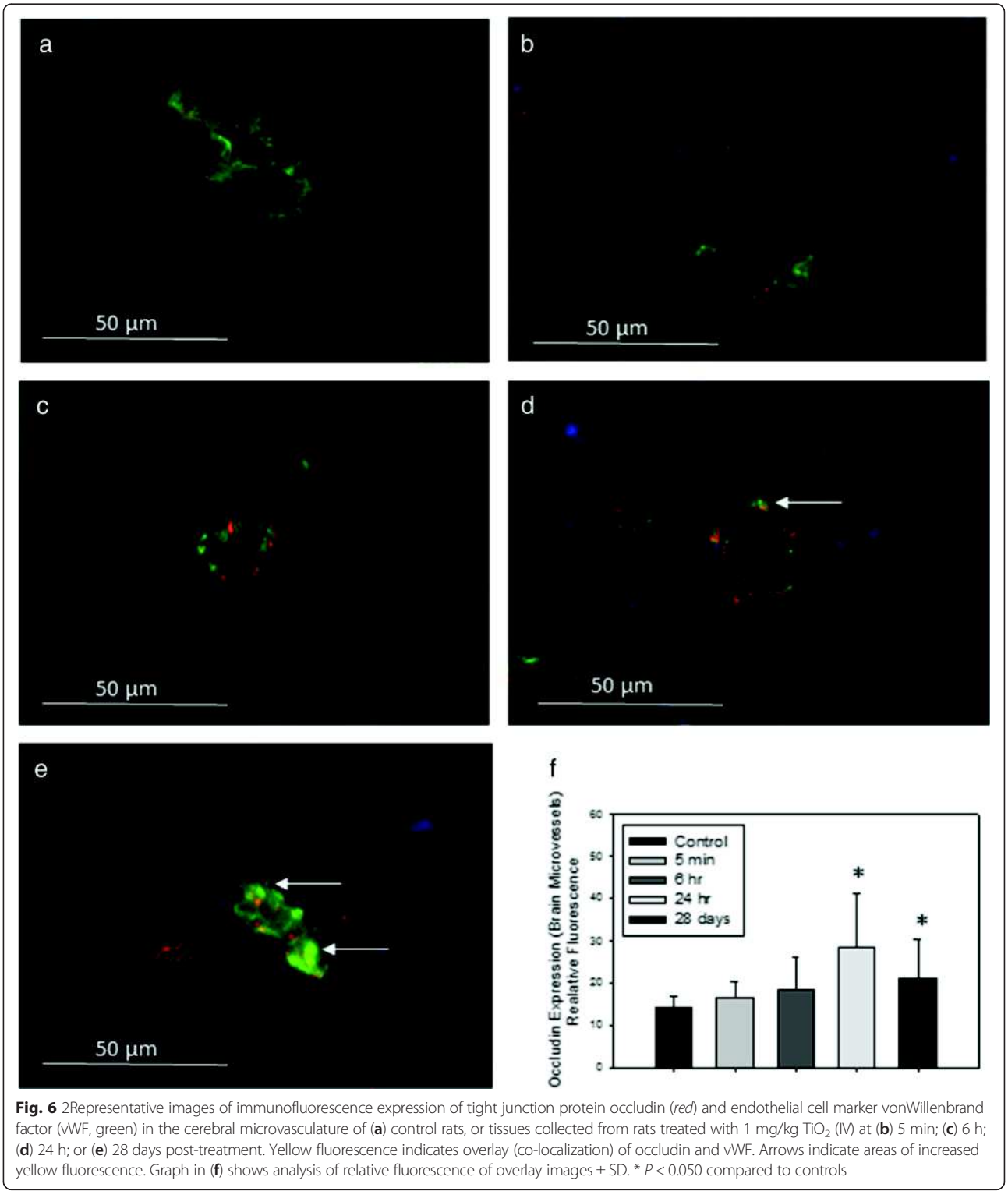

Fig. 6 2Representative images of immunofluorescence expression of tight junction protein occludin (*red*) and endothelial cell marker vonWillenbrand factor (vWF, green) in the cerebral microvasculature of (**a**) control rats, or tissues collected from rats treated with 1 mg/kg TiO_2 (IV) at (**b**) 5 min; (**c**) 6 h; (**d**) 24 h; or (**e**) 28 days post-treatment. Yellow fluorescence indicates overlay (co-localization) of occludin and vWF. Arrows indicate areas of increased yellow fluorescence. Graph in (**f**) shows analysis of relative fluorescence of overlay images ± SD. * $P < 0.050$ compared to controls

potential brain dysfunction. Indeed, a link between persistent neuro-inflammation and brain pathologies as already been established [43]. Second, modifications of P-gp and structural tight junction protein mRNA expressions come with modulation of cytokines and chemokines 28 days after TiO_2 NPs administration to rats. This is not correlated with measurable Ti brain and plasma content. In this context, an indirect mechanism of interactions between NPs and BECs could be suggested. It is likely that soluble mediators interacts with

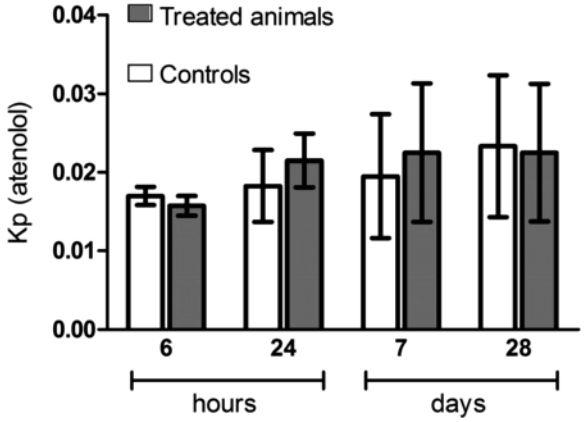

Fig. 7 BBB integrity assessment. The integrity was estimated by the ratio between atenolol concentrations in brain and plasma (partition coefficient or Kp) at 6 h, 24 h, 7 days and 28 days after IV administration. Each data point represents the mean ± SD of n = 4 rats. Statistical comparison was performed by two-way ANOVA

their BBB targets and elicit BECs activation and neurovascular inflammation. For example, pro-inflammatory mediators such as TNFα distributed through the systemic circulation affect ABC transporter expression and activity [44, 45]. We thus suggest that 28 days after exposure, circulating cytokines and chemokines released probably by organs containing high amounts of Ti induce activation of BECs and initiate the release of IL-1β, IP-10 and CXCL1, which act in a paracrine way to activate astrocytes/microglia cells in the brain parenchyma. Immunofluorescence staining revealed an increase of IL-1β in the rostral and caudal diencephalon (Fig. 10). Because of its massive and biopersistence of Ti, liver could be a key organ for induction of oxidative stress, lipid composition modifications, and immune response as reported elsewhere [25, 46–48]. Mediators such as cytokines, chemokines and lipids circulating in the blood may be responsible indirectly for BBB deregulation at late end points. Transposition of the effect evidenced at the BBB on other endothelial cells by blood circulating factors could not be excluded.

Circulating serum factors from rats treated with TiO_2 NPs induce an inflammatory response in a cell-based BBB model

To demonstrate whether circulating cytokines/mediators that may be released by organs bioaccumulating Ti can lead to neurovascular inflammation and BBB physiology alterations, we performed *in vitro* studies on the primary rat cell-based BBB model described previously [26]. The model was exposed to diluted sera from untreated and treated animals collected 28 days after exposure to TiO_2 NPs. Exposure of the apical compartment mimics blood-borne exposure. After 24 h of exposure to serum, the integrity of the BECs monolayer was checked and BECs and glial cells were recovered for mRNA profiling.

After 24 h of exposure, the integrity of the BECs monolayer remained intact in the control group as well as in the treated group (Fig. 11f), thus confirming the maintenance of BBB integrity observed 28 days after exposure *in vivo* (apparent permeability (P_{app}) for Lucifer Yellow (LY) was 2.08 ± 0.99 cm/s for controls vs 2.17 ± 0.77 cm/s for the treated group). In BECs, we noted a tendency of increase for occludin mRNA expression ($P = 0.057$), which is in accordance with *in vivo* observations. The mRNA expressions of IL6, CXCL1 and glial fibrillary acid protein (GFAP) in astrocytes were upregulated. These inflammatory markers are key proteins for communication between glial and BECs [49–54]. This *in vitro* mRNA upregulation in glial cells of the BBB model suggests that the mediators are present 28 days after exposure in the serum of treated rats and allows to consolidate our hypothesis of circulating mediators.

Conclusions

The major findings of our study are depicted in Fig. 12 and Fig. 3d. They show a Ti burden in the liver, spleen and lungs up to 356 days after IV administration of TiO_2 NPs to rats, with very low clearance rate observed until one year after administration. Additionally, we describe for the first time the *in vivo* uptake and clearance by BECs of TiO_2 NPs after exposure. Furthermore, this is the first study reporting the link between deregulation of BBB physiology and the presence of TiO_2 NPs in distal organs. Upregulation of tight junction proteins, modulation of P-gp mRNA expression and persistent brain inflammation markers such as IL-1β, IP-10 and CXCL1 were highlighted. Thus, regardless of where the peripheral signal originates from, our findings raise the question of circulating biomarkers potentially released by organs accumulating Ti to promote dysregulation of BBB physiology and neuroinflammation. Substantial research remains to be done to identify such peripheral biomarkers. Our findings point out for the first time that TiO_2 NPs can exert indirect effect on the CNS that seems dependent on the circulation.

Materials and methods

Chemicals

Human serum, bovine serum albumin (BSA), N-alpha-tosyl-L-lysinyl-chloromethylketone (TLCK) and Lucifer yellow (LY), Digoxin, Prazosin, Atenolol and Atenolol-d7 were from Sigma Aldrich (Saint-Quentin Fallavier, France). Collagenase/dispase and DNAse I were from Roche Applied Science (Basel, Switzerland). Digoxien-d3 was from Artmolecule (Poitier, France).

All chemicals used for ICP-MS were of analytical grade. Nitric acid was used to prepare 0.2 % HNO_3 (*v/v*) with ultrapure water. All single element stock solutions

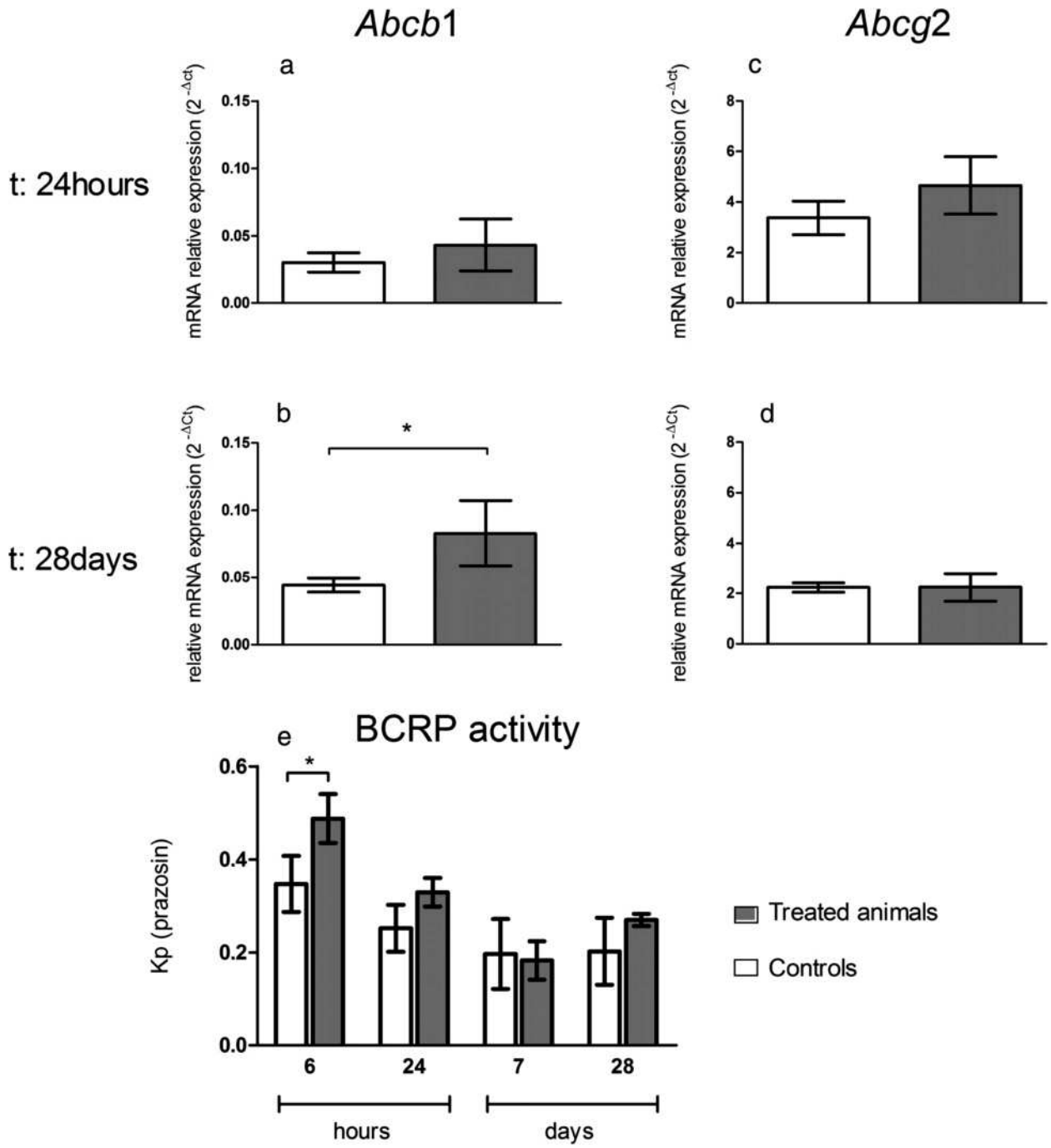

Fig. 8 mRNA expression of transporters *Abcb1* (P-gp) and *Abcg2* (BCRP) transporters in isolated brain microvasculature endothelial cells and BCRP activity assessment at the BBB after IV injection of 1 mg/kg TiO_2 NPs in rats. mRNA transcription profiles for *Abcb1* (**a; b**) and *Abcg2* (**c; d**) were performed by RT-qPCR in isolated rat brain microvasculature endothelial cells of control and treated animals. Each data point represents the mean ± SEM of n = 4 animals and RT-qPCR was performed in duplicate for each single preparation of brain microvasculature endothelial cells. Statistical comparison was performed by two tailed Mann-Whitney test, $^{*}P < 0.05$. BCRP activity (**e**) was estimated by the ratio between prazosin concentrations in brain and plasma (partition coefficient or Kp). Each data point represents the mean ± SD of n = 4 rats. Statistical comparison was performed by two-way ANOVA, $^{*}P < 0.05$

(1000 mg/L) were delivered by SCP Science and certified for purity and concentration. From these stock solutions, a mixed working standard solution with a concentration of 10 mg/L for each element was prepared by putting 1 mL of each stock solution in a 100 mL measuring flask, adding 5 mL of purified

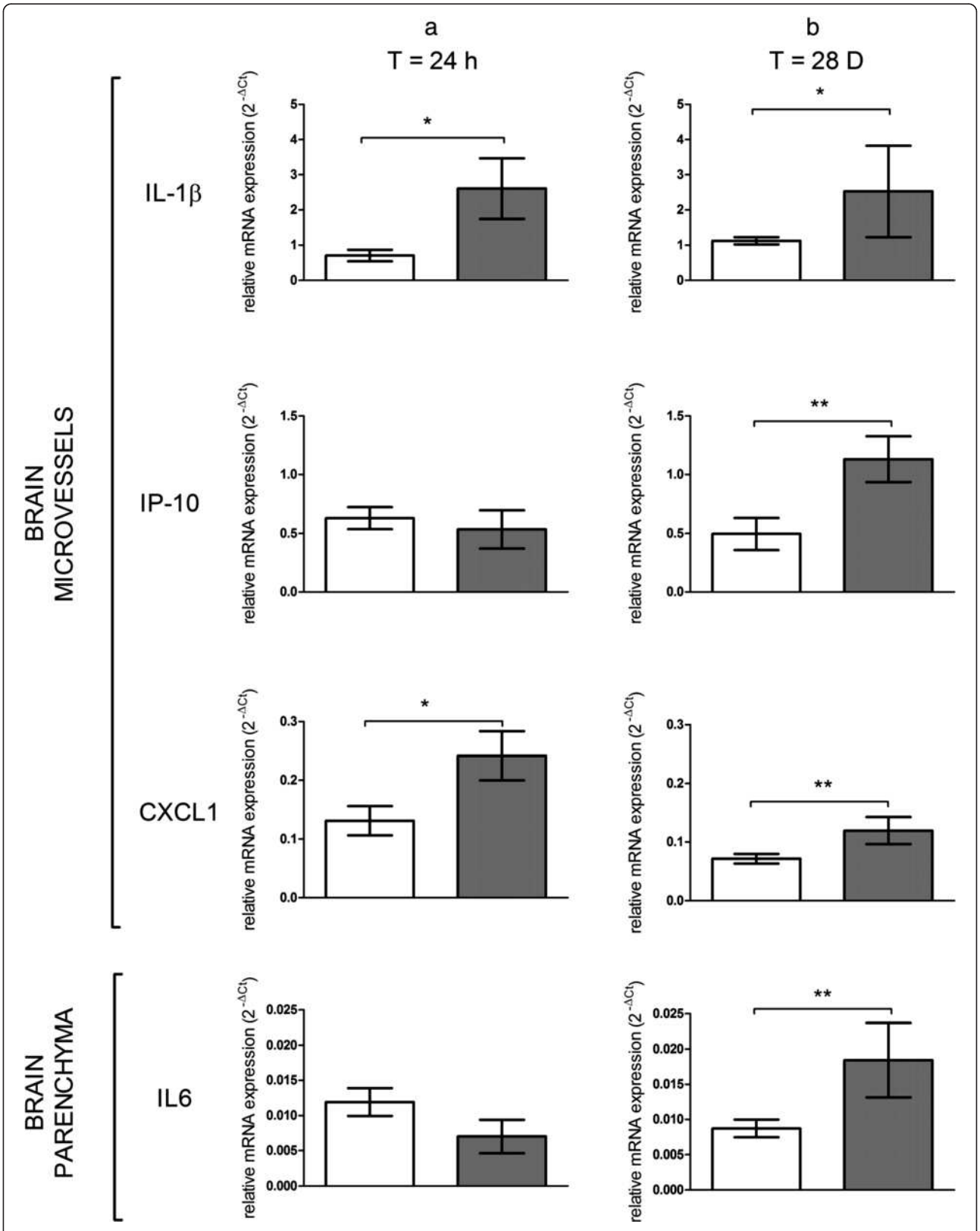

Fig. 9 (See legend on next page.)

(See figure on previous page.)
Fig. 9 mRNA expression of cytokines and chemokines in isolated brain microvasculature endothelial cells and parenchyma fraction after IV injection of 1 mg/kg TiO_2 NPs in rats. mRNA transcription profiles for IL-1β, IP-10 and CXCL1 in isolated rat brain microvasculature endothelial cells and IL6 in parenchyma fractions of control and treated animals performed by RT-qPCR at 24 h (**a**) and 28 days (**b**) after IV injection. Each data point represents the mean ± SEM of n = 4 animals and RT-qPCR were performed in duplicate for each single preparation of brain microvasculature endothelial cells. Statistical comparison was performed by one tailed Mann Whitney test, *$P < 0.05$; ** $P < 0.01$

HNO_3 and diluting to 100 mL with ultrapure water (MilliQ, Millipore, Germany).

TiO_2 nanoparticles

TiO_2 P25 NPs (Aeroxide® P25, 75 % anatase 25 % rutile, Evonik®) were from Sigma Aldrich (Saint-Quentin Fallavier, France). For *in vivo* experiments, TiO_2 NPs were suspended in sterile physiological salt solution at a stock concentration of 1 mg/mL. No other treatment was performed. A thorough characterization of NPs was conducted through a panel of complementary techniques. NPs were imaged by Transmission Electron Microscopy (TEM) with a JEOL 1400 instrument (JEOL, Tokyo, Japan) operating at 80 keV (Imagif platform, Gif-sur-Yvette) and Scanning Electron Microscopy (SEM) (Carl Zeiss, Ultra 55) equipped with an Energy Dispersive X-ray spectrometer (EDX) allowing elemental analysis. For both TEM and SEM analyses, samples were prepared as follows: 3 μL droplet of the dispersion was cast on formvar/ carbon-coated copper grids for 5 min. The Brunauer-Emmett-Teller (BET) method (Micromeritics FlowsorbII 2300) was applied to determine the specific surface area (SSA) of the nanopowder and diameter was calculated from the SSA value, as $D = 6\ 000/(\rho.SSA)$, where D is BET diameter (nm), and $\rho = 3.9\ g.cm^{-3}$ is the density of anatase TiO_2. The crystalline phases were measured by X-Ray Diffraction (XRD) with a Siemens D5000 instrument using the Cu-Kα radiation and using the Match software (crystal impact). Hydrodynamic diameter was measured by Dynamic Light Scattering (DLS) using a ZetaSizer ZEN3600 (Malvern, Herenberg, Germany) equipped with a 633 nm laser.

Animals and intravenous TiO_2 NPs administration protocol

Male Fisher F344 rats (from Charles River Laboratories, France), 8 weeks old and weight 180–250 g, were housed in standard environmental conditions (room humidity and temperature controlled 19 °C–23 °C; room under a 12 : 12 h light dark cycle) and maintained with free access to water and standard laboratory diet. The control animals were injected intravenously via the tail vein with 1 mL/kg of sterile saline buffer and the treated animals were injected with TiO_2 NPs suspension at the dose of 1 mg/kg. TiO_2 NPs suspension was vortex for 5 min before administration. No other dispersion protocol was used to avoid false positive results that would be due to inappropriate handling of the dispersion protocol of NPs.

30 min, 1 h, 2 h, 6 h, 24 h, 7 days, 28 days, 90 days or 356 days after IV injection, animals were anesthetized with isoflurane and euthanized. Additional time points at 5 min and 15 min was set up for brain and blood collection. Blood, liver, brain, spleen, kidneys and lungs were collected and stored at −80 °C until assayed. All procedures were approved by the CEA Institute's Animal Care and Use Committee and conform to the Guide for the Care and Use of Laboratory Animals published by the European community's council (directives 86/609/EEC, November 24, 1986), and the French directives concerning the use of laboratory animals (February 2013).

Sample Preparation and Ti analysis by ICP-MS

Tissues from 6 controls and 6 treated rats were used for biodistribution studies. Tissues were thawed and about 0.1–0.3 g of each tissue was weighed, digested and analyzed for Ti content. Each sample was added to a 55 mL microwave digestion vessel along with 8 mL of nitric acid and 2 mL of hydrofluoric acid and digested using a Microwave Assisted Reaction System (MARS) Express instrument. The microwave digestion program was 15 min; 150 °C; 1200 W then 15 min; 180 °C; 1200 W followed by 20 min cooling. After cooling, the sample was rinsed 3 times using approximately 20 mL of 2 % nitric acid solution in a polytetrafluoroethylene (PTFE or Teflon) beaker. 2 mL of hydrogen peroxide was added to each beaker to digest any remaining organic matter. The beaker was then heated on a hot plate at 180 °C until between 0.1 and 0.5 mL of solution remained. The beakers were removed from the hot plate, allowed to cool and rinsed 3 times with 2 % nitric acid solution into a 25 mL volumetric flask before being stored for analysis. Samples were refrigerated at −20 °C while not in use.

This digestion method was evaluated for the recovery of a known amount of TiO_2 and the ability to digest organic material sufficiently for analysis. The method was applied to a number of blank samples, containing only the reagents and no sample, in order to measure the amount of Ti contamination.

Analysis of Ti with ICP-MS

Ti standard solutions for ICP-MS calibration were prepared at concentrations of 2, 4, 8, 10, 30, 50 and 100 ng/

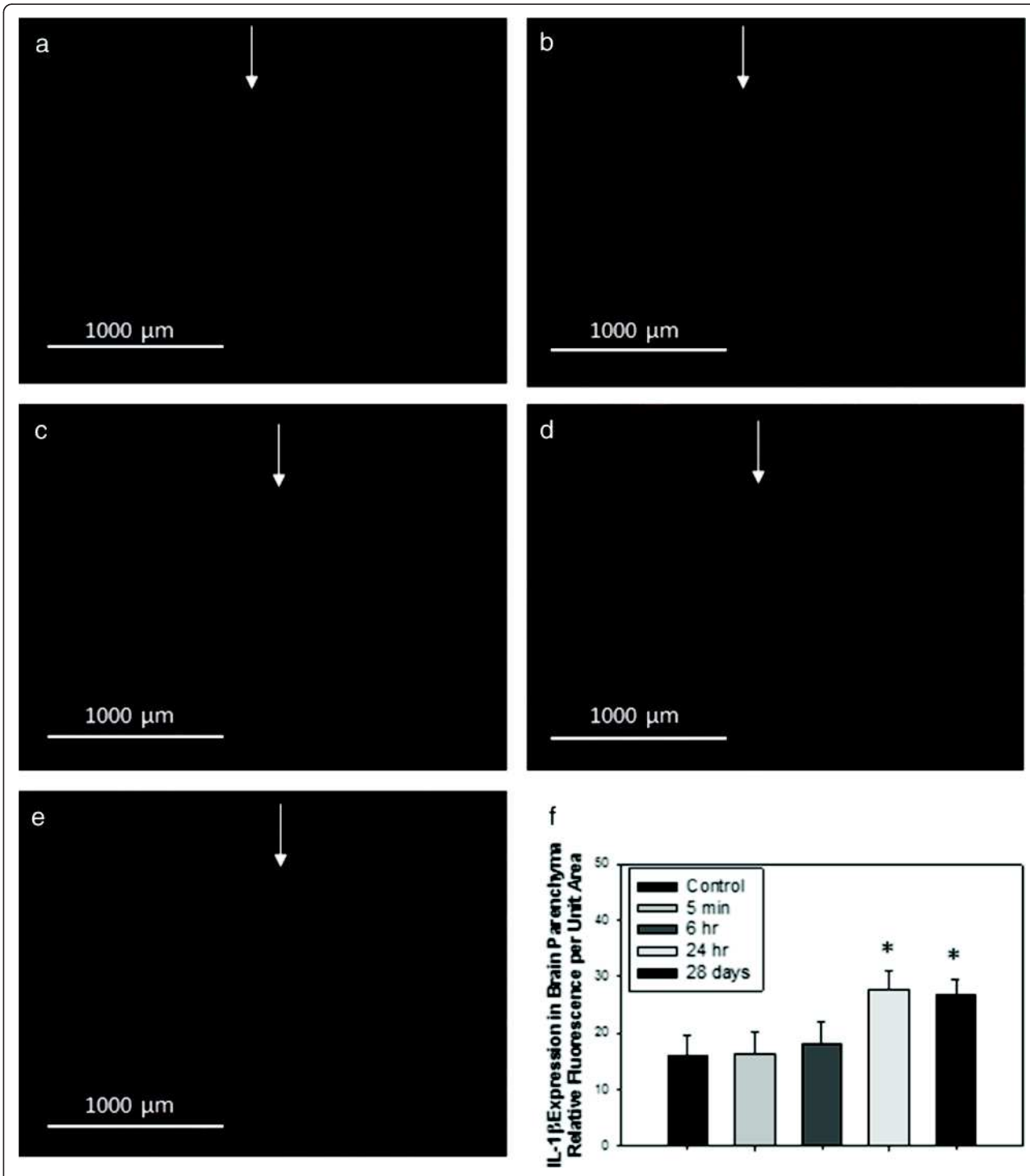

Fig. 10 Representative images of immunofluorescence expression of IL-1β in the cerebral parenchyma of (**a**) control rats, or tissues collected from rats treated with 1 mg/kg TiO_2 (IV) at (**b**) 5 min; (**c**) 6 h; (**d**) 24 h; or (**e**) 28 days post-treatment. Arrows indicate sagittal suture (coronal cut, sections cut and analyzed between rostral and caudal diencephalon). Graph in (**f**) shows analysis of relative fluorescence of overlay images ± SD. *$P < 0.050$ compared to controls

L, by diluting a 1 g/L Ti standard stock solution (1.70363.0100, SCP Science) with 2 % *v/v* HNO_3 and 0.01 % *v/v* Triton X-100. An internal standard solution, containing 25 μg/L of Ge was prepared by diluting a 1000 mg/L internal standard stock solution (1.70320.0100, Merck) with 2 % *v/v* HNO_3. The internal standard (25 μg/

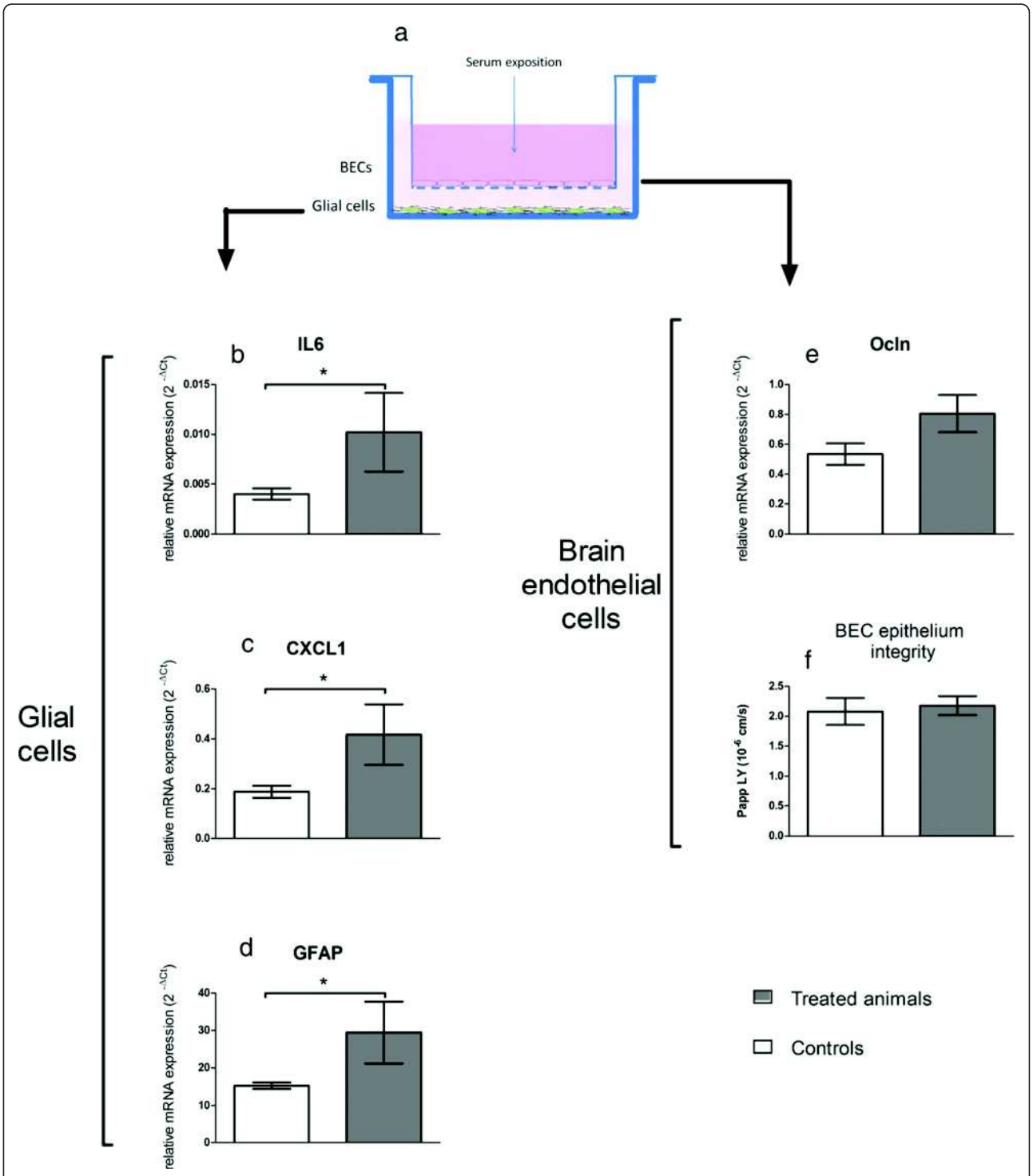

Fig. 11 Impact of exposure to sera from treated animals on the *in vitro* BBB model. (**a**) is a schematic view of the model architecture. BECs were grown on a semipermeable membrane whereas glial cells lay on the well bottom. mRNA expressions were quantified by RT-qPCR after 24 h exposure to sera from control and treated rats. For glial cells, expressionsof cytokines and chemokines (IL6 (**b**), CXCL1 (**c**)) and of GFAP (**d**) are presented. For BECs, tight junction protein occludin (Ocln (**e**)) is reported and integrity of the BECs monolayer was checked in terms of apparent permeability to Lucifer yellow (**f**). Sera diluted in culture medium were applied to the BECs compartment for 24 h. Each data point represents the mean ± SEM of n = 4 samples, each sample representing the mRNA pool from 6 wells. RT-qPCR was performed in duplicate for each single sample. Statistical comparison was performed by one tailed Mann Whitney test, * $P < 0.05$ for IL-6, CXCL1 and GFAP mRNA expressions. Statistical comparison was performed by two tailed Mann Whitney test for Ocln mRNA expression ($P = 0{,}057$)

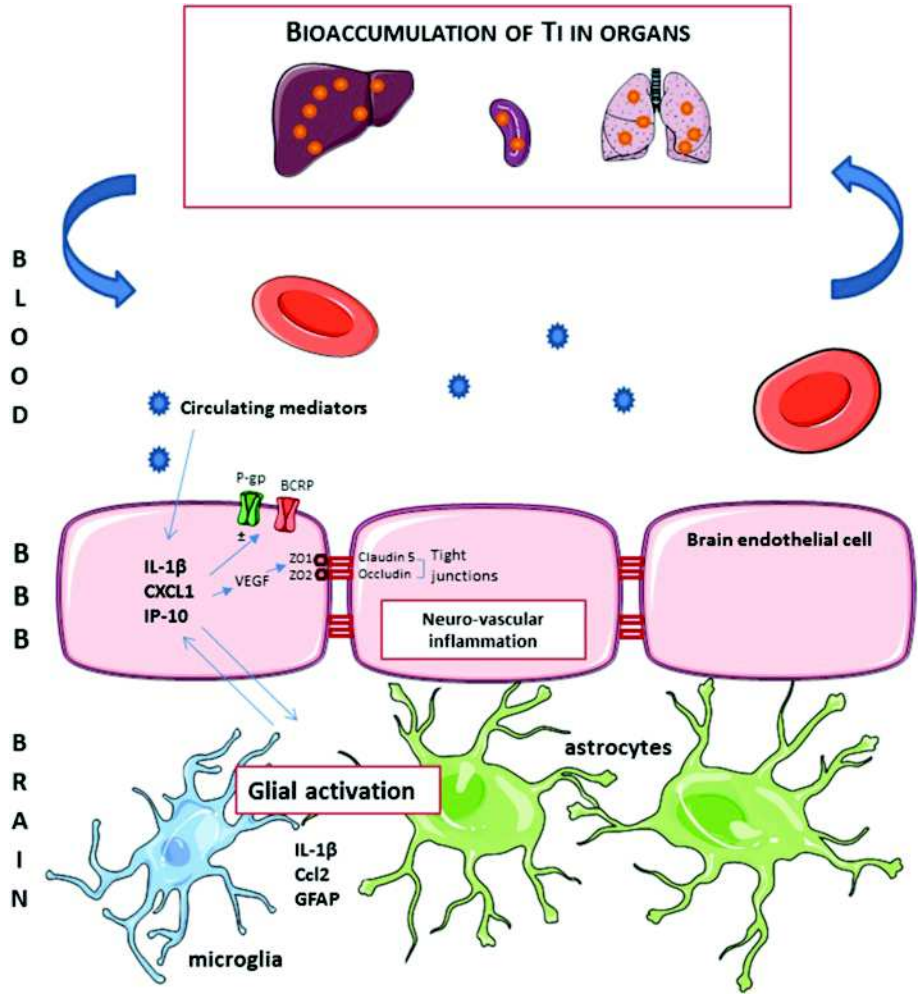

Fig. 12 Schematic summary of the events and potential effects on BBB physiology in the case of bioaccumulation of TiO_2 NPs in organs. Exposure to circulating mediators that maybe originate from organs bioaccumulating titanium leads to neurovascular inflammation. Overexpression of IL-1β, CXCL1 and IP-10 may contribute to modification of brain endothelial cell physiology in terms of expression of tight junction proteins (occludin and claudin-5) and ABC transporters (P-gp and BCRP). In parallel, key inflammatory markers for glial and endothelial cells interactions were upregulated

L Ge) was added in all samples and standards. Ti analysis of acidified samples was carried out using a Varian 820-MS. Samples in 2 % *v/v* HNO_3 were directly analyzed with the Varian-820-MS for Ti determination.

BBB permeability and P-Glycoprotein and BCRP transport activity measurement

Four hours before sacrifice, 4 control and 4 treated rats were subcutaneously implanted with mini-osmotic pumps (Alzet model 2001D; DURECT Corp., Cupertino, California). Pumps were filled with atenolol, digoxin and prazosin dissolved in PEG200/DMSO (50/50) to deliver at 0.25 mg/kg/h, 0.5 mg/kg/h or 0.25 mg/kg/h rates, respectively. The relevance of distribution study of atenolol, digoxin and prazosin in plasma and brain for BBB integrity and transport function assessment was previously demonstrated [26, 29]. 6 h, 24 h, 7 d or 28 d after IV injection, animals were anesthetized with isoflurane and euthanized. Plasma samples and brain were collected and weighed immediately after death. The administered substrates were quantified in the two compartments using mass spectrometry coupled with liquid chromatography (LC/MS). BBB integrity was estimated by the ratio of atenolol brain to plasma concentration (C_{brain} and C_{plasma}, respectively). This ratio is described by the partition coefficient (Kp).

$$Kp = \frac{C_{brain}}{C_{plasma}}$$

The P-gp and BCRP transport activities were estimated by means of the digoxin and prazosin Kp, respectively.

LC/MS assay for digoxin, prazosin and atenolol quantification

Brains were mixed in ultrapure water (2 mL/g of tissue) using an Ultraturrax T65 system (IKA-Werke, Staufen, Germany). Extract suspensions (400 μL) were submitted to protein precipitation with 1 mL of methanol previously spiked with internal standard (digoxin-d3 and atenolol-d7 4 μg/mL). After centrifugation (20000 g; 15 min; 4 °C) the supernatant was dried under nitrogen at 40 °C. The dried extracts were resuspended in 1 mL 0.75 M NH_4OH / methanol (80:20 *v/v*). Plasma (150 μL) was diluted with 150 μL of 0.75 M NH_4OH / methanol (80:20 *v/v*) previously spiked with internal standard. Both brain and plasma extracts were submitted to solid-liquid extraction on isolute SLE+ columns 1 or 6 mL (Biotage). The two eluates (3 mL of dichloromethane/isopropanol (70:30 *v/v*) then 3 mL of dichloromethane/isopropanol (70:30 *v/v*) + 0.2 % formic acid) were pooled and evaporated to dryness. The dry extracts were resuspend in 200 μL of 5 mM ammonium acetate/methanol (95:5 *v/v*). Chromatography was performed using a Shimadzu HPLC system LC 20 AD on a Kinetex C18 column (Phenomenex). The total run time was 5 min and the flow rate was 0.4 mL/min. Analyte (20 μL) was injected onto the column placed in an oven at 40 °C.

Detection was done by tandem mass spectrometry (Finnigan TSQ Quantum Discovery with Xcalibur and LC Quan softwares, Thermo) in positive electrospray mode. Tuning parameters were: capillary voltage 3 kV, source temperature 200 °C. The multiple reaction monitoring transitions for analytes were as follows: m/z digoxin 798.5 > 651.4, m/z prazosin 384.19 > 247.14, m/z atenolol 267.18 > 145.1. Analytes were quantified by means of calibration curves using digoxin-d3 or atenolol-d7 as internal standard. For plasma and brain extract assay, calibration ranges were from 1.0 to 200 ng/mL.

Isolation of brain microvasculature endothelial cells

Rat brain capillaries were isolated as described previously [26, 55]. 6 rats from three relevant time groups (5 min; 2 h and 28 days) were used. Brains were extracted and stored in Hanks balanced salt solution (HBSS) supplemented with 1 % (*v/v*) PSN on ice. The remainder of the isolation took place under aseptic conditions. The brains were cut sagittally into two halves and the cerebral cortices emptied of white matter. The meninges and the associated vessels were cleaned off by rolling on Whatman 3 mm chromatography paper. The homogenized tissue was pelleted by centrifugation at 1500 rpm for 5 min. The pellet containing the microvessels was digested in HBSS-1 % PSN solution, 1 mg/mL collagenase/dispase, 10 U/μL DNase-I, and 1 μg/mL TLCK for 1 h at 37 °C. Digested tissue was then pelleted by centrifugation at 1500 rpm for 5 min at 4 °C. To remove myelin, the pellet was resuspended in 20 % (*w/v*) BSA in HBSS-1 % PSN solution and centrifuged at 2800 rpm for 30 min. The resulting floating white matter corresponding to the brain parenchyma fraction and centrifugation medium were removed carefully. The microvessel pellets were washed then frozen at −80 °C. The remaining parenchyma fraction was resuspended in centrifugation medium then half-dissolved in HBSS-1 % PSN solution and pelleted by centrifugation at 1500 rpm for 15 min. The brain parenchyma pellet was then washed several times before being frozen at −80 °C.

Cell culture

Rat primary BECs and glial cells were isolated and cultured as previously described [26]. Briefly, for BECs, brain tissues were digested enzymatically (1 g/L collagenase/dispase, 20 U/mL DNAse I, 0.147 mg/L TCLK in HBSS, 1 h at 37 °C). A 20 % BSA gradient was used for isolation of capillaries. After a second enzymatic digestion, cells were plated in 75 cm^2 coated culture flasks in EBM medium completed by the EGM-2 MV SingleQuots kit (Lonza, Basel, Switzerland). Cultures were maintained at 37 °C in a humidified 5 % CO_2 atmosphere for 5–6 days before being trypsinized and frozen.

BBB cell-based model

For BBB modeling, glial cells were seeded at a density of 5700 cells/cm^2 on transwell plates in a glial-specific basal medium as previously reported [26]. BECs were plated on the upper side of a coated polyester transwell membrane (pore size 0.4 mm, Costar, Dutscher sa, Brumath, France) at a density of 71400 cells/cm^2 in a BEC-specific medium. Microplates were then incubated at 37 °C in a humidified 5 % CO_2 atmosphere for 5 to 7 days before treatment. Upper and lower chambers will be referred to as apical and basal compartments, respectively, throughout this manuscript. 4 sera from controls and 4 sera from treated animals were tested. Each collected serum from controls and treated animals were diluted at 1/16 in the BEC medium. BECs were exposed to diluted rat serum in the apical compartment for 24 h. Transport experiments were performed in six wells for each serum.

Transport experiments

After exposure to sera, exposure medium were removed then transwells with BECs were transferred to new plates. 0.5 and 1.5 mL of transfer buffer (150 mM NaCl, 5.2 mM KCl, 2.2 mM $CaCl_2$, 0.2 mM $MgCl_2$, 6 mM $NaHCO_3$, 2.8 mM glucose and 5 mM Hepes) was added to the apical and basolateral compartments or donor and acceptor chambers, respectively. Lucifer yellow (LY) was added to the donor chamber to a final concentration

of 0.1 mM and, after 30 min, aliquots from acceptor and donor chambers were collected for determination of tracer concentration by fluorescence counting. The apparent permeability (P_{app}) value for LY was calculated as follows:

$$P_{app} = dQ = dT \times A \times C_0$$

where dQ/dT is the amount of LY transported per time-point, A is the membrane surface area and C_0 the initial donor concentration. The mass balance (R) was calculated as:

$$R(\%) = 100 \times [(A + D)/D_0]$$

where A and D are the amounts of LY in the acceptor and donor chambers and D_0 is the amount introduced at t: 0. Mass balances of LY were between 80 and 120 %. As LY permeability values on the order of 10^{-6} cm/s were obtained previously in various *in vitro* BBB models [33, 56–58] , we considered that beyond 5.10^{-6} cm/s the monolayer is disrupted.

Transcription profiling

RNA was isolated from rat BECs, brain parenchyma fraction or cells isolated from the BBB *in vitro* model using the RNeasy plus universal tissue minikit or the RNeasy Mini kit, respectively (Qiagen, France), according to the manufacturer's instructions. The concentration and purity of the RNA samples were assessed spectrophotometrically at 260 and 280 nm using the NanoDrop ND-1000 instrument (NanoDrop Technologies, Wilmington, DE, USA). The A260/280 ratio ranged between 1.8 and 2.

A sample of 0.5 μg of total RNA was converted to cDNA with random primers in a total of 10 μL using an RT2 first stand kit (Qiagen, France). The cDNA was diluted with DNA/RNAse-free distilled water to a volume of 110 μL.

The quantitative expression of various cytokines, chemokines, transporters and structural proteins was determined using 0.4 μM cDNA for each primer set in the RT2 Pathway Focus profiler array from Qiagen. The RT2 Profiler array consists of a previously validated qRT-PCR primer set (1 μL) for relevant cytokines, chemokines: Il-1β, CXCL1 and IP-10; tight junction proteins: Cldn5 and Ocln; ABC transporters: *Abcb1* and *Abcg2* and housekeeping genes (Hprt, GAPDH). Thermocycling was carried out in a CFX96 real-time PCR detection system (Bio-Rad) using SYBR green fluorescence detection. The final reaction mixture contained 2 μL of diluted cDNA, 1 μL of one of the specific primer, 12.5 μL of distilled water and 9.5 μL of SYBR green master mix. The specific amplification conditions were 2 min at 50 °C, 10 min at 95 °C followed by 40 amplification cycles at 95 °C for 0.5 min, and 60 °C for 1 min to reinitialize the cycle again. The specificity of each reaction was also assessed by melting curve analysis to ensure the presence of only one product. Relative gene expression values were calculated as $2^{-\Delta CT}$, where ΔCT is the difference between the amplification curve (CT) values for genes of interest and housekeeping genes (hypoxanthine guanine phosphoryltransferase or Hprt; glyceraldehyde phosphodehydrogenase or GAPDH). If the CT was higher than 35, we considered the expression level too low to be applicable.

Immunofluorescence

Brain sections embedded in OCT and cut on a cryostat (10 μm) were prepared for either occludin or claudin-5, and von Willebrand factor (vWF) double immunofluorescence, or IL-1β. Brain sections were air-dried for 30 min and fixed in ice-cold acetone for 30 min and then rinsed in PBS. Sections were then incubated with 3 % BSA for 60 min at RT, rinsed in PBS, and incubated with 150 μL per section of the appropriate primary antibody (occludin: 1:1000, Abcam, Cambridge, MA; clauin-5: 1:100, Invitrogen/Life Technologies, Carlbad, CA) and an FITC-tagged vWF (1:1000 dilution, Abcam) or IL-1β (1:1000, Abcam) alone; diluted in wash buffer [1 part 5 % blocking solution (0.5 mL normal rabbit serum in 10 mL 3 % *w/v* bovine serum albumin) and 4 parts phosphate-buffered saline (PBS)] for 1 h at room temperature (RT) and then rinsed 3 times with PBS. The slides were incubated in 150 μL per section of the appropriate secondary antibody with either Alexa Fluor 555 or Alexa Fluor 546 (1:1000 dilution, Vector Laboratories, Biovalley, Marne la Vallée, France) in the dark for 1 h at RT. Slides were rinsed 3 times in PBS and subsequently incubated with Hoechst nuclear stain (1 μL/mL; 150 μL/section) for one minute, rinsed again then coverslipped with Aqueous Gel Mount (TBS, Fisher Scientific, Waltham, MA). Slides were imaged by fluorescence microscopy at 10x and 40x, using the appropriate excitation/emission filters, digitally recorded, and analyzed by image densitometry using Image J software (NIH). A minimum of 3 locations on each section (2 sections per slide), 3 slides and n = 3 per group were processed/analyzed. Only vessels >50 μm were used for analysis.

Statistical Analysis

Analyses were performed using the Prism 5.1 program (GraphPad Software, Inc, San Diego CA). Statistical comparisons conducted herein were accomplished using variance analysis (two-way ANOVA) two determinants being time and treatment for organs Ti distribution followed by the Bonferroni post test. mRNA expression of cytokines and chemokines were analyzed using one tailed Mann-Whitney test and two tailed Man Whitney

test for other mRNA expressions (tight junctions proteins and transporters). Immunofluorescence end points were analyzed using one-way ANOVA between treatment groups followed by the Holm-Sidak post hoc test (SigmaPlot SyStat Software Inc, San Joes, CA) and data were expressed as mean ± SD. Changes were considered statistically significant at $P < 0.05$.

Additional files

Additional file 1: BBB integrity assessment after IV injection of 10 mg/kg TiO_2 NPs in rats. BBB integrity was estimated by the ratio between atenolol concentrations in brain and plasma (partition coefficient or Kp). Each data point represents the mean ± SD of n = 8 rats. Statistical comparison was performed by two tailed Mann-Whitney test, * $P < 0.05$. (TIFF 4945 kb)

Additional file 2: Effect of 24 h TiO_2NPs exposure on BEC epithelium integrity. TiO_2 NPs concentrations from 0 to 100 μg/mL were applied to the apical pole of the *in vitro* BBB model for 24 h. Data are apparent permeability coefficient of sucrose. Each data point represents the mean ± SD of at least 2 experiments. The horizontal dotted line represents the usual limit value of 8.3 10^{-6} $cm.s^{-1}$ beyond which the BEC monolayer is considered to be disrupted. The blue zone represents sucrose apparent permeability coefficient for the controls (Mean ± SD). (TIFF 61 kb)

Abbreviations

TiO_2NPs: Titanium dioxide nanoparticles; CNS: Central nervous system; IV: Intravenous; IL-1β: Interleukin-1β; CXCL1: Chemokine Ligand 1; IP-10: Gamma inductible protein-10; BECs: Brain endothelial cells; P-gp: P-glycoprotein; BCRP: Breast cancer resistance protein; TEM: Transmission electron microscopy; SEM: Scanning electron microscopy; EDX: Energy dispersive X ray; BET: Brunauer-Emmett-Teller; DLS: Dynamic light scattering; ICP-MS: Inductively couple plasma mass spectrometry; LOQ: Limit of quantification; Kp: Partition coefficient; P_{app}: Apparent permeability; LY: Lucifer yellow; GFAP: Glial fibrillary acid protein; RT: Room temperature; TNF-α: Tumor Necrosis Factor - α; TNF-R1: Tumor necrosis factor receptor 1.

Competing interest

The authors declare that they have no competing interests.

Author's contributions

CD participated in the design of the studies, animal experiments, *in vitro* BBB studies, real-Time RT PCR studies and LC/MS/MS studies. JD and MC carried out titanium quantification studies in biological samples and analyzed final data. AC coordinated in vitro BBB studies, NH and EB carried out titanium dioxide nanoparticles characterization studies. AL participated in the study design and oversaw immunohistochemistry studies. AM conceived of the study, participated in its design and coordination and assisted with drafting the manuscript. All authors read and approved the final manuscript prior to submission.

Acknowledgements

The authors would like to thank Emilie Jaumain for her contribution in animal experiments and Gael Noyalet for LC-MS analyse. The authors would like to thank JoAnn Lucero for her contribution to this manuscript in processing and analyzing the samples for immunofluorescence. This research was supported by the University of North Texas Department of Biology. This work has benefited from the facilities and expertise of the Imagif Cell Biology Unit of the Gif campus (www.imagif.cnrs.fr).

Author details

[1]CEA, Direction des Sciences du Vivant, iBiTec-S, Service de Pharmacologie et d'Immunoanalyse, Equipe Pharmacologie Neurovasculaire, 91191 Gif-sur-Yvette, France. [2]INRS, Département Polluants et Santé, Rue du Morvan, CS 60027, 54519 Vandœuvre Cedex, France. [3]DSM, IRAMIS, NIMBE (UMR 3685), laboratory of Nanometric Structures, CEA Saclay, 91191 Gif/Yvette, France. [4]Laboratoire de Chimie Physique, UMR CNRS 8000, Université de Paris-Sud, 91405 Orsay, France. [5]Department of Biological Sciences, University of North Texas, Denton, TX, USA.

Received: 30 April 2015 Accepted: 24 August 2015
Published online: 04 September 2015

References

1. Chen X, Mao SS. Titanium dioxide nanomaterials: synthesis, properties, modifications, and applications. Chem Rev. 2007;107:2891–959.
2. Weir A, Westerhoff P, Fabricius L, Hristovski K, von Goetz N. Titanium dioxide nanoparticles in food and personal care products. Environ Sci Technol. 2012;46:2242–50.
3. Peters RJB, van Bemmel G, Herrera-Rivera Z, Helsper HPFG, Marvin HJP, Weigel S, et al. Characterization of titanium dioxide nanoparticles in food products: analytical methods to define nanoparticles. J Agric Food Chem. 2014;62:6285–93.
4. Brun E, Barreau F, Veronesi G, Fayard B, Sorieul S, Chaneac C, et al. Titanium dioxide nanoparticle impact and translocation through ex vivo, in vivo and in vitro gut epithelia. Part Fibre Toxicol. 2014;11:13.
5. Shi H, Magaye R, Castranova V, Zhao J. Titanium dioxide nanoparticles: a review of current toxicological data. Part Fibre Toxicol. 2013;10:15.
6. Iavicoli I, Leso V, Bergamaschi A. Toxicological effects of titanium dioxide nanoparticles: a review of in vivo studies. Journal of Nanomaterials. 2012;15(5):481–508.
7. Abbott NJ, Ronnback L, Hansson E. Astrocyte-endothelial interactions at the blood-brain barrier. Nat Rev Neurosci. 2006;7:41–53.
8. Abbott NJ, Patabendige AAK, Dolman DEM, Yusof SR, Begley DJ. Structure and function of the blood-brain barrier. Neurobiol Dis. 2010;37:13–25.
9. Abbott NJ, Friedman A. Overview and introduction: the blood-brain barrier in health and disease. Epilepsia. 2012;53:1–6.
10. Abbott NJ. Blood-brain barrier structure and function and the challenges for CNS drug delivery. J Inherit Metab Dis. 2013;36:437–49.
11. Keller A. Breaking and building the wall: the biology of the blood-brain barrier in health and disease. Swiss Med Wkly. 2013;143:w13892.
12. Begley DJ. ABC transporters and the blood-brain barrier. Curr Pharm Des. 2004;10:1295–312.
13. Loscher W, Potschka H. Role of drug efflux transporters in the brain for drug disposition and treatment of brain diseases. Prog Neurobiol. 2005;76:22–76.
14. Omidi Y, Barar J. Impacts of blood-brain barrier in drug delivery and targeting of brain tumors. BioImpacts. 2012;2:5–22.
15. Fabian E, Landsiedel R, Ma-Hock L, Wiench K, Wohlleben W, van Ravenzwaay B. Tissue distribution and toxicity of intravenously administered titanium dioxide nanoparticles in rats. Arch Toxicol. 2008;82:151–7.
16. Shinohara N, Danno N, Ichinose T, Sasaki T, Fukui H, Honda K, et al. Tissue distribution and clearance of intravenously administered titanium dioxide (TiO(2)) nanoparticles. Nanotoxicology. 2013;8(2):132–41.
17. Xie G, Wang C, Sun J, Zhong G. Tissue distribution and excretion of intravenously administered titanium dioxide nanoparticles. Toxicol Lett. 2011;205:55–61.
18. Geraets L, Oomen AG, Krystek P, Jacobsen NR, Wallin H, Laurentie M, et al. Tissue distribution and elimination after oral and intravenous administration of different titanium dioxide nanoparticles in rats. Part Fibre Toxicol. 2014;11:30.
19. Wang J, Zhou G, Chen C, Yu H, Wang T, Ma Y, et al. Acute toxicity and biodistribution of different sized titanium dioxide particles in mice after oral administration. Toxicol Lett. 2007;168:176–85.
20. Wang J, Chen C, Liu Y, Jiao F, Li W, Lao F, et al. Potential neurological lesion after nasal instillation of TiO(2) nanoparticles in the anatase and rutile crystal phases. Toxicol Lett. 2008;183:72–80.
21. Takahashi Y, Mizuo K, Shinkai Y, Oshio S, Takeda K. Prenatal exposure to titanium dioxide nanoparticles increases dopamine levels in the prefrontal cotex and neostriatum of mice. J Toxicol Sci. 2010;35:749–56.
22. Shin JA, Lee EJ, Seo SM, Kim HS, Kang JL, Park EM. Nanosized titanium dioxide enhanced inflammatory responses in the septic brain of mouse. Neuroscience. 2010;165:445–54.
23. Ze Y, Zheng L, Zhao X, Gui S, Sang X, Su J, et al. Molecular mechanism of titanium dioxide nanoparticles-induced oxidative injury in the brain of mice. Chemosphere. 2013;92:1183–9.
24. Ze Y, Hu R, Wang X, Sang X, Ze X, Li B, et al. Neurotoxicity and gene-expressed profile in brain-injured mice caused by exposure to titanium dioxide nanoparticles. J Biomed Mater Res A. 2014;102:470–8.

25. Shrivastava R, Raza S, Yadav A, Kushwaha P, Flora SJS. Effects of sub-acute exposure to TiO2, ZnO and Al2O3 nanoparticles on oxidative stress and histological changes in mouse liver and brain. Drug Chem Toxicol. 2014;37:336–47.
26. Lacombe O, Videau O, Chevillon D, Guyot A-C, Contreras C, Blondel S, et al. In vitro primary human and animal cell-based blood-brain barrier models as a screening tool in drug discovery. Mol Pharm. 2011;8:651–63.
27. Brun E, Carriere M, Mabondzo A. In vitro evidence of dysregulation of blood-brain barrier function after acute and repeated/long-term exposure to TiO(2) nanoparticles. Biomaterials. 2012;33:886–96.
28. van Ravenzwaay B, Landsiedel R, Fabian E, Burkhardt S, Strauss V, Ma-Hock L. Comparing fate and effects of three particles of different surface properties: nano-TiO2, pigmentary TiO2 and quartz. Toxicol Lett. 2009;186:152–9.
29. Harati R, Benech H, Villegier AS, Mabondzo A. P-Glycoprotein, breast cancer resistance protein, organic anion transporter 3, and transporting peptide 1a4 during blood-brain barrier maturation: involvement of Wnt/beta-Catenin and Endothelin-1 signaling. Mol Pharm. 2013;10:1566–80.
30. Daneman R. The blood-brain barrier in health and disease. Ann Neurol. 2012;72:648–72.
31. van Vliet EA, Araujo SC, Redeker S, van Schaik R, Aronica E, Gorter JA. Blood-brain barrier leakage may lead to progression of temporal lobe epilepsy. Brain. 2007;130:521–34.
32. Marchi N, Granata T, Alexopoulos A, Janigro D. The blood-brain barrier hypothesis in drug resistant epilepsy. Brain. 2012;135(Pt 4):e211.
33. Hellinger E, Veszelka S, Toth AE, Walter F, Kittel A, Bakk ML, et al. Comparison of brain capillary endothelial cell-based and epithelial (MDCK-MDR1, Caco-2, and VB-Caco-2) cell-based surrogate blood-brain barrier penetration models. Eur J Pharm Biopharm. 2012;82:340–51.
34. Wang X, Campos CR, Peart JC, Smith LK, Boni JL, Cannon RE, et al. Nrf2 upregulates ATP binding cassette transporter expression and activity at the blood-brain and blood-spinal cord barriers. J Neurosci. 2014;34:8585–93.
35. Sugimoto H, Hirabayashi H, Amano N, Moriwaki T. Retrospective analysis of P-Glycoprotein-Mediated Drug-drug interactions at the blood-brain barrier in humans. Drug Metab Dispos. 2013;41:683–8.
36. Schinkel AH, Wagenaar E, Vandeemter L, Mol C, Borst P. Absence of the MDR1A P-Glycoprotein in mice affects tissue distribution and pharmacokinetics of dexamethasone, digoxin, and cyclosporine-A. J Clin Invest. 1995;96:1698–705.
37. Schinkel AH, Mayer U, Wagenaar E, Mol C, van Deemter L, Smit JJM, et al. Normal viability and altered pharmacokinetics in mice lacking mdr1-type (drug-transporting) P-glycoproteins (vol 94, pg 4028, 1997). Proc Natl Acad Sci U S A. 2003;100:8036–6.
38. Mayer U, Wagenaar E, Dorobek B, Beijnen JH, Borst P, Schinkel AH. Full blockade of intestinal P-glycoprotein and extensive inhibition of blood-brain barrier P-glycoprotein by oral treatment of mice with PSC833. J Clin Invest. 1997;100:2430–6.
39. Liu Y-C, Liu H-Y, Yang H-W, Wen T, Shang Y, Liu X-D, et al. Impaired expression and function of breast cancer resistance protein (Bcrp) in brain cortex of streptozocin-induced diabetic rats. Biochem Pharmacol. 2007;74:1766–72.
40. Hartz AMS, Bauer B, Fricker G, Miller DS. Rapid modulation of p-glycoprotein-mediated transport at the blood-brain barrier by tumor necrosis factor-alpha and lipopolysaccharide. Mol Pharmacol. 2006;69:462–70.
41. Miller DS. Regulation of ABC transporters blood-brain barrier: the good, the bad, and the ugly. Adv Cancer Res. 2015;125:43–70.
42. Ma L, Liu J, Li N, Wang J, Duan Y, Yan J, et al. Oxidative stress in the brain of mice caused by translocated nanoparticulate TiO2 delivered to the abdominal cavity. Biomaterials. 2010;31:99–105.
43. Carvalho da Fonseca AC, Matias D, Garcia C, Amaral R, Geraldo LH, Freitas C, et al. The impact of microglial activation on blood-brain barrier in brain diseases. Front Cell Neurosci. 2014;8:362.
44. Miller DS. Regulation of P-glycoprotein and other ABC drug transporters at the blood-brain barrier. Trends Pharmacol Sci. 2010;31:246–54.
45. Bauer B, Hartz AMS, Miller DS. Tumor necrosis factor alpha and endothelin-1 increase P-glycoprotein expression and transport activity at the blood-brain barrier. Mol Pharmacol. 2007;71:667–75.
46. Sha B, Gao W, Wang S, Gou X, Li W, Liang X, et al. Oxidative stress increased hepatotoxicity induced by nano-titanium dioxide in BRL-3A cells and Sprague-Dawley rats. J Appl Toxicol. 2014;34:345–56.
47. Wang Y, Chen ZJ, Ba T, Pu J, Cui XX, Jia G. Effects of TiO2 nanoparticles on antioxidant function and element content of liver and kidney tissues in young and adult rats. Journal of Peking University Health sciences. 2014;46:395–9.
48. Hong J, Wang L, Zhao X, Yu X, Sheng L, Xu B, et al. Th2 factors may be involved in TiO2 NP-induced hepatic inflammation. J Agric Food Chem. 2014;62:6871–8.
49. Didier N, Romero IA, Creminon C, Wijkhuisen A, Grassi J, Mabondzo A. Secretion of interleukin-1 beta by astrocytes mediates endothelin-1 and tumour necrosis factor-alpha effects on human brain microvascular endothelial cell permeability. J Neurochem. 2003;86:246–54.
50. Argaw AT, Zhang Y, Snyder BJ, Zhao M-L, Kopp N, Lee SC, et al. IL-1beta regulates blood-brain barrier permeability via reactivation of the hypoxia-angiogenesis program. J Immunol. 2006;177:5574–84.
51. Labus J, Haeckel S, Lucka L, Danker K. Interleukin-1 beta induces an inflammatory response and the breakdown of the endothelial cell layer in an improved human THBMEC-based in vitro blood-brain barrier model. J Neurosci Methods. 2014;228:35–45.
52. Poller B, Drewe J, Krahenbuhl S, Huwyler J, Gutmann H. Regulation of BCRP (ABCG2) and P-glycoprotein (ABCB1) by cytokines in a model of the human blood-brain barrier. Cell Mol Neurobiol. 2010;30:63–70.
53. Zhang K, Tian L, Liu L, Feng Y, Dong Y-B, Li B, et al. CXCL1 contributes to beta-Amyloid-induced transendothelial migration of monocytes in Alzheimer's disease. PloS One. 2013;8(8):e72744.
54. Campbell IL, Erta M, Lim SL, Frausto R, May U, Rose-John S, et al. Trans-signaling is a dominant mechanism for the pathogenic actions of Interleukin-6 in the brain. J Neurosci. 2014;34:2503–13.
55. Harati R, Villegier A-S, Banks WA, Mabondzo A. Susceptibility of juvenile and adult blood-brain barrier to endothelin-1: regulation of P-glycoprotein and breast cancer resistance protein expression and transport activity. J Neuroinflammation. 2012;9:273.
56. Cecchelli R, Berezowski V, Lundquist S, Culot M, Renftel M, Dehouck M-P, et al. Modelling of the blood-brain barrier in drug discovery and development. Nat Rev Drug Discov. 2007;6:650–61.
57. Deli MA, Abraham CS, Kataoka Y, Niwa M. Permeability studies on in vitro blood-brain barrier models: physiology, pathology, and pharmacology. Cell Mol Neurobiol. 2005;25:59–127.
58. Reichel A, Begley DJ, Abbott NJ. An overview of in vitro techniques for blood-brain barrier studies. Methods Mol Med. 2003;89:307–24.

Additional file 1:

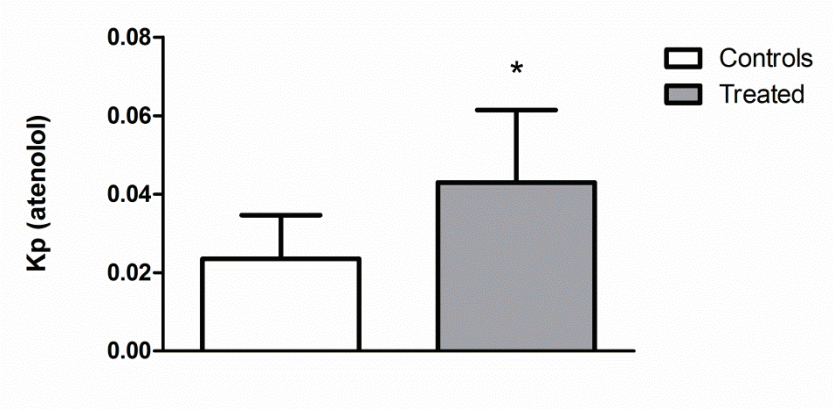

BBB integrity assessment after IV injection of 10 mg/kg TiO_2 NPs in rats. BBB integrity was estimated by the ratio between atenolol concentrations in brain and plasma (partition coefficient or Kp). Each data point represents the mean ± SD of n = 8 rats. Statistical comparison was performed by two tailed Mann-Whitney test, * $P < 0.05$.

Additional file 2:

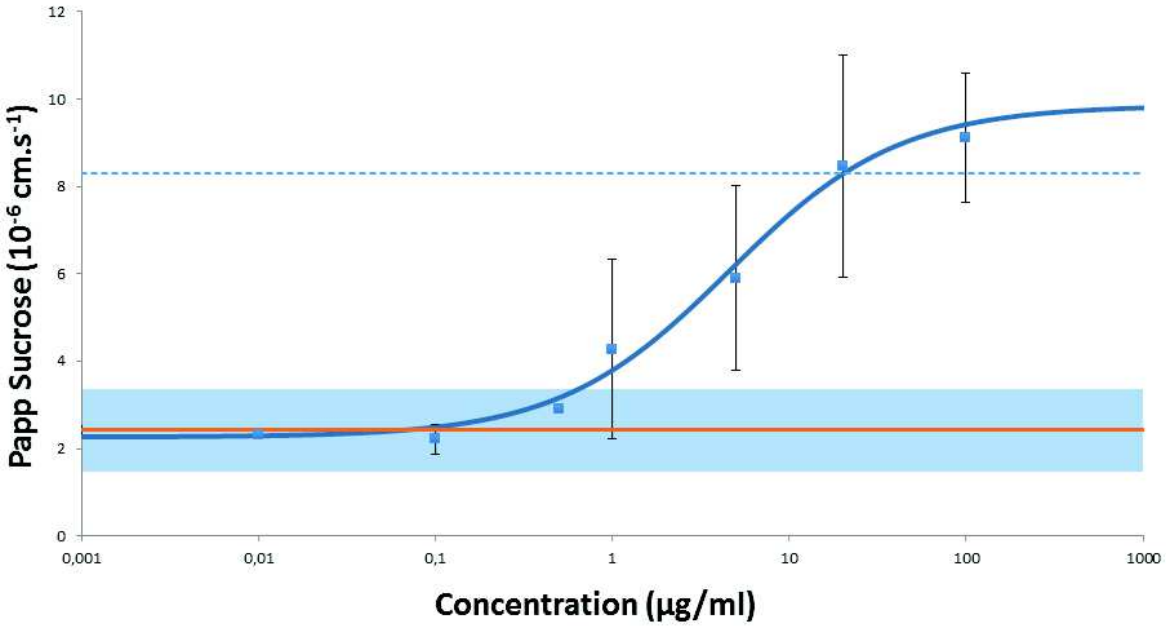

Effect of 24 h TiO_2 NPs exposure on BEC epithelium integrity. TiO_2 NPs concentrations from 0 to 100 µg/mL were applied to the apical pole of the *in vitro* BBB model for 24 h. Data are apparent permeability coefficient of sucrose. Each data point represents the mean ± SD of at least 2 experiments. The horizontal dotted line represents the usual limit value of 8.3 10^{-6} $cm.s^{-1}$ beyond which the BEC monolayer is considered to be disrupted. The blue zone represents sucrose apparent permeability coefficient for the controls (Mean ± SD).

Part II: inhalation exposure study

1. Distribution description

1.1. Context and introduction

Inhalation is one of the major routes for TiO_2 NPs to gain access into the human organism especially in occupational settings. Indeed, in the workplace NP aerosol are easily generated during production or handling. Thus beside dermal contact, inhalation appears as a very important route of exposure to NPs.

The consequences of pulmonary exposure to TiO_2 nano-aerosol have been described by multiple *in vivo* studies (see background part II.). But even if translocation of other inorganics NPs was demonstrated *in vivo*, data on absorption after inhalation exposure to TiO_2 NPs remains scarce.

Because age is the greatest risk factor for neurodegenerative diseases and has been suggesting as an aggravating risk factor in response to the particulate air pollution, we focused our study on the CNS potential adverse effect of TiO_2 NPs exposure on young adults and aging rats.

We have implemented a protocol of sub-acute exposure to TiO_2 nano-aerosol. NPs powders and nano-aerosols have been characterized in term of concentration and aggregation state. The characteristics of the aerosol were followed in real time throughout the duration of the experiment in order to ensure a constant and reproducible exposure. Young adults and aging animals were exposed over periods of six hours a day, five days a week for four weeks. Control animals inhaled filtered air. At the end of this period of exposure, the main organs and tissues were collected at various time points for ICP-MS titanium assay in order to describe the biodistribution up to 180 days after the end of exposure. Given the advanced age of the animals in the elderly group, the study had to be limited to 90 days after exposure because of animal well-being concerns. A distribution in extra-pulmonary organs was investigated with particular attention paid to the cerebral TiO_2 NPs distribution.

1.2. Major findings and Discussion

After subacute inhalation of TiO_2 NPs aerosol, the ICP-MS analysis of major organs and tissues revealed a biopersistence of titanium in lungs and a slow clearance over time. In term of lungs burden, no major age related differences was noticed.

It is important to note that we measured very high variations in titanium tissue concentrations in the exposed groups suggesting differences level of responses between animals. Indeed the variance homogeneity problems did not allow us to apply parametric tests directly. The Box Cox transformation applied on the variable "titanium tissue concentration" homogenizes the variances. Statistical analyzes by two way ANOVA test after Box Cox transformation highlighted an exposure effect in spleen and liver tissue in both age groups. After Bonferroni correction, there is a difference in spleen titanium concentration between exposed and controls animals from 28 days in young adult rats and 90 days in elderly rats. Translocation and biopersistence in spleen and liver is in accordance with the biodistribution described after IV administration. Indeed, liver and spleen appeared as major bioaccumulating organs after blood distribution. Even if the follow up period was limited here to 180 days for young adults group and 90 days for elderly group, a long term biopersistence is suggested.
Several hypotheses of translocation pathways can be formulated from these observations and are summarized in Figure 32.

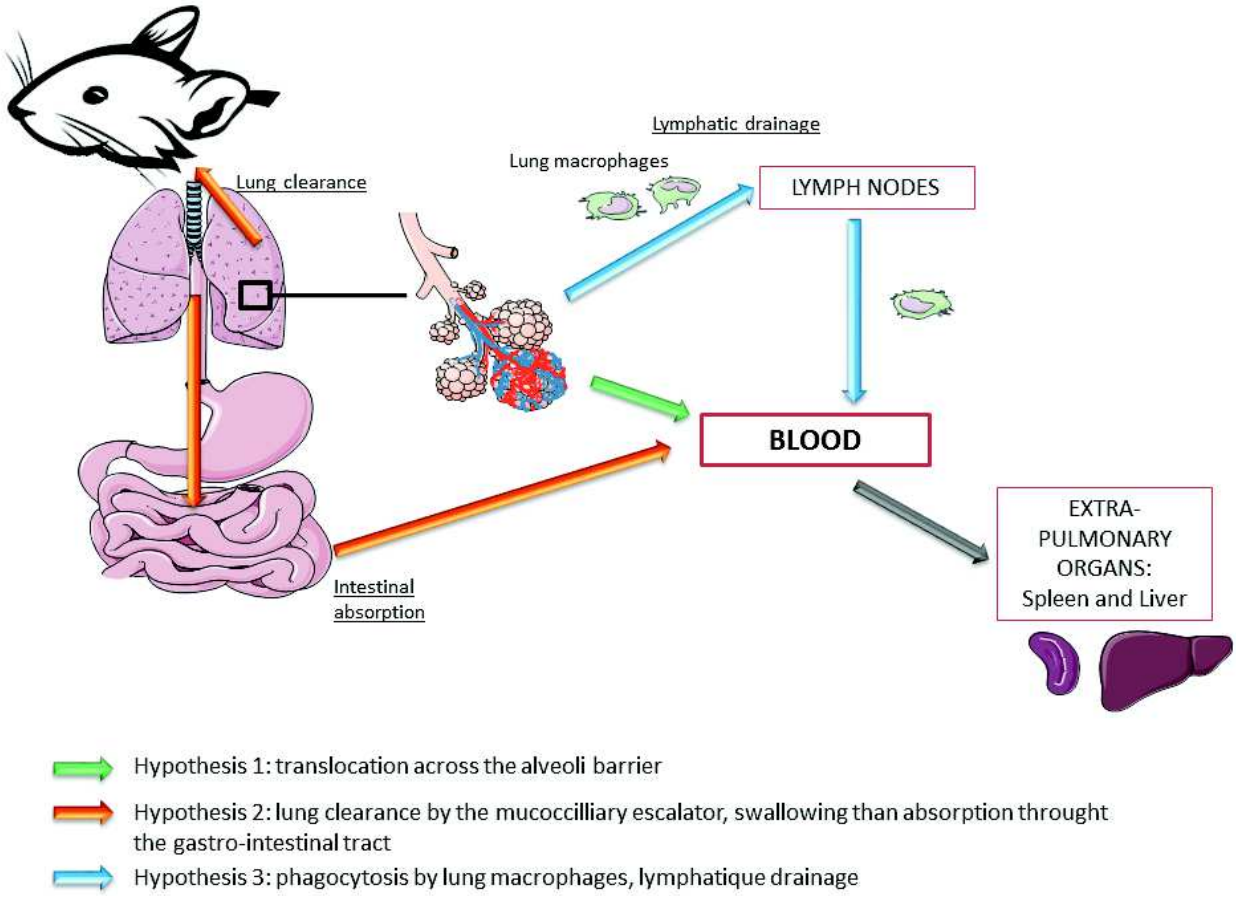

Figure 34: translocation to extra-pulmonary pathways hypothesis.

Comparing both age groups, several differences in biodistribution profile were noticed: 1) a delayed significant translocation of titanium in extra-pulmonary organs, 2) greater inter-individual variability and 3) higher amount of titanium recovered in extra-pulmonary organs.

Concerning the brain distribution, two translocation hypotheses were made (Figure 33) and the analyses in total brain, didn't evidenced CNS translocation of TiO_2 NPs partly rejecting both hypothesis:

1) Passage through the BBB in the case of a blood distribution. Given the low concentrations found in the extrapulmonary organs, it is not surprising that we did not found titanium here. Indeed, cerebral distribution after IV injection showed that the distribution to the brain was very low (6 hours after administration, about 0.1% of the dose administered was recovered in the total brain).

2) Translocation by the olfactory nerve from the nasal mucosa to directly reach the olfactory bulb before distribution to other brain areas. Several studies from the same research team had after nasal instillation in mice demonstrated this route of entry into the CNS [225, 233]. They described a titanium concentration in the olfactory bulb and hippocampus. Assays in different brain areas have not been achieved because of the limited amount of tissue for the ICP-MS method used. We have measured that titanium in the total brain and a very low concentration in small areas of the brain such as the olfactory bulb and the hippocampus may go unnoticed.

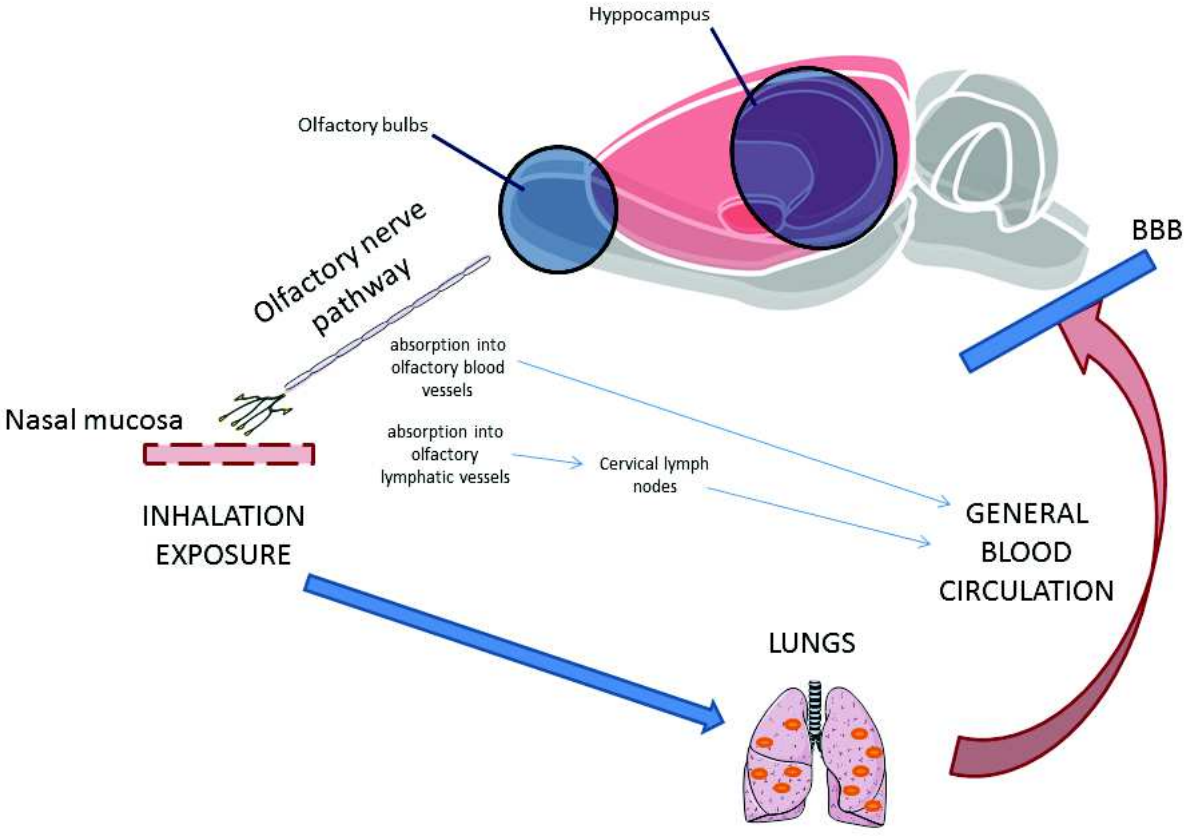

Figure 35: Entry pathways to the CNS after inhalation exposure.

The lack of detectable brain translocation does not mean the absence of neurotoxicity and adverse effect on the BBB physiology. After IV administration, we found indirect effects on the BBB at late time points affecting the tight junction proteins expressions and transport functions associated with brain inflammation. This was observed when no titanium was detectable in the brain. Therefore, the kinetics evidenced after subacute inhalation exposure with biopersistence in the lungs, spleen and liver could induce BBB dysregulation and brain effect such as brain inflammation. Moreover, potential trace of titanium in the olfactory bulbs that we weren't able to detect may induce local inflammatory response and promote generalized neuro-toxicity.

1.3. Article 2: Biopersistence and Translocation to Extrapulmonary Organs of Titanium Dioxide Nanoparticles after Subacute Inhalation Exposure to Aerosol in Adult and Elderly Rats.

Submitted to Nanotoxicology on 2016/02/26

Nanotoxicology

Biopersistence and Translocation to Extrapulmonary Organs of Titanium Dioxide Nanoparticles after Subacute Inhalation Exposure to Aerosol in Adult and Elderly Rats.

Laurent Gaté[#1], Clémence Disdier[#2], Frédéric Cosnier[1], François Gagnaire[1], Jérôme Devoy[1], Wadad Saba[3], Emilie Brun[4], Monique Chalansonnet*[1], Aloise Mabondzo*[2].

1. INRS, Département Toxicologie et Biométrologie, Rue du Morvan, CS 60027, 54519 Vandœuvre Cedex, France
2. CEA, Direction des Sciences du Vivant, iBiTec-S, Service de Pharmacologie et d'Immunoanalyse, Equipe Pharmacologie Neurovasculaire, 91191 Gif-sur-Yvette, France
3. Inserm / CEA / Université Paris Sud, UMR 1023 - ERL 9218 CNRS, IMIV, Orsay, F-91406, France
4. Laboratoire de Chimie Physique, UMR CNRS 8000, Université Paris Sud 91405 Orsay, France

[#] These authors contributed equally to this work.

* To whom correspondence should be addressed: A. Mabondzo, aloise.mabondzo@cea.fr; CEA Saclay, 91191 Gif-sur-Yvette, France.

co-author e -mail addresses: laurent.gate@inrs.fr, clemence.disdier@cea.fr, frederic.cosnier@inrs.fr, francois.gagnaire@inrs.fr, jerome.devoy@inrs.fr, wadad.saba@inrs.fr, emilie.brun@u-psud.fr, monique.chalansonnet@inrs.fr

Abstract

The increasing uses of nanoparticles (NPs) have raised concern about their impact on health. Since aging and exposure to environmental factors are linked to the risk for developing diseases, we address the question of TiO_2 NPs biodistribution in the context of a realistic environmental exposure. We report biodistribution in healthy young adults (12-13-week-old) and in aged rats (19-month-old) after subacute air-born exposure to 10 mg/m^3 of a TiO_2 nano-aerosol. The TiO_2 nano-aerosol was characterized all along inhalation experiment: 2 periods of 3 hr / day, 5 days / week for 4 weeks. We followed up Ti content in major organs using inductively coupled plasma mass spectrometry. Titanium were initially found in the lung and slowly cleared during the follow-up period. From day 28, a small amount of Ti was found in the spleen and liver of young adults exposed rats. Ti was never found in blood, kidneys nor brain. In the elderly group, translocation to extra-pulmonary organs was significant from day 90. Ti recovered in spleen and liver of elderly exposed rats was higher than in exposed young adults. These data suggest that TiO_2 NPs are able to translocate from the lung to extra-pulmonary organs and could promote systemic side effect.

Key words: titanium dioxide; nanoparticles aerosol; inhalation exposure; biodistribution

Introduction

Due to their remarkable properties, nanoparticles (NPs) are currently used in a large array of applications, from electronics to medicine, and thus introduced in a growing number of commercial products. According to the project on emerging nanotechnologies, the number of nanotechnology-based products increased nearly thirty times from 2005 to 2015, reaching a total of 1,814 items produced by companies located in 32 countries (Vance et al., 2015). Titanium dioxide NPs (TiO_2 NPs), the second most widely used NPs, are present in a tenth of the abovementioned manufactured products (Chen and Mao, 2007), including cosmetics and food products. Until recently, TiO_2 was considered inert, but the International Agency for Research in Cancer (IARC) has recently classified TiO_2 NPs as a possible carcinogen (group 2B) for humans (Baan, 2007). The reason for this re-classification arises from a study reporting that high concentrations of ultrafine (<100 nm) TiO_2 dusts are associated with cancer of the respiratory tract in exposed rats (Dankovic et al., 2007). Recent *in vivo* studies also introduced the concept that repeated inhalation of TiO_2 nano-aerosol, both in the workplace and as a consumer, may cause extrapulmonary adverse health effects (Christensen et al., 2011, Baisch et al., 2014, Landsiedel et al., 2014). Due to their small size, NPs may present a different bio-kinetic profile compared to bulk material. Consequently, in a case of a facilitated absorption or/and slower elimination of NPs, the potential risk upon exposure is expected to be increased. It is supported by several inhalation studies in rodents showing the distribution of various types of NPs to various organs outside of the pulmonary system, including the liver, spleen, heart and brain. For example, Takenaka *et al.* report that after a 6-hour inhalation exposure to silver NPs (4-10 nm), a small amount of particles was recovered from the liver, spleen, brain, heart, and blood of rats 30 minutes after inhalation (Takenaka et al., 2001);

Braakhuis et al. highlighted distribution of silver to the liver from 24 hours after the end of a 4-day inhalation period to silver NPs (15nm) (Braakhuis et al., 2014)**;** Yu *et al.* observed gold NPs after 15 days of recovery in the heart, liver, pancreas, spleen, kidney, brain and testis in rats exposed to gold NPs by inhalation during 5 days (majority with a size <35 nm)(Yu et al., 2007); Geraets *et al.* highlighted translocation to extrapulmonary organs of cerium oxide NPs (5-10 nm) observed 6 hours after the end of a 28 days exposure (Geraets et al., 2012). In these reported studies, the translocation to extra-pulmonary organs was described after a short recovery period. Furthermore, two separate studies reported long-term NP biokinetics in secondary target organs over six months after a single short-term inhalation of iridium NPs (15-20 nm)(Kreyling et al., 2002, Kreyling et al., 2009). Taken together, these findings suggest that inhalation of various types of NPs can result in their translocation across the lung air-blood barrier. As for TiO_2, some authors did not observe any translocation to extrapulmonary organs (Ma-Hock et al., 2009, van Ravenzwaay et al., 2009, Landsiedel et al., 2014) even though few studies have shown such translocation after intratracheal or intranasal instillation to rodents (Shinohara et al., 2014, Zhang et al., 2013, Shinohara N, 2015, Husain et al., 2015). Such discrepancy can be due to the differences in NPs physical properties (for example size), doses and exposure route. Moreover, in the studies by Ma Hock *et al.,* Van Ravenzwaay *et al.* and Landsiedel *et al.*, the recovery period was limited to 16, 14 or 21 days and analyses were conducted in only 3 rats per groups. Observations on possible translocation to extra-pulmonary organs after inhalation therefore warrant further research taking into account long term bio-kinetics in secondary organs. This is one of our main objective.

Besides, the nano-toxic effects on susceptible populations (such as pregnant, neonate, diseased, and aged populations) have been mostly ignored (Yang et al., 2014). And yet, Chen

et al. observed age-dependent pulmonary inflammation, cardiovascular injuries, and serum biomarkers after exposure of old (20 months), adult (8 weeks) and young (3 weeks) rats to SiO_2 NPs by inhalation for a period of 4 weeks (24.1 mg/m^3 40 min/day)(Chen et al., 2008). Their toxicity was higher in old rats than in younger age groups. Such results emphasize both the differences in response to inhaled NPs in normal and susceptible populations, as well as a need for further research to elucidate alterations of pathways involved in these age-related responses. In this context, the present study is the first designed to determine the biokinetics of TiO_2 NPs after subacute nose-only inhalation exposure of elderly rats in comparison to adult rats. To accomplish this aim, both elderly (19-month-old) and healthy young adult (12-13-week-old) Fisher F344 rats were exposed to either 10 mg/m^3 TiO_2 nano-aerosol (2 periods of 3 hours a day, 5 days a week for 4 weeks) or filtered air. The chosen concentration of 10 mg/m^3 corresponds to the 8 hours time-weighted average French OEL (Occupational Exposure Limit) value for particles without known significant toxicity (INRS, 2012). The aerosol generation was characterized throughout the inhalation period in order to ensure consistent and reproducible exposure. At the end of the 28-day inhalation period, animals were held for a recovery period of 3, 28, 90 and 180 days for adult rats. For elderly rats, it was shortened to 3, 28 and 90 days because of their old age. At each time point (n=6-12 rats per time point), organs were collected for titanium (Ti) analysis by inductively coupled plasma mass spectrometry (ICP-MS), as described previously (Devoy et al. 2016; accepted paper).

Methods

TiO_2 NPs

TiO_2 P25 NPs (Aeroxide® P25, 75% anatase 25% rutile, Evonik®) were from Sigma Aldrich (Saint-Quentin Fallavier, France).

Animals

The animal experiments were performed according to European (Directive 2010/63/EC) and French (Décret n°2013-118) legislations regarding the protection of animals used for scientific purposes. The INRS animal facility has full accreditation (authorization n° D54-547-10) from the French Ministry of Agriculture. This study was approved by the regional ethical committee appointed by the Ministry of Higher Education and Research (Authorisation n°00692.01).

Male Fisher F344 rats (from Charles River Laboratories, France), 12-13 weeks old and weight 300-320 g referred as young adults and 19 months old , weight 400-425 g referred as aging group (Sengupta, 2013), were housed in standard environmental conditions (room humidity 55±10% and temperature 22±2 °C ; room under a 12 : 12 hrs light-dark cycle) and maintained with free access to water and standard laboratory diet. The aging rats were fed separately with free access to A04 diet (Safe diet) from 1 month of age to 7 months then with A05 diet (Safe diet) adapted to long term studies.

Generation and monitoring of TiO_2 nano-aerosol

The inhalation system described previously (Cosnier et al, submited) is mainly composed of an aerosol generation system and inhalation towers for nose-only exposure. Exposure capability is around 100 rats: 50 NPs exposed rats (in 6 × 9 ports manifold) and 50 control rats (in 2 × 27

ports manifold). Controls were exposed to filtered air. During the 6-hrs exposure, rats did not have access to food or water. The system has been fully validated according to OECD guidelines for chemicals testing.

The integrated control of the exposure conditions (airflow, temperature and relative humidity, depression) is managed and recorded using dedicated software. Air entering the towers was filtered and conditioned at a temperature of 22°C ± 2°C and a humidity of 55 ± 10 %. To produce test aerosol of aggregates and agglomerates NPs, a dry power with rotating brush generator (RBG) (RBG1000 PALAS) method has been chosen. Aerosol concentration was adjusted with feed rate of the RBG operated at constant air flow rate.

The aerosol monitoring and the characterization is ensured by real time devices (condensation particle counter, electrical low pressure impactor, aerodynamic particle sizer, scanning mobility particle sizer spectrometer, optical light scattering dust monitor,) and off-line analyses (gravimetric filter, particle size-distribution by cascade impactor, sampling for TEM observations).

Mass concentrations were measured on the basis of gravimetric samplings taken twice to 4 times a day on 25 mm cassettes with GLA-5000 PVC filters (5 µm pore size).

***In vivo* experimental design**

One week before the beginning of the exposure period, rats were acclimated to the restraining tubes following the daily scheme of experiment: 2 periods of 3 hrs exposure. Rats were then exposed to filtered air for controls group or TiO_2 nano-aerosol for the treated group during 2 periods of 3 hrs a day, 5 days/week for 4 weeks. 0, 3, 28, 90 or 180 days after the end of the inhalation exposure period, animals were anesthetized with pentobarbital 200 mg/kg and

euthanized. Blood, liver, brain, spleen, kidneys and lungs were collected and stored at −80 ºC until assayed.

Sample Preparation and Ti analysis by ICP-MS

Sample preparation and ICP-MS analysis has been previously described (Disdier et al., 2015). Briefly, about 0.1-0.3 g of each sample was digested in 8 mL of concentrated nitric acid and 2 mL of concentrated hydrofluoric acid using a Microwave Assisted Reaction System (MARS) Express instrument. After cooling, the sample was rinsed using 2% nitric acid solution in a polytetrafluoroethylene (PTFE or Teflon) beaker. 2 mL of hydrogen peroxide was added to digest any remaining organic matter. Beakers were then heated at 180 °C until between 0.1 and 0.5 mL of solution remained then allowed to cool and rinsed 3 times with 2% nitric acid solution into a 25 mL volumetric flask before being stored for analysis. Ti standard solutions for ICP-MS calibration were prepared at concentrations from 2 to 100 ng/L, by diluting 1 g/L Ti standard stock solution (1.70363.0100, SCP Science) with 2% v/v HNO_3 and 0.01% v/v Triton X-100. The internal standard (25 µg/L Ge) was added in all samples and standards. Samples in 2% v/v HNO_3 were directly analyzed with the Varian-820-MS for Ti determination.

Statistical Analysis

Statistical analysis was performed using Stata 14 (StataCorp LP,TX ,USA) After Box cox transformation on Ti concentration variable, statistical comparisons were accomplished using two-way ANOVA (the two determinants being treatment and time) followed by Bonferroni post-hoc test. Changes were considered statistically significant at $p < 0.05$.

Results

Aerosol generation

The morphology and size of TiO_2 NPs have been previously described (Disdier et al., 2015) (spherical particle with primary size of 21.5 ± 7.2 nm), as well as the methodologies for TiO_2 nano-aerosol generation and characterization (Cosnier et al., submitted). The achieved concentrations of TiO_2 nano-aerosol were consistently near the target concentration of 10 mg/m^3 and comparable between both inhalation campaigns: 10.17 ± 3.29 mg/m^3 and 10.42 ± 1.80 mg/m^3 for the exposure of adult and elderly rats, respectively. These mass concentrations correspond to a number concentration of 24,000 ± 6400 particles/cm^3. Particle size distributions demonstrated a quasi monomodal aerosol in mass- and count-median aerodynamic diameters are around 905 and 270 nm, respectively and the geometric standard deviation of the distributions equal 2.2**.**

Biodistribution of TiO_2 NPs after subacute inhalation exposure

Ti burdens in exposed rat lungs from the young adult and elderly groups were significantly higher than those of the corresponding control groups at each of the time points analyzed, and decreased over time. At the end of the inhalation period, the Ti concentration in lung tissue was 1.43 ± 0.08 mg/g in the exposed group *vs.* 55.3 x10^{-6} ± 8.1 x 10^{-6} mg/g in the control group for young adults, and 1.1 ± 0.2 mg/g in the exposed group *vs.* 84.8 x10^{-6} ± 20.0 x 10^{-6} mg/g in the control group for elderly rats (Figures 1a and 2a). As previously described, the deposited fraction of Ti in the lung of young rats was 21.0 ± 1.1% of the cumulative inhalable dose of NPs whereas in elderly rats the deposited fraction was 17.7 ± 3.3%. The deposited fractions were calculated using the respiratory parameters described by Hsieh et al. (Hsieh et

al., 1999). In exposed young adults, a decrease of Ti burden in lung tissue was observed between 0 and 180 days after the end of the inhalation exposure period, suggesting a clearance of particles. After 90 days of recovery, the mean lung burden in the exposed young adult group corresponded to a 54% decrease of the lung burden at day 0 (mean Ti content in lung being 2.09 mg/lung at day 0 and 0.95 mg/lung at day 90), suggesting a slow clearance rate. The clearance observed in Ti lung burden in the elderly group was even slower. Indeed, in elderly group after 90 days of recovery, the mean lung burden in exposed animals was 1.2 mg/lung compared to 2.19 mg/lung at day 0 thus corresponding to a decrease of approximately 45%. However, no significant age-related difference in Ti lung burden from day 0 to day 90 was observed between the young adult and elderly exposed groups.

Ti analysis in other organs of exposed young adult rats indicated an increase in measurable concentration in the spleen from day 28 to 180 (Figure 1c). The total amount of Ti in the spleen at day 90 was 28.0 ± 6.4 ng/g in the control group *vs.* 78.4 ± 52.2 ng/g in the exposed group, with an even further increase observed at day 180 (555.7 ± 1089 ng/g). In the elderly group, an increase of Ti concentration in the spleen was also observed significantly at day 90 (Ti in the spleen at this time point was 35.4 ±6.5 ng/g in the control group *vs.* 319.5± 275.2 ng/g in the exposed group) (Figure 2c). In both age groups, the impact of TiO_2 NPs exposure on liver Ti concentrations was also observed**.** It is worth noticing that even if intra-group variability is greater, the amount of Ti detected in extra-pulmonary organs of exposed aged rats is much higher than in the young adult group (319.5± 275.2 ng/g in the TiO_2-exposed elderly group vs. 78.4 ± 52.2 ng/g in the exposed young adults group). In addition, when exposed animals were taken individually, a link between the levels of Ti in spleen and liver was observed. Indeed when in a given animal a higher amount of Ti in the spleen was observed, the same trend was

found in the liver. This may suggest some kind of heterogeneity between animals in the translocation of NPs from the lung to secondary organs. There was no significant increase of Ti measured in the kidneys of either the young adult or elderly TiO_2-exposed groups, compared with controls. Moreover, we provide evidence in a translatable occupational exposure that there was no detectable Ti translocation into the brain of both young adult and elderly TiO_2-exposed rats, compared with controls (Figures 2f and 3f).

Discussion

In this study, we described the distribution of TiO_2 after subacute inhalation exposure in rats. Animals were exposed to a well characterized nano-aerosol composed of agglomerated TiO_2 NPs. A nano-aerosol is defined as a fluid nano-dispersion with gaseous matrix and at least one liquid or solid nanophase including nano-objects (ISO). In our case, the nano-objects are nanostructured agglomerates composed of TiO_2 NPs of 21.5 nm. Aerosol found in workplace resulting from nano-powder handling and processing are composed of agglomerates. Therefore, the exposure conditions used in this study could be considered representative of an occupational exposure scenario. Moreover, it is worth noticing that agglomerated NPs present a greater surface reactivity than bulk material; this may promote their capabilities to interact with biological system and their adverse effects (Oberdorster et al., 2005).

Titanium in major organs were assessed by ICP-MS. Major finding from this study are: (a) biopersistence of titanium in lungs and a slow clearance over time. In term of lungs burden, no major age related differences was noticed (b) late translocation to spleen and liver with an age-difference profil (c) lack of translocated titanium recovered in brain. To our knowledge, this study is the first to report uptake of TiO_2 NPs in the lungs with a redistribution to the

spleen and liver after sub-acute nose-only inhalation of TiO_2 nano-aerosol in elderly rats. Regarding the slow pulmonary particle clearance, these results confirm for TiO_2 NPs what was observed for metallic NPs. For example, Anderson *et al.* showed, for silver NPs, a significant decrease in the amount of Ag in lung tissue 56 days post-exposure but 33% of the day-one dose was still present (Anderson et al., 2015). Spleen was also depicted as the second most accumulative organ for 13 nm gold NPs (Han et al., 2015). After a 5 day inhalation campaign (6hr/day, 12.8±2.4 µg/m^3), and 28 days of recovery, gold content was found significantly different between exposed and control animals only in lungs and spleen. In our previous study dealing with intravenous administration and a one-year follow-up period after administration, we showed that liver and spleen are key organs in TiO_2 NPs biodistribution and that the clearance from liver and spleen was minimal (Disdier et al., 2015). This fact, combined with a still high Ti lung burden at day 180 (approximately 30% of the initial lung burden remains at 180 days), suggests a long-term NPs accumulation potentially leading to alteration of pulmonary functions, but also potential systemic impact. It has to be noticed that other studies have reported varied results after short-term inhalation of TiO_2 NPs. For example, in studies where rats were exposed to a range of 2-50 mg/m^3 of TiO_2 nano-aerosol 6 hours/day for 5 days (Ma-Hock et al., 2009, Landsiedel et al., 2014, van Ravenzwaay et al., 2009), no Ti was observed in extrapulmonary organs after 14,16 or 21-day post-exposure recovery period. Several reasons can be proposed to explain such a discrepancy. The rats from the aforementioned studies received a relatively short-term exposure (5 days) compared to the subacute exposure protocol used in our study (5 days/week for 4 weeks). Thus, for the same exposure concentration (10 mg/m^3), the cumulative inhalable dose in our system was four times higher. Tissues were only analyzed at 14, 16 or 21 post-exposure days compared to the

180 days post-exposure time point used in our study. Since we did not observe a significant increase of Ti in the spleen until after 28 days, in the young adult TiO_2-exposed group, their recovery period may have been too short to detect the redistribution to these extra pulmonary organs. Moreover, they designed their study with only 3 animals per tested group, an insufficient number knowing that we noticed a heterogeneity between animals in the translocation to extra pulmonary organs. Finally the difference between these studies and ours may also be explained by the sensitivity of the ICP-MS method used (Devoy et al.; 2016 accepted paper). Altogether, the experimental design and the number of animals included in our study allow to reassess previous conclusions.

The route by which TiO_2 NPs are transported to the extrapulmonary organs cannot be directly determined from the results of this study. Given the low levels found in the extrapulmonary organs, several hypotheses are plausible and are summarized in figure 3.

First, Ti clearance from the lungs can occur via mucociliary clearance and swallowing, ending up in the gastrointestinal tract, this may be followed by an absorption across the intestinal mucosa and a subsequent systemic distribution. Orally administered TiO_2 NPs have previously been shown to accumulate in both the liver and spleen, testifying of a possible transport through the gastro-intestinal barrier (Wang et al., 2007, Cui et al., 2011, Brun et al., 2014, Dorier et al., 2015, Sang et al., 2014). *In vitro* studies using an epithelial intestinal model, such as Caco2 cell lines, have also confirmed the ability of NPs to translocate across the intestinal barrier, allowing them to reach the systemic circulation, as well as other tissues/organs (Koeneman et al., 2010, Brun et al., 2014). Another route by which TiO_2 NPs may also be distributed to other organs after inhalation is through macrophage-mediated transport. Phagocytosis of TiO_2 NPs by lung macrophages could lead to their migration to the lymphatic

system and subsequently their possible release into the blood circulation. Indeed, alveolar macrophages play a critical role in the respiratory system by phagocytizing foreign bodies including NPs. After pulmonary exposure, several other studies have reported TiO_2 NPs into alveolar macrophages (Grassian et al., 2007, Geiser, 2002, Warheit et al., 2006, Silva et al., 2013, Geiser et al., 2008, van Ravenzwaay et al., 2009). Furthermore, Ti was also found in draining lymph nodes after a 5-day inhalation study (Ma-Hock et al., 2009, Landsiedel et al., 2014, van Ravenzwaay et al., 2009) or 90-day sub-chronic inhalation exposure(Bermudez et al., 2004), suggesting transportation via the lymphatic system. Finally, Ti present in organs such as the spleen may have occurred due to translocation of NPs across the respiratory membrane of the lung, where we observed clearance during the follow-up period. An *in vitro* study on Calu-3 cells confirmed the ability of TiO_2 NPs to cross the epithelia lung blood barrier (George et al., 2015). In each of these possible mechanisms of NP translocation, there is a transient passage via the blood circulation, even though we did not observed significantly increased Ti in total blood from exposed *vs.* control animals in our study. The quantification limit of Ti in the blood is however about 11.7 ± 2.0 ng/mL. In this context, a very low blood concentration of Ti cannot be ruled out.

A hot topic concerning NPs biodistribution is their translocation to the CNS. Except across the blood brain barrier in case of blood distribution, there are two main direct routes of entry to the brain after intranasal administration: the olfactory and the trigeminal pathways. These paths connect directly the nasal mucosa and the brain (Lochhead et al., 2015) and thus bypass the BBB. NPs can pass between the nasal epithelium through the intercellular spaces. Additionally, there are also transcellular processes in which NPs can be transported across the nasal epithelium by transcytosis. After crossing the epithelium, NPs can use nerve pathways

to reach deep regions of the brain (Lochhead and Thorne, 2012).Lack of detectable titanium in the brain observed in this study is in good agreement with our recently published paper showing absence of brain parenchyma translocation after intravenous injection of TiO_2 NPs(Disdier et al., 2015). In contrast, Wang *et al.* reported the presence of Ti in the olfactory bulb, hippocampus, cerebral cortex, and the cerebellum after nasal instillation in a mouse model (500 µg/mouse; TiO_2 80 nm rutile; daily for 30 days)(Wang et al., 2008). The route of exposure, the concentrations used combined with a high dose rate delivery may increase NP translocation via the olfactory nerve pathway through non physiological mechanisms and may explain the differences between both studies. These observations on possible direct translocation of inhaled NPs to the brain warrant further research such as investigation on brain functions to confirm or reject the hypothesis of NPs association with various brain diseases. Despite the lack of aged-related difference in CNS distribution, we observed an increased in BBB permeability and an exacerbated neuro-inflammation in the aging group (data not shown). These observations underscore susceptibility for developing brain diseases of the elderly population in response to inhaled NPs.

Conclusions

Overall, our study shows the lung uptake, clearance, and redistribution of Ti in young adults and elderly rats after subacute inhalation exposure to TiO_2 nano-aerosol with primary particle size of 21.5 nm. After a 4-week inhalation period, TiO_2 NPs were observed to accumulate in the lungs, with a gradual clearance rate over the time points measured. Due to the sensitivity of the ICP-MS method used, a small amount of the applied dose was observed to translocate into the spleen and liver between 28 to 180 post-exposure days. Observations made

previously with the same TiO_2 NPs after intravenous administration suggest a persistence of these NPs in such extrapulmonary organs during at least one year (Disdier et al., 2015). Comparison of biodistribution profiles between both ages revealed delay in translocation, greater intra-animals variability but also higher amount of titanium in spleen and liver of the elderly group. This redistribution of Ti highlights a need for future mechanistic studies to elucidate the transport mechanisms involved, as well as potential systemic side effects.

Acknowledgements

This work was supported by the French Agency for Food, Environmental and Occupational Health Safety (ANSES). The authors gratefully acknowledge Aurélie Remy for the statistical analysis, Guillaume Antoine and Mathieu Melczer for titanium quantification; Céline Brochard, Stéphane Grossmann, Hervé Nunge and Stéphane Viton for aerosol generation and characterization; Stéphane Boucard, Mylène Lorcin, Lise Merlen, Jean-Claude Miccilino and Sylvie Sébillaud for animal exposure and tissue collection; and Marie-Josèphe Décret, Laurine Douteau, Lionel Dussoul and Sylvie Michaux for animal care and husbandry.

Competing interests:

The authors declare that they have no competing interests

References

ANDERSON, D. S., PATCHIN, E. S., SILVA, R. M., UYEMINAMI, D. L., SHARMAH, A., GUO, T., DAS, G. K., BROWN, J. M., SHANNAHAN, J., GORDON, T., CHEN, L. C., PINKERTON, K. E. & VAN WINKLE, L. S. 2015. Influence of Particle Size on Persistence and Clearance of Aerosolized Silver Nanoparticles in the Rat Lung. *Toxicological Sciences,* 144**,** 366-381.

BAAN, R. A. 2007. Carcinogenic hazards from inhaled carbon black, titanium dioxide, and talc not containing asbestos or asbestiform fibers: Recent evaluations by an IARC Monographs working group. *Inhalation Toxicology,* 19.

BAISCH, B. L., CORSON, N. M., WADE-MERCER, P., GELEIN, R., KENNELL, A. J., OBERDOERSTER, G. & ELDER, A. 2014. Equivalent titanium dioxide nanoparticle deposition by intratracheal instillation and whole body inhalation: the effect of dose rate on acute respiratory tract inflammation. *Particle and Fibre Toxicology,* 11.

BERMUDEZ, E., MANGUM, J. B., WONG, B. A., ASGHARIAN, B., HEXT, P. M., WARHEIT, D. B. & EVERITT, J. I. 2004. Pulmonary responses of mice, rats, and hamsters to subchronic inhalation of ultrafine titanium dioxide particles. *Toxicological Sciences,* 77**,** 347-357.

BRAAKHUIS, H. M., GOSENS, I., KRYSTEK, P., BOERE, J. A. F., CASSEE, F. R., FOKKENS, P. H. B., POST, J. A., VAN LOVEREN, H. & PARK, M. V. D. Z. 2014. Particle size dependent deposition and pulmonary inflammation after short-term inhalation of silver nanoparticles. *Particle and Fibre Toxicology,* 11.

BRUN, E., BARREAU, F., VERONESI, G., FAYARD, B., SORIEUL, S., CHANEAC, C., CARAPITO, C., RABILLOUD, T., MABONDZO, A., HERLIN-BOIME, N. & CARRIERE, M. 2014. Titanium dioxide nanoparticle impact and translocation through ex vivo, in vivo and in vitro gut epithelia. *Particle and Fibre Toxicology,* 11.

CHEN, X. & MAO, S. S. 2007. Titanium dioxide nanomaterials: Synthesis, properties, modifications, and applications. *Chemical Reviews,* 107**,** 2891-2959.

CHEN, Z., MENG, H., XING, G., YUAN, H., ZHAO, F., LIU, R., CHANG, X., GAO, X., WANG, T., JIA, G., YE, C., CHAI, Z. & ZHAO, Y. 2008. Age-Related Differences in Pulmonary and Cardiovascular Responses to SiO(2) Nanoparticle Inhalation: Nanotoxicity Has Susceptible Population. *Environmental Science & Technology,* 42**,** 8985-8992.

CHRISTENSEN, F. M., JOHNSTON, H. J., STONE, V., AITKEN, R. J., HANKIN, S., PETERS, S. & ASCHBERGER, K. 2011. Nano-TiO(2)-feasibility and challenges for human health risk assessment based on open literature. *Nanotoxicology,* 5**,** 110-124.

CUI, Y., LIU, H., ZHOU, M., DUAN, Y., LI, N., GONG, X., HU, R., HONG, M. & HONG, F. 2011. Signaling pathway of inflammatory responses in the mouse liver caused by TiO2 nanoparticles. *Journal of Biomedical Materials Research Part A,* 96A**,** 221-229.

DANKOVIC, D., KUEMPEL, E. & WHEELER, M. 2007. An approach to risk assessment for TiO2. *Inhalation Toxicology,* 19**,** 205-212.

DISDIER, C., DEVOY, J., COSNEFROY, A., CHALANSONNET, M., HERLIN-BOIME, N., BRUN, E., LUND, A. & MABONDZO, A. 2015. Tissue biodistribution of intravenously administrated titanium dioxide nanoparticles revealed blood-brain barrier clearance and brain inflammation in rat. *Particle and fibre toxicology,* 12**,** 27-27.

DORIER, M., BRUN, E., VERONESI, G., BARREAU, F., PERNET-GALLAY, K., DESVERGNE, C., RABILLOUD, T., CARAPITO, C., HERLIN-BOIME, N. & CARRIERE, M. 2015. Impact of anatase and rutile titanium dioxide nanoparticles on uptake carriers and efflux pumps in Caco-2 gut epithelial cells. *Nanoscale,* 7**,** 7352-7360.

GEISER, M. 2002. Morphological aspects of particle uptake by lung phagocytes. *Microscopy Research and Technique,* 57**,** 512-522.

GEISER, M., CASAULTA, M., KUPFERSCHMID, B., SCHULZ, H., SEMIRRILER-BEHINKE, M. & KREYLING, W. 2008. The role of macrophages in the clearance of inhaled ultrafine titanium dioxide particles. *American Journal of Respiratory Cell and Molecular Biology,* 38**,** 371-376.

GEORGE, I., NAUDIN, G., BOLAND, S., MORNET, S., CONTREMOULINS, V., BEUGNON, K., MARTINON, L., LAMBERT, O. & BAEZA-SQUIBAN, A. 2015. Metallic oxide nanoparticle translocation across the human bronchial epithelial barrier. *Nanoscale,* 7**,** 4529-4544.

GERAETS, L., OOMEN, A. G., SCHROETER, J. D., COLEMAN, V. A. & CASSEE, F. R. 2012. Tissue Distribution of Inhaled Micro- and Nano-sized Cerium Oxide Particles in Rats: Results From a 28-Day Exposure Study. *Toxicological Sciences,* 127**,** 463-473.

GRASSIAN, V. H., ADAMCAKOVA-DODD, A., PETTIBONE, J. M., O'SHAUGHNESSY, P. T. & THORNE, P. S. 2007. Inflammatory response of mice to manufactured titanium dioxide nanoparticles: Comparison of size effects through different exposure routes. *Nanotoxicology,* 1**,** 211-226.

HAN, S. G., LEE, J. S., AHN, K., KIM, Y. S., KIM, J. K., LEE, J. H., SHIN, J. H., JEON, K. S., CHO, W. S., SONG, N. W., GULUMIAN, M., SHIN, B. S. & YU, I. J. 2015. Size-dependent clearance of gold nanoparticles from lungs of Sprague-Dawley rats after short-term inhalation exposure. *Archives of Toxicology,* 89**,** 1083-1094.

HSIEH, T. H., YU, C. P. & OBERDORSTER, G. 1999. Modeling of deposition and clearance of inhaled Ni compounds in the human lung. *Regulatory Toxicology and Pharmacology,* 30**,** 18-28.

HUSAIN, M., WU, D., SABER, A. T., DECAN, N., JACOBSEN, N. R., WILLIAMS, A., YAUK, C. L., WALLIN, H., VOGEL, U. & HALAPPANAVAR, S. 2015. Intratracheally instilled titanium dioxide nanoparticles translocate to heart and liver and activate complement cascade in the heart of C57BL/6 mice. *Nanotoxicology,* 9**,** 1013-22.

INRS 2012. Occupational Exposure Limit Values to Chemical Agents in France. Paris: Institut National de Recherche de Sécurité.

ISO TS 80004-4:2011 Nanotechnology-Vocabulary-Part4: Nanostructured materials.

KOENEMAN, B. A., ZHANG, Y., WESTERHOFF, P., CHEN, Y., CRITTENDEN, J. C. & CAPCO, D. G. 2010. Toxicity and cellular responses of intestinal cells exposed to titanium dioxide. *Cell Biology and Toxicology,* 26**,** 225-238.

KREYLING, W. G., SEMMLER, M., ERBE, F., MAYER, P., TAKENAKA, S., SCHULZ, H., OBERDORSTER, G. & ZIESENIS, A. 2002. Translocation of ultrafine insoluble iridium particles from lung epithelium to extrapulmonary organs is size dependent but very low. *Journal of Toxicology and Environmental Health-Part A,* 65.

KREYLING, W. G., SEMMLER-BEHNKE, M., SEITZ, J., SCYMCZAK, W., WENK, A., MAYER, P., TAKENAKA, S. & OBERDORSTER, G. 2009. Size dependence of the translocation of inhaled iridium and carbon

nanoparticle aggregates from the lung of rats to the blood and secondary target organs. *Inhalation toxicology,* 21 Suppl 1.

LANDSIEDEL, R., MA-HOCK, L., HOFMANN, T., WIEMANN, M., STRAUSS, V., TREUMANN, S., WOHLLEBEN, W., GROETERS, S., WIENCH, K. & VAN RAVENZWAAY, B. 2014. Application of short-term inhalation studies to assess the inhalation toxicity of nanomaterials. *Particle and Fibre Toxicology,* 11.

LOCHHEAD, J. J. & THORNE, R. G. 2012. Intranasal delivery of biologics to the central nervous system. *Advanced Drug Delivery Reviews,* 64**,** 614-628.

LOCHHEAD, J. J., WOLAK, D. J., PIZZO, M. E. & THORNE, R. G. 2015. Rapid transport within cerebral perivascular spaces underlies widespread tracer distribution in the brain after intranasal administration. *Journal of Cerebral Blood Flow and Metabolism,* 35**,** 371-381.

MA-HOCK, L., BURKHARDT, S., STRAUSS, V., GAMER, A. O., WIENCH, K., VAN RAVENZWAAY, B. & LANDSIEDEL, R. 2009. Development of a Short-Term Inhalation Test in the Rat Using Nano-Titanium Dioxide as a Model Substance. *Inhalation Toxicology,* 21**,** 102-118.

OBERDORSTER, G., OBERDORSTER, E. & OBERDORSTER, J. 2005. Nanotoxicology: An emerging discipline evolving from studies of ultrafine particles. *Environmental Health Perspectives,* 113**,** 823-839.

SANG, X., FEI, M., SHENG, L., ZHAO, X., YU, X., HONG, J., ZE, Y., GUI, S., SUN, Q., ZE, X., WANG, L. & HONG, F. 2014. Immunomodulatory effects in the spleen-injured mice following exposure to titanium dioxide nanoparticles. *Journal of Biomedical Materials Research Part A,* 102**,** 3562-3572.

SENGUPTA, P. 2013. The Laboratory Rat: Relating Its Age With Human's. *International journal of preventive medicine,* 4**,** 624-30.

SHINOHARA, N., OSHIMA, Y., KOBAYASHI, T., IMATANAKA, N., NAKAI, M., ICHINOSE, T., SASAKI, T., ZHANG, G., FUKUI, H. & GAMO, M. 2014. Dose-dependent clearance kinetics of intratracheally administered titanium dioxide nanoparticles in rat lung. *Toxicology,* 325**,** 1-11.

SHINOHARA N, O. Y., KOBAYASHI T, IMATANAKA N, NAKAI M, ICHINOSE T, SASAKI T, KAWAGUCHI K, ZHANG G, GAMO M. 2015. Pulmonary clearance kinetics and extrapulmonary translocation of seven titanium dioxide nano- and submicron materials following intratracheal administration in rats. Nanotoxicology.

SILVA, R. M., TEESY, C., FRANZI, L., WEIR, A., WESTERHOFF, P., EVANS, J. E. & PINKERTON, K. E. 2013. Biological response to nano-scale titanium dioxide (TiO2): role of particle dose, shape, and retention. *Journal of Toxicology and Environmental Health-Part a-Current Issues,* 76**,** 953-972.

TAKENAKA, S., KARG, E., ROTH, C., SCHULZ, H., ZIESENIS, A., HEINZMANN, U., SCHRAMEL, P. & HEYDER, J. 2001. Pulmonary and systemic distribution of inhaled ultrafine silver particles in rats. *Environmental Health Perspectives,* 109**,** 547-551.

VAN RAVENZWAAY, B., LANDSIEDEL, R., FABIAN, E., BURKHARDT, S., STRAUSS, V. & MA-HOCK, L. 2009. Comparing fate and effects of three particles of different surface properties: Nano-TiO2, pigmentary TiO2 and quartz. *Toxicology Letters,* 186**,** 152-159.

VANCE, M. E., KUIKEN, T., VEJERANO, E. P., MCGINNIS, S. P., HOCHELLA, M. F., JR., REJESKI, D. & HULL, M. S. 2015. Nanotechnology in the real world: Redeveloping the nanomaterial consumer products inventory. *Beilstein Journal of Nanotechnology,* 6**,** 1769-1780.

WANG, J., LIU, Y., JIAO, F., LAO, F., LI, W., GU, Y., LI, Y., GE, C., ZHOU, G., LI, B., ZHAO, Y., CHAI, Z. & CHEN, C. 2008. Time-dependent translocation and potential impairment on central nervous system by intranasally instilled TiO(2) nanoparticles. *Toxicology,* 254**,** 82-90.

WANG, J., ZHOU, G., CHEN, C., YU, H., WANG, T., MA, Y., JIA, G., GAO, Y., LI, B., SUN, J., LI, Y., JIAO, F., ZHAO, Y. & CHAI, Z. 2007. Acute toxicity and biodistribution of different sized titanium dioxide particles in mice after oral administration. *Toxicology Letters,* 168**,** 176-185.

WARHEIT, D. B., WEBB, T. R., SAYES, C. M., COLVIN, V. L. & REED, K. L. 2006. Pulmonary instillation studies with nanoscale TiO2 rods and dots in rats: Toxicity is not dependent upon particle size and surface area. *Toxicological Sciences,* 91.

YANG, L., YI, Z. & BING, Y. 2014. Nanotoxicity Overview: Nano-threat to Susceptible Populations. *International Journal of Molecular Science,* 15**,** 3671-97.

YU, L. E., YUNG, L.-Y. L., ONG, C.-N., TAN, Y.-L., BALASUBRAMANIAM, K. S., HARTONO, D., SHUI, G., WENK, M. R. & ONG, W.-Y. 2007. Translocation and effects of gold nanoparticles after inhalation exposure in rats. *Nanotoxicology,* 1**,** 235-242.

ZHANG, J., LI, B., ZHANG, Y., LI, A., YU, X., HUANG, Q., FANA, C. & CAI, X. 2013. Synchrotron radiation X-ray fluorescence analysis of biodistribution and pulmonary toxicity of nanoscale titanium dioxide in mice. *Analyst,* 138**,** 6511-6516.

Figures:

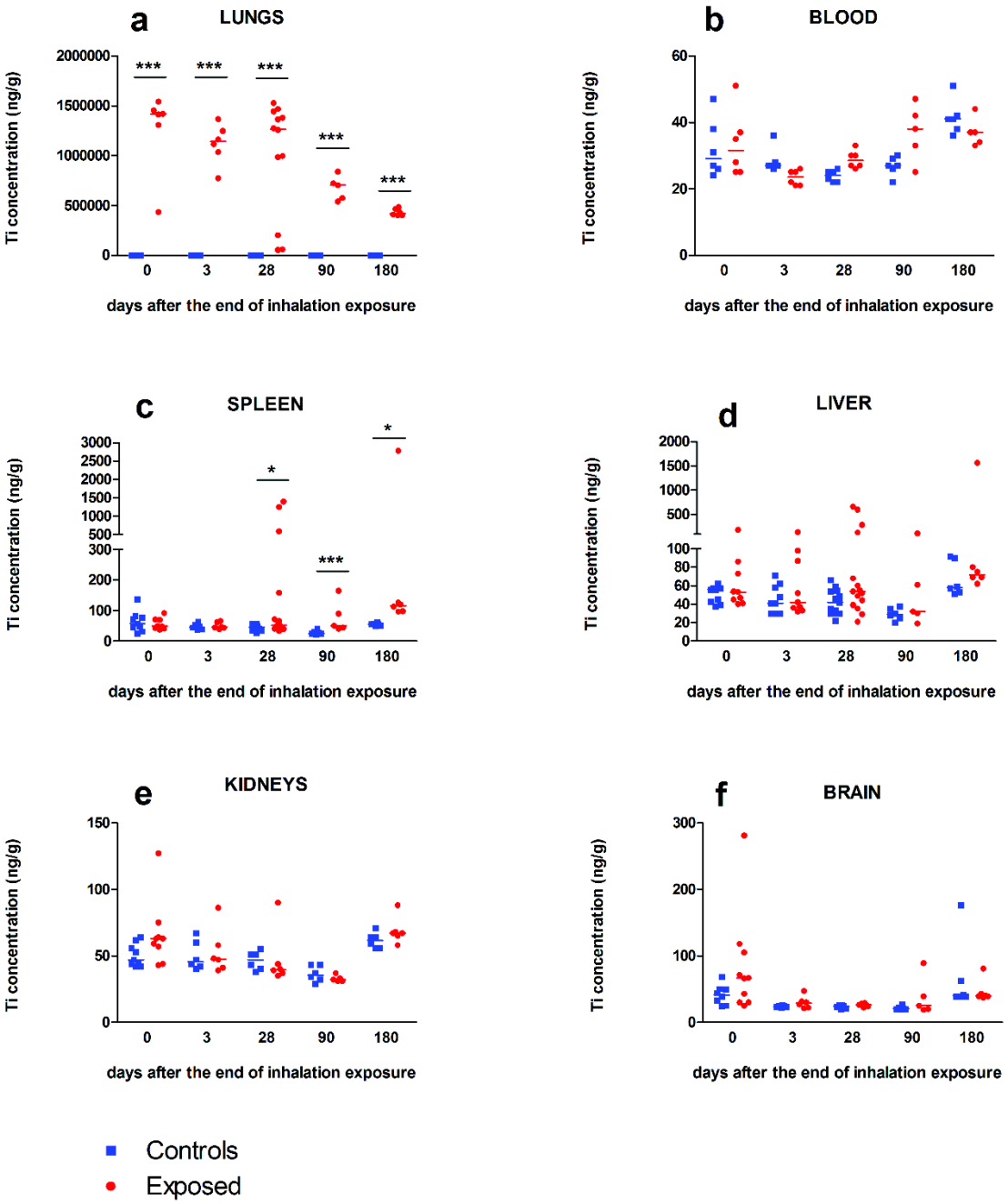

Figure 1: Tissue distribution of titanium after subacute TiO_2 nano-aerosol exposure in young adult rats.

Titanium quantification in lungs (a); blood (b); spleen (c); liver (d); kidneys (e) and brain (f) of exposed and control animals. Quantification by inductively coupled plasma mass spectrometry (ICP-MS). Results represents the median of n = 5 to 13 animals. Statistical comparison between treated and control groups was by two way ANOVA after Box-Cox transformation on Ti concentration variable and Bonferroni post hoc test, *P <0.05; **P <0.01; ***P <0.001.

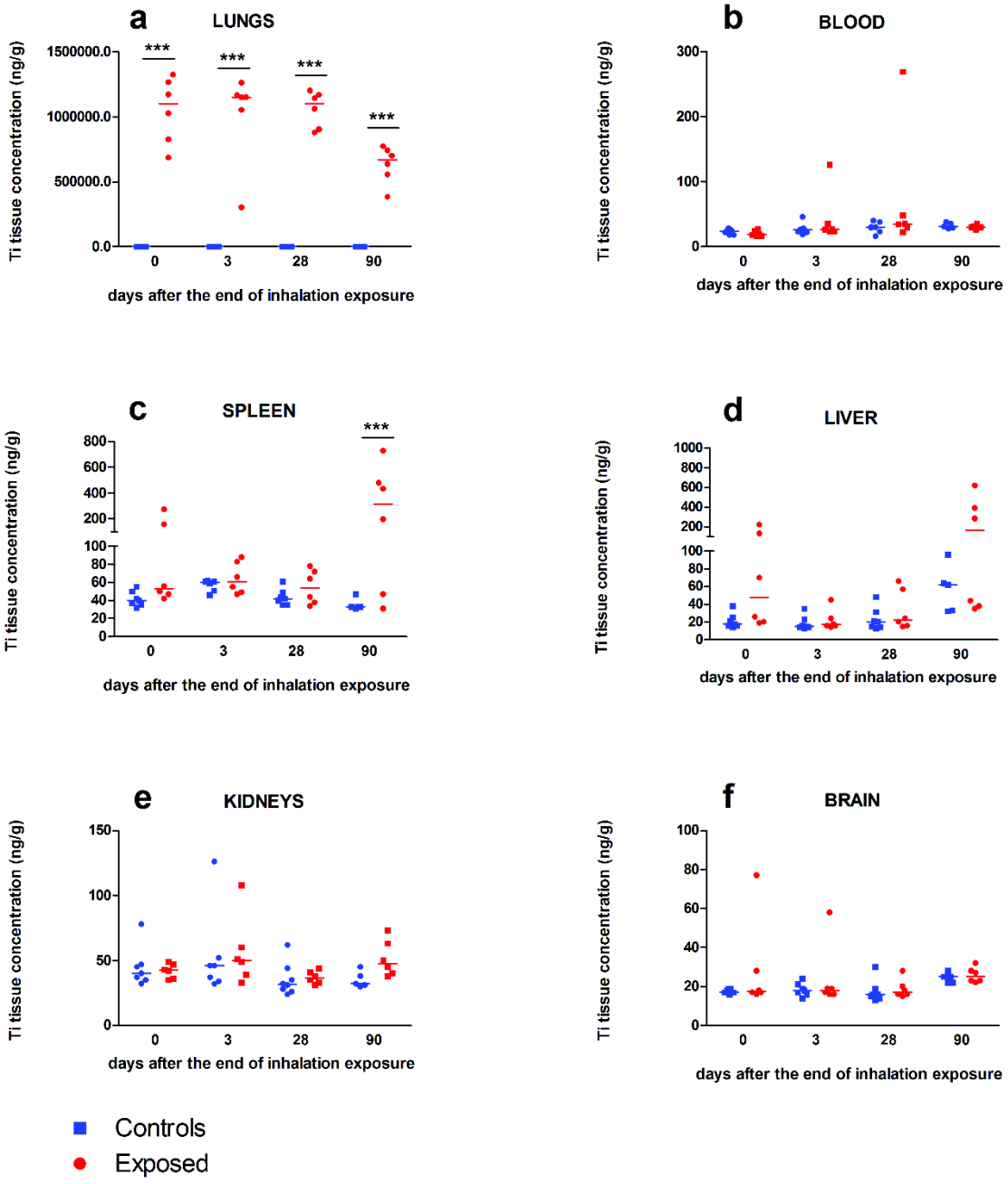

Figure 2: Tissue distribution of titanium after sub-acute TiO_2 nano-aerosol exposure in vulnerable elderly rats.

Titanium quantification in lungs (a); blood (b); spleen (c); liver (d); kidneys (e) and brain (f) of exposed and control animals. Quantification by inductively coupled plasma mass spectrometry (ICP-MS). Results represents the median of n = 6 to 8 animals. Statistical comparison between treated and control groups was performed was by two way ANOVA after Box-Cox transformation on Ti concentration variable and Bonferroni post hoc test, ***P <0.001.

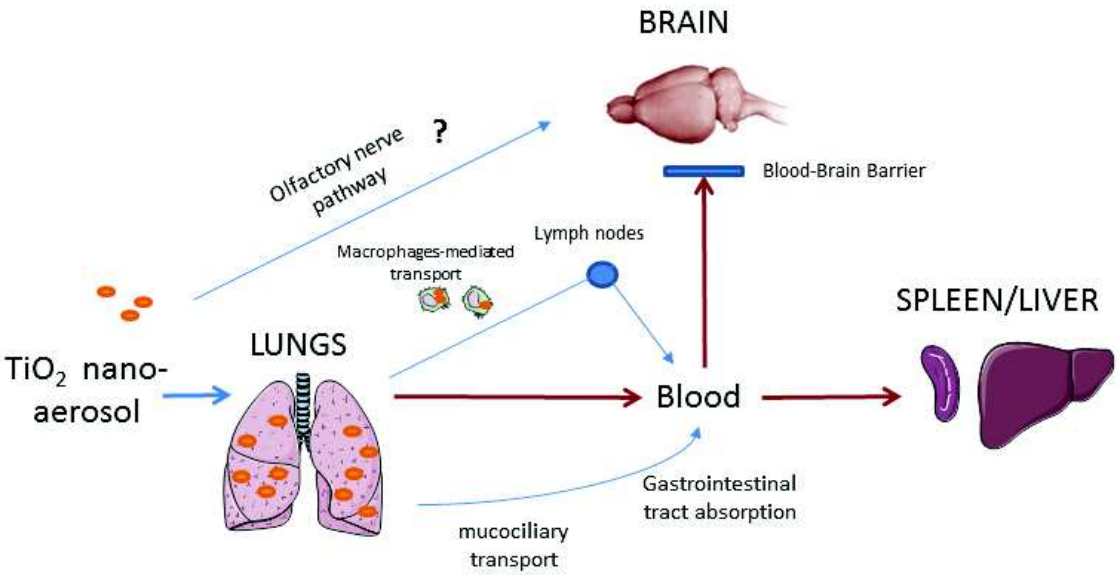

Figure 3: Schematic summary of the distribution and potential way of translocation to extra-pulmonary organs of inhaled TiO_2 NPs.

2. Impact on the central nervous system and the BBB physiology

2.1. Context and introduction

Studies after intratracheal or intranasal instillation in rodents demonstrated CNS adverse effects but no data are available under representative environmental conditions. The biodistribution study after subacute inhalation exposure to TiO_2 NPs aerosols showed titanium biopersistence in lung tissue, spleen and liver. Despite lack of brain translocation evidence, potential neurotoxic effects and impact on the BBB need to be considered. Indeed, undetectable Ti trace in olfactory bulbs cannot be ruled out. Such trace in the olfactory bulbs may be responsible for local effects but also mediated neurotoxicity. Furthermore, indirect effect associated with circulating mediators secretion due to Ti biopersistence in peripheral organs could have an impact on the BBB functions. Taken together, the barrier permeability and neuro-inflammation parameters have therefore been investigated extensively in young adults and aging rats after subacute inhalation exposure.

After subacute inhalation exposure, we investigated the same parameters of BBB integrity than after IV administration using several methods: *in vivo* evaluation by studying atenolol brain to plasma partition coefficient and evaluation of tight junction proteins expressions by immunohistochemistry. The neuro-inflammation as well as systemic inflammation was assessed by a multiplexed approach and immunohistochemistry.

2.2. Major findings and discussion

Major findings highlighted impact of TiO_2 NPs subacute exposure by inhalation on BBB permeability. The expression of claudin-5 protein expression is decrease in both age group. This decrease of one major tight junction protein didn't affect the low paracellular passage at the BBB in exposed young adults. Unlike, in aging group, we observed an increased in the BBB permeability characterized by the increased of atenolol Kp. These modulations were associated with acute neuro-inflammation in both age groups. Several cytokines and chemokines were over-expressed in brain cortexes of exposed animals. The response in term of BBB permeability alteration and neuro-inflammation was exacerbated in aging brain. Since it is found that in a barrier already structurally more permeable, a decrease in the expression of a tight junction protein causes a worsening integrity loss, this exacerbated response in the aging brain confirms the vulnerability status of the aging BBB.

The results indicate induction of brain inflammation in the absence of detectable translocation of the titanium in the brain. This significant inflammation at late times points suggest 1) an indirect mechanism due certainly to the circulating mediators or 2) direct interactions due to undetectable titanium circulating in blood. We can note that research of pro-inflammatory mediators in sera was performed by the multiplex method. We have targeted 11 pro-inflammatory cytokines and chemokines (Il1β, IL6, EGF, MIP2, IFNγ, MCP1, IP10, VEGF, Fractalkine, RANTES, TNFα) among which only 5 have been quantified in sera (MCP1, IP10, VEGF, Fractalkine, RANTES). No overexpression of these pro-inflammatory cytokines was evidenced in the blood of exposed rats (Figure 36).

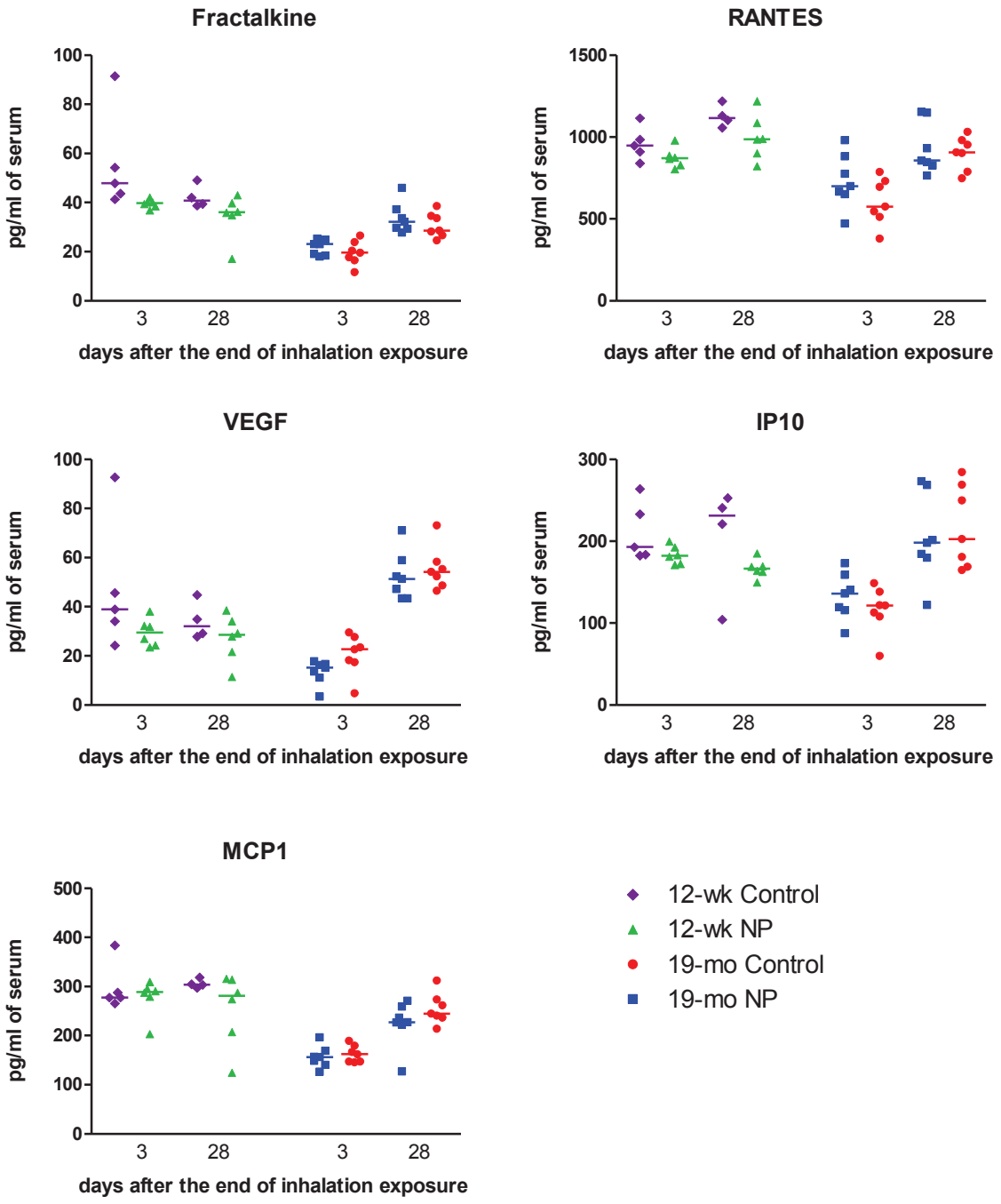

Figure 36: Detection of 5 inflammatory markers in young adults and aging rat sera after subacute inhalation exposure to TiO_2 nano-aerosol. Measure was done in sera collected 3 or 28 days after the end of the inhalation exposure by multiplexing approach. Each data point represent one animal with median of n = 4 to 7 animals.

As in the IV study, we intended to use the *in vitro* BBB model to explore existence of circulating mediators or trace titanium in the blood of exposed rats. The *in vitro* BBB model was exposed to diluted plasmas collected 28 days after the end of the inhalation period from control and exposed rats. At the end of the 24 hours exposure in the apical compartment, the permeability

of BECs monolayer was figured out using ^{14}C sucrose or Lucifer yellow (LY). Exposure of the *in vitro* cell based BBB model to plasmas did not affect the integrity of the cell monolayers. Indeed, the apparent permeability for LY and ^{14}C sucrose were under the integrity threshold after exposure to young adult plasmas. These findings are consistent with *in vivo* observations. However, exposure to aging rats' plasmas did not reveal alteration in permeability in contrast to *in vivo* observations. The use of a primary young adult cell based model may explain such discrepancy. The development of an aging BBB *in vitro* model will shed light in this age related differences in the TiO_2 NPs exposure response.

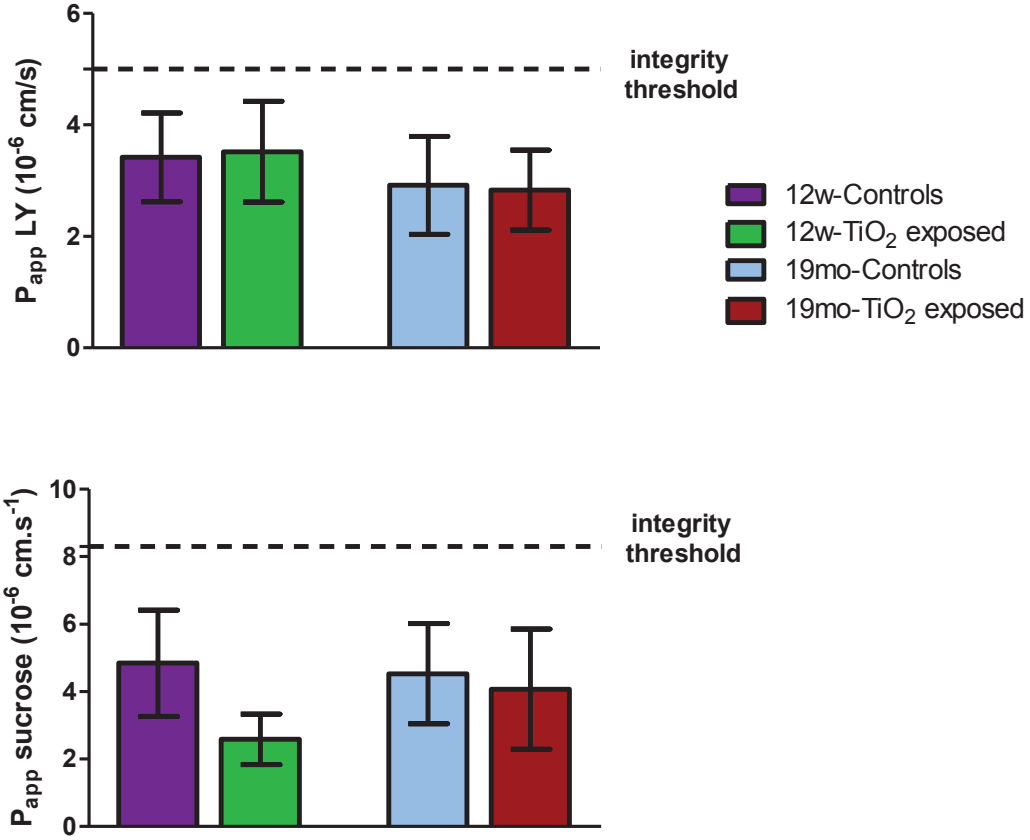

Figure 37: Impact of exposure to plasma from exposed animals on the *in vitro* BBB model. Plasmas collected from controls and exposed animals 28 days after the end of the inhalation period were applied on the apical compartment for 24 hours. The endothelial cell monolayer integrity was check using ^{14}C-sucrose and/or lucifer yellow (LY). Each data point represent mean ± SD of n = 6 samples; each sample representing a pool of 3 or 6 culture wells.

The BECs and astrocytes composing the model were recovered for mRNA profiling by RT-qPCR. After exposure to plasmas from aging exposed rats, we have observed a decrease of expression of claudin 5 (P = 0.12) emphasize with *in vivo* observations (Figure 35b). Moreover, after exposure to plasmas from both age group, we noticed a decrease in expression of INSR (Figure 35d and h; P = 0.24 after exposure to young adults plasmas) suggesting potential alteration of insulin metabolism at the BBB. It has been suggested that neurodegeneration might

be a consequence of a dysfunctional insulin signaling in AD patients [3]. In astrocytes, we have highlighted an increase IBA1 (ionized calcium-binding adapter molecule 1) mRNA expression after exposure to young adults plasmas suggesting microglia activation (Figure 35i) and thereby potential cytokines/chemokines release.

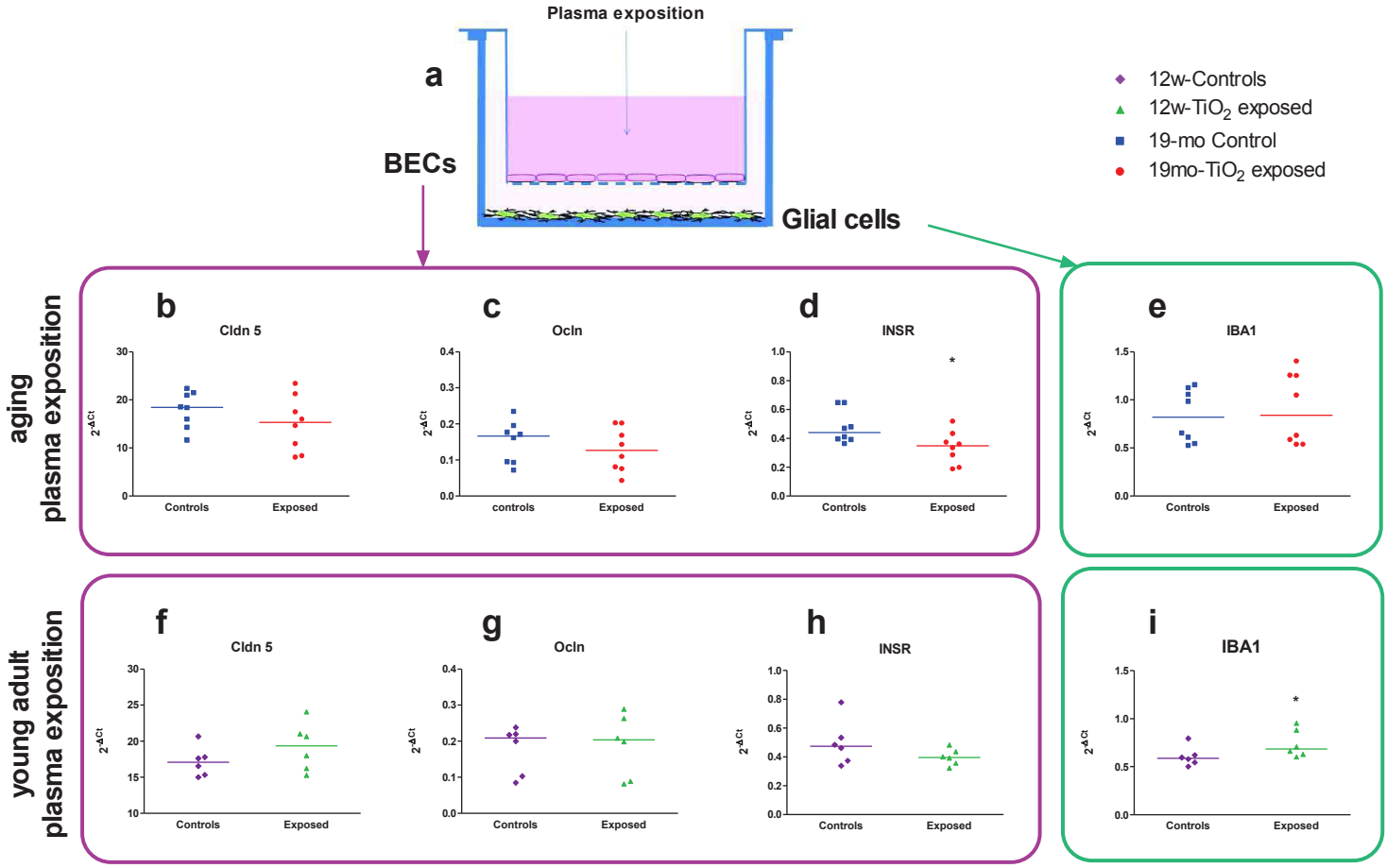

Figure 38: Impact of exposure to plasma from aging and young adults exposed animals on the *in vitro* BBB model. (a) schematic view of the model architecture. BECs were grown on a semipermeable membrane whereas glial cells were seeded on the well bottom. mRNA expressions were quantified by RT-qPCR after 24 hours exposure to plasmas from control and exposed rats. For BECs, expression of tight junction protein claudin 5 (b and f), occludin (c and g) and INSR (e and h) are represented. For glial cells, expressions of IBA 1 (e and i) is represented. Data represent a median of n=8 or 6 samples, each sample representing the mRNA pool from 6 wells. RT-qPCR was performed in duplicate for each single sample. Statistical comparison performed by two-tailed Student t test and one-tailed for claudin 5 after homogeneity of variance confirmation by Hartley test; *P<0.05.

2.3. Article 3: Brain Inflammation and Blood Brain Barrier dyfunction after Sub acute Inhalation Exposure to Titanium Dioxide Nano-aerosol in Aging Rats

Submitted to Particle and Fibre Toxicology on 2016/02/26

Particle and Fibre Toxicology

Brain Inflammation and Blood Brain Barrier dysfunction after Sub acute Inhalation Exposure to Titanium Dioxide Nano-aerosol in Aging Rats

Clémence Disdier[1], Monique Chalansonnet[2], François Gagnaire[2], Susie Barbeau[1], Laurent Gaté[2], Frédéric Cosnier[2], Jérome Devoy[2], Wadad Saba[3], Amie Lund[4], Emilie Brun[5], Aloïse Mabondzo[1*]

1. CEA, Direction des Sciences du Vivant, iBiTec-S, Service de Pharmacologie et d'Immunoanalyse, Equipe Pharmacologie Neurovasculaire, 91191 Gif-sur-Yvette, France
2. INRS, Département Toxicologie et Biométrologie, Rue du Morvan, CS 60027, 54519 Vandœuvre Cedex, France
3. Inserm / CEA / Université Paris Sud, UMR 1023 - ERL 9218 CNRS, IMIV, Orsay, F-91406, France
4. Department of Biological Sciences, Institute of Applied Sciences, University of North Texas, Denton, TX, USA
5. Laboratoire de Chimie Physique, UMR CNRS 8000 Université Paris-Sud 91405 Orsay, France

Address correspondence to: Aloïse Mabondzo

Phone number: 33 1 69081321 e-mail address: aloise.mabondzo@cea.fr

Abstract

Background: Notwithstanding potential neurotoxicity of titanium dioxide nanoparticles (TiO_2 NPs), the toxicokinetics and consequences on blood brain barrier (BBB) functions remain poorly characterized. To improve risk assessment, we needed to evaluate the impact on BBB under realistic environmental conditions and to take into account vulnerability status such as age. Previous experiments highlighted that after a 4 wk inhalation period, TiO_2 NPs were observed to accumulate in the lungs and to translocate to extrapulmonary organs (spleen and liver).

Methods: 12-13 week and 19-month-old male rats were exposed by inhalation to 10mg/m^3 of TiO_2 nano-aerosol for 6 hr/day, 5 d/wk, for 4 wk. Resulting *in vivo* BBB permeability and structural components were evaluated. The brain inflammatory profile was assessed by multiplexing analysis and quantified/localized by immuno-fluorescence.

Results: Despite the lack of evidence of TiO_2 translocation to the central nervous system (CNS), we noted an age-dependent modulation of BBB integrity parameters (increase of cerebral concentrations of a paracellular marker associated with a decrease of tight junction proteins expressions), suggesting increased BBB permeability in vulnerable aging rats. The TiO_2 NP-mediated BBB permeability alteration was associated with a significant increase of cytokines/chemokines in the brain, including interleukin-1β, interferon-γ, and fractalkine. These observations, in absence of detectable titanium in the brain, may suggests an indirect effect that may be mediated by signal transduction pathways initiated by circulating factors.

Conclusion: Despite the lack of CNS translocation, we observed an association between the presence of TiO_2 NPs in organs and the dysregulation of BBB physiology associated with neuro-inflammation, which was further exacerbated in the brain of aged animals. Moreover,

observations in term of BBB permeability and inflammation response in the brain underline age susceptibility.

Introduction

Due to their remarkable properties, nanoparticles (NPs) could potentially be used in a large array of applications, from electronics to medicine. Nanomaterials are currently being utilized in the production or the manufacturing process of a number of commercial products [1]. In this context, there are increasing concerns regarding the potential adverse effects of NPs on human health. Among the wide variety of nanomaterials, titanium dioxide NPs (TiO_2 NPs) are produced in a large industrial scale and can be found in commercial products such as paints, food additives [2], cosmetics [3], and also environmental decontamination systems [4]. Published data from studies in rodents show that TiO_2 NPs can enter the circulation from the respiratory and the gastro-intestinal tract [5-10], and therefore translocation across the epithelial barriers (nasal, bronchial, alveolar, gastro- intestinal) is observed. After inhalation exposure, there is larger concern about translocation of NPs into the brain, either directly *via* the olfactory pathway or indirectly across the blood brain barrier (BBB). Indeed, ambient air particles and NPs have been previously demonstrated to translocate into the brain after inhalation, and thus may potentially influence the central nervous system (CNS). For example, translocation of 36 nm ^{13}C particles was observed *via* the olfactory bulb of rats, most likely originating from entry in the olfactory mucosa of the nose [11]. Brain translocation of gold NPs were also observed in rat exposure models [12], and 15-20 nm iridium NPs could be detected in the rat brain up to 6 months after inhalation exposure [13, 14]. Despite these observations, the effects of NPs on the CNS, have been studied to a limited extent. The few reports to date reveal increased oxidative stress, activated inflammatory response, modulation of neurotransmitter

levels in the brain, and impairment of spacial recognition associated with the presence of Ti in the brain [15-22]. Moreover, recent evidence suggests that exposure to air pollution containing fine particles can increase the risk of fatal stroke, cause cerebrovascular damage and neuroinflammation that may trigger neurodegenerative diseases such as Alzheimer's and Parkinson's diseases [23-26]. Altogether, these observations warrant further research to investigate the potential effects of TiO_2 NPs on cerebrovascular function.

If consequences of NP exposure on cerebrovascular functions are explored, aging must be considered. Indeed, increased BBB permeability has been demonstrated in the aging brain, as well as age-related elevations in inflammation, *via* redox imbalance, which could ultimately result in a cytotoxic activation of glia cells and neurodegeneration [27-29]. Aging is likely a critical vulnerability parameter to consider with NPs exposures, and thus warrants further investigation.

We have previously reported Ti tissue distribution after subacute inhalation of a well characterized TiO_2 nano-aerosol in adult and aging rats up to 180 days post-exposure, which revealed evidence of TiO_2 NPs biopersistence in lung and translocation to extrapulmonary organs such as liver and spleen but not to the brain (Gate et al., submitted). The observed biokinetics raise the questions of the impact of TiO_2 NPs on extrapulmonary organs, especially on the CNS *via* interaction at the BBB. Hence to the two hypothesis for the current study: inhalation exposure to TiO_2 NPs inhalation could result in BBB permeability alteration and subsequent brain inflammation, and aged rats could be more susceptible to CNS dysfunctions following NP exposure. To investigate these hypothesis, both young adult (12-13 wks old) and aged (19 mo old) rats were exposed to 10 mg/m^3 of TiO_2 nano-aerosol for 6 hr/d, 5 d/wk for a period of 28 days. Resulting *in vivo* BBB permeability was evaluated with a marker of

paracellular transport and brains were analyzed for neuroinflammation, after a recovery period of 3 and 28 days.

Results and discussion

Our previous findings highlighted a lack of TiO_2 NPs in the brain after subacute inhalation (Gate et al. submitted). In light of these observations, two possible mechanisms of TiO_2 NPs – exposure impact on the CNS can be hypothesized: (1) Accumulation of titanium in the lungs and/or extrapulmonary translocation of TiO_2 NPs, as evidenced by quantification in the spleen and liver, may result in either direct NP-interaction or initiation of signaling cascades at the BBB; and/or (2) trace amounts of Ti were actually present in small concentration in regions of the brain (such as olfactory bulbs) that we were not able to accurately quantify due to the methodology used for this study. We have previously demonstrated that after intravenous administration of TiO_2 NPs, the Ti biopersistence in peripheral organs was associated with dysregulation of the BBB and neuroinflammation [30], which suggests that either TiO_2 NPs are acting on the BBB, directly, or mediating expression of a secondary factor or signaling cascade at the BBB resulting in the observed alterations in barrier integrity.

BBB integrity assessment

The BBB is a physical barrier that limits the paracellular passage of xenobiotics in the brain. This limitation is explained by the presence of protein junctions between neighboring brain endothelial cells (BECs). To assess indirect effect of Ti on BBB integrity, the expression of tight junction (TJ) protein Claudin 5, as well as the partition coefficient (Kp) of atenolol (a known marker of paracellular transport across the BBB), were determined. Under normal

physiological conditions, atenolol does not cross the BBB, and thus concentrations and cerebral Kp should remain low. Conversely, an increase in cerebral Kp of atenolol suggests a permeability alteration of the BBB, allowing for atenolol to cross into the brain and accumulate. The average cerebral atenolol Kp in the young control rats was lower than that observed in the aged control rat brains, attesting to the increase in BBB permeability with aging (0.16 ± 0.018 vs 0.028 ± 0.0058, respectively) (Figure 1B and 1D). This age related difference in BBB permeability emphasizes the structural alteration of the BBB with aging.

In the young adults group, cerebral atenolol concentrations (Figure 1A) and atenolol Kp (Figure 1B) between the control and exposed animals remained unchanged, suggesting a lack of BBB permeability modulation. In contrast, results from the aged rat brains showed that atenolol Kp remain unchanged at day 3, but significantly increased at day 28 post TiO_2 NPs-exposure (Figure 1D; 0.23 ± 0.054 in exposed vs 0.15 ± 0.033 in controls). These facts suggest that TiO_2 nano-aerosol exposure results in exacerbation of BBB integrity loss that is associated with age-related alterations in BBB integrity.

To characterize more precisely the permeability modulations at the BBB level observed after 28 days of recovery, brains from controls and exposed animals were sampled and protein expressions of TJ proteins were assessed by double-immunofluorescence. Expression of claudin-5, one of the primary proteins expressed in TJ intercellular connections between adjacent BECs that contribute to BBB structural integrity, was down-regulated at 28 days after the end of the TiO_2 nano-aerosol inhalation period in both the young and aged rat brains, compared to control animals (Figure 2E and 2F, and Figure 3E and 3F). The even further decrease of TJ protein expression in the cerebrum of the TiO_2 NPs-exposed aged rat, compared to that in the young rats, correlates with an increased alteration of BBB integrity

(quantification graphs represented in Figures 2 and 3). Interestingly, the claudin-5 expression decrease observed in the microvasculature of the young rat brains (Figure 2) was not accompanied with an alteration of BBB permeability, as shown in Figure 1A and 1B. This further underscores age-related baseline vulnerability and differences in response of the BBB to TiO_2 NP exposure (or possibly other stressors). Moreover, other mechanisms involving for example the other junction proteins regulating the BBB permeability, may occur at the barrier level. For example severe decreases in occludin and/or zonula occludens expression that we did not explore may explain increase permeability of the BBB in the aging brain.

Neuroinflammation assessment

BBB permeability alteration is a common response in the inflamed brain [31]. Indeed, The BBB integrity is affected by pro-inflammatory mediators (cytokines and chemokines)[30, 32, 33]. These mediators could initiate changes in permeability and adhesions properties of BECs that allow immune cells to infiltrate the CNS. Inflammation within the CNS and BBB permeability alterations has been associated with chronic neurodegenerative disease including Alzheimer's diseases (AD), multiple sclerosis and Parkinson's disease [34-39]. Many of these changes have been linked to alterations in BBB TJ. Moreover, we have previously described increased cerebral neuroinflammation after TiO_2 NPs i.v. administration to rats [30]. To determine whether TiO_2 NP exposure *via* inhalation results in neuroinflammation, phenomenon that can promote increased BBB permeability, we quantified cytokines and chemokines in the serum, olfactory bulbs, and cerebral tissues (cerebrum and cerebellum) from control and exposed rats of both age groups. Interestingly, assays in the olfactory bulb homogenates did not reveal any modulation in levels of inflammatory markers (data not shown). These results contradict the observations of Wang et al. which showed a translocation of 80 or 150 nm TiO_2 NPs associated

with inflammation in the olfactory bulb level after nasal instillation in mice [15, 16]. Apart from different sizes of NPs, the dose of 500 µg of TiO_2 suspension up to 15 times per mouse might have overestimated translocation of NPs *via* nerves pathways. Indeed, after nasal instillation of 65,3 µg, 653,8 µg or 1,3 mg during 10 days per rat of our NPs we didn't recover titanium in olfactory bulbs of exposed rats 24 hours after instillation (data not shown). Altogether, our observations in the olfactory bulb after nasal instillation and subacute inhalation exposure suggest that it is unlikely that TiO_2 NPs can gain access to the CNS *via* the olfactory pathway.

In both age groups, we noted a significant increase in the expression of several pro-inflammatory cytokines and chemokines in the cerebral tissues extracts (Figure 4). Interleukin- -1β (IL-1β) was found to be significantly upregulated 28 days after the end of the inhalation exposure in both age groups. Furthermore, the increase in IL-1β expression in the cerebrum of TiO_2 exposed animals (both young and aged), compared to controls, was confirmed by immunofluorescence staining (Figures 5 and 6). In particular, we observed an increase in IL-1β localization in the midbrain (Figure 5B and 5D) and forebrain (Figure 6B and 6D) in TiO_2 exposed brains compared to the respective age-matched controls (Figures 5A and 5B and Figures 6A and 6B). IL-1β is a key mediator of neuroinflammation, particularly in the context of neurodegenerative diseases such as AD or Parkinson's disease [40]. Both aging and inflammation in the brain are also known to mediate memory deficits *via* IL-1β [41, 42]. Our results show that in aged rat brains, TiO_2 nano-aerosol exposure results in an even further increase in IL-1β expression than in young rat brains.

We also observed an increase in VEGF (Vascular Endothelial Growth Factor) and fractalkine at 28 days post-inhalation in both age groups. VEGF is a factor that is responsible for regulating microvascular permeability to blood plasma proteins [43], amongst other functions. Therefore,

the reported increase BBB permeability in the aged group may be due in part to the increased expression of VEGF. Fractalkine, which is expressed on the surface of endothelial cells, regulates trafficking and adhesion of immune cells at endothelium [44]. As a soluble chemokine, it acts as a chemoattractant for T cells and monocytes, and promotes leukocytes adhesion. Increased IFNγ (Interferon-gamma), IP-10 (IFN-gamma-inducible protein 10) at 3 days and RANTES (Regulated on Activation, Normal T cell Expressed and Secreted) at 28 days after the end of the inhalation period in young adults group brains underscores the inflamed environment in the brain of exposed animals [45]. In aging group, the increase in IFNγ expression was only significant at the 28 day-post exposure time point, suggesting a delay in the brain inflammatory response. Altogether, up-regulation of cytokines/chemokines and adhesion molecules in the brain of TiO_2 NP-exposed rats suggest infiltration of immune cells in the brain. Importantly, this inflammatory process occurs in the brain in the absence of detectable Ti accumulation. Additionally, as there was no expression of these pro-inflammatory markers present in the olfactory bulbs, the neuroinflammatory response observed in the cerebral tissue suggest involvement of TiO_2 NP (or another circulating factor) mediating expression of these makers of inflammation *via* signaling at the BBB. This premise is further confirmed through a similar induction of cerebral inflammation following i.v. administration of the same TiO_2 NPs to rats[30]. Cytokine and chemokine concentrations were also assessed in the serum from controls and treated rats in both age groups. Among the 11 cytokines and chemokines targeted, we were able to quanty only 5 analytes. These non-exhaustive assays did not demonstrate the upregulation of pro-inflammatory markers in the blood of exposed animals (data not shown). Even though an exposure-mediated induction of a systemic pro-inflammatory factor cannot be conclusively be ruled out, it is plausible that other biological

circulating mediators, such as lipids or other metabolites, may be mediating the response at the BBB and thus warrants further investigations.

Multiple previous studies have demonstrated an increased secretion of pro-inflammatory mediators in neurodegenerative diseases conditions such as AD [46, 47]. For example, elevated expressions of RANTES has been previously reported in the brains of AD patients, and is believed to play a role in a neuroprotective response [48]. IL-1β has also been detected in microglial cells surrounding Aβ plaques in brains from patients with AD [47]. Thus, our results raise the question as to whether the BBB dysfunction and the neuroinflammation induced after TiO_2 nano-aerosol exposure may be involved in the neurodegenerative process, particularly in the aging brain. Furthermore, findings such as these suggest a role for environmental (or occupational) exposures to NPs in the pathogenesis of neuroinflammatory-mediated disease states.

The neuro-inflammation is described in both age groups but is associated with BBB integrity loss only in the aging group. This raise the question of the BBB impairment of repair mechanism or of adaptive response to stress in the aging brain. It further underscore the need of investigation of NPs toxicity in at risk population such as the elderly.

Conclusions

We investigated the impact of TiO_2 nano-aerosols subacute inhalation exposure in altering BBB integrity and in driving inflammation in the brains of young and aged rats. While we did not observe any evidence of brain TiO_2 NPs translocation, our findings highlighted the promotion of BBB dysregulation and neuroinflammation under realistic environmental exposure conditions in both young and aged rats. Dysregulation of BBB structural integrity

and permeability were observed in aged exposed rats in contrast with only an alteration in TJ protein (claudin-5), without increased permeability in young exposed rats 28-days post TiO_2 NP-exposure, compared to control animals. Dysregulation of BBB function was associated with acute neuroinflammation, characterized by a significant increase in cerebral expressions of several pro-inflammatory markers (IL-1β, RANTES, fractalkine, VEGF, IP-10 and IFNγ). Along with our results, this emphasizes the need of further research to investigate neurodegenerative process that may occur, as a result of exposure to NPs, in the aging exposed. Importantly, the hypothesis of direct translocation of TiO_2 NPs from the nasal mucosa *via* the olfactory bulb appeared unlikely due to the absence of Ti in that region after nasal instillation and inflammation after subacute inhalation exposure. Altogether, the major findings of our study reveal a potential link between dysregulation of BBB structure and function, and the presence of titanium in peripheral tissues (lung, spleen, or liver). Additional research is needed to identify the mediators responsible for this indirect neurotoxic effect of TiO_2 NPs.

Materials and methods

Chemicals

TiO_2 P25 NPs (Aeroxide® P25, 75% anatase 25% rutile, Evonik®) were from Sigma Aldrich (Saint-Quentin Fallavier, France).

Animals

The animal facilities have full accreditation (D54-547-10) and while conducting the research described in this article, investigators adhered to the guide for care and use of laboratory

animals promulgated by the European Parliament and Council (Directive 2010/63/EC, 2010/63/EU, 22 September 2010). The present study was approved by our local ethical committee appointed by the French Ministry of Research and Higher Education (Project n° 00692.01).

Male Fisher F344 rats (from Charles River Laboratories, France), 12-13 weeks old and weight 300-320 g referred as young adults and 19 months old , weight 400-425 g referred as aging group [49], were housed in standard environmental conditions (room humidity 55±10% and temperature 22±2 °C ; room under a 12 : 12 hrs light dark cycle) and maintained with free access to water and standard laboratory diet. The aging rats were fed separately with A04 diet (Safe diet) from 1 month of age to 7 months then with A05 diet (Safe diet) adapted to long term studies.

Generation and monitoring of TiO_2 nano-aerosol

The inhalation which has already been described (Cosnier et al, submitted) system is mainly composed of an aerosol generation system and inhalation towers for nose-only exposure. Exposure capability is around 100 rats: 50 NPs exposed rats (in 6 × 9 ports manifold) and 50 control rats (in 2 × 27 ports manifold). Controls were exposed to filtered air. During the 6-hrs exposure, rats did not have access to food or water. The system has been fully validated according to OCDE guidelines for chemicals testing. The integrated control of the exposure conditions (airflow, temperature and relative humidity, depression) is managed and recorded using dedicated software. Air entering the towers was filtered and conditioned at a temperature of 22°C ± 2°C and a humidity of 55 ± 10 %. To produce test aerosol of aggregates and agglomerates NPs, a dry power with rotating brush generator (RBG) (RBG1000 PALAS)

method was chosen. Aerosol concentration was adjusted with feed rate of the RBG operated at constant air flow rate. The aerosol monitoring and the characterization was ensured by real time devices (condensation particle counter, electrical low pressure impactor, aerodynamic particle sizer, scanning mobility particle sizer spectrometer, optical light scattering dust monitor,) and off-line analyses (gravimetric filter, particle size-distribution by cascade impactor, sampling for TEM observations). Mass concentrations were measured on the basis of gravimetric samplings taken twice to 4 times a day on 25 mm cassettes with GLA-5000 PVC filters (5 µm pore size).

***In vivo* experimental design**

Before the beginning of the aerosol exposure period, rats were acclimated to the restraining tubes according to the daily scheme of experiment: 2 periods of 3 hrs exposure. Rats were then exposed to filtered air (controls) or TiO_2 nano-aerosol (exposed) during 2 periods of 3 hrs a day, 5 days/week for 4 weeks. 3 and 28 days after the end of the inhalation exposure period, animals were anesthetized with isoflurane and euthanized. Organs were collected, sampled, and store at -80°C until assay.

Neuroinflammation assessment using multiplexing approach

The cerebral cortex and olfactory bulbs were dissected, crushed in 10 volumes of TRIS lysis buffer 50mM (Sigma) added with proteases inhibitor (Calbiochem) using homogenization for 60 sec in TeenPrep (15ml) Lysing Matrix D (MP Biomedicals). The homogenates were first centrifuged for 5 min at 2000G then the supernatant was recovered for ultracentrifugation for 30 min at 26184G and stored at -80 ° C until assayed.

Multiple cytokines/chemokines (Il1β, IL6, EGF, MIP2, IFNγ, MCP1, IP10, VEGF, Fractalkine, RANTES, TNFα) were analysed in extracts from either the cerebral tissues (cerebrum+ cerebellum), olfactory bulbs, or sera using a MILLIPLEX MAP (Merck Millipore, Billerica, US) kit and the Biorad Bioplex-200 analysis instrument (Bio-Rad laboratories, Hercules, US) all according to manufacturer's instructions. Bioplex manager software was used to generate standard curves and calculate sample cytokines/chemokines concentrations. Assays were performed in duplicate for each brain extract. Results are expressed as mean of duplicate.

BBB Permeability Measurement

4 hours before animal necropsy, control and exposed rats were anesthetized with isoflurane and subcutaneously implanted with mini-osmotic pumps (Alzet model 2001D; DURECT Corp., Cupertino, California). Pumps were filled with atenolol dissolved in PEG200/DMSO (50/50) to deliver at 0.25 mg/kg/h. At day 3 and 28, animals were anesthetized with isoflurane and euthanized. Plasma samples and brain were collected and weighed immediately after death. The atenolol concentration were quantified in the two compartments using tandem mass spectrometry coupled with liquid chromatography (LC/MSMS). BBB integrity was estimated by the ratio of atenolol brain to plasma concentration (C_{brain} and C_{plasma}, respectively). This ratio is described by the partitioning coefficient (Kp).

$$Kp = \frac{C_{brain}}{C_{plasma}}$$

LC/MSMS Assay for Atenolol Quantification

Brains were mixed in ultrapure water (2 mL/g of tissue) using an Ultraturrax T65 system (IKA-Werke, Staufen, Germany). Extract suspensions (400 µL) were submitted to protein precipitation with 1 mL of methanol previously spiked with internal standard (atenolol-d7 4

µg/mL). After centrifugation (20000G; 15 min; 4 °C) the supernatant was dried under nitrogen at 40 °C. The dried extracts were resuspended in 1 mL 0.75 M NH_4OH / methanol (80:20 v/v). Plasma (150 µL) was diluted with 150 µL of 0.75 M NH_4OH / methanol (80:20 v/v) previously spiked with internal standard. Both brain and plasma extracts were submitted to solid-liquid extraction on isolute SLE+ columns 1 or 6 mL (Biotage). The two eluates (3 mL of dichloromethane/isopropanol (70:30 v/v) then 3 mL of dichloromethane/isopropanol (70:30 v/v) + 0.2 % formic acid) were pooled and evaporated to dryness. The dry extracts were resuspended in 200 µL of 5 mM ammonium acetate/methanol (95:5 v/v). Chromatography was performed using a Shimadzu HPLC system LC 20AD on a Kinetex C18 column (Phenomenex).The total run time was 5 min and the flow rate was 0.4 mL/min. Analyte (20 µL) was injected onto the column placed in an oven at 40 °C.

Detection was done by tandem mass spectrometry (Finnigan TSQ Quantum Discovery with Xcalibur and LC Quan softwares, Thermo) in positive electrospray mode. Tuning parameters were: capillary voltage 3 kV, source temperature 200 °C. The multiple reaction monitoring transitions for atenolol were m/z atenolol 267.18 > 145.1. Analyte was quantified by means of calibration curves using atenolol-d7 as internal standard. For plasma and brain extract assay, calibration ranges were from 1.0 to 200 ng/mL.

Immunofluorescence

Midsagittal brain sections sampled at 28 days after the end of the inhalation period were embedded in OCT and cut on a cryostat (10 µm) were prepared for either claudin-5 and vonWillebrand factor (vWF) double immunofluorescence, or IL-1β. Brain sections were air dried for 30 minutes and fixed in ice-cold acetone for 30 minutes and then rinsed in PBS. Sections were then incubated with 3% BSA for 60 min at RT, rinsed in PBS, and incubated with

150 µl per section of the appropriate primary antibody (claudin-5: 1:100, Invitrogen/Life Technologies, Carlbad, CA) and a FITC-tagged vWF (1:1000 dilution, Abcam) or IL-1β (1:1000, Abcam) alone; diluted in rinse wash buffer [1 part 5% blocking solution (0.5 ml Normal Rabbit Serum in 10 ml 3% w/v Bovine Serum Albumin) and 4 parts Phosphate Buffered Saline (PBS)] for 1 hr at RT and then rinsed 3 times with PBS. The slides were then incubated in 150 µl per section of the appropriate secondary antibody either Alexa Fluor 555 or Alexa Fluor 546 (1:1000 dilution, Vector Laboratories, Biovalley, Marne la Vallée, France) in the dark for 1 hr at RT. Slides were then rinsed 3 times in PBS and subsequently incubated with Hoescht nuclear stain (1 µl/ml; 150 µl/section) for one minute, rinsed again then coverslipped with Aqueous Gel Mount (TBS, Fisher Scientific, Waltham, MA). Slides were imaged by fluorescent microscopy at 10x and 40x, using the appropriate excitation/emission filters, digitally recorded, and analyzed by image densitometry using Image J software (NIH). A minimum of 3 locations on each section (2 sections per slide), 3 slides and n=3 per group were processed/analyzed. IL-1β was quantified by total amount of fluorescence per unit area (consistent across regions/slides). Midbrain analysis included regions of midbrain, brainstem, hippocampal formation, and cerebral cortex (somatosensory); Forebrain analysis included regions of the cerebral cortex (somatomotor) and cerebral nuclei/caudoputamen/striatum. Only vessels <50 µm were used for claudin-5 analysis.

Statistical Analysis

After homogeneity of variance confirmation by Hartley or Bartlett test, atenolol partition coefficients were analyzed using one way ANOVA between control and exposed groups followed by Tukey post hoc test (Prism 5.1 program, GraphPad Software, Inc, San Diego CA), Changes were considered statistically significant at $p < 0.05$. Cytokines and chemokines assays

were analyzed either using one way ANOVA followed by Tukey post hoc test when Hartley or Bartlett test confirmed homogeneity of variances (Il1β, IFNγ, VEGF and IP10 for both aged groups; RANTES for aging group) or Kruskal-Wallis test followed by test by Dunn's post hoc test (RANTES for young adult groups). Immunofluorescence endpoints were analyzed using a one way ANOVA between treatment groups followed by Holm-Sidak post hoc test (SigmaPlot SyStat Software Inc, San Joes, CA) and data expressed as mean ± SE. Changes were considered statistically significant at $p < 0.05$.

Abbreviations

AD: Alzheimer's diseases

BBB: Blood Brain Barrier

BECs: Brain Endothelial Cells

CNS: Central Nervous System

IARC: the International Agency for Research on Cancer

IFNγ: Interferon-gamma

Il1 β: Interleukin-1β

INF γ: Interferon-γ

IP-10: IFN-gamma-inducible protein 10

i.v.: intravenous

Kp: partition coefficient

NIOSH: The National Institute for occupational safety and health

RANTES: Regulated on Activation, Normal T cell Expressed and Secreted

TiO_2 NPs: titanium dioxide nanoparticles

TJ: tight junction

VEGF: Vascular Endothelial Growth Factor

Competing interests

The authors declare that they have no competing interests.

Author's contributions

CD participated in the design of the studies, animal experiments, LC/MSMS and multiplex studies. AL oversaw immunohistochemistry studies. FC designed the procedure for aerosol generation and characterization. LG and MC coordinate the animal exposure and necropsy. All authors participated in the design of the study. Manuscript was written by CD, corrected and approved by all authors. AM participated in the study design and coordination and assisted with drafting the manuscript. All authors read and approved the final manuscript prior to submission.

Acknowledgements

This work was supported by the French Agency for Food, Environmental and Occupational Health Safety (ANSES). The authors would like to thank Lise Merlen for her contribution in *in vivo* experiments and sample preparation. The authors gratefully acknowledge the INRS staff for animal care, husbandry, animal exposure and tissue collection. This research was supported by the University of North Texas.

References

1. Vance, M. E.; Kuiken, T.; Vejerano, E. P.; McGinnis, S. P.; Hochella, M. F., Jr.; Rejeski, D.; Hull, M. S., Nanotechnology in the real world: Redeveloping the nanomaterial consumer products inventory. *Beilstein Journal of Nanotechnology* **2015**, *6*, 1769-1780.
2. Lomer, M. C.; Thompson, R. P.; Powell, J. J., Fine and ultrafine particles of the diet: influence on the mucosal immune response and association with Crohn's disease. *Proc Nutr Soc* **2002**, *61*, 123-30.
3. Kaida, T.; Kobayashi, K.; Adachi, M.; Suzuki, F., Optical characteristics of titanium oxide interference film and the film laminated with oxides and their applications for cosmetics. *J Cosmet Sci* **2004**, *55*, 219-20.
4. Chen, X.; Mao, S. S., Titanium dioxide nanomaterials: Synthesis, properties, modifications, and applications. *Chemical Reviews* **2007**, *107*, 2891-2959.
5. Shinohara N, O. Y., Kobayashi T, Imatanaka N, Nakai M, Ichinose T, Sasaki T, Kawaguchi K, Zhang G, Gamo M., Pulmonary clearance kinetics and extrapulmonary translocation of seven titanium dioxide nano- and submicron materials following intratracheal administration in rats. In Nanotoxicology: 2015; Vol. 4.
6. Shinohara, N.; Oshima, Y.; Kobayashi, T.; Imatanaka, N.; Nakai, M.; Ichinose, T.; Sasaki, T.; Zhang, G.; Fukui, H.; Gamo, M., Dose-dependent clearance kinetics of intratracheally administered titanium dioxide nanoparticles in rat lung. *Toxicology* **2014**, *325*, 1-11.
7. Zhang, J.; Li, B.; Zhang, Y.; Li, A.; Yu, X.; Huang, Q.; Fana, C.; Cai, X., Synchrotron radiation X-ray fluorescence analysis of biodistribution and pulmonary toxicity of nanoscale titanium dioxide in mice. *Analyst* **2013**, *138*, 6511-6516.
8. Husain, M.; Wu, D.; Saber, A. T.; Decan, N.; Jacobsen, N. R.; Williams, A.; Yauk, C. L.; Wallin, H.; Vogel, U.; Halappanavar, S., Intratracheally instilled titanium dioxide nanoparticles translocate to heart and liver and activate complement cascade in the heart of C57BL/6 mice. *Nanotoxicology* **2015**, *9*, 1013-22.
9. Wang, J.; Zhou, G.; Chen, C.; Yu, H.; Wang, T.; Ma, Y.; Jia, G.; Gao, Y.; Li, B.; Sun, J.; Li, Y.; Jiao, F.; Zhao, Y.; Chai, Z., Acute toxicity and biodistribution of different sized titanium dioxide particles in mice after oral administration. *Toxicology Letters* **2007**, *168*, 176-185.
10. Hong, J.; Wang, L.; Zhao, X.; Yu, X.; Sheng, L.; Xu, B.; Liu, D.; Zhu, Y.; Long, Y.; Hong, F., Th2 Factors May Be Involved in TiO2 NP-Induced Hepatic Inflammation. *Journal of Agricultural and Food Chemistry* **2014**, *62*, 6871-6878.
11. Oberdorster, G.; Sharp, Z.; Atudorei, V.; Elder, A.; Gelein, R.; Kreyling, W.; Cox, C., Translocation of inhaled ultrafine particles to the brain. *Inhalation Toxicology* **2004**, *16*, 437-445.
12. Yu, L. E.; Yung, L.-Y. L.; Ong, C.-N.; Tan, Y.-L.; Balasubramaniam, K. S.; Hartono, D.; Shui, G.; Wenk, M. R.; Ong, W.-Y., Translocation and effects of gold nanoparticles after inhalation exposure in rats. *Nanotoxicology* **2007**, *1*, 235-242.
13. Semmler, M.; Seitz, J.; Erbe, F.; Mayer, P.; Heyder, J.; Oberdorster, G.; Kreyling, W. G., Long-term clearance kinetics of inhaled ultrafine insoluble iridium particles from the rat lung, including transient translocation into secondary organs. *Inhalation Toxicology* **2004**, *16*, 453-459.
14. Kreyling, W. G.; Semmler-Behnke, M.; Seitz, J.; Scymczak, W.; Wenk, A.; Mayer, P.; Takenaka, S.; Oberdorster, G., Size dependence of the translocation of inhaled iridium and carbon nanoparticle aggregates from the lung of rats to the blood and secondary target organs. *Inhalation toxicology* **2009**, *21 Suppl 1*.
15. Wang, J.; Chen, C.; Liu, Y.; Jiao, F.; Li, W.; Lao, F.; Li, Y.; Li, B.; Ge, C.; Zhou, G.; Gao, Y.; Zhao, Y.; Chai, Z., Potential neurological lesion after nasal instillation of TiO(2) nanoparticles in the anatase and rutile crystal phases. *Toxicology Letters* **2008**, *183*, 72-80.

16. Wang, J.; Liu, Y.; Jiao, F.; Lao, F.; Li, W.; Gu, Y.; Li, Y.; Ge, C.; Zhou, G.; Li, B.; Zhao, Y.; Chai, Z.; Chen, C., Time-dependent translocation and potential impairment on central nervous system by intranasally instilled TiO(2) nanoparticles. *Toxicology* **2008**, *254*, 82-90.
17. Li, Y.; Li, J.; Yin, J.; Li, W.; Kang, C.; Huang, Q.; Li, Q., Systematic Influence Induced by 3 nm Titanium Dioxide Following Intratracheal Instillation of Mice. *Journal of Nanoscience and Nanotechnology* **2010**, *10*, 8544-8549.
18. Zhang, L.; Bai, R.; Li, B.; Ge, C.; Du, J.; Liu, Y.; Le Guyader, L.; Zhao, Y.; Wu, Y.; He, S.; Ma, Y.; Chen, C., Rutile TiO(2) particles exert size and surface coating dependent retention and lesions on the murine brain. *Toxicology Letters* **2011**, *207*, 73-81.
19. Ze, Y.; Zheng, L.; Zhao, X.; Gui, S.; Sang, X.; Su, J.; Guan, N.; Zhu, L.; Sheng, L.; Hu, R.; Cheng, J.; Cheng, Z.; Sun, Q.; Wang, L.; Hong, F., Molecular mechanism of titanium dioxide nanoparticles-induced oxidative injury in the brain of mice. *Chemosphere* **2013**, *92*, 1183-1189.
20. Ze, Y.; Sheng, L.; Zhao, X.; Ze, X.; Wang, X.; Zhou, Q.; Liu, J.; Yuan, Y.; Gui, S.; Sang, X.; Sun, Q.; Hong, J.; Yu, X.; Wang, L.; Li, B.; Hong, F., Neurotoxic characteristics of spatial recognition damage of the hippocampus in mice following subchronic peroral exposure to TiO2 nanoparticles. *Journal of Hazardous Materials* **2014**, *264*, 219-229.
21. Ze, Y.; Hu, R.; Wang, X.; Sang, X.; Ze, X.; Li, B.; Su, J.; Wang, Y.; Guan, N.; Zhao, X.; Gui, S.; Zhu, L.; Cheng, Z.; Cheng, J.; Sheng, L.; Sun, Q.; Wang, L.; Hong, F., Neurotoxicity and gene-expressed profile in brain-injured mice caused by exposure to titanium dioxide nanoparticles. *Journal of Biomedical Materials Research Part A* **2014**, *102*, 470-478.
22. Ze, Y.; Sheng, L.; Zhao, X.; Hong, J.; Ze, X.; Yu, X.; Pan, X.; Lin, A.; Zhao, Y.; Zhang, C.; Zhou, Q.; Wang, L.; Hong, F., TiO2 Nanoparticles Induced Hippocampal Neuroinflammation in Mice. *Plos One* **2014**, *9*.
23. Block, M. L.; Calderon-Garciduenas, L., Air pollution: mechanisms of neuroinflammation and CNS disease. *Trends in Neurosciences* **2009**, *32*, 506-516.
24. Palacios, N.; Fitzgerald, K. C.; Hart, J. E.; Weisskopf, M. G.; Schwarzschild, M. A.; Ascherio, A.; Laden, F., Particulate matter and risk of parkinson disease in a large prospective study of women. *Environmental Health* **2014**, *13*.
25. Calderon-Garciduenas, L.; Reed, W.; Maronpot, R. R.; Henriquez-Roldan, C.; Delgado-Chavez, R.; Calderon-Garciduenas, A.; Dragustinovis, I.; Franco-Lira, M.; Aragon-Flores, M.; Solt, A. C.; Altenburg, M.; Torres-Jordon, R.; Swenberg, J. A., Brain inflammation and Alzheimer's-like pathology in individuals exposed to severe air pollution. *Toxicologic Pathology* **2004**, *32*, 650-658.
26. Peters, A.; Veronesi, B.; Calderon-Garciduenas, L.; Gehr, P.; Chen, L. C.; Geiser, M.; Reed, W.; Rothen-Rutishauser, B.; Schurch, S.; Schulz, H., Translocation and potential neurological effects of fine and ultrafine particles a critical update. *Particle and fibre toxicology* **2006**, *3*, 13.
27. Palmer, A. M., The Role of the Blood Brain Barrier in Neurodegenerative Disorders and their Treatment. *Journal of Alzheimers Disease* **2011**, *24*, 643-656.
28. Elahy, M.; Jackaman, C.; Mamo, J. C. L.; Lam, V.; Dhaliwal, S. S.; Giles, C.; Nelson, D.; Takechi, R., Blood-brain barrier dysfunction developed during normal aging is associated with inflammation and loss of tight junctions but not with leukocyte recruitment. *Immunity & Ageing* **2015**, *12*.
29. Grammas, P.; Martinez, J.; Miller, B., Cerebral microvascular endothelium and the pathogenesis of neurodegenerative diseases. *Expert Reviews in Molecular Medicine* **2011**, *13*.
30. Disdier, C.; Devoy, J.; Cosnefroy, A.; Chalansonnet, M.; Herlin-Boime, N.; Brun, E.; Lund, A.; Mabondzo, A., Tissue biodistribution of intravenously administrated titanium dioxide nanoparticles revealed blood-brain barrier clearance and brain inflammation in rat. *Particle and fibre toxicology* **2015**, *12*, 27-27.
31. Miller, D. W., Immunobiology of the blood-brain barrier. *Journal of Neurovirology* **1999**, *5*, 570-578.
32. Abbott, N. J.; Patabendige, A. A. K.; Dolman, D. E. M.; Yusof, S. R.; Begley, D. J., Structure and function of the blood-brain barrier. *Neurobiology of Disease* **2010**, *37*, 13-25.

33. Didier, N.; Romero, I. A.; Creminon, C.; Wijkhuisen, A.; Grassi, J.; Mabondzo, A., Secretion of interleukin-1 beta by astrocytes mediates endothelin-1 and tumour necrosis factor-alpha effects on human brain microvascular endothelial cell permeability. *Journal of Neurochemistry* **2003**, *86*, 246-254.
34. Abbott, N. J.; Friedman, A., Overview and introduction: The blood-brain barrier in health and disease. *Epilepsia* **2012**, *53*, 1-6.
35. Daneman, R., The blood-brain barrier in health and disease. *Annals of Neurology* **2012**, *72*, 648-672.
36. Akiyama, H., Inflammation in Alzheimer's disease. *Brain Pathology* **2000**, *10*, 707-708.
37. Hirsch, E. C.; Vyas, S.; Hunot, S., Neuroinflammation in Parkinson's disease. *Parkinsonism & related disorders* **2012**, *18 Suppl 1*, S210-2.
38. Farrall, A. J.; Wardlaw, J. M., Blood brain barrier: ageing and microvascular disease-systematic review and meta-analysis. *Journal of the Neurological Sciences* **2009**, *283*, 261-261.
39. Starr, J. M.; Farrall, A. J.; Armitage, P.; McGurn, B.; Wardlaw, J., Blood-brain barrier permeability in Alzheimer's disease: a case-control MRI study. *Psychiatry Research-Neuroimaging* **2009**, *171*, 232-241.
40. Rothwell, N. J.; Luheshi, G. N., Interleukin I in the brain: biology, pathology and therapeutic target. *Trends in Neurosciences* **2000**, *23*, 618-625.
41. Prieto, G. A.; Snigdha, S.; Baglietto-Vargas, D.; Smith, E. D.; Berchtold, N. C.; Tong, L.; Ajami, D.; LaFerla, F. M.; Rebek, J., Jr.; Cotman, C. W., Synapse-specific IL-1 receptor subunit reconfiguration augments vulnerability to IL-1 beta in the aged hippocampus. *Proceedings of the National Academy of Sciences of the United States of America* **2015**, *112*, E5078-E5087.
42. Lynch, M. A., Age-related impairment in long-term potentiation in hippocampus: A role for the cytokine, interleukin-1 beta? *Progress in Neurobiology* **1998**, *56*, 571-589.
43. Nagy, J. A.; Dvorak, A. M.; Dvorak, H. F., Vascular Hyperpermeability, Angiogenesis, and Stroma Generation. *Cold Spring Harbor Perspectives in Medicine* **2012**, *2*.
44. Imai, T.; Hieshima, K.; Haskell, C.; Baba, M.; Nagira, M.; Nishimura, M.; Kakizaki, M.; Takagi, S.; Nomiyama, H.; Schall, T. J.; Yoshie, O., Identification and molecular characterization of fractalkine receptor CX(3)CR1, which mediates both leukocyte migration and adhesion. *Cell* **1997**, *91*, 521-530.
45. Dufour, J. H.; Dziejman, M.; Liu, M. T.; Leung, J. H.; Lane, T. E.; Luster, A. D., IFN-gamma-Inducible protein 10 (IP-10; CXCL10)-deficient mice reveal a role for IP-10 in effector T cell generation and trafficking. *Journal of Immunology* **2002**, *168*, 3195-3204.
46. McGeer, P. L.; Rogers, J.; McGeer, E. G., Inflammation, anti-inflammatory agents and Alzheimer disease: The last 12 years. *Journal of Alzheimers Disease* **2006**, *9*, 271-276.
47. Heneka, M. T.; Carson, M. J.; El Khoury, J.; Landreth, G. E.; Brosseron, F.; Feinstein, D. L.; Jacobs, A. H.; Wyss-Coray, T.; Vitorica, J.; Ransohoff, R. M.; Herrup, K.; Frautschy, S. A.; Finsen, B.; Brown, G. C.; Verkhratsky, A.; Yamanaka, K.; Koistinaho, J.; Latz, E.; Halle, A.; Petzold, G. C.; Town, T.; Morgan, D.; Shinohara, M. L.; Perry, V. H.; Holmes, C.; Bazan, N. G.; Brooks, D. J.; Hunot, S.; Joseph, B.; Deigendesch, N.; Garaschuk, O.; Boddeke, E.; Dinarello, C. A.; Breitner, J. C.; Cole, G. M.; Golenbock, D. T.; Kummer, M. P., Neuroinflammation in Alzheimer's disease. *Lancet Neurology* **2015**, *14*, 388-405.
48. Tripathy, D.; Thirumangalakudi, L.; Grammas, P., RANTES upregulation in the Alzheimer's disease brain: A possible neuroprotective role. *Neurobiology of Aging* **2010**, *31*, 8-16.
49. Sengupta, P., The Laboratory Rat: Relating Its Age With Human's. *International journal of preventive medicine* **2013**, *4*, 624-30.

Figures legends:

Figure 1: BBB permeability assessment. The permeability was estimated by the atenolol cerebral concentration and the ratio between atenolol in the brain and plasma (partition coefficient or Kp) at 3 days and 28 days after the end of the inhalation exposure in young adults (A and B) and aging groups (C and D). Each data point represents one animal with median of n= 7 to 9 rats. *P<0.05;**P<0.01 compared to corresponding control.

Figure 2: Representative expression of (A,D) von Willenbrand factor, green fluorescence; (B, E) claudin-5, red fluorescence; (C, F) vessel-specific claudin-5, yellow overlay in midbrain microvessels (<100 µm in diameter) of (young) 12-13 wk control (A, B, C) or nanoparticle-exposed (D, E, F) rats at 28 days after the end of nano-aerosol exposure. Graph shows quantification of fluorescence shown in panels C and F. Scale bar = 100 µm. *p<0.050 compared to control rat microvessels.

Figure 3: Representative expression of (A, D) von Willebrand factor, green fluorescence; (B, E) claudin-5, red fluorescence; (C, F) vessel-specific claudin-5, yellow overlay in midbrain microvessels (<100 µm in diameter) of (aged) 19 mo control (A, B, C) or nanoparticle-exposed (D, E, F) rats at 28 days after the end of nano-aerosol exposure. Graph shows quantification of fluorescence shown in panels C and F. Scale bar = 100 µm. *p<0.050 compared to control rat microvessels.

Figure 4: Detection of 6 inflammatory markers in young adults and aging rat cerebral tissues (cerebrum + cerebelum) after subacute inhalation exposure to TiO_2 nano-aerosol. Measure was done in cerebral tissues extracts collected 3 or 28 days after the end of the inhalation

exposure by multiplexing approach. Each data point represents one animal with medians of 4 to 7 animals. *P<0.05; **P<0.01 compared to corresponding controls.

Figure 5: IL-1β expression (red fluorescence) in the midbrain of (A) 12-13 wk control, (B) 12-13 wk nanoparticle (NP)-exposed; (C) 19 mo control; and (D) 19 mo NP-exposed rats at 28 days after the end of nano-aerosol exposure. Relative fluorescence per unit area is represented in graph shown. *p<0.050 compared to 12-13 wk control; †p<0.050 compared to 19 mo control. Scale bar = 1000μm.

Figure 6: IL-1β expression (red fluorescence) in the forebrain of (A) 12-13 wk control, (B) 12-13 wk nanoparticle (NP)-exposed; (C) 19 mo control; and (D) 19 mo NP-exposed rats at 28 days after the end of nano-aerosol exposure. Relative fluorescence per unit area is represented in graph shown. *p<0.050 compared to 12-13 wk control; †p<0.050 compared to 19 mo control. Scale bar = 1000μm.

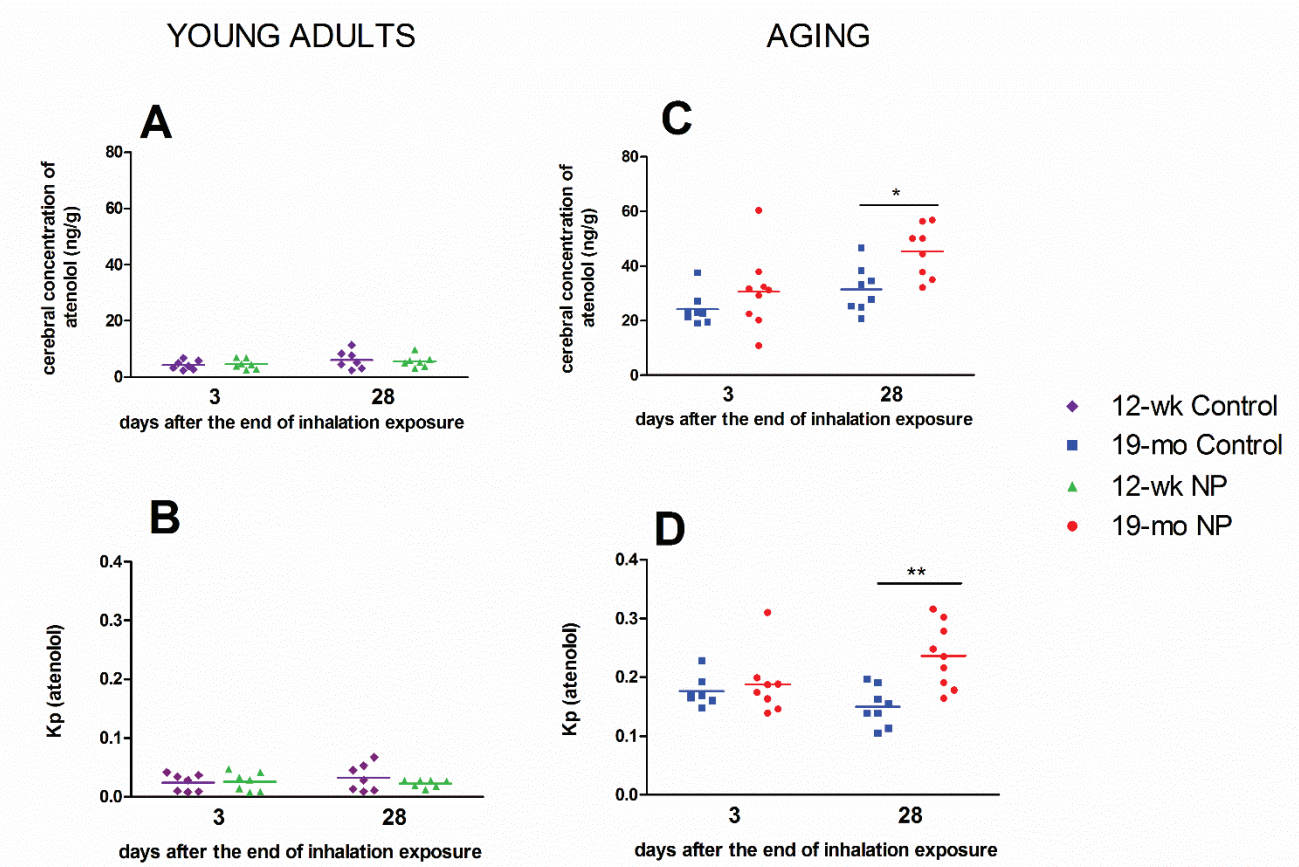

Figure 1: BBB permeability assessment. The permeability was estimated by the atenolol cerebral concentration and the ratio between atenolol in the brain and plasma (partition coefficient or Kp) at 3 days and 28 days after the end of the inhalation exposure in young adults (A and B) and aging groups (C and D). Each data point represents one animal with median of n= 7 to 9 rats.*P<0.05 ;**P<0.01 compared to corresponding control.

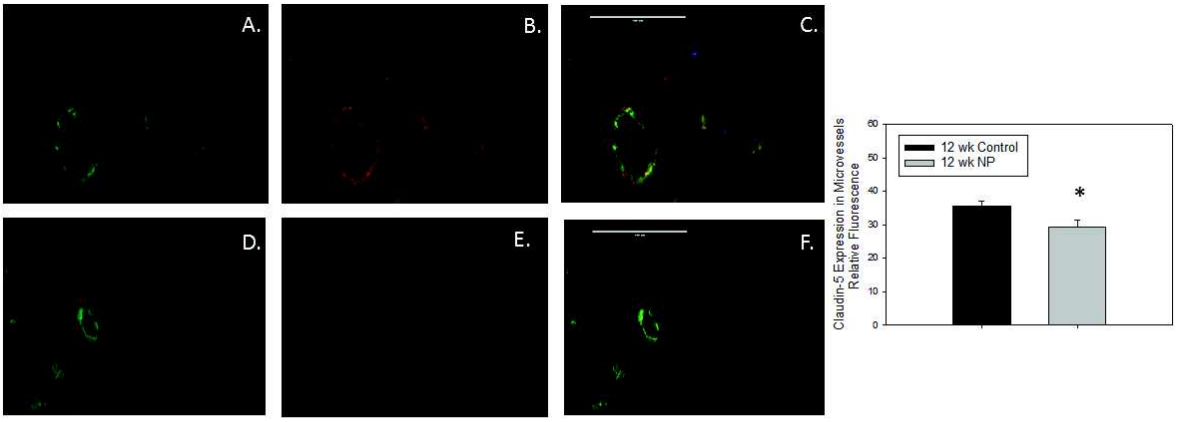

Figure 2: Representative expression of (A,D) von Willenbrand factor, green fluorescence; (B, E) claudin-5, red fluorescence; (C, F) vessel-specific claudin-5, yellow overlay in midbrain microvessels (<100 µm in diameter) of (young) 12-13 wk control (A, B, C) or nanoparticle-exposed (D, E, F) rats at 28 days after the end of nano-aerosol exposure. Graph shows quantification of fluorescence shown in panels C and F. Scale bar = 100 µm. *p<0.050 compared to control rat microvessels.

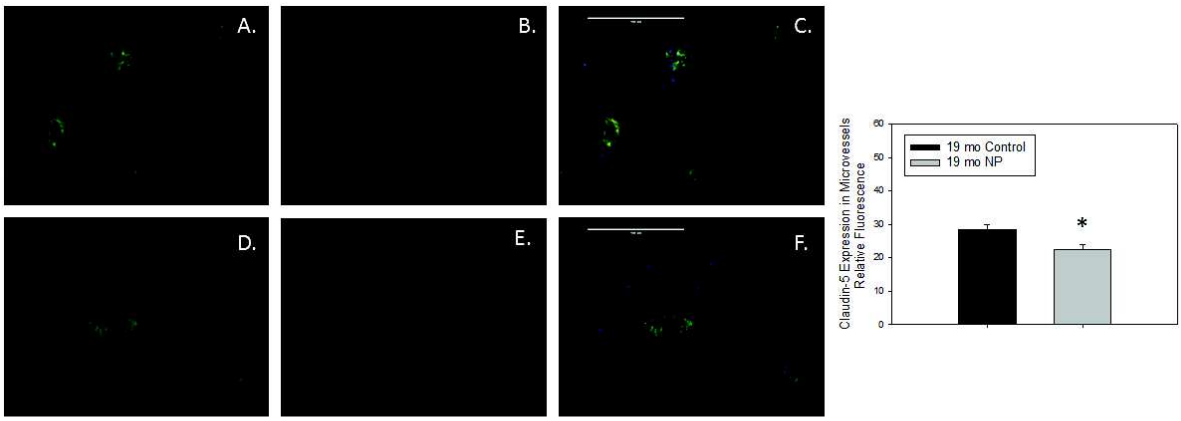

Figure 3: Representative expression of (A, D) von Willebrand factor, green fluorescence; (B, E) claudin-5, red fluorescence; (C, F) vessel-specific claudin-5, yellow overlay in midbrain microvessels (<100 µm in diameter) of (aged) 19 mo control (A, B, C) or nanoparticle-exposed (D, E, F) rats at 28 days after the end of nano-aerosol exposure. Graph shows quantification of fluorescence shown in panels C and F. Scale bar = 100 µm. *p<0.050 compared to control rat microvessels.

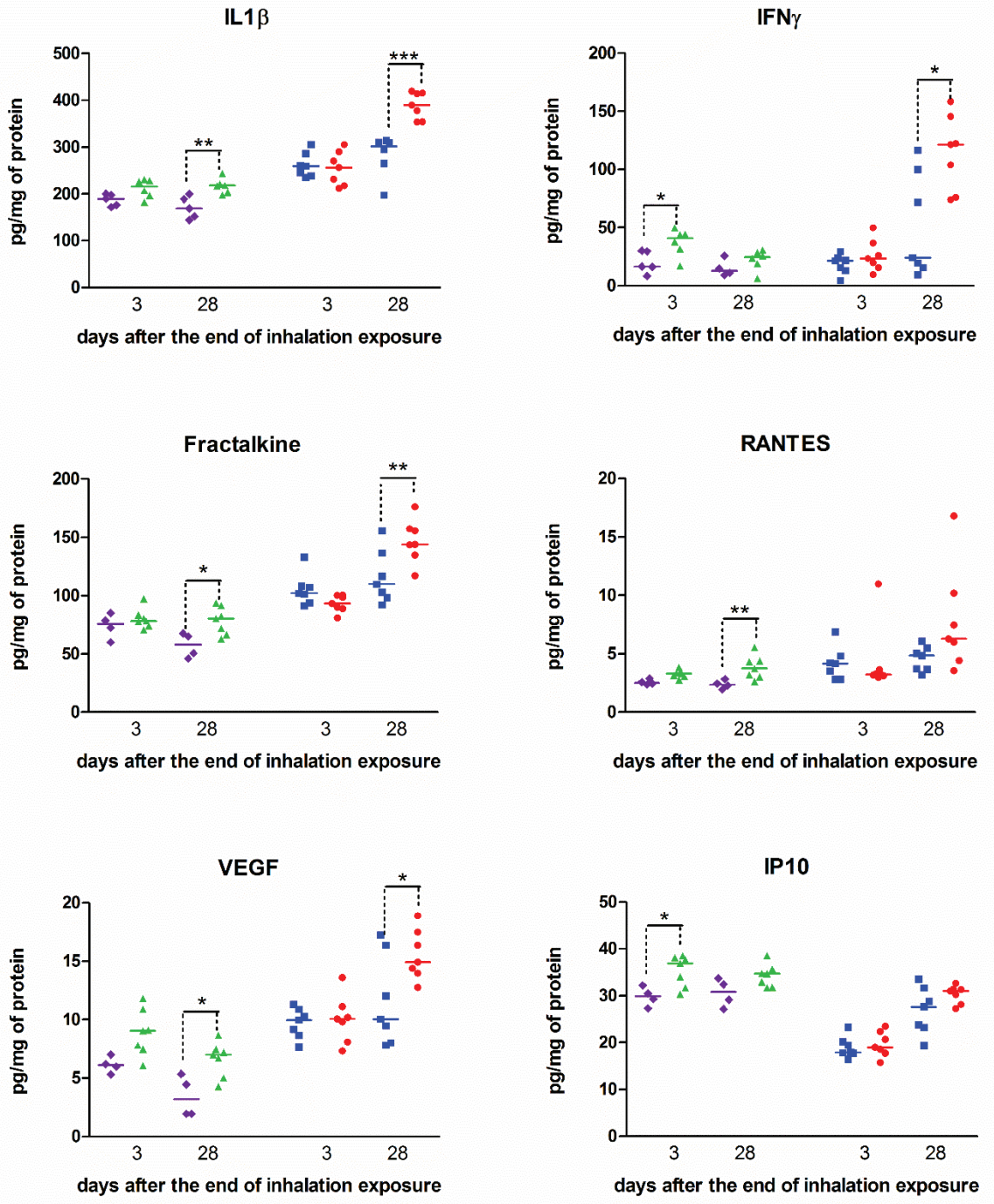

Figure 4: Detection of 6 inflammatory markers in young adults and aging rat cerebral tissues (cerebrum + cerebelum) after subacute inhalation exposure to TiO_2 nano-aerosol. Measure was done in cerebral tissues extracts collected 3 or 28 days after the end of the inhalation exposure by multiplexing approach. Each data point represents one animal with medians of 4 to 7 animals. *P<0.05; **P<0.01 compared to corresponding controls.

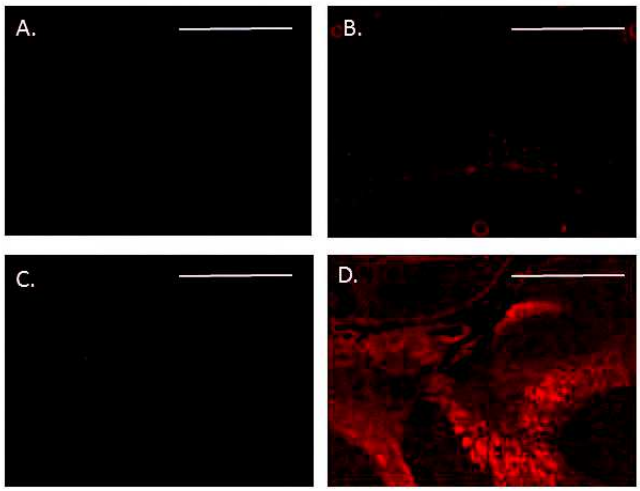

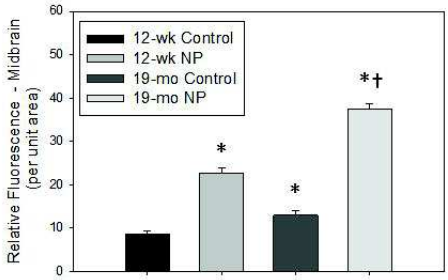

Figure 5: IL-1β expression (red fluorescence) in the midbrain of (A) 12-13 wk control, (B) 12-13 wk nanoparticle (NP)-exposed; (C) 19 mo control; and (D) 19 mo NP-exposed rats at 28 days after the end of nano-aerosol exposure. Relative fluorescence per unit area is represented in graph shown. *p<0.050 compared to 12-13 wk control; †p<0.050 compared to 19 mo control. Scale bar = 1000µm.

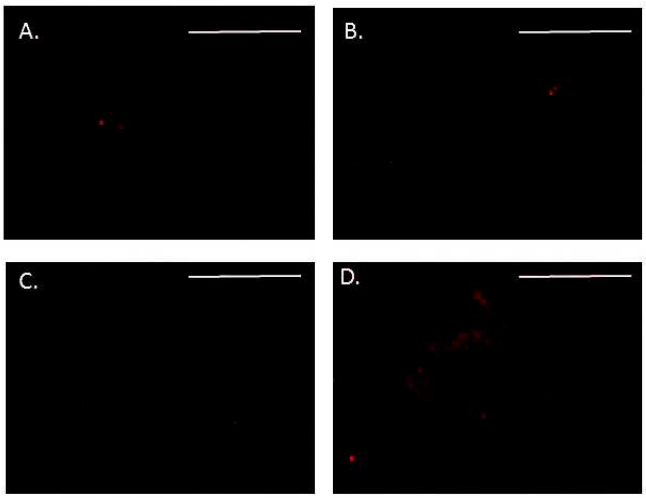

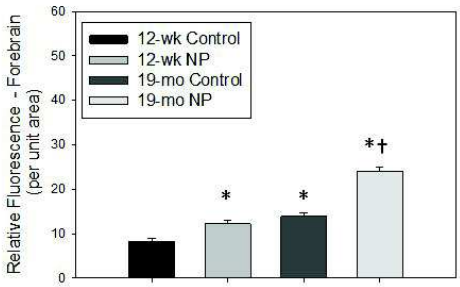

Figure 6: IL-1β expression (red fluorescence) in the forebrain of (A) 12-13 wk control, (B) 12-13 wk nanoparticle (NP)-exposed; (C) 19 mo control; and (D) 19 mo NP-exposed rats at 28 days after the end of nano-aerosol exposure. Relative fluorescence per unit area is represented in graph shown. *p<0.050 compared to 12-13 wk control; †p<0.050 compared to 19 mo control. Scale bar = 1000µm.

Conclusions and perspectives

Conclusions:

Previous laboratory results underscore the importance of *in vivo* assessment of the consequences of TiO_2 NPs on the brain and the BBB functions. Because of the BBB involvement in many brain diseases (e.g. neurodegenerative diseases), we suggest that exposure to TiO_2 NPs may regulate BBB functions, neuro-inflammation and promote neuro-toxicity in adult and aging brain. Therefore, the objective of this PhD project was to explore *in vivo* impact of TiO_2 NPs exposure on the BBB and brain functions in young adults and aging population.

The initial approach proposed in this project was firstly to conduct *in vivo* experiments by IV injection of TiO_2 NPs in rats. The IV corresponding to a 100% bioavailability, this study overcomes the interactions with other physiological barriers before the passage of NPs into the blood. For titanium quantification in tissues and organs samples, a mineralization methods was validated. This method allow sensitive ICP-MS quantification of titanium with a recovery of 96% recovery and a limit of quantification down to 0.9 µg/L for a titanium suspension. The assays carried out by ICP-MS showed a titanium bioaccumulation in various organs, particularly in the liver up to a year after IV administration of TiO_2 NPs. At the brain level, titanium is found in significant amounts during the first 6 hours after administration. The deep analysis of brain microvessels showed a rapid sequestration of titanium in the BECs, rapid elimination and limited translocation to the brain parenchyma.

Assessment of BBB functions showed a down regulation of the BCRP activity at early time point (6 hours). The *in vitro* BBB model was used to further characterized interactions between TiO_2 NPs and BECs. Results of 24 hours direct exposure to NPs suggest alteration of P-gp activities. Moreover, despite the absence of titanium in the brain parenchyma, 28 days after IV administration, we noticed an increase in transcriptional expression of P-gp in BECs, of structure proteins (claudin 5 and occludin) and of cytokines such as interleukin-1β, CXCL1 and IP-10, suggesting a neurovascular inflammation associated with BECs activation. The dysfunction of the BBB physiology in the absence of titanium in the brain is probably related to extra-cerebral titanium bioaccumulation associated with the secretion of circulating mediators such as pro-inflammatory cytokines / chemokines or metabolite products. The concept of circulating mediators was confirmed by exposing the *in vitro* BBB model to sera from exposed animals. The up regulation of inflammatory markers in the *in vitro* model evidenced emphasizes our hypothesis.

This first part of the project shed light on the TiO_2 NPs brain distribution and pointed out the role of the BBB in the limitation of translocation to the CNS. In addition, we report for the first time the role of circulating mediators, released by organs bioaccumulating titanium, on the regulation of the BBB physiology leading to neuro-inflammation.

In order to draw a comparative study with the IV route, we discussed the second part of the project with the exposure by inhalation to TiO_2 NPs. Experiments showed a bio-persistence in the lungs with a slow clearance and a translocation to extra-pulmonary organs: spleen and liver. We have not confirmed data previously published suggesting brain distribution transport pathway of TiO_2 NPs along the olfactory nerve. Despite the lack of brain translocation evidence, we observed modification in structure protein expression leading to BBB integrity loss in aging exposed rats. Like after IV administration, the effects were associated with acute brain inflammation characterized by up regulation of pro-inflammatory cytokines and chemokines secretions in the brain cortex.

Early and long term events occurring at the BBB as well as discussed mechanisms are summarized in Figure 36. Altogether, the experimental strategy developed in this work described TiO_2 NPs kinetics precisely and showed that indeed, TiO_2 NPs exposure induced BBB dysregulation and neuro-inflammation. This is the first study which report indirect impact on the CNS linking bioaccumulation of titanium in extra-cerebral organs, BBB physiology and neuro-inflammation. Exacerbated response in the aging brain emphasize with aging as a vulnerability factor.

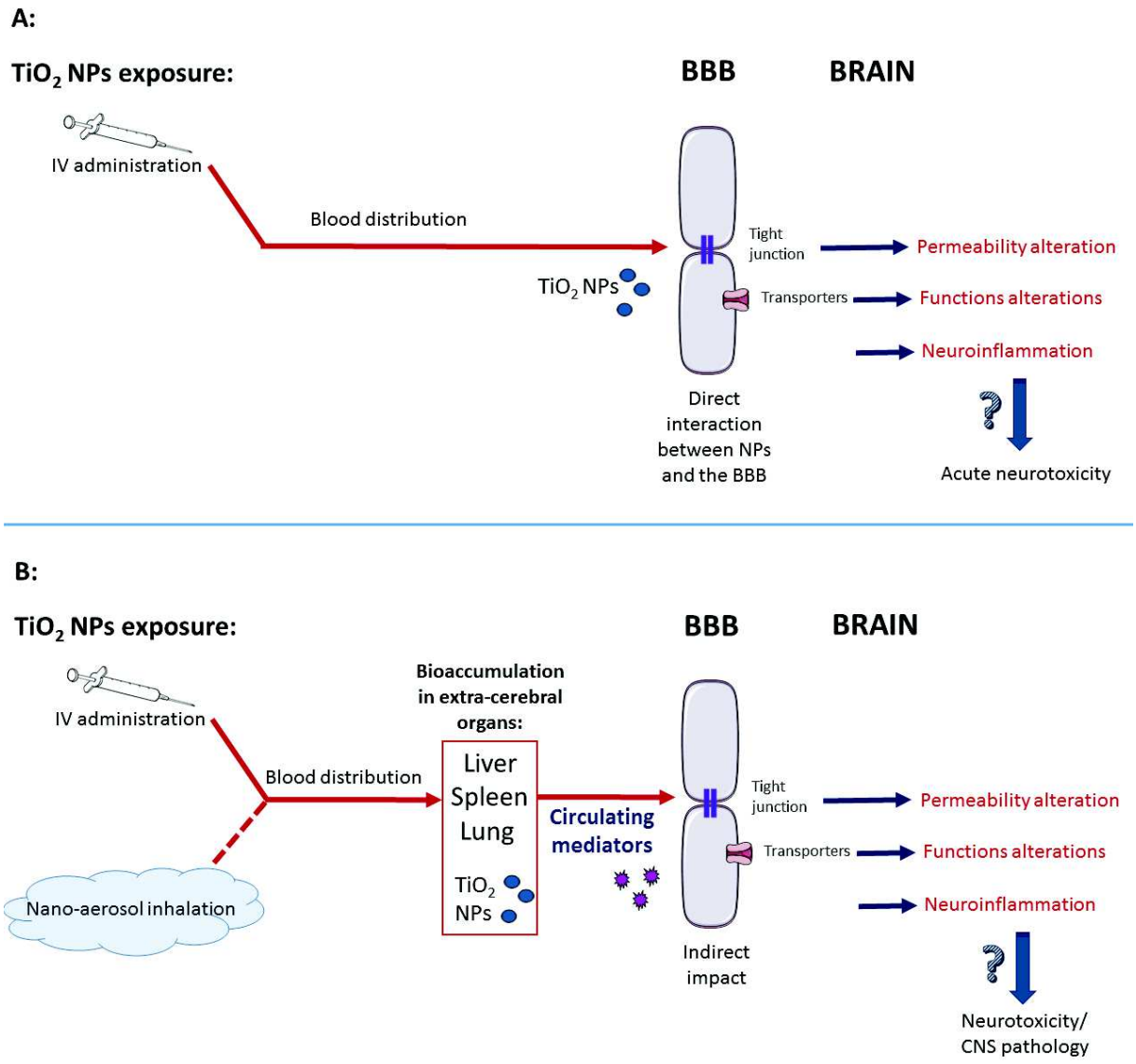

Figure 39: Schematic summary of the early events (A) and indirect long term consequences (B) of TiO_2 NPs exposure on the BBB physiology and on inflammation in the brain.

Perspectives

We have demonstrated, for the first time that the accumulation of TiO_2 NPs in peripheral organs can impact the CNS by indirect mechanisms. These indirect effects show the sensitivity of the CNS to all the physiological modulations in the organism as well as the link between the peripheral organs such as the liver, spleen, lungs and the brain. This relationship seems to be dependent on circulating factors which remain to be determined. Indeed, the long term titanium accumulation in extra-cerebral organs such as the liver after IV administration may lead to local impairment of metabolism. The factors released from these organs may circulate in blood and act at the CNS level. For example, ceramide and sphingosine are lipid species that have demonstrated to be implicated in transport functions regulation in the brain, amyloidogenesis and neurotoxicity [281-283]. The crucial role of lipids metabolites is demonstrated by the large number of CNS diseases in which lipid metabolism is altered [279]. For example, systemic ceramides accumulation has been described as involved in the early brain changes in AD [278]. In this context, lipidomics studies will be undertaken to shed light on the role of circulating lipid species in the brain function after exposure to TiO_2 NPs.

In the elderly we noted modulations and inflammation at the brain levels of a certain number of parameters that can suggest an exacerbation of neurodegenerative processes. Indeed, inflammation within the CNS and BBB permeability alterations has been associated with chronic neurodegenerative disease including AD [204-206, 208, 209]. Neurodegenerative diseases such as AD are multifactorial but exposure to air pollution induced by ultrafine particles has already been mentioned as one of those risk factors. The research of neurodegenerative disease biomarkers such as beta amyloid plaque formation or Tau protein hyper-phosphorylation would be interesting to highlight in the context of inhalation exposure particularly in aging animals.

In the inflamed brain, many processes are dysregulated. For example, metal homeostasis and metabolism process such as carbohydrates metabolism. The brain being highly sensitive to such homeostasis modulations, it may lead to alteration of neuronal functions. Indeed metal homeostasis can be used as a marker of toxicity in the brain. Metal ions such as iron, copper or zinc fulfill important biological functions at the brain level and particularly in the synaptic connections. In normal conditions, the brain strictly regulates the homeostasis of metal ions. The metal ions are present in healthy brains at relatively high concentrations where they are involved in neuronal activity. Deregulation (either excess or deficiency) will cause malfunctions. Indeed, metal ions Fe^{III} and Cu^{II} are usually initiators of toxicity and are due to their redox properties, *via* the production of reactive oxygen species (ROS) ($HO^{\bullet}$, $O_2^{\bullet -}$). Metals are part of the enzyme function and conduction of intracellular signals. Moreover, during aging, homeostatic mechanisms involving metals may be disturbed. For example, in AD pathological contexts, homeostatic mechanisms are disrupted, causing an aberrant functioning of the metal-dependent enzymes, a mitochondrial dysfunction and an ROS generation. In addition, because of their affinity for various proteins, metals can promote the aggregation of proteins. For

example, in the context of AD, copper has a high affinity for Aβ and APP proteins. The assessment of the distribution and metal homeostasis in our study showed therefore a twofold advantage: as a marker of neurotoxicity and as a sign that can be associated with neuro-degenerative process-toxicity in aging rats. Therefore we proposed to characterize brain metal homeostasis after inhalation exposure using PIXE (particle induced X-ray emission).

In addition, glucose metabolism alteration can be proposed as neurotoxic consequences of exposure to TiO_2 NPs. Indeed, glucose transport at the BBB level play a critical role in brain energy supplies and several evidence suggest that brain glucose hypo-metabolism may be the first sign to AD cognitive decline [3, 284]. As example, reduced glucose transport in metabolic active brain regions and reduced component of the insulin signaling pathway were noticed in the brain of AD patients. Impaired energy metabolism correlates with progression of neurodegeneration in these patients. Thus, altered glucose utilization and metabolism could appear as a contributing factor in AD. Metabolomic approach will be used for the assessment of the impact of exposure to TiO_2 NPs on carbohydrates metabolism at the brain level.

.

REFERENCES

1. Brun, E.; Carriere, M.; Mabondzo, A., In vitro evidence of dysregulation of blood-brain barrier function after acute and repeated/long-term exposure to TiO(2) nanoparticles. *Biomaterials* **2012**, *33*, 886-896.
2. Mooradian, A. D.; Chung, H. C.; Shah, G. N., GLUT-1 expression in the cerebra of patients with Alzheimer's disease. *Neurobiology of Aging* **1997**, *18*, 469-474.
3. Shah, K.; DeSilva, S.; Abbruscato, T., The Role of Glucose Transporters in Brain Disease: Diabetes and Alzheimer's Disease. *International Journal of Molecular Sciences* **2012**, *13*, 12629-12655.
4. Gray, M. T.; Woulfe, J. M., Striatal blood-brain barrier permeability in Parkinson's disease. *Journal of Cerebral Blood Flow and Metabolism* **2015**, *35*, 747-750.
5. Calderon-Garciduenas, L.; Reed, W.; Maronpot, R. R.; Henriquez-Roldan, C.; Delgado-Chavez, R.; Calderon-Garciduenas, A.; Dragustinovis, I.; Franco-Lira, M.; Aragon-Flores, M.; Solt, A. C.; Altenburg, M.; Torres-Jordon, R.; Swenberg, J. A., Brain inflammation and Alzheimer's-like pathology in individuals exposed to severe air pollution. *Toxicologic Pathology* **2004**, *32*, 650-658.
6. Calderon-Garciduenas, L.; Franco-Lira, M.; Henriquez-Roldan, C.; Osnaya, N.; Gonzalez-Maciel, A.; Reynoso-Robles, R.; Villarreal-Calderon, R.; Herritt, L.; Brooks, D.; Keefe, S.; Palacios-Moreno, J.; Villarreal-Calderon, R.; Torres-Jardon, R.; Medina-Cortina, H.; Delgado-Chavez, R.; Aiello-Mora, M.; Maronpot, R. R.; Doty, R. L., Urban air pollution: Influences on olfactory function and pathology in exposed children and young adults. *Experimental and Toxicologic Pathology* **2010**, *62*, 91-102.
7. Calderon-Garciduenas, L.; Engle, R.; Mora-Tiscareno, A.; Styner, M.; Gomez-Garza, G.; Zhu, H.; Jewells, V.; Torres-Jardon, R.; Romero, L.; Monroy-Acosta, M. E.; Bryant, C.; Oscar Gonzalez-Gonzalez, L.; Medina-Cortina, H.; D'Angiulli, A., Exposure to severe urban air pollution influences cognitive outcomes, brain volume and systemic inflammation in clinically healthy children. *Brain and Cognition* **2011**, *77*, 345-355.
8. Villarreal-Calderon, R.; Osnaya, N.; Medina-Cortina, H.; Maronpot, R.; Calderon-Garciduenas, L., Olfactory Dysfunction and Olfactory Bulb Pathology induced by Urban Air Pollution. *Faseb Journal* **2009**, *23*.
9. Calderon-Garciduenas, L.; Franco-Lira, M.; Mora-Tiscareno, A.; Medina-Cortina, H.; Torres-Jardon, R.; Kavanaugh, M., Early Alzheimer's and Parkinson's disease pathology in urban children: Friend versus Foe responses--it is time to face the evidence. *BioMed research international* **2013**, *2013*, 161687-161687.
10. Lucchini, R. G.; Guazzetti, S.; Zoni, S.; Donna, F.; Peter, S.; Zacco, A.; Salmistraro, M.; Bontempi, E.; Zimmerman, N. J.; Smith, D. R., Tremor, olfactory and motor changes in Italian adolescents exposed to historical ferro-manganese emission. *Neurotoxicology* **2012**, *33*, 687-696.
11. Iavicoli, I.; Leso, V.; Fontana, L.; Bergamaschi, A., Toxicological effects of titanium dioxide nanoparticles: a review of in vitro mammalian studies. *European Review for Medical and Pharmacological Sciences* **2011**, *15*, 481-508.
12. Iavicoli, I.; Leso, V.; Bergamaschi, A., Toxicological Effects of Titanium Dioxide Nanoparticles: A Review of In Vivo Studies. *Journal of Nanomaterials* **2012**.
13. Song, B.; Liu, J.; Feng, X.; Wei, L.; Shao, L., A review on potential neurotoxicity of titanium dioxide nanoparticles. *Nanoscale research letters* **2015**, *10*, 1042-1042.
14. Marques, F.; Sousa, J. C.; Sousa, N.; Palha, J. A., Blood-brain-barriers in aging and in Alzheimer's disease. *Molecular Neurodegeneration* **2013**, *8*.
15. Buzea, C.; Pacheco, I. I.; Robbie, K., Nanomaterials and nanoparticles: Sources and toxicity. *Biointerphases* **2007**, *2*, MR17-MR71.
16. Oberdorster, G.; Oberdorster, E.; Oberdorster, J., Nanotoxicology: An emerging discipline evolving from studies of ultrafine particles. *Environmental Health Perspectives* **2005**, *113*, 823-839.
17. Borm, P. J. A.; Robbins, D.; Haubold, S.; Kuhlbusch, T.; Fissan, H.; Donaldson, K.; Schins, R.; Stone, V.; Kreyling, W.; Lademann, J.; Krutmann, J.; Warheit, D.; Oberdorster, E., The potential risks of nanomaterials: a review carried out for ECETOC. *Particle and fibre toxicology* **2006**, *3*.

18. Lahiri, D.; Ghosh, S.; Agarwal, A., Carbon nanotube reinforced hydroxyapatite composite for orthopedic application: A review. *Materials Science & Engineering C-Materials for Biological Applications* **2012**, *32*, 1727-1758.
19. Zhan, G. D.; Kuntz, J. D.; Garay, J. E.; Mukherjee, A. K., Electrical properties of nanoceramics reinforced with ropes of single-walled carbon nanotubes. *Applied Physics Letters* **2003**, *83*, 1228-1230.
20. Vance, M. E.; Kuiken, T.; Vejerano, E. P.; McGinnis, S. P.; Hochella, M. F., Jr.; Rejeski, D.; Hull, M. S., Nanotechnology in the real world: Redeveloping the nanomaterial consumer products inventory. *Beilstein Journal of Nanotechnology* **2015**, *6*, 1769-1780.
21. ANSES, Evaluation des risques liés aux nanomatériaux, enjeux et mise à jour des connaissances. In 2014.
22. Honnert B., V. R., Industrial production and uses of nanostructured particles. In INRS: 2007; Vol. cahiers de notes documentaires 4e trimestre 2277-209-07.
23. Linsebigler, A. L.; Lu, G. Q.; Yates, J. T., Photocatalysis on TiO2 surfaces- principles, mechanisms and selected results. *Chemical Reviews* **1995**, *95*, 735-758.
24. Weir, A.; Westerhoff, P.; Fabricius, L.; Hristovski, K.; von Goetz, N., Titanium Dioxide Nanoparticles in Food and Personal Care Products. *Environmental Science & Technology* **2012**, *46*, 2242-2250.
25. Peters, R. J. B.; van Bemmel, G.; Herrera-Rivera, Z.; Helsper, H. P. F. G.; Marvin, H. J. P.; Weigel, S.; Tromp, P. C.; Oomen, A. G.; Rietveld, A. G.; Bouwmeester, H., Characterization of Titanium Dioxide Nanoparticles in Food Products: Analytical Methods To Define Nanoparticles. *Journal of Agricultural and Food Chemistry* **2014**, *62*, 6285-6293.
26. repport, A., State of knowledge on titanium dioxide and zinc oxide nanoparticles in coosmetic products in terms of skin penetration, cytotoxicity and carcinogenicity. In 2011; Vol. adopted by the cosmetic commissionon march 2011.
27. Chen, X.; Mao, S. S., Titanium dioxide nanomaterials: Synthesis, properties, modifications, and applications. *Chemical Reviews* **2007**, *107*, 2891-2959.
28. Fei Yin, Z.; Wu, L.; Gui Yang, H.; Hua Su, Y., Recent progress in biomedical applications of titanium dioxide. *Physical chemistry chemical physics : PCCP* **2013**, *15*, 4844-58.
29. Yaghoubi, H.; Taghavinia, N.; Alamdari, E. K., Self cleaning TiO2 coating on polycarbonate: Surface treatment, photocatalytic and nanomechanical properties. *Surface & Coatings Technology* **2010**, *204*, 1562-1568.
30. Wang, R.-M.; Wang, B.-Y.; He, Y.-F.; Lv, W.-H.; Wang, J.-F., Preparation of composited Nano-TiO2 and its application on antimicrobial and self-cleaning coatings. *Polymers for Advanced Technologies* **2010**, *21*, 331-336.
31. Banerjee, S.; Gopal, J.; Muraleedharan, P.; Tyagi, A. K.; Rai, B., Physics and chemistry of photocatalytic titanium dioxide: Visualization of bactericidal activity using atomic force microscopy. *Current Science* **2006**, *90*, 1378-1383.
32. Lingzhou, Z.; Hairong, W.; Kaifu, H.; Lingyun, C.; Wenrui, Z.; Hongwei, N.; Yumei, Z.; Zhifen, W.; Chu, P. K., Antibacterial nano-structured titania coating incorporated with silver nanoparticles. *Biomaterials* **2011**, *32*, 5706-16.
33. Kubacka, A.; Ferrer, M.; Martinez-Arias, A.; Fernandez-Garcia, M., Ag promotion of TiO2-anatase disinfection capability: Study of Escherichia coli inactivation. *Applied Catalysis B-Environmental* **2008**, *84*, 87-93.
34. Sung, W. P.; Tsai, T. T.; Wu, M. J.; Wang, H. J.; Surampalli, R. Y., Removal of Indoor Airborne Bacteria by Nano-Ag/TiO2 as Photocatalyst: Feasibility Study in Museum and Nursing Institutions. *Journal of Environmental Engineering-Asce* **2011**, *137*, 163-170.
35. Dastjerdi, R.; Montazer, M., A review on the application of inorganic nano-structured materials in the modification of textiles: Focus on anti-microbial properties. *Colloids and Surfaces B-Biointerfaces* **2010**, *79*, 5-18.

36. Tsuang, Y.-H.; Sun, J.-S.; Huang, Y.-C.; Lu, C.-H.; Chang, W. H.-S.; Wang, C.-C., Studies of photokilling of bacteria using titanium dioxide nanoparticles. *Artificial Organs* **2008**, *32*, 167-174.
37. Goto, K.; Hashimoto, M.; Takadama, H.; Tamura, J.; Fujibayashi, S.; Kawanabe, K.; Kokubo, T.; Nakamura, T., Mechanical, setting, and biological properties of bone cements containing micron-sized titania particles. *Journal of Materials Science-Materials in Medicine* **2008**, *19*, 1009-1016.
38. Kulkarni, M.; Mazare, A.; Gongadze, E.; Perutkova, S.; Kralj-Iglic, V.; Milosev, I.; Schmuki, P.; Iglic, A.; Mozetic, M., Titanium nanostructures for biomedical applications. *Nanotechnology* **2015**, *26*.
39. Roy, S. C.; Paulose, M.; Grimes, C. A., The effect of TiO2 nanotubes in the enhancement of blood clotting for the control of hemorrhage. *Biomaterials* **2007**, *28*, 4667-4672.
40. Chen, Y.; Yan, L.; Yuan, T.; Zhang, Q.; Fan, H., Asymmetric Polyurethane Membrane with In Situ-Generated Nano-TiO2 as Wound Dressing. *Journal of Applied Polymer Science* **2011**, *119*, 1532-1541.
41. Liu, L.; Miao, P.; Xu, Y.; Tian, Z.; Zou, Z.; Li, G., Study of Pt/TiO2 nanocomposite for cancer-cell treatment. *Journal of Photochemistry and Photobiology B-Biology* **2010**, *98*, 207-210.
42. Mendonca, G.; Mendonca, D. B. S.; Aragao, F. J. L.; Cooper, L. F., Advancing dental implant surface technology - From micron- to nanotopography. *Biomaterials* **2008**, *29*, 3822-3835.
43. Yi, H.; Linxia, G.; Watanabe, H., Micromechanical analysis of nanoparticle-reinforced dental composites. *International Journal of Engineering Science* **2013**, *69*, 69-76.
44. Xia, Y.; Zhang, F.; Xie, H.; Gu, N., Nanoparticle-reinforced resin-based dental composites. *Journal of Dentistry* **2008**, *36*, 450-455.
45. Donaldson, K.; Stone, V.; Tran, C. L.; Kreyling, W.; Borm, P. J. A., Nanotoxicology. *Occupational and Environmental Medicine* **2004**, *61*, 727-728.
46. Nel, A.; Xia, T.; Madler, L.; Li, N., Toxic potential of materials at the nanolevel. *Science* **2006**, *311*, 622-627.
47. Suh, W. H.; Suslick, K. S.; Stucky, G. D.; Suh, Y.-H., Nanotechnology, nanotoxicology, and neuroscience. *Progress in Neurobiology* **2009**, *87*.
48. Jones, C. F.; Grainger, D. W., In vitro assessments of nanomaterial toxicity. *Advanced Drug Delivery Reviews* **2009**, *61*.
49. Arora, S.; Rajwade, J. M.; Paknikar, K. M., Nanotoxicology and in vitro studies: The need of the hour. *Toxicology and Applied Pharmacology* **2012**, *258*, 151-165.
50. Ostiguy C., R. B., Woods C., Soucy B., Synthetic nanoparticles, current knowledge about risks and prevention measures in workplaces. In IRSST: 2010.
51. Chen, Z.; Meng, H.; Xing, G.; Yuan, H.; Zhao, F.; Liu, R.; Chang, X.; Gao, X.; Wang, T.; Jia, G.; Ye, C.; Chai, Z.; Zhao, Y., Age-Related Differences in Pulmonary and Cardiovascular Responses to SiO(2) Nanoparticle Inhalation: Nanotoxicity Has Susceptible Population. *Environmental Science & Technology* **2008**, *42*, 8985-8992.
52. Burtscher, H.; Schueepp, K., The occurrence of ultrafine particles in the specific environment of children. *Paediatric Respiratory Reviews* **2012**, *13*, 89-94.
53. Yang, L.; Yi, Z.; Bing, Y., Nanotoxicity Overview: Nano-threat to Susceptible Populations. *International Journal of Molecular Science* **2014**, *15*, 3671-97.
54. (NIOSH), t. n. i. f. o. s. a. h., NIOSH current intelligence bulletin 63: Occupational exposure to titanium. In NIOSH publication: Atlanta, GA, USA, 2011.
55. Oberdorster, G., Pulmonary effects of inhaled ultrafine particles. *International Archives of Occupational and Environmental Health* **2001**, *74*.
56. Nemmar, A.; Hoet, P. H. M.; Vanquickenborne, B.; Dinsdale, D.; Thomeer, M.; Hoylaerts, M. F.; Vanbilloen, H.; Mortelmans, L.; Nemery, B., Passage of inhaled particles into the blood circulation in humans. *Circulation* **2002**, *105*.
57. Peters, A.; Veronesi, B.; Calderon-Garciduenas, L.; Gehr, P.; Chen, L. C.; Geiser, M.; Reed, W.; Rothen-Rutishauser, B.; Schurch, S.; Schulz, H., Translocation and potential neurological effects of fine and ultrafine particles a critical update. *Particle and fibre toxicology* **2006**, *3*, 13.

58. Shi, H.; Magaye, R.; Castranova, V.; Zhao, J., Titanium dioxide nanoparticles: a review of current toxicological data. *Particle and Fibre Toxicology* **2013**, *10*.
59. Gustafsson, A.; Lindstedt, E.; Elfsmark, L. S.; Bucht, A., Lung exposure of titanium dioxide nanoparticles induces innate immune activation and long-lasting lymphocyte response in the Dark Agouti rat. *Journal of Immunotoxicology* **2011**, *8*.
60. Yazdi, A. S.; Guarda, G.; Riteau, N.; Drexler, S. K.; Tardivel, A.; Couillin, I.; Tschopp, J., Nanoparticles activate the NLR pyrin domain containing 3 (Nlrp3) inflammasome and cause pulmonary inflammation through release of IL-1 alpha and IL-1 beta. *Proceedings of the National Academy of Sciences of the United States of America* **2010**, *107*.
61. Park, E.-J.; Yoon, J.; Choi, K.; Yi, J.; Park, K., Induction of chronic inflammation in mice treated with titanium dioxide nanoparticles by intratracheal instillation. *Toxicology* **2009**, *260*.
62. Chen, H.-W.; Su, S.-F.; Chien, C.-T.; Lin, W.-H.; Yu, S.-L.; Chou, C.-C.; Chen, J. J. W.; Yang, P.-C., Titanium dioxide nanoparticles induce emphysema-like lung injury in mice. *Faseb Journal* **2006**, *20*.
63. Rossi, E. M.; Pylkkanen, L.; Koivisto, A. J.; Vippola, M.; Jensen, K. A.; Miettinen, M.; Sirola, K.; Nykasenoja, H.; Karisola, P.; Stjernvall, T.; Vanhala, E.; Kiilunen, M.; Pasanen, P.; Makinen, M.; Hameri, K.; Joutsensaari, J.; Tuomi, T.; Jokiniemi, J.; Wolff, H.; Savolainen, K.; Matikainen, S.; Alenius, H., Airway Exposure to Silica-Coated TiO2 Nanoparticles Induces Pulmonary Neutrophilia in Mice. *Toxicological Sciences* **2010**, *113*.
64. Renwick, L. C.; Donaldson, K.; Clouter, A., Impairment of alveolar macrophage phagocytosis by ultrafine particles. *Toxicology and Applied Pharmacology* **2001**, *172*.
65. Renwick, L. C.; Brown, D.; Clouter, A.; Donaldson, K., Increased inflammation and altered macrophage chemotactic responses caused by two ultrafine particle types. *Occupational and Environmental Medicine* **2004**, *61*.
66. Sager, T. M.; Kommineni, C.; Castranova, V., Pulmonary response to intratracheal instillation of ultrafine versus fine titanium dioxide: role of particle surface area. *Particle and Fibre Toxicology* **2008**, *5*.
67. Inoue, K.; Takano, H.; Ohnuki, M.; Yanagisawa, R.; Sakurai, M.; Shimada, A.; Mizushima, K.; Yoshikawa, T., Size effects of nanomaterials on lung inflammation and coagulatory disturbance. *International Journal of Immunopathology and Pharmacology* **2008**, *21*, 197-206.
68. Li, J.; Li, Q.; Xu, J.; Li, J.; Cai, X.; Liu, R.; Li, Y.; Ma, J.; Li, W., Comparative study on the acute pulmonary toxicity induced by 3 and 20 nm TiO2 primary particles in mice. *Environmental Toxicology and Pharmacology* **2007**, *24*.
69. Zhang, Q. W.; Kusaka, Y.; Sato, K.; Nakakuki, K.; Kohyama, N.; Donaldson, K., Differences in the extent of inflammation caused by intratracheal exposure to three ultrafine metals: Role of free radicals. *Journal of Toxicology and Environmental Health-Part A* **1998**, *53*.
70. Sun, Q.; Tan, D.; Ze, Y.; Sang, X.; Liu, X.; Gui, S.; Cheng, Z.; Cheng, J.; Hu, R.; Gao, G.; Liu, G.; Zhu, M.; Zhao, X.; Sheng, L.; Wang, L.; Tang, M.; Hong, F., Pulmotoxicological effects caused by long-term titanium dioxide nanoparticles exposure in mice. *Journal of Hazardous Materials* **2012**, *235*, 47-53.
71. Chang, X.; Fu, Y.; Zhang, Y.; Tang, M.; Wang, B., Effects of Th1 and Th2 cells balance in pulmonary injury induced by nano titanium dioxide. *Environmental Toxicology and Pharmacology* **2014**, *37*, 275-283.
72. Warheit, D. B.; Webb, T. R.; Sayes, C. M.; Colvin, V. L.; Reed, K. L., Pulmonary instillation studies with nanoscale TiO2 rods and dots in rats: Toxicity is not dependent upon particle size and surface area. *Toxicological Sciences* **2006**, *91*.
73. Rehn, B.; Seiler, F.; Rehn, S.; Bruch, J.; Maier, M., Investigations on the inflammatory and genotoxic lung effects of two types of titanium dioxide: untreated and surface treated. *Toxicology and Applied Pharmacology* **2003**, *189*.
74. Leppanen, M.; Korpi, A.; Miettinen, M.; Leskinen, J.; Torvela, T.; Rossi, E. M.; Vanhala, E.; Wolff, H.; Alenius, H.; Kosma, V.-M.; Joutsensaari, J.; Jokiniemi, J.; Pasanen, P., Nanosized TiO2 caused minor airflow limitation in the murine airways. *Archives of Toxicology* **2011**, *85*, 827-839.

75. Halappanavar, S.; Jackson, P.; Williams, A.; Jensen, K. A.; Hougaard, K. S.; Vogel, U.; Yauk, C. L.; Wallin, H., Pulmonary Response to Surface-Coated Nanotitanium Dioxide Particles Includes Induction of Acute Phase Response Genes, Inflammatory Cascades, and Changes in MicroRNAs: A Toxicogenomic Study. *Environmental and Molecular Mutagenesis* **2011**, *52*.
76. Simon-Deckers, A.; Gouget, B.; Mayne-L'Hermite, M.; Herlin-Boime, N.; Reynaud, C.; Carriere, M., In vitro investigation of oxide nanoparticle and carbon nanotube toxicity and intracellular accumulation in A549 human pneumocytes. *Toxicology* **2008**, *253*.
77. Val, S.; Hussain, S.; Boland, S.; Hamel, R.; Baeza-Squiban, A.; Marano, F., Carbon black and titanium dioxide nanoparticles induce pro-inflammatory responses in bronchial epithelial cells: need for multiparametric evaluation due to adsorption artifacts. *Inhalation toxicology* **2009**, *21 Suppl 1*.
78. Soto, K.; Garza, K. M.; Murr, L. E., Cytotoxic effects of aggregated nanomaterials. *Acta Biomaterialia* **2007**, *3*.
79. Park, E.-J.; Yi, J.; Chung, Y.-H.; Ryu, D.-Y.; Choi, J.; Park, K., Oxidative stress and apoptosis induced by titanium dioxide nanoparticles in cultured BEAS-2B cells. *Toxicology Letters* **2008**, *180*.
80. Singh, S.; Shi, T.; Duffin, R.; Albrecht, C.; van Berlo, D.; Hoehr, D.; Fubini, B.; Martra, G.; Fenoglio, I.; Borm, P. J. A.; Schins, R. P. F., Endocytosis, oxidative stress and IL-8 expression in human lung epithelial cells upon treatment with fine and ultrafine TiO2: Role of the specific surface area and of surface methylation of the particles. *Toxicology and Applied Pharmacology* **2007**, *222*.
81. Sayes, C. M.; Wahi, R.; Kurian, P. A.; Liu, Y. P.; West, J. L.; Ausman, K. D.; Warheit, D. B.; Colvin, V. L., Correlating nanoscale titania structure with toxicity: A cytotoxicity and inflammatory response study with human dermal fibroblasts and human lung epithelial cells. *Toxicological Sciences* **2006**, *92*.
82. Rothen-Rutishauser, B.; Muhlfeld, C.; Blank, F.; Musso, C.; Gehr, P., Translocation of particles and inflammatory responses after exposure to fine particles and nanoparticles in an epithelial airway model. *Particle and fibre toxicology* **2007**, *4*.
83. Monteiller, C.; Tran, L.; MacNee, W.; Faux, S.; Jones, A.; Miller, B.; Donaldson, K., The pro-inflammatory effects of low-toxicity low-solubility particles, nanoparticles and fine particles, on epithelial cells in vitro: the role of surface area. *Occupational and Environmental Medicine* **2007**, *64*.
84. Shi, Y.; Wang, F.; He, J.; Yadav, S.; Wang, H., Titanium dioxide nanoparticles cause apoptosis in BEAS-2B cells through the caspase 8/t-Bid-independent mitochondrial pathway. *Toxicology Letters* **2010**, *196*.
85. Hussain, S.; Boland, S.; Baeza-Squiban, A.; Hamel, R.; Thomassen, L. C. J.; Martens, J. A.; Billon-Galland, M. A.; Fleury-Feith, J.; Moisan, F.; Pairon, J.-C.; Marano, F., Oxidative stress and proinflammatory effects of carbon black and titanium dioxide nanoparticles: Role of particle surface area and internalized amount. *Toxicology* **2009**, *260*.
86. Gurr, J. R.; Wang, A. S. S.; Chen, C. H.; Jan, K. Y., Ultrafine titanium dioxide particles in the absence of photoactivation can induce oxidative damage to human bronchial epithelial cells. *Toxicology* **2005**, *213*, 66-73.
87. Sen, C. K.; Packer, L., Antioxidant and redox regulation of gene transcription. *Faseb Journal* **1996**, *10*.
88. (NIOSH), t. n. i. f. o. s. a. h., NIOSH current intelligence bulletin 63: Occupational exposure to titanium dioxide. In NIOSH publication: Atlanta, GA, USA, 2011.
89. Takenaka, S.; Karg, E.; Roth, C.; Schulz, H.; Ziesenis, A.; Heinzmann, U.; Schramel, P.; Heyder, J., Pulmonary and systemic distribution of inhaled ultrafine silver particles in rats. *Environmental Health Perspectives* **2001**, *109*, 547-551.
90. Yu, L. E.; Yung, L.-Y. L.; Ong, C.-N.; Tan, Y.-L.; Balasubramaniam, K. S.; Hartono, D.; Shui, G.; Wenk, M. R.; Ong, W.-Y., Translocation and effects of gold nanoparticles after inhalation exposure in rats. *Nanotoxicology* **2007**, *1*, 235-242.
91. Geraets, L.; Oomen, A. G.; Schroeter, J. D.; Coleman, V. A.; Cassee, F. R., Tissue Distribution of Inhaled Micro- and Nano-sized Cerium Oxide Particles in Rats: Results From a 28-Day Exposure Study. *Toxicological Sciences* **2012**, *127*, 463-473.

92. Kwon, J.-T.; Hwang, S.-K.; Jin, H.; Kim, D.-S.; Mina-Tehrani, A.; Yoon, H.-J.; Chop, M.; Yoon, T.-J.; Han, D.-Y.; Kang, Y.-W.; Yoon, B.-I.; Lee, J.-K.; Cho, M.-H., Body distribution of inhaled fluorescent magnetic nanoparticles in the mice. *Journal of Occupational Health* **2008**, *50*, 1-6.
93. Kreyling, W. G.; Semmler, M.; Erbe, F.; Mayer, P.; Takenaka, S.; Schulz, H.; Oberdorster, G.; Ziesenis, A., Translocation of ultrafine insoluble iridium particles from lung epithelium to extrapulmonary organs is size dependent but very low. *Journal of Toxicology and Environmental Health-Part A* **2002**, *65*.
94. Geiser, M.; Rothen-Rutishauser, B.; Kapp, N.; Schurch, S.; Kreyling, W.; Schulz, H.; Semmler, M.; Hof, V. I.; Heyder, J.; Gehr, P., Ultrafine particles cross cellular membranes by nonphagocytic mechanisms in lungs and in cultured cells. *Environmental Health Perspectives* **2005**, *113*.
95. Shinohara, N.; Oshima, Y.; Kobayashi, T.; Imatanaka, N.; Nakai, M.; Ichinose, T.; Sasaki, T.; Zhang, G.; Fukui, H.; Gamo, M., Dose-dependent clearance kinetics of intratracheally administered titanium dioxide nanoparticles in rat lung. *Toxicology* **2014**, *325*, 1-11.
96. Zhang, J.; Li, B.; Zhang, Y.; Li, A.; Yu, X.; Huang, Q.; Fana, C.; Cai, X., Synchrotron radiation X-ray fluorescence analysis of biodistribution and pulmonary toxicity of nanoscale titanium dioxide in mice. *Analyst* **2013**, *138*, 6511-6516.
97. Shinohara N, O. Y., Kobayashi T, Imatanaka N, Nakai M, Ichinose T, Sasaki T, Kawaguchi K, Zhang G, Gamo M., Pulmonary clearance kinetics and extrapulmonary translocation of seven titanium dioxide nano- and submicron materials following intratracheal administration in rats. In Nanotoxicology: 2015; Vol. 4.
98. Husain, M.; Wu, D.; Saber, A. T.; Decan, N.; Jacobsen, N. R.; Williams, A.; Yauk, C. L.; Wallin, H.; Vogel, U.; Halappanavar, S., Intratracheally instilled titanium dioxide nanoparticles translocate to heart and liver and activate complement cascade in the heart of C57BL/6 mice. *Nanotoxicology* **2015**, *9*, 1013-22.
99. Takenaka, S.; Dornhofertakenaka, H.; Muhle, H., Alveolar distribution of fly-ash and of titanium dioxide after long-term inhalation by wistar rats. *Journal of Aerosol Science* **1986**, *17*, 361-364.
100. Ferin, J.; Oberdorster, G.; Penney, D. P., pulmonary retention of ultrafine and fine particles in rats. *American Journal of Respiratory Cell and Molecular Biology* **1992**, *6*, 535-542.
101. Muhlfeld, C.; Geiser, M.; Kapp, N.; Gehr, P.; Rothen-Rutishauser, B., Re-evaluation of pulmonary titanium dioxide nanoparticle distribution using the "relative deposition index": Evidence for clearance through microvasculature. *Particle and fibre toxicology* **2007**, *4*.
102. van Ravenzwaay, B.; Landsiedel, R.; Fabian, E.; Burkhardt, S.; Strauss, V.; Ma-Hock, L., Comparing fate and effects of three particles of different surface properties: Nano-TiO2, pigmentary TiO2 and quartz. *Toxicology Letters* **2009**, *186*, 152-159.
103. Ma-Hock, L.; Burkhardt, S.; Strauss, V.; Gamer, A. O.; Wiench, K.; van Ravenzwaay, B.; Landsiedel, R., Development of a Short-Term Inhalation Test in the Rat Using Nano-Titanium Dioxide as a Model Substance. *Inhalation Toxicology* **2009**, *21*, 102-118.
104. Landsiedel, R.; Ma-Hock, L.; Hofmann, T.; Wiemann, M.; Strauss, V.; Treumann, S.; Wohlleben, W.; Groeters, S.; Wiench, K.; van Ravenzwaay, B., Application of short-term inhalation studies to assess the inhalation toxicity of nanomaterials. *Particle and Fibre Toxicology* **2014**, *11*.
105. Takenaka, S.; Karg, E.; Roth, C.; Schulz, H.; Ziesenis, A.; Heinzmann, U.; Schramel, P.; Heyder, J., Pulmonary and systemic distribution of inhaled ultrafine silver particles in rats. *Environmental Health Perspectives* **2001**, *109*.
106. Wang, J.; Zhou, G.; Chen, C.; Yu, H.; Wang, T.; Ma, Y.; Jia, G.; Gao, Y.; Li, B.; Sun, J.; Li, Y.; Jiao, F.; Zhao, Y.; Chai, Z., Acute toxicity and biodistribution of different sized titanium dioxide particles in mice after oral administration. *Toxicology Letters* **2007**, *168*, 176-185.
107. Sycheva, L. P.; Zhurkov, V. S.; Iurchenko, V. V.; Daugel-Dauge, N. O.; Kovalenko, M. A.; Krivtsova, E. K.; Durnev, A. D., Investigation of genotoxic and cytotoxic effects of micro- and nanosized titanium dioxide in six organs of mice in vivo. *Mutation Research-Genetic Toxicology and Environmental Mutagenesis* **2011**, *726*.

108. Botelho, M. C.; Costa, C.; Silva, S.; Costa, S.; Dhawan, A.; Oliveira, P. A.; Teixeira, J. P., Effects of titanium dioxide nanoparticles in human gastric epithelial cells in vitro. *Biomedicine & Pharmacotherapy* **2014**, *68*, 59-64.
109. Koeneman, B. A.; Zhang, Y.; Westerhoff, P.; Chen, Y.; Crittenden, J. C.; Capco, D. G., Toxicity and cellular responses of intestinal cells exposed to titanium dioxide. *Cell Biology and Toxicology* **2010**, *26*, 225-238.
110. Zhang, A.-P.; Sun, Y.-P., Photocatalytic killing effect of TiO(2) nanoparticles on Ls-174-t human colon carcinoma cells. *World Journal of Gastroenterology* **2004**, *10*.
111. Brun, E.; Barreau, F.; Veronesi, G.; Fayard, B.; Sorieul, S.; Chaneac, C.; Carapito, C.; Rabilloud, T.; Mabondzo, A.; Herlin-Boime, N.; Carriere, M., Titanium dioxide nanoparticle impact and translocation through ex vivo, in vivo and in vitro gut epithelia. *Particle and Fibre Toxicology* **2014**, *11*.
112. Dorier, M.; Brun, E.; Veronesi, G.; Barreau, F.; Pernet-Gallay, K.; Desvergne, C.; Rabilloud, T.; Carapito, C.; Herlin-Boime, N.; Carriere, M., Impact of anatase and rutile titanium dioxide nanoparticles on uptake carriers and efflux pumps in Caco-2 gut epithelial cells. *Nanoscale* **2015**, *7*, 7352-7360.
113. Gatti, A. M., Biocompatibility of micro- and nano-particles in the colon. Part II. *Biomaterials* **2004**, *25*.
114. Lomer, M. C. E.; Thompson, R. P. H.; Powell, J. J., Fine and ultrafine particles of the diet: influence on the mucosal immune response and association with Crohn's disease. *Proceedings of the Nutrition Society* **2002**, *61*.
115. Lomer, M. C. E.; Hutchinson, C.; Volkert, S.; Greenfield, S. M.; Catterall, A.; Thompson, R. P. H.; Powell, J. J., Dietary sources of inorganic microparticles and their intake in healthy subjects and patients with Crohn's disease. *British Journal of Nutrition* **2004**, *92*.
116. Stern, S. T.; McNeil, S. E., Nanotechnology safety concerns revisited. *Toxicological Sciences* **2008**, *101*.
117. Hillery, A. M.; Jani, P. U.; Florence, A. T., Comparative, quantitative study of lymphoid and nonlymphoid uptake of 60 nm polystyrene particles. *Journal of Drug Targeting* **1994**, *2*.
118. Jani, P.; Halbert, G. W.; Langridge, J.; Florence, A. T., Nanoparticle uptake by the rat gastrointestinal mucosa- quantification and particle size dependency. *Journal of Pharmacy and Pharmacology* **1990**, *42*.
119. Jani, P. U.; McCarthy, D. E.; Florence, A. T., Titanium dioxide (rutile) particle uptake from tha rat GI tract and translocation to systemic organs after oral-administration. *International Journal of Pharmaceutics* **1994**, *105*, 157-168.
120. Cho, W.-S.; Kang, B.-C.; Lee, J. K.; Jeong, J.; Che, J.-H.; Seok, S. H., Comparative absorption, distribution, and excretion of titanium dioxide and zinc oxide nanoparticles after repeated oral administration. *Particle and Fibre Toxicology* **2013**, *10*.
121. Geraets, L.; Oomen, A. G.; Krystek, P.; Jacobsen, N. R.; Wallin, H.; Laurentie, M.; Verharen, H. W.; Brandon, E. F. A.; de Jong, W. H., Tissue distribution and elimination after oral and intravenous administration of different titanium dioxide nanoparticles in rats. *Particle and Fibre Toxicology* **2014**, *11*.
122. Hong, J.; Wang, L.; Zhao, X.; Yu, X.; Sheng, L.; Xu, B.; Liu, D.; Zhu, Y.; Long, Y.; Hong, F., Th2 Factors May Be Involved in TiO2 NP-Induced Hepatic Inflammation. *Journal of Agricultural and Food Chemistry* **2014**, *62*, 6871-6878.
123. Jones, K.; Morton, J.; Smith, I.; Jurkschat, K.; Harding, A.-H.; Evans, G., Human in vivo and in vitro studies on gastrointestinal absorption of titanium dioxide nanoparticles. *Toxicology Letters* **2015**, *233*, 95-101.
124. Skocaj, M.; Filipic, M.; Petkovic, J.; Novak, S., Titanium dioxide in our everyday life; is it safe? *Radiology and Oncology* **2011**, *45*, 227-247.
125. Johnston, H. J.; Hutchison, G. R.; Christensen, F. M.; Peters, S.; Hankin, S.; Stone, V., Identification of the mechanisms that drive the toxicity of TiO(2) particulates: the contribution of physicochemical characteristics. *Particle and Fibre Toxicology* **2009**, *6*.

126. Dunford, R.; Salinaro, A.; Cai, L. Z.; Serpone, N.; Horikoshi, S.; Hidaka, H.; Knowland, J., Chemical oxidation and DNA damage catalysed by inorganic sunscreen ingredients. *Febs Letters* **1997**, *418*.
127. Sadrieh, N.; Wokovich, A. M.; Gopee, N. V.; Zheng, J.; Haines, D.; Parmiter, D.; Siitonen, P. H.; Cozart, C. R.; Patri, A. K.; McNeil, S. E.; Howard, P. C.; Doub, W. H.; Buhse, L. F., Lack of Significant Dermal Penetration of Titanium Dioxide from Sunscreen Formulations Containing Nano- and Submicron-Size TiO2 Particles. *Toxicological Sciences* **2010**, *115*, 156-166.
128. Wu, J.; Liu, W.; Xue, C.; Zhou, S.; Lan, F.; Bi, L.; Xu, H.; Yang, X.; Zeng, F.-D., Toxicity and penetration of TiO2 nanoparticles in hairless mice and porcine skin after subchronic dermal exposure. *Toxicology Letters* **2009**, *191*, 1-8.
129. Blundell, G.; Henderson, W. J.; Price, E. W., Soil particles in the tissues of the foot in endemic elephantiasis of the lower legs. *Annals of Tropical Medicine and Parasitology* **1989**, *83*.
130. Schulz, J.; Hohenberg, H.; Pflucker, F.; Gartner, E.; Will, T.; Pfeiffer, S.; Wepf, R.; Wendel, V.; Gers-Barlag, H.; Wittern, K. P., Distribution of sunscreens on skin. *Advanced Drug Delivery Reviews* **2002**, *54*.
131. Menzel, F.; Reinert, T.; Vogt, J.; Butz, T., Investigations of percutaneous uptake of ultrafine TiO2 particles at the high energy ion nanoprobe LIPSION. *Nuclear Instruments & Methods in Physics Research Section B-Beam Interactions with Materials and Atoms* **2004**, *219*.
132. Kertesz, Z.; Szikszai, Z.; Gontier, E.; Moretto, P.; Surleve-Bazeille, J. E.; Kiss, B.; Juhasz, I.; Hunyadi, J.; Kiss, A. Z., Nuclear microprobe study of TiO2-penetration in the epidermis of human skin xenografts. *Nuclear Instruments & Methods in Physics Research Section B-Beam Interactions with Materials and Atoms* **2005**, *231*.
133. Gamer, A. O.; Leibold, E.; van Ravenzwaay, B., The in vitro absorption of microfine zinc oxide and titanium dioxide through porcine skin. *Toxicology in Vitro* **2006**, *20*.
134. Senzui, M.; Tamura, T.; Miura, K.; Ikarashi, Y.; Watanabe, Y.; Fujii, M., Study on penetration of titanium dioxide (TiO2) nanoparticles into intact and damaged skin in vitro. *Journal of Toxicological Sciences* **2010**, *35*, 107-113.
135. Monteiro-Riviere, N. A.; Wiench, K.; Landsiedel, R.; Schulte, S.; Inman, A. O.; Riviere, J. E., Safety Evaluation of Sunscreen Formulations Containing Titanium Dioxide and Zinc Oxide Nanoparticles in UVB Sunburned Skin: An In Vitro and In Vivo Study. *Toxicological Sciences* **2011**, *123*.
136. Miquel-Jeanjean, C.; Crepel, F.; Raufast, V.; Payre, B.; Datas, L.; Bessou-Touya, S.; Duplan, H., Penetration Study of Formulated Nanosized Titanium Dioxide in Models of Damaged and Sun-Irradiated Skins. *Photochemistry and Photobiology* **2012**, *88*, 1513-1521.
137. Kimura, E.; Kawano, Y.; Todo, H.; Ikarashi, Y.; Sugibayashi, K., Measurement of Skin Permeation/Penetration of Nanoparticles for Their Safety Evaluation. *Biological & Pharmaceutical Bulletin* **2012**, *35*, 1476-1486.
138. Xie, G.; Wang, C.; Sun, J.; Zhong, G., Tissue distribution and excretion of intravenously administered titanium dioxide nanoparticles. *Toxicology Letters* **2011**, *205*, 55-61.
139. De Jong, W. H.; Hagens, W. I.; Krystek, P.; Burger, M. C.; Sips, A. J. A. M.; Geertsma, R. E., Particle size-dependent organ distribution of gold nanoparticles after intravenous administration. *Biomaterials* **2008**, *29*, 1912-1919.
140. Hirn, S.; Semmler-Behnke, M.; Schleh, C.; Wenk, A.; Lipka, J.; Schaeffler, M.; Takenaka, S.; Moeller, W.; Schmid, G.; Simon, U.; Kreyling, W. G., Particle size-dependent and surface charge-dependent biodistribution of gold nanoparticles after intravenous administration. *European Journal of Pharmaceutics and Biopharmaceutics* **2011**, *77*.
141. Lankveld, D. P. K.; Oomen, A. G.; Krystek, P.; Neigh, A.; Troost-de Jong, A.; Noorlander, C. W.; Van Eijkeren, J. C. H.; Geertsma, R. E.; De Jong, W. H., The kinetics of the tissue distribution of silver nanoparticles of different sizes. *Biomaterials* **2010**, *31*.
142. Oberdorster, G.; Maynard, A.; Donaldson, K.; Castranova, V.; Fitzpatrick, J.; Ausman, K.; Carter, J.; Karn, B.; Kreyling, W.; Lai, D.; Olin, S.; Monteiro-Riviere, N.; Warheit, D.; Yang, H.; Toxicity, I. R. F. R. S. I. N.; Screening Working, G., Principles for characterizing the potential human health effects from

exposure to nanomaterials: elements of a screening strategy. *Particle and fibre toxicology* **2005**, *2*, 8-8.
143. Liang, G.; Pu, Y.; Yin, L.; Liu, R.; Ye, B.; Su, Y.; Li, Y., Influence of Different Sizes of Titanium Dioxide Nanoparticles on Hepatic and Renal Functions in Rats with Correlation to Oxidative Stress. *Journal of Toxicology and Environmental Health-Part a-Current Issues* **2009**, *72*, 740-745.
144. Guo, L.-l.; Liu, X.-h.; Qin, D.-x.; Gao, L.; Zhang, H.-m.; Liu, J.-y.; Cui, Y.-g., Effects of nanosized titanium dioxide on the reproductive system of male mice. *Zhonghua nan ke xue = National journal of andrology* **2009**, *15*, 517-22.
145. Chen, J.; Dong, X.; Zhao, J.; Tang, G., In vivo acute toxicity of titanium dioxide nanoparticles to mice after intraperitioneal injection. *Journal of Applied Toxicology* **2009**, *29*, 330-337.
146. Ma, L.; Zhao, J.; Wang, J.; Liu, J.; Duan, Y.; Liu, H.; Li, N.; Yan, J.; Ruan, J.; Wang, H.; Hong, F., The Acute Liver Injury in Mice Caused by Nano-Anatase TiO(2). *Nanoscale Research Letters* **2009**, *4*, 1275-1285.
147. Wang, J.-X.; Fan, Y.-B.; Gao, Y.; Hu, Q.-H.; Wang, T.-C., TiO2 nanoparticles translocation and potential toxicological effect in rats after intraarticular injection. *Biomaterials* **2009**, *30*, 4590-4600.
148. Meng, T.; Ting, Z.; Yuying, X.; Shu, W.; Mingming, H.; Yang, Y.; Minyu, L.; Hao, L.; Lu, K.; Pu, Y., Dose dependent in vivo metabolic characteristics of titanium dioxide nanoparticles. *Journal of Nanoscience and Nanotechnology* **2010**, *10*, 8575-83.
149. Yanmei, D.; Jie, L.; Linglan, M.; Na, L.; Huiting, L.; Jue, W.; Lei, Z.; Chao, L.; Xuefeng, W.; Xiaoyang, Z.; Jingying, Y.; Sisi, W.; Han, W.; Xueguang, Z.; Fashui, H., Toxicological characteristics of nanoparticulate anatase titanium dioxide in mice. *Biomaterials* **2010**, *31*, 894-9.
150. Cui, Y.; Gong, X.; Duan, Y.; Li, N.; Hu, R.; Liu, H.; Hong, M.; Zhou, M.; Wang, L.; Wang, H.; Hong, F., Hepatocyte apoptosis and its molecular mechanisms in mice caused by titanium dioxide nanoparticles. *Journal of Hazardous Materials* **2010**, *183*, 874-880.
151. Bu, Q.; Yan, G.; Deng, P.; Peng, F.; Lin, H.; Xu, Y.; Cao, Z.; Zhou, T.; Xue, A.; Wang, Y.; Cen, X.; Zhao, Y.-L., NMR-based metabonomic study of the sub-acute toxicity of titanium dioxide nanoparticles in rats after oral administration. *Nanotechnology* **2010**, *21*.
152. Tang, M.; Zhang, T.; Xue, Y.; Wang, S.; Huang, M.; Yang, Y.; Lu, M.; Lei, H.; Kong, L.; Wang, Y.; Pu, Y., Metabonomic Studies of Biochemical Changes in the Serum of Rats by Intratracheally Instilled TiO2 Nanoparticles. *Journal of Nanoscience and Nanotechnology* **2011**, *11*, 3065-3074.
153. Nemmar, A.; Melghit, K.; Al-Salam, S.; Zia, S.; Dhanasekaran, S.; Attoub, S.; Al-Amri, I.; Ali, B. H., Acute respiratory and systemic toxicity of pulmonary exposure to rutile Fe-doped TiO2 nanorods. *Toxicology* **2011**, *279*, 167-175.
154. Cui, Y.; Liu, H.; Zhou, M.; Duan, Y.; Li, N.; Gong, X.; Hu, R.; Hong, M.; Hong, F., Signaling pathway of inflammatory responses in the mouse liver caused by TiO2 nanoparticles. *Journal of Biomedical Materials Research Part A* **2011**, *96A*, 221-229.
155. Umbreit, T. H.; Francke-Carroll, S.; Weaver, J. L.; Miller, T. J.; Goering, P. L.; Sadrieh, N.; Stratmeyer, M. E., Tissue distribution and histopathological effects of titanium dioxide nanoparticles after intravenous or subcutaneous injection in mice. *Journal of Applied Toxicology* **2012**, *32*, 350-357.
156. Jeon, Y.-M.; Kim, W.-J.; Lee, M.-Y., Studies on liver damage induced by nanosized-titanium dioxide in mouse. *Journal of Environmental Biology* **2013**, *34*, 283-287.
157. Jia, X.; Guo, X.; Li, H.; An, X.; Zhao, Y., Characteristics and popular topics of latest researches into the effects of air particulate matter on cardiovascular system by bibliometric analysis. *Inhalation Toxicology* **2013**, *25*, 211-218.
158. Nelin, T. D.; Joseph, A. M.; Gorr, M. W.; Wold, L. E., Direct and indirect effects of particulate matter on the cardiovascular system. *Toxicology Letters* **2012**, *208*, 293-299.
159. Liu, H.; Ma, L.; Zhao, J.; Liu, J.; Yan, J.; Ruan, J.; Hong, F., Biochemical Toxicity of Nano-anatase TiO(2) Particles in Mice. *Biological Trace Element Research* **2009**, *129*, 170-180.

160. Nurkiewicz, T. R.; Porter, D. W.; Hubbs, A. F.; Cumpston, J. L.; Chen, B. T.; Frazer, D. G.; Castranova, V., Nanoparticle inhalation augments particle-dependent systemic microvascular dysfunction. *Particle and Fibre Toxicology* **2008**, *5*.
161. Nurkiewicz, T. R.; Porter, D. W.; Hubbs, A. F.; Stone, S.; Chen, B. T.; Frazer, D. G.; Boegehold, M. A.; Castranova, V., Pulmonary Nanoparticle Exposure Disrupts Systemic Microvascular Nitric Oxide Signaling. *Toxicological Sciences* **2009**, *110*, 191-203.
162. LeBlanc, A. J.; Cumpston, J. L.; Chen, B. T.; Frazer, D.; Castranova, V.; Nurkiewicz, T. R., Nanoparticle Inhalation Impairs Endothelium-Dependent Vasodilation in Subepicardial Arterioles. *Journal of Toxicology and Environmental Health-Part a-Current Issues* **2009**, *72*, 1576-1584.
163. LeBlanc, A. J.; Moseley, A. M.; Chen, B. T.; Frazer, D.; Castranova, V.; Nurkiewicz, T. R., Nanoparticle Inhalation Impairs Coronary Microvascular Reactivity via a Local Reactive Oxygen Species-Dependent Mechanism. *Cardiovascular Toxicology* **2010**, *10*, 27-36.
164. Sha, B.; Gao, W.; Wang, S.; Li, W.; Liang, X.; Xu, F.; Lu, T. J., Nano-titanium dioxide induced cardiac injury in rat under oxidative stress. *Food and Chemical Toxicology* **2013**, *58*, 280-288.
165. Wang, Y.; Chen, Z.; Ba, T.; Pu, J.; Chen, T.; Song, Y.; Gu, Y.; Qian, Q.; Xu, Y.; Xiang, K.; Wang, H.; Jia, G., Susceptibility of Young and Adult Rats to the Oral Toxicity of Titanium Dioxide Nanoparticles. *Small* **2013**, *9*, 1742-1752.
166. Savi, M.; Rossi, S.; Bocchi, L.; Gennaccaro, L.; Cacciani, F.; Perotti, A.; Amidani, D.; Alinovi, R.; Goldoni, M.; Aliatis, I.; Lottici, P. P.; Bersani, D.; Campanini, M.; Pinelli, S.; Petyx, M.; Frati, C.; Gervasi, A.; Urbanek, K.; Quaini, F.; Buschini, A.; Stilli, D.; Rivetti, C.; Macchi, E.; Mutti, A.; Miragoli, M.; Zaniboni, M., Titanium dioxide nanoparticles promote arrhythmias via a direct interaction with rat cardiac tissue. *Particle and fibre toxicology* **2014**, *11*, 63-63.
167. Kan, H.; Wu, Z.; Lin, Y.-C.; Chen, T.-H.; Cumpston, J. L.; Kashon, M. L.; Leonard, S.; Munson, A. E.; Castranova, V., The role of nodose ganglia in the regulation of cardiovascular function following pulmonary exposure to ultrafine titanium dioxide. *Nanotoxicology* **2014**, *8*, 447-454.
168. Chen, Z.; Wang, Y.; Zhuo, L.; Chen, S.; Zhao, L.; Luan, X.; Wang, H.; Jia, G., Effect of titanium dioxide nanoparticles on the cardiovascular system after oral administration. *Toxicology letters* **2015**, *239*, 123-30.
169. Nemmar, A.; Melghit, K.; Ali, B. H., The acute proinflammatory and prothrombotic effects of pulmonary exposure to rutile TiO2 nanorods in rats. *Experimental Biology and Medicine* **2008**, *233*, 610-619.
170. C., L., The immunomodulatory effects of titanium dioxide and silver nanoparticles. In Food and Chyemical Toxicology: 2015; Vol. 1, p 6.
171. Li, N.; Duan, Y.; Hong, M.; Zheng, L.; Fei, M.; Zhao, X.; Wang, J.; Cui, Y.; Liu, H.; Cai, J.; Gong, S.; Wang, H.; Hong, F., Spleen injury and apoptotic pathway in mice caused by titanium dioxide nanoparticules. *Toxicology Letters* **2010**, *195*, 161-168.
172. Moon, E.-Y.; Yi, G.-H.; Kang, J.-S.; Lim, J.-S.; Kim, H.-M.; Pyo, S., An increase in mouse tumor growth by an in vivo immunomodulating effect of titanium dioxide nanoparticles. *Journal of Immunotoxicology* **2011**, *8*, 56-67.
173. Wang, J.; Li, N.; Zheng, L.; Wang, S.; Wang, Y.; Zhao, X.; Duan, Y.; Cui, Y.; Zhou, M.; Cai, J.; Gong, S.; Wang, H.; Hong, F., P38-Nrf-2 Signaling Pathway of Oxidative Stress in Mice Caused by Nanoparticulate TiO2. *Biological Trace Element Research* **2011**, *140*, 186-197.
174. Sang, X.; Zheng, L.; Sun, Q.; Li, N.; Cui, Y.; Hu, R.; Gao, G.; Cheng, Z.; Cheng, J.; Gui, S.; Liu, H.; Zhang, Z.; Hong, F., The chronic spleen injury of mice following long-term exposure to titanium dioxide nanoparticles. *Journal of Biomedical Materials Research Part A* **2012**, *100A*, 894-902.
175. Sang, X.; Li, B.; Ze, Y.; Hong, J.; Ze, X.; Gui, S.; Sun, Q.; Liu, H.; Zhao, X.; Sheng, L.; Liu, D.; Yu, X.; Wang, L.; Hong, F., Toxicological Mechanisms of Nanosized Titanium Dioxide-Induced Spleen Injury in Mice after Repeated Peroral Application. *Journal of Agricultural and Food Chemistry* **2013**, *61*, 5590-5599.

176. Fu, Y.; Zhang, Y.; Chang, X.; Zhang, Y.; Ma, S.; Sui, J.; Yin, L.; Pu, Y.; Liang, G., Systemic Immune Effects of Titanium Dioxide Nanoparticles after Repeated Intratracheal Instillation in Rat. *International Journal of Molecular Sciences* **2014**, *15*, 6961-6973.
177. Sheng, L.; Wang, L.; Sang, X.; Zhao, X.; Hong, J.; Cheng, S.; Yu, X.; Liu, D.; Xu, B.; Hu, R.; Sun, Q.; Cheng, J.; Cheng, Z.; Gui, S.; Hong, F., Nano-sized titanium dioxide-induced splenic toxicity: A biological pathway explored using microarray technology. *Journal of Hazardous Materials* **2014**, *278*, 180-188.
178. Rolfe, D. F. S.; Brown, G. C., Cellular energy utilization and molecular origin of standard metabolic rate in mammals. *Physiological Reviews* **1997**, *77*, 731-758.
179. Czajka, M.; Sawicki, K.; Sikorska, K.; Popek, S.; Kruszewski, M.; Kapka-Skrzypczak, L., Toxicity of titanium dioxide nanoparticles in central nervous system. *Toxicology in Vitro* **2015**, *29*, 1042-1052.
180. Cipolla., M. J., *The Cerebral Circulation*. 2009; Vol. Chapter 1, Introduction.
181. Iadecola, C.; Nedergaard, M., Glial regulation of the cerebral microvasculature. *Nature Neuroscience* **2007**, *10*, 1369-1376.
182. Ballabh, P.; Braun, A.; Nedergaard, M., The blood-brain barrier: an overview - Structure, regulation, and clinical implications. *Neurobiology of Disease* **2004**, *16*, 1-13.
183. Zlokovic, B. V., The blood-brain barrier in health and chronic neurodegenerative disorders. *Neuron* **2008**, *57*, 178-201.
184. Hawkins, B. T.; Davis, T. P., The blood-brain barrier/neurovascular unit in health and disease. *Pharmacological Reviews* **2005**, *57*, 173-185.
185. Duvernoy, H. M.; Risold, P.-Y., The circumventricular organs: An atlas of comparative anatomy and vascularization. *Brain Research Reviews* **2007**, *56*, 119-147.
186. Kim, J. H.; Kim, J. H.; Park, J. A.; Lee, S.-W.; Kim, W. J.; Yu, Y. S.; Kim, K.-W., Blood-neural barrier: Intercellular communication at glio-vascular interface. *Journal of Biochemistry and Molecular Biology* **2006**, *39*, 339-345.
187. Bushnell, C. D.; Hurn, P.; Colton, C.; Miller, V. M.; del Zoppo, G.; Elkind, M. S. V.; Stern, B.; Herrington, D.; Ford-Lynch, G.; Gorelick, P.; James, A.; Brown, C. A.; Choi, E.; Bray, P.; Newby, L. K.; Goldstein, L. B.; Simpkins, J., Advancing the study of stroke in women - Summary and recommendations for future research from an NINDS-sponsored multidisciplinary working group. *Stroke* **2006**, *37*, 2387-2399.
188. Brown, A. M.; Ransom, B. R., Astrocyte glycogen and brain energy metabolism. *Glia* **2007**, *55*, 1263-1271.
189. Fellin, T.; D'Ascenzo, M.; Haydon, P. G., Astrocytes control neuronal excitability in the nucleus accumbens. *TheScientificWorldJournal* **2007**, *7*, 89-97.
190. Dong, Y. S.; Benveniste, E. N., Immune function of astrocytes. *Glia* **2001**, *36*, 180-190.
191. Gordon, G. R. J.; Mulligan, S. J.; MacVicar, B. A., Astrocyte control of the cerebrovasculature. *Glia* **2007**, *55*, 1214-1221.
192. Abbott, N. J.; Ronnback, L.; Hansson, E., Astrocyte-endothelial interactions at the blood-brain barrier. *Nature Reviews Neuroscience* **2006**, *7*, 41-53.
193. Bandopadhyay, R.; Orte, C.; Lawrenson, J. G.; Reid, A. R.; De Silva, S.; Allt, G., Contractile proteins in pericytes at the blood-brain and blood-retinal barriers. *Journal of Neurocytology* **2001**, *30*, 35-44.
194. Cardoso, F. L.; Brites, D.; Brito, M. A., Looking at the blood-brain barrier: Molecular anatomy and possible investigation approaches. *Brain Research Reviews* **2010**, *64*, 328-363.
195. Dore-Duffy, P., Pericytes: Pluripotent cells of the blood brain barrier. *Current Pharmaceutical Design* **2008**, *14*, 1581-1593.
196. Dalkara, T.; Gursoy-Ozdemir, Y.; Yemisci, M., Brain microvascular pericytes in health and disease. *Acta Neuropathologica* **2011**, *122*, 1-9.
197. Dore-Duffy, P.; Cleary, K., Morphology and properties of pericytes. *Methods in molecular biology (Clifton, N.J.)* **2011**, *686*, 49-68.

198. Hirschi, K. K.; Damore, P. A., Pericytes in the microvasculature. *Cardiovascular Research* **1996**, *32*, 687-698.
199. Engelhardt, B.; Sorokin, L., The blood-brain and the blood-cerebrospinal fluid barriers: function and dysfunction. *Seminars in Immunopathology* **2009**, *31*, 497-511.
200. Lampugnani, M. G.; Corada, M.; Caveda, L.; Breviario, F.; Ayalon, O.; Geiger, B.; Dejana, E., The molecular-organization of endothelial-cell to cell-junctions - Differential association of plakoglobin, beta-catenin, and alpha-catenin with vascular endothelial cadherin (VE-cadherin). *Journal of Cell Biology* **1995**, *129*, 203-217.
201. MJ, C., *The Cerebral Circulation*. 2009; Vol. Chapter 1, Introduction.
202. Huber, J. D.; Egleton, R. D.; Davis, T. P., Molecular physiology and pathophysiology of tight junctions in the blood-brain barrier. *Trends in Neurosciences* **2001**, *24*, 719-725.
203. Miller, D. W., Immunobiology of the blood-brain barrier. *Journal of Neurovirology* **1999**, *5*, 570-578.
204. Abbott, N. J.; Friedman, A., Overview and introduction: The blood-brain barrier in health and disease. *Epilepsia* **2012**, *53*, 1-6.
205. Daneman, R., The blood-brain barrier in health and disease. *Annals of Neurology* **2012**, *72*, 648-672.
206. Akiyama, H., Inflammation in Alzheimer's disease. *Brain Pathology* **2000**, *10*, 707-708.
207. Hirsch, E. C.; Vyas, S.; Hunot, S., Neuroinflammation in Parkinson's disease. *Parkinsonism & related disorders* **2012**, *18 Suppl 1*, S210-2.
208. Farrall, A. J.; Wardlaw, J. M., Blood brain barrier: ageing and microvascular disease-systematic review and meta-analysis. *Journal of the Neurological Sciences* **2009**, *283*, 261-261.
209. Starr, J. M.; Farrall, A. J.; Armitage, P.; McGurn, B.; Wardlaw, J., Blood-brain barrier permeability in Alzheimer's disease: a case-control MRI study. *Psychiatry Research-Neuroimaging* **2009**, *171*, 232-241.
210. van Vliet, E. A.; Araujo, S. d. C.; Redeker, S.; van Schaik, R.; Aronica, E.; Gorter, J. A., Blood-brain barrier leakage may lead to progression of temporal lobe epilepsy. *Brain* **2007**, *130*, 521-534.
211. Banks, W. A., Blood-Brain Barrier as a Regulatory Interface. *Frontiers in Eating and Weight Regulation* **2010**, *63*, 102-110.
212. Bartels, A. L.; Kortekaas, R.; Bart, J.; Willemsen, A. T. M.; de Klerk, O. L.; de Vries, J. J.; van Oostrom, J. C. H.; Leenders, K. L., Blood-brain barrier P-glycoprotein function decreases in specific brain regions with aging: A possible role in progressive neurodegeneration. *Neurobiology of Aging* **2009**, *30*, 1818-1824.
213. Bartels, A. L., Blood-Brain Barrier P-Glycoprotein Function in Neurodegenerative Disease. *Current Pharmaceutical Design* **2011**, *17*, 2771-2777.
214. Dauchy, S.; Dutheil, F.; Weaver, R. J.; Chassoux, F.; Daumas-Duport, C.; Couraud, P.-O.; Scherrmann, J.-M.; De Waziers, I.; Decleves, X., ABC transporters, cytochromes P450 and their main transcription factors: expression at the human blood-brain barrier. *Journal of Neurochemistry* **2008**, *107*, 1518-1528.
215. Miller, D. S., Regulation of ABC Transporters Blood-Brain Barrier: The Good, the Bad, and the Ugly. *Advances in cancer research* **2015**, *125*, 43-70.
216. Miller, D. S., Regulation of P-glycoprotein and other ABC drug transporters at the blood-brain barrier. *Trends in Pharmacological Sciences* **2010**, *31*, 246-254.
217. Miller, D. S.; Cannon, R. E., Signaling Pathways that Regulate Basal ABC Transporter Activity at the Blood-Brain Barrier. *Current Pharmaceutical Design* **2014**, *20*, 1463-1471.
218. Qosa H., M. D., Pasinelli; P., T. D., Regulation of ABC efflux transporters at the Blood Brain Barrier. In Brain Res. : 2015.
219. Winkler, E. A.; Nishida, Y.; Sagare, A. P.; Rege, S. V.; Bell, R. D.; Perlmutter, D.; Sengillo, J. D.; Hillman, S.; Kong, P.; Nelson, A. R.; Sullivan, J. S.; Zhao, Z.; Meiselman, H. J.; Wenby, R. B.; Soto, J.; Abel,

E. D.; Makshanoff, J.; Zuniga, E.; De Vivo, D. C.; Zlokovic, B. V., GLUT1 reductions exacerbate Alzheimer's disease vasculo-neuronal dysfunction and degeneration. *Nature Neuroscience* **2015**, *18*, 521-+.
220. Liu, Y.; Liu, F.; Iqbal, K.; Grundke-Lqbal, I.; Gong, C.-X., Decreased glucose transporters correlate to abnormal hyperphosphorylation of tau in Alzheimer disease. *Febs Letters* **2008**, *582*, 359-364.
221. Deng, Y.; Li, B.; Lu, Y.; Iqbal, K.; Grundke-Iqbal, I.; Gong, C.-X., Dysregulation of Insulin Signaling, Glucose Transporters, O-GlcNAcylation, and Phosphorylation of Tau and Neurofilaments in the Brain Implication for Alzheimer's Disease. *American Journal of Pathology* **2009**, *175*, 2089-2098.
222. Liu, F.; Shi, J.; Tanimukai, H.; Gu, J.; Gu, J.; Grundke-Iqbal, I.; Iqbal, K.; Gong, C.-X., Reduced O-GlcNAcylation links lower brain glucose metabolism and tau pathology in Alzheimer's disease. *Brain* **2009**, *132*, 1820-1832.
223. Gizurarson, S., Anatomical and Histological Factors Affecting Intranasal Drug and Vaccine Delivery. *Current Drug Delivery* **2012**, *9*, 566-582.
224. Lochhead, J. J.; Thorne, R. G., Intranasal delivery of biologics to the central nervous system. *Advanced Drug Delivery Reviews* **2012**, *64*, 614-628.
225. Wang, J.; Liu, Y.; Jiao, F.; Lao, F.; Li, W.; Gu, Y.; Li, Y.; Ge, C.; Zhou, G.; Li, B.; Zhao, Y.; Chai, Z.; Chen, C., Time-dependent translocation and potential impairment on central nervous system by intranasally instilled TiO(2) nanoparticles. *Toxicology* **2008**, *254*, 82-90.
226. Zhang, L.; Bai, R.; Li, B.; Ge, C.; Du, J.; Liu, Y.; Le Guyader, L.; Zhao, Y.; Wu, Y.; He, S.; Ma, Y.; Chen, C., Rutile TiO(2) particles exert size and surface coating dependent retention and lesions on the murine brain. *Toxicology Letters* **2011**, *207*, 73-81.
227. Ze, Y.; Hu, R.; Wang, X.; Sang, X.; Ze, X.; Li, B.; Su, J.; Wang, Y.; Guan, N.; Zhao, X.; Gui, S.; Zhu, L.; Cheng, Z.; Cheng, J.; Sheng, L.; Sun, Q.; Wang, L.; Hong, F., Neurotoxicity and gene-expressed profile in brain-injured mice caused by exposure to titanium dioxide nanoparticles. *Journal of Biomedical Materials Research Part A* **2014**, *102*, 470-478.
228. Oberdorster, G.; Sharp, Z.; Atudorei, V.; Elder, A.; Gelein, R.; Kreyling, W.; Cox, C., Translocation of inhaled ultrafine particles to the brain. *Inhalation Toxicology* **2004**, *16*, 437-445.
229. Semmler, M.; Seitz, J.; Erbe, F.; Mayer, P.; Heyder, J.; Oberdorster, G.; Kreyling, W. G., Long-term clearance kinetics of inhaled ultrafine insoluble iridium particles from the rat lung, including transient translocation into secondary organs. *Inhalation Toxicology* **2004**, *16*, 453-459.
230. Kenzaoui, B. H.; Bernasconi, C. C.; Guney-Ayra, S.; Juillerat-Jeanneret, L., Induction of oxidative stress, lysosome activation and autophagy by nanoparticles in human brain-derived endothelial cells. *Biochemical Journal* **2012**, *441*, 813-821.
231. Patri, A.; Umbreit, T.; Zheng, J.; Nagashima, K.; Goering, P.; Francke-Carroll, S.; Gordon, E.; Weaver, J.; Miller, T.; Sadrieh, N.; McNeil, S.; Stratmeyer, M., Energy dispersive X-ray analysis of titanium dioxide nanoparticle distribution after intravenous and subcutaneous injection in mice. *Journal of Applied Toxicology* **2009**, *29*, 662-672.
232. Sugibayashi, K.; Todo, H.; Kimura, E., Safety evaluation of titanium dioxide nanoparticles by their absorption and elimination profiles (vol 33, pg 293, 2008). *Journal of Toxicological Sciences* **2008**, *33*, 668-669.
233. Wang, J.; Chen, C.; Liu, Y.; Jiao, F.; Li, W.; Lao, F.; Li, Y.; Li, B.; Ge, C.; Zhou, G.; Gao, Y.; Zhao, Y.; Chai, Z., Potential neurological lesion after nasal instillation of TiO(2) nanoparticles in the anatase and rutile crystal phases. *Toxicology Letters* **2008**, *183*, 72-80.
234. Takeda, K.; Suzuki, K. I.; Ishihara, A.; Kubo-Irie, M.; Fujimoto, R.; Tabata, M.; Oshio, S.; Nihei, Y.; Ihara, T.; Sugamata, M., Nanoparticles Transferred from Pregnant Mice to Their Offspring Can Damage the Genital and Cranial Nerve Systems. *Journal of Health Science* **2009**, *55*, 95-102.
235. Hu, R.; Gong, X.; Duan, Y.; Li, N.; Che, Y.; Cui, Y.; Zhou, M.; Liu, C.; Wang, H.; Hong, F., Neurotoxicological effects and the impairment of spatial recognition memory in mice caused by exposure to TiO2 nanoparticles. *Biomaterials* **2010**, *31*, 8043-8050.
236. Shin, J. A.; Lee, E. J.; Seo, S. M.; Kim, H. S.; Kang, J. L.; Park, E. M., Nanosized titanium dioxide enhanced inflammatory response in the septic brain of mouse. *Neuroscience* **2010**, *165*, 445-454.

237. Ze, Y.; Zheng, L.; Zhao, X.; Gui, S.; Sang, X.; Su, J.; Guan, N.; Zhu, L.; Sheng, L.; Hu, R.; Cheng, J.; Cheng, Z.; Sun, Q.; Wang, L.; Hong, F., Molecular mechanism of titanium dioxide nanoparticles-induced oxidative injury in the brain of mice. *Chemosphere*.
238. Jinglong, T.; Ling, X.; Guofeng, Z.; Shuo, W.; Jianyu, W.; Li, L.; Jiage, L.; Fuqiang, Y.; Songfang, L.; Ziyi, W.; Laisheng, C.; Tingfei, X., Silver Nanoparticles Crossing Through and Distribution in the Blood-Brain Barrier In Vitro. *Journal of Nanoscience and Nanotechnology* **2010**, *10*.
239. Trickler, W. J.; Lantz, S. M.; Murdock, R. C.; Schrand, A. M.; Robinson, B. L.; Newport, G. D.; Schlager, J. J.; Oldenburg, S. J.; Paule, M. G.; Slikker, W., Jr.; Hussain, S. M.; Ali, S. F., Brain microvessel endothelial cells responses to gold nanoparticles: In vitro pro-inflammatory mediators and permeability. *Nanotoxicology* **2011**, *5*, 479-492.
240. Trickler, W. J.; Lantz, S. M.; Murdock, R. C.; Schrand, A. M.; Robinson, B. L.; Newport, G. D.; Schlager, J. J.; Oldenburg, S. J.; Paule, M. G.; Slikker, W., Jr.; Hussain, S. M.; Ali, S. F., Silver Nanoparticle Induced Blood-Brain Barrier Inflammation and Increased Permeability in Primary Rat Brain Microvessel Endothelial Cells. *Toxicological Sciences* **2010**, *118*.
241. Trickler, W. J.; Lantz, S. M.; Schrand, A. M.; Robinson, B. L.; Newport, G. D.; Schlager, J. J.; Paule, M. G.; Slikker, W.; Biris, A. S.; Hussain, S. M.; Ali, S. F., Effects of copper nanoparticles on rat cerebral microvessel endothelial cells. *Nanomedicine* **2012**, *7*, 835-846.
242. Chen, L.; Yokel, R. A.; Hennig, B.; Toborek, M., Manufactured Aluminum Oxide Nanoparticles Decrease Expression of Tight Junction Proteins in Brain Vasculature. *Journal of Neuroimmune Pharmacology* **2008**, *3*.
243. Abbott, N. J., Astrocyte-endothelial interactions and blood-brain barrier permeability. *Journal of Anatomy* **2002**, *200*, 629-638.
244. Blamire, A. M.; Anthony, D. C.; Rajagopalan, B.; Sibson, N. R.; Perry, V. H.; Styles, P., Interleukin-1 beta-induced changes in blood-brain barrier permeability, apparent diffusion coefficient, and cerebral blood volume in the rat brain: A magnetic resonance study. *Journal of Neuroscience* **2000**, *20*, 8153-8159.
245. Didier, N.; Romero, I. A.; Creminon, C.; Wijkhuisen, A.; Grassi, J.; Mabondzo, A., Secretion of interleukin-1 beta by astrocytes mediates endothelin-1 and tumour necrosis factor-alpha effects on human brain microvascular endothelial cell permeability. *Journal of Neurochemistry* **2003**, *86*, 246-254.
246. Roberts, D. J.; Goralski, K. B., A critical overview of the influence of inflammation and infection on P-glycoprotein expression and activity in the brain. *Expert Opinion on Drug Metabolism & Toxicology* **2008**, *4*, 1245-1264.
247. Carvey, P. M.; Hendey, B.; Monahan, A. J., The blood-brain barrier in neurodegenerative disease: a rhetorical perspective. *Journal of Neurochemistry* **2009**, *111*, 291-314.
248. Shimizu, M.; Tainaka, H.; Oba, T.; Mizuo, K.; Umezawa, M.; Takeda, K., Maternal exposure to nanoparticulate titanium dioxide during the prenatal period alters gene expression related to brain development in the mouse. *Particle and Fibre Toxicology* **2009**, *6*.
249. Takahashi, Y.; Mizuo, K.; Shinkai, Y.; Oshio, S.; Takeda, K., Prenatal exposure to titanium dioxide nanoparticles increases dopamine levels in the prefrontal cotex and neostriatum of mice. *Journal of Toxicological Sciences* **2010**, *35*, 749-756.
250. Mohammadipour, A.; Fazel, A.; Haghir, H.; Motejaded, F.; Rafatpanah, H.; Zabihi, H.; Hosseini, M.; Bideskan, A. E., Maternal exposure to titanium dioxide nanoparticles during pregnancy; impaired memory and decreased hippocampal cell proliferation in rat offspring. *Environmental Toxicology and Pharmacology* **2014**, *37*, 617-625.
251. Long, T. C.; Saleh, N.; Tilton, R. D.; Lowry, G. V.; Veronesi, B., Titanium dioxide (P25) produces reactive oxygen species in immortalized brain microglia (BV2): Implications for nanoparticle neurotoxicity. *Environmental Science & Technology* **2006**, *40*, 4346-4352.
252. Long, T. C.; Tajuba, J.; Sama, P.; Saleh, N.; Swartz, C.; Parker, J.; Hester, S.; Lowry, G. V.; Veronesi, B., Nanosize titanium dioxide stimulates reactive oxygen species in brain microglia and damages neurons in vitro. *Environmental Health Perspectives* **2007**, *115*, 1631-1637.

253. Lai, J. C. K.; Lai, M. B.; Jandhyam, S.; Dukhande, V. V.; Bhushan, A.; Daniels, C. K.; Leung, S. W., Exposure to titanium dioxide and other metallic oxide nanoparticles induces cytotoxicity on human neural cells and fibroblasts. *International Journal of Nanomedicine* **2008**, *3*, 533-545.
254. Li, X.; Xu, S.; Zhang, Z.; Schluesener, H. J., Apoptosis induced by titanium dioxide nanoparticles in cultured murine microglia N9 cells. *Chinese Science Bulletin* **2009**, *54*, 3830-3836.
255. Xiaoyan, L.; Xiufang, R.; Xiaoyong, D.; Yinan, H.; Jiang, X.; Hai, H.; Zheng, J.; Minghong, W.; Yuanfang, L.; Tieqiao, W., A protein interaction network for the analysis of the neuronal differentiation of neural stem cells in response to titanium dioxide nanoparticles. *Biomaterials* **2010**, *31*, 3063-70.
256. Liu, S.; Xu, L.; Zhang, T.; Ren, G.; Yang, Z., Oxidative stress and apoptosis induced by nanosized titanium dioxide in PC12 cells. *Toxicology* **2010**, *267*, 172-177.
257. Wu, J.; Sun, J.; Xue, Y., Involvement of JNK and P53 activation in G2/M cell cycle arrest and apoptosis induced by titanium dioxide nanoparticles in neuron cells. *Toxicology Letters* **2010**, *199*.
258. Xue, Y.; Wu, J.; Sun, J., Four types of inorganic nanoparticles stimulate the inflammatory reaction in brain microglia and damage neurons in vitro. *Toxicology Letters* **2012**, *214*, 91-98.
259. Gissela Marquez-Ramirez, S.; Laura Delgado-Buenrostro, N.; Irasema Chirino, Y.; Gutierrez Iglesias, G.; Lopez-Marure, R., Titanium dioxide nanoparticles inhibit proliferation and induce morphological changes and apoptosis in glial cells. *Toxicology* **2012**, *302*, 146-156.
260. Valdiglesias, V.; Costa, C.; Sharma, V.; Kilic, G.; Pasaro, E.; Teixeira, J. P.; Dhawan, A.; Laffon, B., Comparative study on effects of two different types of titanium dioxide nanoparticles on human neuronal cells. *Food and Chemical Toxicology* **2013**, *57*, 352-361.
261. Huerta-García, E.; Pérez-Arizti, J. A.; Márquez-Ramírez, S. G.; Delgado-Buenrostro, N. L.; Chirino, Y. I.; Iglesias, G. G.; López-Marure, R., Titanium dioxide nanoparticles induce strong oxidative stress and mitochondrial damage in glial cells. *Free Radical Biology and Medicine* **2014**, *73*, 84-94.
262. Fujioka, K.; Hanada, S.; Inoue, Y.; Sato, K.; Hirakuri, K.; Shiraishi, K.; Kanaya, F.; Ikeda, K.; Usui, R.; Yamamoto, K.; Kim, S. U.; Manome, Y., Effects of Silica and Titanium Oxide Particles on a Human Neural Stem Cell Line: Morphology, Mitochondrial Activity, and Gene Expression of Differentiation Markers. *International Journal of Molecular Sciences* **2014**, *15*, 11742-11759.
263. Sheng, L.; Ze, Y.; Wang, L.; Yu, X.; Hong, J.; Zhao, X.; Ze, X.; Liu, D.; Xu, B.; Zhu, Y.; Long, Y.; Lin, A.; Zhang, C.; Zhao, Y.; Hong, F., Mechanisms of TiO2 nanoparticle-induced neuronal apoptosis in rat primary cultured hippocampal neurons. *Journal of Biomedical Materials Research Part A* **2015**, *103*, 1141-1149.
264. Ma, L.; Liu, J.; Li, N.; Wang, J.; Duan, Y.; Yan, J.; Liu, H.; Wang, H.; Hong, F., Oxidative stress in the brain of mice caused by translocated nanoparticulate TiO2 delivered to the abdominal cavity. *Biomaterials* **2010**, *31*, 99-105.
265. Li, Y.; Li, J.; Yin, J.; Li, W.; Kang, C.; Huang, Q.; Li, Q., Systematic Influence Induced by 3 nm Titanium Dioxide Following Intratracheal Instillation of Mice. *Journal of Nanoscience and Nanotechnology* **2010**, *10*, 8544-8549.
266. Hougaard, K. S.; Jackson, P.; Jensen, K. A.; Sloth, J. J.; Loeschner, K.; Larsen, E. H.; Birkedal, R. K.; Vibenholt, A.; Boisen, A.-M. Z.; Wallin, H.; Vogel, U., Effects of prenatal exposure to surface-coated nanosized titanium dioxide (UV-Titan). A study in mice. *Particle and Fibre Toxicology* **2010**, *7*.
267. Hu, R.; Zheng, L.; Zhang, T.; Gao, G.; Cui, Y.; Cheng, Z.; Cheng, J.; Hong, M.; Tang, M.; Hong, F., Molecular mechanism of hippocampal apoptosis of mice following exposure to titanium dioxide nanoparticles. *Journal of Hazardous Materials* **2011**, *191*, 32-40.
268. Gao, X.; Yin, S.; Tang, M.; Chen, J.; Yang, Z.; Zhang, W.; Chen, L.; Yang, B.; Li, Z.; Zha, Y.; Ruan, D.; Wang, M., Effects of Developmental Exposure to TiO2 Nanoparticles on Synaptic Plasticity in Hippocampal Dentate Gyrus Area: an In Vivo Study in Anesthetized Rats. *Biological Trace Element Research* **2011**, *143*, 1616-1628.
269. Ze, Y.; Zheng, L.; Zhao, X.; Gui, S.; Sang, X.; Su, J.; Guan, N.; Zhu, L.; Sheng, L.; Hu, R.; Cheng, J.; Cheng, Z.; Sun, Q.; Wang, L.; Hong, F., Molecular mechanism of titanium dioxide nanoparticles-induced oxidative injury in the brain of mice. *Chemosphere* **2013**, *92*, 1183-1189.

270. Cui, Y.; Chen, X.; Zhou, Z.; Lei, Y.; Ma, M.; Cao, R.; Sun, T.; Xu, J.; Huo, M.; Wen, C.; Che, Y., Prenatal exposure to nanoparticulate titanium dioxide enhances depressive-like behaviors in adult rats. *Chemosphere* **2014**, *96*, 99-104.
271. Ze, Y.; Sheng, L.; Zhao, X.; Ze, X.; Wang, X.; Zhou, Q.; Liu, J.; Yuan, Y.; Gui, S.; Sang, X.; Sun, Q.; Hong, J.; Yu, X.; Wang, L.; Li, B.; Hong, F., Neurotoxic characteristics of spatial recognition damage of the hippocampus in mice following subchronic peroral exposure to TiO2 nanoparticles. *Journal of Hazardous Materials* **2014**, *264*, 219-229.
272. Ze, Y.; Sheng, L.; Zhao, X.; Hong, J.; Ze, X.; Yu, X.; Pan, X.; Lin, A.; Zhao, Y.; Zhang, C.; Zhou, Q.; Wang, L.; Hong, F., TiO2 Nanoparticles Induced Hippocampal Neuroinflammation in Mice. *Plos One* **2014**, *9*.
273. Younes, N. R. B.; Amara, S.; Mrad, I.; Ben-Slama, I.; Jeljeli, M.; Omri, K.; El Ghoul, J.; El Mir, L.; Rhouma, K. B.; Abdelmelek, H.; Sakly, M., Subacute toxicity of titanium dioxide (TiO2) nanoparticles in male rats: emotional behavior and pathophysiological examination. *Environmental science and pollution research international* **2015**, *22*, 8728-37.
274. Lacombe, O.; Videau, O.; Chevillon, D.; Guyot, A.-C.; Contreras, C.; Blondel, S.; Nicolas, L.; Ghettas, A.; Benech, H.; Thevenot, E.; Pruvost, A.; Bolze, S.; Krzaczkowski, L.; Prevost, C.; Mabondzo, A., In Vitro Primary Human and Animal Cell-Based Blood-Brain Barrier Models as a Screening Tool in Drug Discovery. *Molecular Pharmaceutics* **2011**, *8*, 651-663.
275. Fabian, E.; Landsiedel, R.; Ma-Hock, L.; Wiench, K.; Wohlleben, W.; van Ravenzwaay, B., Tissue distribution and toxicity of intravenously administered titanium dioxide nanoparticles in rats. *Archives of Toxicology* **2008**, *82*, 151-157.
276. Shinohara, N.; Danno, N.; Ichinose, T.; Sasaki, T.; Fukui, H.; Honda, K.; Gamo, M., Tissue distribution and clearance of intravenously administered titanium dioxide (TiO(2)) nanoparticles. *Nanotoxicology* **2013**.
277. Jeon, S.-B.; Yoon, H. J.; Park, S.-H.; Kim, I.-H.; Park, E. J., Sulfatide, A Major Lipid Component of Myelin Sheath, Activates Inflammatory Responses as an Endogenous Stimulator in Brain-Resident Immune Cells. *Journal of Immunology* **2008**, *181*, 8077-8087.
278. Alayoubi, A. M.; Wang, J. C. M.; Au, B. C. Y.; Carpentier, S.; Garcia, V.; Dworski, S.; El-Ghamrasni, S.; Kirouac, K. N.; Exertier, M. J.; Xiong, Z. J.; Prive, G. G.; Simonaro, C. M.; Casas, J.; Fabrias, G.; Schuchman, E. H.; Turner, P. V.; Hakem, R.; Levade, T.; Medin, J. A., Systemic ceramide accumulation leads to severe and varied pathological consequences. *Embo Molecular Medicine* **2013**, *5*, 827-842.
279. Adibhatla, R. M.; Hatcher, J. F., Role of lipids in brain injury and diseases. *Future Lipidology* **2007**, *2*, 403-422.
280. Abbott, N. J.; Patabendige, A. A. K.; Dolman, D. E. M.; Yusof, S. R.; Begley, D. J., Structure and function of the blood-brain barrier. *Neurobiology of Disease* **2010**, *37*, 13-25.
281. Cannon, R. E.; Peart, J. C.; Hawkins, B. T.; Campos, C. R.; Miller, D. S., Targeting blood-brain barrier sphingolipid signaling reduces basal P-glycoprotein activity and improves drug delivery to the brain. *Proceedings of the National Academy of Sciences of the United States of America* **2012**, *109*, 15930-15935.
282. Martinez, T. N.; Chen, X.; Bandyopadhyay, S.; Merrill, A. H.; Tansey, M. G., Ceramide sphingolipid signaling mediates Tumor Necrosis Factor (TNF)-dependent toxicity via caspase signaling in dopaminergic neurons. *Molecular Neurodegeneration* **2012**, *7*.
283. Asle-Rousta, M.; Oryan, S.; Ahmadiani, A.; Rahnema, M., Activation of sphingosine 1-phosphate receptor-1 by SEW2871 improves cognitive function in Alzheimer's disease model rats. *Excli Journal* **2013**, *12*, 449-461.
284. Cunnane, S.; Nugent, S.; Roy, M.; Courchesne-Loyer, A.; Croteau, E.; Tremblay, S.; Castellano, A.; Pifferi, F.; Bocti, C.; Paquet, N.; Begdouri, H.; Bentourkia, M. h.; Turcotte, E.; Allard, M.; Barberger-Gateau, P.; Fulop, T.; Rapoport, S. I., Brain fuel metabolism, aging, and Alzheimer's disease. *Nutrition* **2011**, *27*, 3-20.

ANNEXES

ANNEXE 1:

Mineralization of TiO_2 nanoparticles for the determination of titanium in rat tissues

Jérôme Devoy*[1], Emilie Brun[**], Anne Cosnefroy[***], Clémence Disdier[***], Mathieu Melczer[*], Guillaume Antoine[*], Monique Chalansonnet[*], Aloïse Mabondzo[***].

[*]*Department of Biomonitoring and Toxicology, Institut National de Recherche et de Sécurité, Rue du Morvan, CS 60027, F-54519 Vandoeuvre-les-Nancy, France.*

[1]*E-mail address: jerome.devoy@inrs.fr*

[**]*Laboratoire de Chimie Physique, UMR CNRS 8000, Université Paris-Sud, F-91140 Orsay, France.*

[***]*CEA, Direction des Sciences du Vivant, iBiTec-S, Service de Pharmacologie et d'Immunoanalyse, F-91191, Gif-sur-Yvette, France.*

Accepted on july 2015 in Journal of Analytical in Chemistry

ЖУРНАЛ АНАЛИТИЧЕСКОЙ ХИМИИ, 2016, том 71, № 4, с. 436–442

ОРИГИНАЛЬНЫЕ СТАТЬИ

УДК 543

MINERALIZATION OF TiO_2 NANOPARTICLES FOR THE DETERMINATION OF TITANIUM IN RAT TISSUES

Jérôme Devoy*, [1], Emilie Brun, Anne Cosnefroy***, Clémence Disdier***, Mathieu Melczer *, Guillaume Antoine*, Monique Chalansonnet*, Aloïse Mabondzo*****

*Department of Biomonitoring and Toxicology, Institut National de Recherche et de Sécurité Rue du Morvan, CS 60027, F-54519 Vandoeuvre-les-Nancy, France

**Laboratoire de Chimie Physique, UMR CNRS 8000, Université Paris-Sud F-91140 Orsay, France

***CEA, Direction des Sciences du Vivant, iBiTec-S, Service de Pharmacologie et d'Immunoanalyse F-91191, Gif-sur-Yvette, France

[1] E-mail: jerome.devoy@inrs.fr

Received March 15, 2015; in final form, July 27, 2015

In order to draw appropriate conclusions about the possible adverse biological effects of titanium dioxide nanoparticles (**TiO_2-NPs**), the so-called "dose–effect" relationship must be explored. This requires proper quantification of titanium in complex matrices such as animal organs for future toxicological studies. This study presents the method development for mineralizing TiO_2-NPs for analysis of biological tissues. We compared the recovery and quantification limits of the four most commonly used mineralization methods for metal oxides. Microwave-assisted dissolution in an HNO_3–HF mixture followed by H_2O_2 treatment produced the best results for a TiO_2-NPs suspension, with 96 ± 8% recovery and a limit of quantification as low as 0.9 μg/L. This method was then used for the determination of titanium levels in tissue samples taken from rats. However, our tests revealed that even this method is not sensitive enough for quantifying titanium levels in single olfactory bulbs or hippocampus in control animals.

Keywords: titanium, nanoparticles, mineralization, toxicology, rat, ICP-MS.

DOI: 10.7868/S0044450216040046

Titanium dioxide nanoparticles are widely produced today, with an estimated upper bound of 38000 tons per year manufactured in the United States alone [1]. They are found in many commercial products, including paint, cosmetics, pharmaceutical products, plastics, paper, ceramics, and food as an anticaking or whitening agent [1, 2]. Such massive production raises the question of their human and environmental toxicity.

While TiO_2 particles were used in the past as a negative control in *in vitro* and *in vivo* toxicological studies [3], this practice was challenged after one study reported the development of lung tumors in rats after two years of exposure to high concentrations of fine TiO_2 [4]. The International Agency for Research on Cancer (IARC) has therefore classified TiO_2 as a Group 2B carcinogen (possibly carcinogenic to humans) [5]. Recent studies have also highlighted the ability of TiO_2-NPs to cross biological barriers and reach several organs [6, 7]. However, some absorption routes remain controversial [8–12].

One possible explanation for the discrepancies in the literature might be the difficulties involved in properly quantifying TiO_2-NPs in tissue samples. Inductively coupled plasma-mass spectrometry (**ICP-MS**) is one of the most useful techniques available but the procedure is complicated. Sample preparation that results in acceptable and reproducible recovery, interference caused by different Ti isotopes, and estimation of the correct quantification limit in complex matrices such as biological tissues are among the hurdles to overcome. Only a few papers have dealt with this issue [13–15]. Other analytical tools, such as electrothermal vaporization ICP-MS, might be considered good alternatives for analyzing solid samples, but these often demand substantial financial investment. In this study, we developed and fully-validated a reliable, quantitative ICP-MS method for analyzing titanium contents in rat organ tissues. Different digestion/dissolution techniques are traditionally used to solubilize TiO_2-NPs in organic matter, such as the use of strong acids (e.g., hydrofluoric, sulfuric and nitric acids) and/or hydrogen peroxide together with microwaves and/or heating systems [15–20]. In this study, we compared the four most common mineralization techniques for use with a TiO_2-NP solution. The most appropriate digestion method was then selected on the basis of its recovery rate and quantification limit. This

method was validated and then applied to determination of titanium in different rat organs. The results were compared to available published data. We consider determination of a method's recovery and quantification limit to be a pre-requisite and mandatory step that must be taken before analysing tissues from exposed animals and drawing conclusions about dose-effect relationships.

EXPERIMENTAL

Apparatus. A Varian 820-MS inductively coupled plasma mass spectrometer (ICP–MS) with an external sample introduction assembly with Peltier-cooled spray chamber, glass concentric nebulizer, peristaltic pump mounted outside the torch box and SPS3 auto sampler was used. A discrete dynode electron multiplier detector provides nine decades of dynamic range in an all-digital pulse design. The Varian 820-MS system also features a Collision Reaction Interface (**CRI**) providing fast, flexible, interference-free analysis using simple collision and reaction gases.

A Varian AA280Z Atomic Absorption Spectrophotometer (**AAS**), equipped with a Zeeman background corrector, was used for atomic absorption measurement of titanium at 364.3 nm with a slit-width of 0.5 mm. A hollow cathode lamp of Ti (photron) was operated at 20 mA. Uncoated graphite tube cuvettes were purchased from Schunk Kohlenstofftechnik (Germany).

Transmission electron microscopy (**TEM**) analyses were performed as follows: a 3-μL droplet of the dispersion was cast on formvar/carbon-coated copper grid for 2 min and imaged with a JEOL 1400 instrument (JEOL, Tokyo, Japan) operating at 80 keV (Imagif platform, Gif-sur-Yvette). Images were acquired using a post-column high resolution (11 megapixels) high speed camera (SC1000 Orius, Gatan) and processed with Digital micrograph (Gatan) and ImageJ (Schneider Nat Meth 2012 9671) software. Hydrodynamic diameter was measured by dynamic light scattering using a ZetaSizer ZEN3600 (Malvern, Herenberg, Germany) equipped with a 633 nm laser. Rat samples were weighed thanks to AB204 Mettler Toledo balance.

Reagents and solutions. Certified water was used (Trace Metals 3, RTC, QC1448). All chemicals used in the study were of analytical grade or higher. Nitric acid was used to prepare 2.0% HNO_3 (v/v) with ultrapure water. All single element stock solutions (1000 mg/L) were delivered by SCP Science and certified for purity and concentration. Titanium standard solutions for ICP-MS calibration were prepared (at concentration levels of 50 to 10000 ng/L) by diluting a 10 g/L titanium standard stock solution (140.050.220, SCP Science) with 2% (v/v) HNO_3. An internal standard solution containing 100 μg/L of Ge was prepared by diluting a 1000 mg/L internal standard stock solution (140.051.211, SCP Science) with 2% (v/v) HNO_3. The internal standard was added to all samples and standard solutions.

External quality assurance was performed by participation in the following international comparison programs and quality assessment schemes: German External Quality Assessment Scheme (G-EQUAS) from the Institute and Out-Patient Clinic for Occupational, Social and Environmental Medicine at Friedrich-Alexander-University, Erlangen-Nuremberg, Germany, and Quebec Multielement External Quality Assessment Scheme (QMEQAS) at the Canadian Institut National de Santé Publique du Québec.

Titanium dioxide nanoparticle preparation. The TiO_2-NPs used in this study were in the form of Aeroxide® P25 TiO_2 (Degussa, Sigma Aldrich), which consists of an 81 : 19 mixture of anatase and rutile. A stock solution was prepared by adding the desired weight of P25 to ultrapure water (MilliQ, Millipore, Germany) and sonicating for 30 min in a Branson 2510 bath sonicator at a frequency of 40 kHz. The morphology and size of TiO_2-NPs in stock suspensions were determined by TEM. The mean particle diameter as observed by TEM was 21 ± 7 nm (n = 300). From dynamic light scattering measurements, TiO_2-NPs were found to agglomerate in both water and culture medium (474 ± 96 nm in distilled water and 747 ± 142 nm in culture media). The specific surface area (BET) was 50 ± 15 m^2/g. Various concentrations for the digestion evaluation were made using a serial dilution of the stock solution. First, 125 mg of TiO_2-NPs powder was dispersed in 50 mL of distilled water. The 2.5 g/L suspension was then treated by ultrasound for 20 min and mechanically vibrated for 3 min. An intermediate suspension at 2.5 mg/L was prepared in order to prepare final solutions of 2 μg/L for testing the stability/homogeneity of the solution, and 5 μg/L for testing the mineralization methods.

Animal tissue samples. All experiments in this study were performed in line with the European guidelines related to the protection of animals used for experimental and other scientific purposes [21]. Prior to the study period, 62 eight-week-old male Sprague-Dawley rats (Charles River, Domaine des Oncins, Saint-Germain-sur-l'Arbresle, France), each weighing 250–275 g, were housed under controlled environmental conditions for seven days in polycarbonate cages (43 cm long, 43 cm wide, 19 cm high, each holding six rats) with hardwood-chip bedding. The room temperature (22°C), humidity (55 ± 5%) and light cycle (07:00–19:00 h) were controlled automatically. Filtered tap water (pore size 0.3 μm) and γ-ray-sterilized food (UAR-Alimentation, Villemoisson, Epinay-sur-Orge, France) were provided *ad libitum*.

Animals were deeply anesthetized with pentobarbital (60 mg/kg) and then killed by exsanguinations through the abdominal aorta. Blood samples were taken and red blood cells (**RBC**) were isolated from plasma for the determination of titanium. Tissue and or-

gans (brain, liver, spleen, kidneys, lungs) were collected and weighed. The brains of 46 rats were removed rapidly and then placed on glass plates at 0°C to sample the olfactory bulbs, hippocampus, frontal cortex and cerebellum. Tissue samples were placed in polyethylene microcentrifuge tubes and immediately put into liquid nitrogen storage at −180°C until analysis. All procedures used in this experiment were compliant with the local ethics committee.

Mineralization methods. The four most commonly-used digestion methods were tested (methods A to D, below). Method A is described by Wang [22] and Liu [23], and methods B, C and D are presented in Khosravi [24]. For each method, tissues were removed from storage and thawed. About 0.1–0.3 g of each tissue was weighed and digested.

Method A. Several hundred mg of sample was digested overnight in 2 mL of concentrated nitric acid. After adding 0.5 mL of concentrated H_2O_2, the mixed solutions were digested completely using a Microwave Assisted Reaction System (**MARS**) Express instrument. The microwave digestion program consisted of a temperature ramp to 150°C over 15 min, followed by a ramp from 150°C to 180°C over 15 min and then a 20-min hold at 180°C. Power was at 1200 W during the 50-min cycle. The MARS reactors were rinsed twice with 10 mL of 2% nitric acid and then transferred to a Teflon reaction vessel containing the sample solution. The solutions were heated at 120°C until colourless and clear in order to remove the remaining nitric acid. Finally, the remaining solutions were diluted to 3 mL with 2% nitric acid and then analyzed for titanium content.

Method B. A tri-acid mixture was prepared with concentrated nitric, hydrochloric and hydrofluoric acids mixed in a ratio of 3 : 1 : 3, and 30 mL of this mixture was added to each Teflon reaction vessel containing a sample. The mixed solutions were then completely digested using MARS Express instrument. The microwave digestion program was the same as that used for method A. After cooling, the remaining solution was diluted with 10 mL of ultrapure water. The aqueous solution was transferred to volumetric flasks for appropriate dilution (ten-fold typically) and then analyzed for titanium content.

Method C. Samples were added to a 55 mL microwave digestion vessel with 8 mL of concentrated nitric acid and 2 mL of concentrated HF. The samples were digested using MARS Express instrument, following the same temperature program as that used for methods A and B. After cooling, the vessel was rinsed at least three times into a Teflon beaker using approximately 20 mL of a 2% nitric acid solution, and 2 mL of concentrated hydrogen peroxide was added to each beaker to digest any remaining organics. The beakers were then heated on a hot plate at 180°C until 0.1 to 0.5 mL of each solution remained. The beakers were then removed from the hot plate, allowed to cool and rinsed at least three times into a 25 mL volumetric flask using a 2% nitric acid solution before being stored for analysis. The final concentration of HF in the measured solution was low enough to allow using the routinely applied sample introduction system.

Method D. Samples were transferred to porcelain crucibles for digestion and heated gently to dryness over a hot plate. To optimize the persulfate fusion method, various amounts of ammonium persulfate were added to the crucible. Care was taken to ensure that the residue at the bottom of the crucible was completely covered with ammonium persulfate prior to fusion, and all the steps in the digestion process took place in an acid-resistant fume hood. Fusion was initiated by heating with a laboratory Bunsen burner. Upon heating of the reaction vessel, the mixture began to fume. Fusion was complete once fuming had ceased (after about 3 min). The fusion product was soaked in 10 mL of 2% nitric acid solution in the reaction vessel for 30 min. The solution was then relocated into a 200 mL flask and placed on a hotplate for further digestion by gentle boiling for 10 min. Finally, the clear solution was transferred to a 50 mL volumetric flask and diluted with 2% nitric acid solution.

Determination of titanium. Prior to elemental analysis, the tissues were mineralized according to one of the methods described above. In general, ICP-MS was used to measure titanium concentrations in the samples. The typical method parameters (including CRI settings) used for the analyses are listed in Table 1. Analytical parameters for AAS are presented in Table 2. The internal standard concentration was 50 μg/L Ge for all samples and calibration solutions. Blanks and tissue digests were measured against an external calibration with internal standard correction.

Titanium determination by conventional quadrupole ICP-MS has recently been optimized [15]. Unwanted interferences can also be minimized using collision/reaction cell technology [25]. For titanium determination with Varian 820-MS, the samples were injected directly. In order to avoid potential interferences [13], the analyses were performed in CRI mode on ^{49}Ti, an isotope that has a relatively low natural abundance (5.4%). In order to cross-check the ICP-MS results, the same samples were analyzed by AAS when possible. The data were expressed either as micrograms per liter of digestion solution or as micrograms per gram of fresh tissue. ICP-MS was sensitive enough to quantify all of our samples and there was no need to improve the analytical quantification limit of 0.08 μg/L. In contrast, a significant effort was made to improve the method quantification limits (**MQL**).

Quantification limits. The limit of quantification (**LOQ**) can be estimated by taking 30 repeat measurements of the blank in the same series. The mean and standard deviation (**SD**) of these 30 measurements are expressed in concentration. In this case, the LOQ is equal to the sum of the mean blank concentration plus

Table 1. Instrumental settings for the determination of titanium in HNO_3 solution by ICP-MS

Parameter	Instrument parameter	Setting
Gas flow parameters, L/min	Plasma flow	13.5
	Auxiliary fow	1.35
	Nebulizer flow	1.00
	Sheath flow	0.19
Plasma power	RF power, kW	1.40
Sample introduction	Sampling depth, mm	7.0
	Pump rate, rpm	5.0
Ion optics, V	First extraction lens	−10
	Second extraction lens	−90
	Third extraction lens	−32
	Corner lens	−310
	Mirror lens left	35
	Mirror lens right	19
	Mirror lens bottom	26
	Fringe bias	−7.0
CRI Gas settings	Skimmer gas source	He
	Skimmer flow, mL/min	150
Quadrupole scan	Scan mode	Peak hopping
	Dwell time, ms	100
	Points per peak	1
	Scans/replicate	20
	Replicates/sample	3

ten standard deviations. Alternatively, the LOQ can be evaluated using the dilution of a standard solution or quality control sample at a low concentration with the dilutant. Eleven dilutions are prepared, altering the dilution by 10% each time (i.e., 100 + 0, 90 + 10, 80 + + 20...0 + 100), and each preparation is measured 10 times in a single series. To determine the LOQ, the standard deviation and variation of the average (m) from the theoretical value (fidelity profile) are calculated for each series of measurements. The concentrations and their respective SD values are then used to construct a Horwitz curve from which the LOQ can be extrapolated at SD = 15%. We chose the first way to estimate LOQ and we verified the consistency of this limit with the second way.

Table 2. Instrumental settings for the determination of titanium in HNO_3 solution by GF-AAS

Parameter	Value
Wavelength, nm	364.3
Lamp current, mA	20
Slit width, nm	0.5
Dry temperature, °C	120
Dry time, ramp/hold, s	40/30
Ashing temperature, °C	1300
Ashing time, ramp/hold, s	20/10
Atomisation temperature, °C	2800
Atomisation time, ramp/hold, s	1.2/3
Cleaning temperature, °C	2800
Cleaning time, ramp/hold, s	2/0.4

Method validation. Validation was done as described in our previous paper [26]. The linearity limit, precision (intermediate precision, repeatability and reproducibility), accuracy and sensitivity were estimated for the chosen method. This validation procedure is in good agreement with that proposed by Peters et al. [27].

RESULTS AND DISCUSSION

Stability and homogeneity of TiO_2-NPs solution. To be sure that the solution was homogeneous and stable, the concentration of an initial 2 μg/L TiO_2-NPs aqueous solution (250 mL) was monitored at different times over 360 min; $t = 0$ corresponds to the end of ultrasonic and vibration treatment. An aliquot of 50 μL was sampled at different times (t = 0, 10, 15, 60, 90,

Table 3. Recovery rates and quantification limits for each method (mean values ± SD)

Method	Recovery*, %	Expected titanium concentration, μg/L	Mean titanium concentration, μg/L	Blank mean titanium concentration, μg/L	LOQ**, μg/L
A	56 ± 25	5.4	3.0 ± 1.4	1.2 ± 0.2	3.7
B	98 ± 3	5.0	4.9 ± 0.2	0.5 ± 0.1	1.2
C	96 ± 8	5.2	5.0 ± 0.4	0.3 ± 0.1	0.9
D	92 ± 9	4.8	4.5 ± 0.4	1.3 ± 0.1	2.6

* For recovery, there were 12 sample repetitions, or 12 independent sample digestions; each sample was measured in triplicate.
** For LOQ, there were 30 sample repetitions; each sample was measured in triplicate; LOQ = mean + 10SD; instrumental quantification limit is equal to 0.08 μg/L.

120, 180, 240, 300 and 360 min) and transferred to a 50 mL flask of 2% HNO_3. A ten-fold dilution was performed for each of these aliquots prior to graphite furnace (**GF**)-AAS analysis. At this level of titanium concentration, the GF is capable of direct analysis of solids [28], thus allowing the problem of TiO_2-NPs mineralization to be avoided. Fifteen analyses of this stock solution were performed over 360 min. The mean TiO_2 concentration was 2.0 μg/L with a SD of 0.3 μg/L (RSD = 16%). A review of Cal-Prieto et al. [29] reported the RSD values for elemental analysis of animal tissue with GF-AAS ranging from 14 to 17%. The stock solution was therefore considered stable enough to be analyzed in our experimental conditions.

Recovery. The digestions were first evaluated for the recovery of the 2 μg/L TiO_2 NPs aqueous solution. Twelve aliquots of this solution were used for each digestion method. The results are presented in Table 3. The recovery rates of methods B, C and D were over 92% with standard deviations below 9%. At this concentration level, a SD below 15% is equivalent to the SD values determined for quality control samples. In contrast, method A had a recovery rate of 56% and a SD of about 25%. These data were also used to determine the digestion MDL.

Quantification limits. All digestion methods were applied to blank samples in order to measure the likely amounts of titanium contamination. Teflon tubes, 15 mL polypropylene tubes and chemicals are all potential sources of titanium contamination [15]. One of the main advantages of using real blank samples to estimate the MQL is that any titanium contamination will be entirely integrated into the MQL.

As a further safeguard and quality check for titanium contamination, the vessels were rinsed in between two consecutive quantitative analyses, following the protocol of method C, and the final solution was analyzed. If the titanium content was higher than 0.4 μg/L, the vessels were rinsed again and re-analyzed. This "contamination limit" was arbitrarily chosen but was later found to have yielded the best results. The quantification limits for each method are reported in Table 3. Titanium blank concentrations ranged from 0.3 to 1.3 μg/L depending on the method. MQL averages and standard deviations are also reported. Of the three methods, method C yielded the highest sensitivity (MQL = 0.9 μg/L) and a satisfactory recovery rate (96 ± 8%). This method was therefore chosen for the analyses of biological samples.

Validation of the method. Linearity was investigated using 6 standard solutions with concentrations ranging from 0.8 to 52 μg/L (6 replicates). The linearity of the calibration curves for ^{49}Ti was good over this concentration range ($R^2 > 0.999$). The intermediate precision at any given level is defined as the degree of concordance between individual results obtained from a single sample tested in a single laboratory, but where one or more of the analyst, equipment and/or day varies. The intermediate precision was determined at two titanium concentrations: 1.24 and 6.20 μg/L. Samples were analyzed twice per day over 15 days. The maximum standard deviation was 22%. The standard deviations obtained for 1.24 and 6.20 μg/L solutions were 6.6 and 3.5%, respectively.

The accuracy at any given level is the degree of concordance between the value certified by a recognized organization and the mean result obtained by applying the experimental procedure at least ten times. Accuracy was measured at the two titanium concentrations, 1.24 and 6.20 μg/L. Thirty replicates of the samples were performed. The accuracies were 99.91 and 99.97%, respectively.

Matrix effects and recovery rates were double-checked by analyzing the titanium content of samples by both ICP-MS and AAS. For ICP-MS analysis in CRI mode, no matrix interferences on ^{49}Ti, such as $^{33}S^{16}O$, $^{32}S^{16}O^{1}H$ or $^{31}P^{18}O$, were observed. Direct AAS analysis of non-mineralized samples and ICP-MS analysis of mineralized samples (method C, corrected for recovery) yielded titanium contents that usually differed by no more than 5%.

Application of method C to different types of biological organ tissues. Table 4 presents the titanium contents measured in different rat organs. Mean titanium concentrations are reported as "μg/L of final digestion solution" and "ng/g of tissue". As the MQL is dependent on the sample mass, it is reported as "ng/g of tissue".

Table 4. Quantification limits for rat tissue samples

Rat matrices/organs	Average sample mass, mg	Mean titanium concentration, μg/L	Mean titanium concentration, ng/g	LOQ, ng/g	LOD, ng/g
Brain (n = 16)	1606 ± 388	4.8 ± 1.7	74.8 ± 17.8	13.7	4.1
Liver	*4738 ± 1259*	*21.1 ± 11.8*	108 ± 43	4.7	1.4
Spleen	668 ± 186	2. 6 ± 1.2	93.9 ± 28.8	33.1	9.9
Kidneys	1502 ± 466	7.0 ± 3.6	107 ± 33	14.7	4.4
Lung	1044 ± 192	3.9 ± 1.5	86.3 ± 27.5	21.2	6.4
RBC	1569 ± 344	5.0 ± 3.5	72.5 ± 17.1	14.1	4.2
Plasma	*1984 ± 733*	*2.7 ± 1.3*	34.5 ± 11.2	11.2	3.3
Cerebellum	2978 ± 23	0.7 ± 0.1	**57.4 ± 7.7**	**54.1**	16.2
Olfactory bulb (n = 32)	48.4 ± 5.2	0.3 ± 0.1	150 ± 63	333	99
5 Olfactory bulbs (n = 12)	239 ± 17	0.6 ± 0.1	**61.4 ± 10.9**	**67.5**	20.2
Hippocampus (n = 32)	51.6 ± 8.6	0.2 ± 0.1	116 ± 44	311	93
5 Hippocampus (n = 12)	251 ± 45	0.6 ± 0.1	**66.1 ± 9.2**	**64.0**	19.2
5 Frontal cortex (n = 18)	351 ± 57	0.8 ± 0.1	**57.3 ± 10.1**	**45.8**	13.7
Urine	*3000 ± 281*	*11.0 ± 1.6*	95.6 ± 19.2	7.4	2.2

Data were obtained from 62 rats. Masses in italics mean that the tissue or the sample was not taken entirely. LOQ in this table is equivalent to MQL.

As mentioned above, the LOQ for method C (as determined from blank analyses) was 0.9 μg/L (Table 3). In the rat tissue tests, the MQL ranged from 4.7 (in liver) to 330 ng/g (in a single olfactory bulb), depending on the sample mass and digestion method used. This important finding should be taken into consideration in future toxicological studies. Because the basal titanium content is highly variable from one organ to another, it is necessary to ensure that the measured titanium concentration is above the MQL for meaningful quantification. The number of control animals is also relatively important (n = 62 in this study) in ensuring that statistically significant results are obtained.

In Table 4, even though the titanium contents were measured in different control animals, when the measured concentrations were close to the MQL, such as those of cerebellum, 5 olfactory bulbs, 5 hippocampus and 5 frontal cortices, the respective standard deviations (13.4, 17.7, 13.9 and 17.6%; Table 4) were acceptable. Taking into account the variability between animals, according to the Horwitz test these standard deviations confirm that the method detection and quantification limits are appropriate.

The standard deviations for organs with relatively high titanium concentrations, such as the brain, liver, spleen, kidney, lung or RBC are equal to 23.8, 39.8, 30.7, 31.5, 31.8 and 23.5%, respectively. Standard deviations at this level are frequently reported for the titanium contents of the major rat tissues [15, 18].

The MQL and method detection limit (**MDL**) are on the same order of magnitude as those found in the literature. Krystek et al. [15] proposed an MDL of 5 ng Ti/g tissue for liver, spleen, kidneys and blood. Our MDL are close to that level for kidneys and RBC (4.4 and 4.2 ng Ti/g tissue, respectively) but deviate from this value for liver and spleen (1.4 and 9.9 ng Ti/g tissue, respectively). The MQL and MDL expressed in "ng Ti/g tissue" are tissue mass-dependent and this should be kept in mind when results of future toxicokinetic studies are presented.

The titanium contents measured in brain (75 ± ± 18 ng/g), liver (108 ± 43 ng/g), spleen (94 ± 29 ng/g), kidney (107 ± 34 ng/g), lung (86 ± 27 ng/g) and RBC (73 ± 17 ng/g) are relatively close to those reported by Wang et al. (n = 80) [22] and Liu et al. (n = 70) [23] in CD-1 mice. However, our results differ by one order of magnitude with those obtained by Fabian [8] (e.g., (1.6 ± ± 0.1) × 10^3 ng/g in rat lung compared to 86 ± 27 ng/g in our study) and Shinohara [30] (e.g. 5.0 ± 2.2 ng/g in rat kidney compared to 107 ± 34 ng/g in our study). These discrepancies may be due to the number of rats (n = 3 for Fabian and n = 25 for Shinohara) and/or the species of rat (Wistar and F344/DuCrlCrlj rats, respectively) used in the different studies.

Finally, it is worth mentioning that Krystek et al. [15] compared different digestion methods (using HF) in different laboratories. The inter-laboratory study yielded consistent results for samples over 4 μg/g tissue. However, all control rat tissue samples have titanium contents lower than 0.15 μg/g tissue, their method quantification limit. In our work, the method we chose is sensitive enough to quantify titanium in all control rat organs/tissues except single olfactory bulbs and hippocampus.

* * *

The aim of this study was to compare and validate a method for quantifying titanium content in biological samples. Four mineralization methods were tested for recovery and quantification limit. The best results were obtained for a method that involved mineralization with nitric and hydrofluoric acid, leading to 96 ± ± 8% recovery and an LOQ down to 0.9 μg/L for a TiO_2-NPs suspension. A wide variety of rat organs were then analysed using this method. These showed that the MQL was matrix-dependent. For example, the method is not sensitive enough to quantify titanium levels in a single olfactory bulb and hippocampus in control rats. Bearing this limitation in mind, the method could be applicable to *in vivo* studies of TiO_2-NPs biokinetics and toxicokinetics studies and could also be transposed to human urine for biological monitoring of workers exposed to TiO_2-NPs. The nanotoxicology community is now fully aware of the need for a thorough characterization of the nano-objects used in their studies independently from any information provided by the supplier. This study has highlighted that the same attention should be paid to ICP-MS quantification: no matter how tedious it might be, determining recovery rates and MQL of methods is a *sine qua none* condition for providing valuable data.

ACKNOWLEDGEMENTS

The authors thank the French Alternative Energies and Atomic Energy Commission (CEA) and the National Institute for Research and Safety (INRS). The authors particularly acknowledge the efforts of Alice Williams, Lise Merlen, Stéphane Boucard, Samuel Müller, Frédéric Cosnier and Robert Devoy for their technical assistance. This work has also benefited from the facilities and expertise of the Platform for TEM of Imagif (Centre de Recherche de Gif, wwww.imagif.cnrs.fr).

REFERENCES

1. *Hendren, C.O., Mesnard, X., Dröge, J., and Wiesner, M.R.*, Environ. Sci. Technol., 2011, vol. 45, no 7, p. 2562.
2. Current Intelligence Bulletin 63. 2011 *Occupational Exposure to Titanium Dioxide*. DHHS (NIOSH). Publication number 2011-160.
3. American Conference of Governmental Industrial Hygienists (ACGIH). *Threshold limit values and biological exposure indices for 1992–1993. 1992*, Cincinnati, Ohio: American Conference of Governmental Industrial Hygienists.
4. *Lee, K.P., Trochimowicz, H.J., and Reinhardt, C.F.*, Toxicol. Appl. Pharmacol., 1985, vol. 79, p. 179.
5. IARC: Carbon Black, Titanium Dioxide and Talc. IARC Monographs, 2010, vol. 93.
6. *Iavicoli, I., Leso, V., and Bergamaschi, A.*, J. Nanomater., 2012, Article ID 964381, 36 p.
7. *Shi, H., Magaye, R., Castranova, V., and Zhao J.*, Particle Fibre Toxicol., 2013, vol. 10, no. 15, p. 1.
8. *Fabian, E., Landsiedel, R., Ma-Hock, L., Wiench, K., Wohlleben, W., and van Ravenzwaay, B.*, Arch. Toxicol., 2008, vol. 82, no. 3, p. 151.
9. *Xie, G., Wang, C., Sun, J., and Zhong, G.*, Toxicol. Lett., 2011, vol. 205, p. 55.
10. *Ze, Y., Sheng, L., Zhao, X., Hong, J., Ze, X., Yu, X., Pan, X., Lin, A., Zhao, Y., Zhang, C., Zhou, Q., Wang, L., and Hong, F.*, J. Hazard. Mater., 2014, vol. 264, p. 219.
11. *Janer, G., Mas del Molino, E., Fernández-Rosas, E., Fernández, A., and Vázquez-Campo, S.*, Toxicol. Lett., 2014, vol. 228, no. 2, p. 103.
12. *Bencsik, A. and Lestaevel, P.*, J. Biomed. Mater. Res. A, 2014, p. 1.
13. *Potouridis, T., Völker, J., Alsenz, H., Oetken, M., and Püttmann, W.*, Anal. Bioanal. Chem., 2014, vol. 406, no. 11, p. 2495.
14. *López-Heras, I., Madrid, Y., and Cámara, C.*, Talanta, 2014, vol. 124, p. 71.
15. *Krystek, P., Tentschert, J., Nia, Y., Trouiller, B., Noël, L., Goetz, M.E., Papin, A., Luch, A., Guérin, T., and de Jong, W.H.*, Anal. Bioanal. Chem., 2014, vol. 406, p. 3853.
16. *Korn, M.D.A., Ferreira, A.C., Costa, A.C.S., Nobrega, J.A., and Silva, C.R.*, Microchem. J., 2002, vol. 71, p. 41.
17. *Lomer, M.C.E., Thompson, R.P.H., Commisso, J., Keen, C.L., and Powell, J.J.*, Analyst, 2000, vol. 125, p. 2339.
18. *Sarmiento-Gonzalez, A., Encinar, J.R., Marchante-Gayon, J.M., and Sanz-Medel, A.*, Anal. Bioanal. Chem., 2009, vol. 393, p. 335.
19. *Sun, H.W., Zhang, X.Z., Niu, Q., Chen, Y.S., and Crittenden, J.C.*, Water Air Soil Pollut., 2007, vol. 178, p. 245.
20. *Wildhagen, D., Krivan, V., Gercken, B., and Pavel, J.*, J. Anal. At. Spectrom., 1996, vol. 11, p. 371.
21. European Union. *Directive 2010/63/EU on the approximation of laws*, September 22, 2010.
22. *Wang, J., Zhou, G., Chen, C., Yu, H., Wang, T., Ma, Y., Jia, G., Gao, Y., Li, B., Sun, J., Li, Y., Jiao, F., Zhao, Y., and Chai, Z.*, Toxicol. Lett., 2007, vol. 168, p. 176.
23. *Liu, H., Ma, L., Zhao, J., Liu, J., Yan, J., Ruan, J., and Hong, F.*, Biol. Trace Elem. Res., 2009, vol. 129, p. 170.
24. *Khosravi, K., Hoque, M.E., Dimock, B., Hintelmann, H., and Metcalfe, C.D.*, Anal. Chim. Acta, 2012, vol. 713, p. 86.
25. *Yip, Y. and Sham, W.*, Trends Anal. Chem., 2007, vol. 26, p. 727.
26. *Devoy, J., Melczer, M., Antoine, G., Remy, A., and Heilier, J.F.*, Anal. Bioanal. Chem., 2013, vol. 405, p. 8327.
27. *Peters, F.T., Drummer, O.H., and Musshoff, F.*, Forensic Sci. Int., 2007, vol. 165, p. 216.
28. *Carnrick, G.R., Lumas, B.K., and Barnett, W.B.*, J. Anal. At. Spectrom., 1986, vol. 1, p. 443.
29. *Cal-Prieto, M.J., Felipe-Sotelo, M., Carlosena, A., Andrade, J.M., Lopez-Mahia, P., Muniategui, S., and Prada, D.*, Talanta, 2002, vol. 56, p. 1.
30. *Shinohara, N., Danno, N., Ichinose, T., Sasaki, T., Fukui, H., Honda, K., and Kamo, M.*, Nanotoxicol., 2014, vol. 8, p. 132.

ANNEXE 2:

TiO_2 NPs caracterization data

Microspcopic analysis (TEM: Transmission Electron Microscopy) confirmed irregular spherical shape of the particles with a size distribution centered around 20 nm.

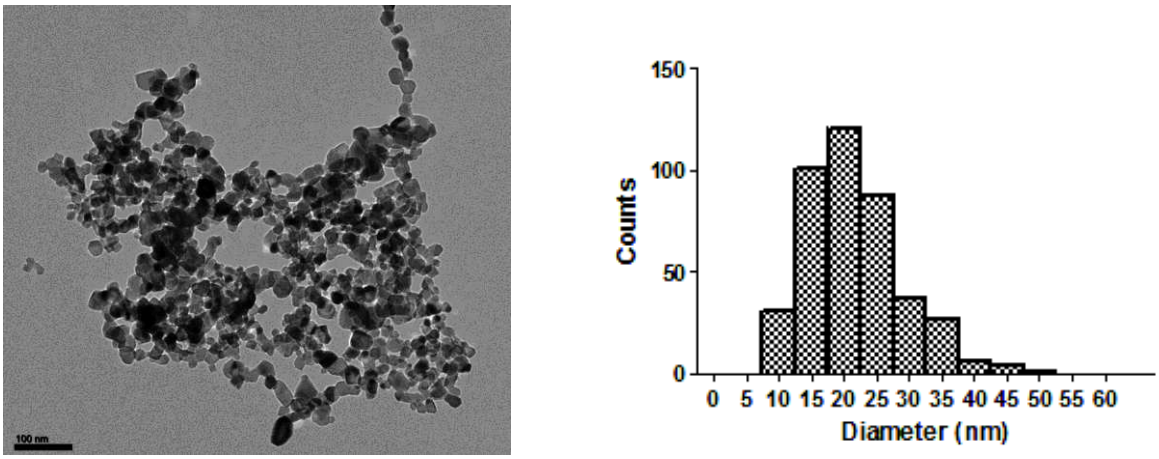

Figure 40: TEM image of TiO_2 P25 Degussa NPs and size distribution diagram.

SEM spectrum (Scanning Electron Microscopy) obtained on the TEM images show the lack of metal contaminants above 1%. The only elements detected were titanium, carbon and oxygen.

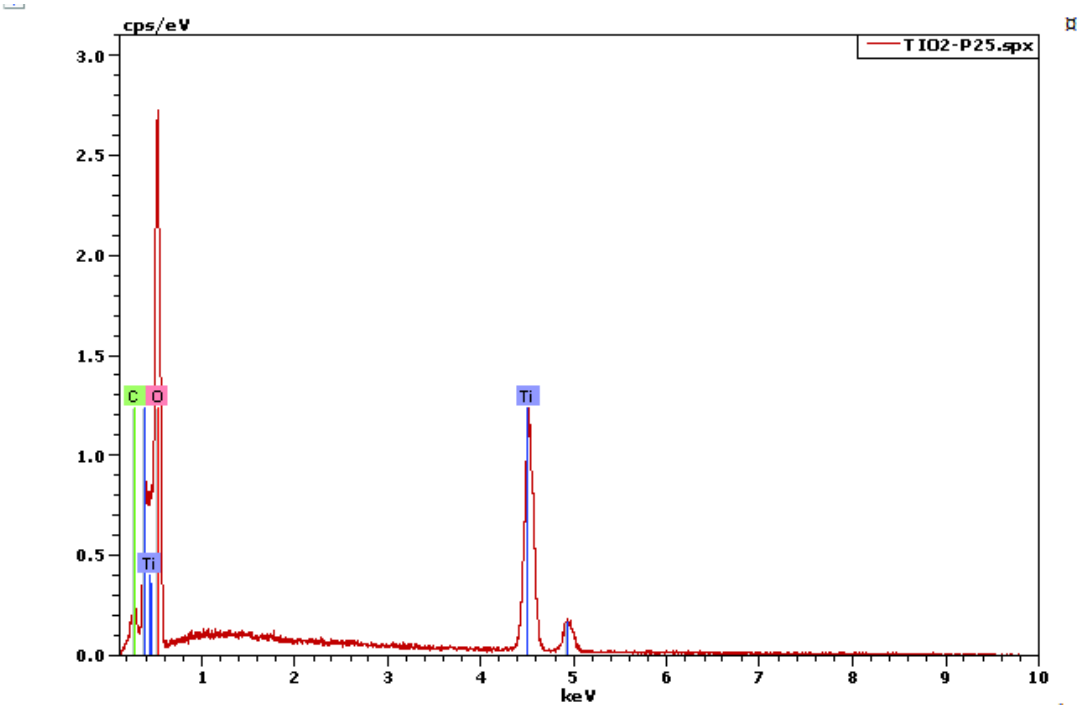

Figure 41: SEM spectrum of TiO_2 P25 Degussa NPs.

The surface area of the particles was measured by BET (Brunauer - Emmett - Teller) and is equal to $51 m^2$ / g.

The spectroscopic analysis by Dynamic Light Scattering (DLS) revealed the presence of clusters and agglomerates in suspension. Two size populations are observed: a small one with approximately 270 nm average diameter and a lager one with an average diameter the upper limit of the measuring range for the equipment used (1200 nm approximately).

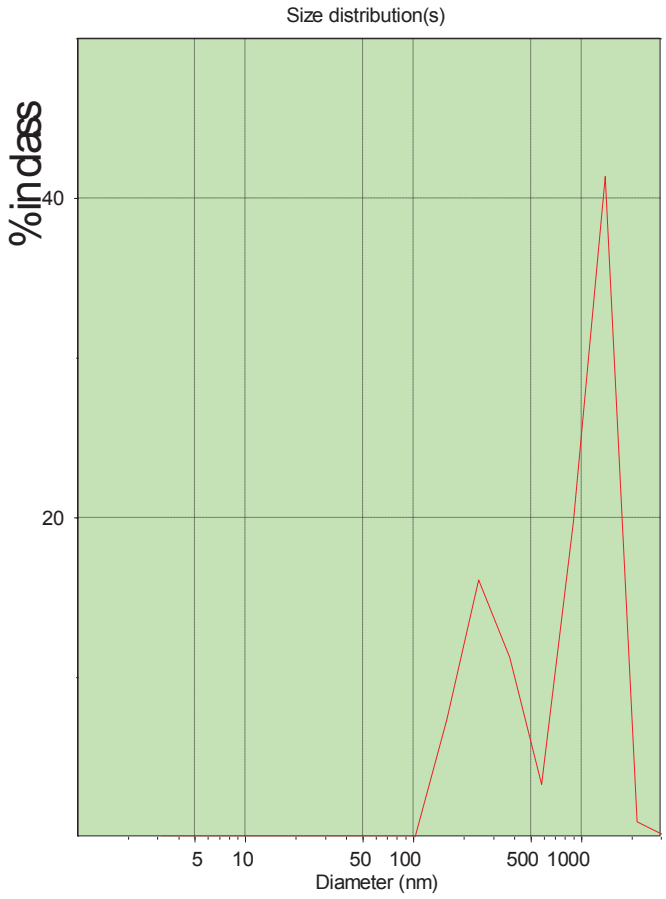

Figure 42: Dynamic light scattering of TiO_2 P25 Degussa NPs in water suspension.

The presence of both anatase and rutile in our powder mixture is proved by X Ray Diffraction study (XRD) after comparison with the X-ray diffraction patterns of anatase and rutile TiO_2.

A :

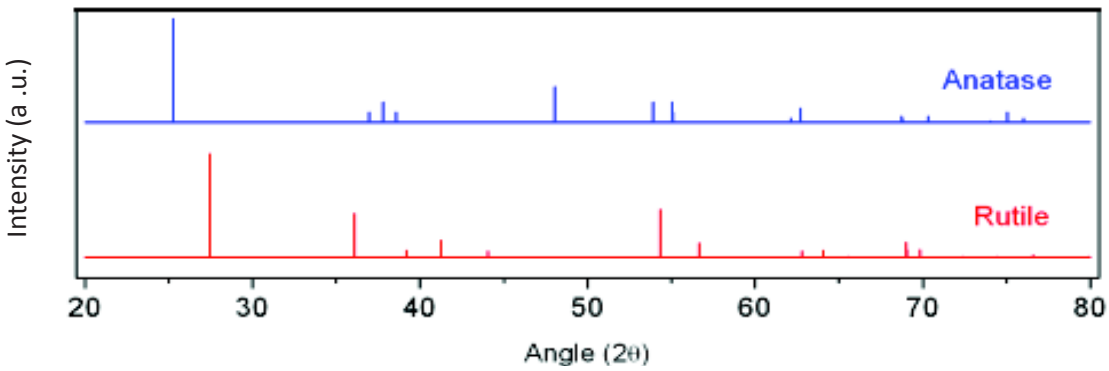

B :

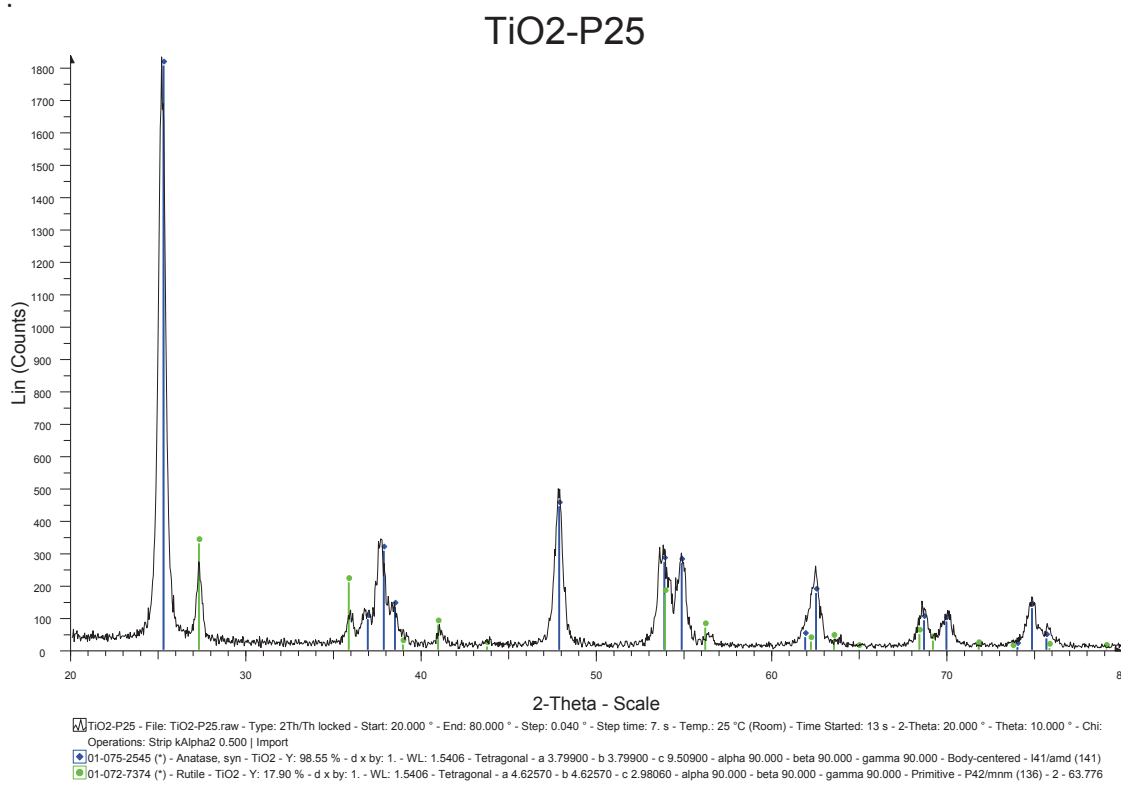

Figure 43: A: Theoretical X-ray diffraction patterns of anatase and rutile TiO_2 and experimental X-ray diffraction patterns of TiO_2 P25 Degussa NPs.

ANNEXE 3:

Bioplex calibration curves

Calibration curve for each analytes is traced by analysing the median fluorescent intensity data of standrads using 5 parameter logistic or spine curve fitting method. Concentration of each analytes in unknown sample were calculated based on corresponding analyte calibration curve. Concentrations where then corrected by dilution factor applied and normalized by sample protein concentration.

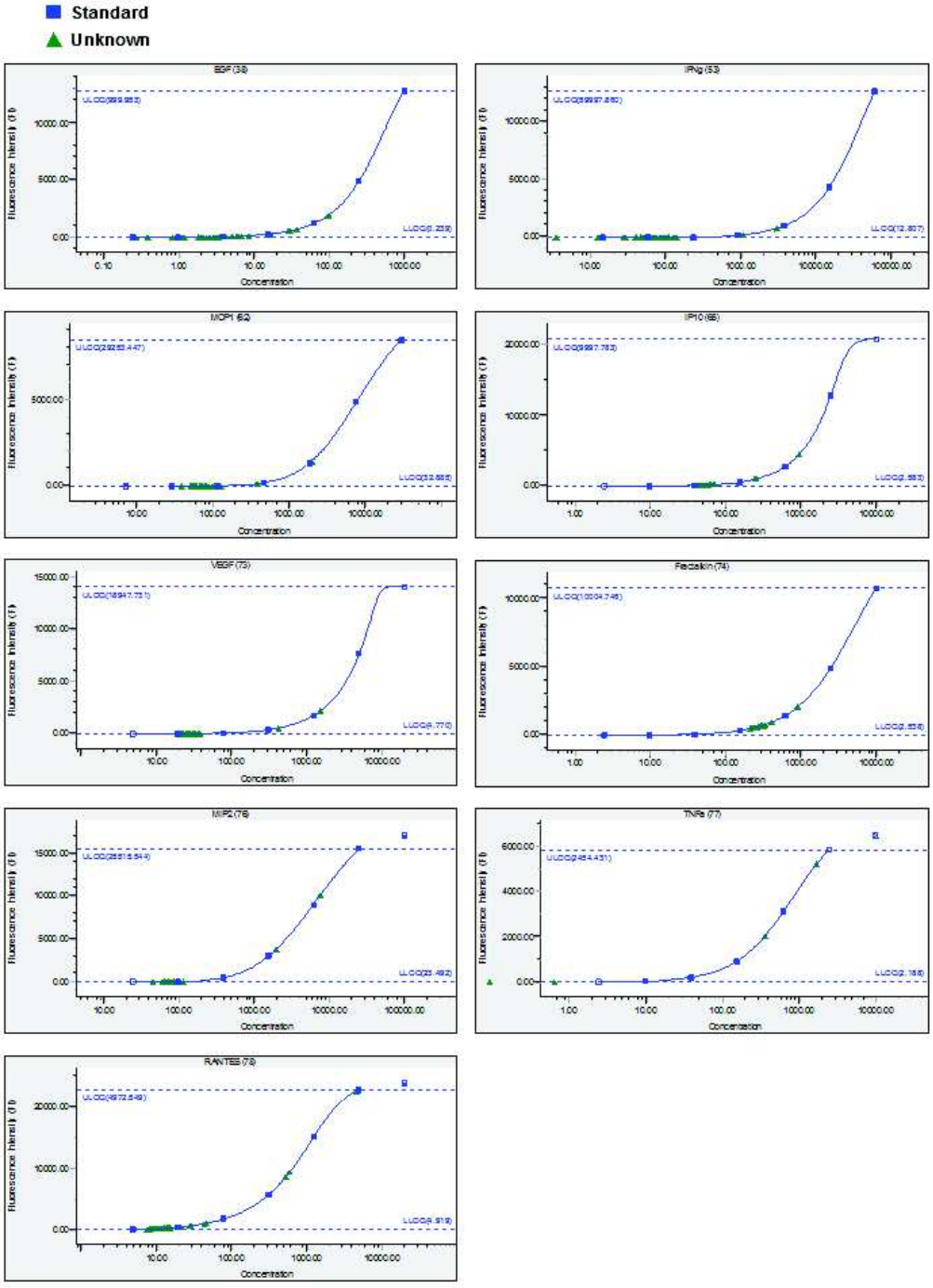

Figure 44 : Example of calibration curves obtained for the 11 analytes targeted in brain cortexes extract matrix.

ANNEXE 4:

MATERIALS

Table 12: Chemical reagents, kits and culture media

PRODUCTS	SUPPLIER
Nanoparticles	
Titanium(IV) oxide nanopowder, 21 nm primary particle size (TEM), ≥99.5% trace metals basis (ref.718467)	Sigma
ICP-MS experiments	
titanium standard stock solution (ref. 140.050.220)	SCP Science
Ge internal standard stock solution (rf. 140.051.211)	SCP Science
LC-MS/MS experiments	
Atenolol (ref. A7655-1G)	Sigma
Digoxin (ref. D6770-1VL)	Sigma
Prazosin hypochloride (ref. P7791-250MG)	Sigma
Dimethyl Sulfoxide DMSO (ref. D4540-500ml)	Sigma
Polyethylen Glycol PEG (ref. P3015-250GR)	Sigma
Alzet pumps (ref. ALZT2001D)	Charles River
Isolute SLE+ 1mL Cartridges (ref. 820-0140-C)	Biotage
Isolute SLE+ 400 µL Cartidges (ref. 820-0055-B)	Biotage
RT-qPCR experiments	
Ethanol	VWR
2 Mercapto-ethanol	Sigma
Chloroform	Merck
UltraPURE Distilled Water Dnase, Rnase Free	Gibco / Life Tech
Rneasy Mini kit (ref. 74104)	Qiagen
QIAshreadder collums (ref. 79654)	Qiagen
Rnase free Dnase set (ref. 79254)	Qiagen
Rneasy Plus Universal Mini kit (ref. 73404)	Qiagen
RT HT First Strand Kit (ref. 330401)	Qiagen
RT SYBR Green/Fluorescein qPCR Master mix (ref. 330503)	Qiagen
RT qPCR Primer Assay: Hprt (RefSeq. NM-012583.2) Gapdh (RefSeq. NM-017008.4) Actab (RefSeq. NM-031144.3) Cldn 5 (RefSeq. NM-031701.2) Ocln (RefSeq. NM-031329.2) Il1b (RefSeq. NM-031512.2) IP10 (RefSeq. NM-139089.1)	Qiagen

Cxcl1 (RefSeq. NM-030845.1)	
Il6 (RefSeq. NM-012589.2)	
Gfap (RefSeq. NM-017009)	
Il2 (RefSeq. NM-053836.1)	
TNFa (RefSeq. NM-012675.3)	
Il10 (RefSeq. NM-012854.2)	
Iba1 (RefSeq. NM-017196.3)	
Insr (RefSeq. NM-017071.2)	
Slc2a1 (RefSeq. NM-138827)	
Pgp (RefSeq. NM-012623.2)	
BCRP (RefSeq. NM-181381.2)	
Asah1 (RefSeq. NM-053407.2)	
Asah2 (RefSeq. NM-053646.1)	
Acer2 (RefSeq. NM-001107943.1)	
Acer3 (RefSeq. Xm-001065019.1)	

Multiplex experiments	
Milliplex MAP Rat Cytokine/Chemokine Magnetic Panel	Merck Millipore
TRIS lysis buffer 50mM	Sigma
proteases inhibitor	Calbiochem
Lysing Matrix D	MP Biomedicals

Immunofluorescence experiments	
antibodies:	
occludin	Abcam
claudin 5	Invitrogen
Il1b	Abcam
vonWillebrand factor	Abcam
Alexa Fluor 555 or Alexa Fluor 546	Biovalley
Aqueous Gel Mount	Fisher Scientific

***in vitro* experiments**	
EBM-2 (Endothelial Basal Medium) + Kit EGM-2 MV SingleQuots (ref. CC-3202/6)	Lonza
MEM-α (Minimum Essential Medium) (ref. 22561-021)	Gibco / Life Tech
F-12 (ref. 21765-029)	Gibco / Life Tech
Fetal Bovine Serum (ref. 10270-106)	Gibco / Life Tech
human serum (ref. H4522)	Sigma
PSN (Polymycin, Streptomycin, Neomycin) (ref. 15640-055)	Gibco / Life Tech
FGF (Fibroblast Growth Factor) (ref. 01-106)	Millipore
D-PBS (Dulbecco's Phosphate- Buffered Saline) without $CaCl_2$ and $MgCl_2$ (ref. 14190-094)	Gibco / Invitrogen
Distilled water (ref. 15230-071)	Gibco / Life Tech
Collagen IV (ref. C5533)	Sigma
Fibronectin (ref. F1141)	Sigma

Trypan Blue (ref. 93595)	Sigma
[^{14}C]- Sucrose (ref. NEC100X250UC)	Perkin Elmer
[^{3}H]- Vinblastine sulphate (ref. NET1176250UC)	Perkin Elmer
Sodium Chloruride, NaCl (ref. 27788.297)	VWR
PotassiumChloride, KCl (ref. 1.04936.0500)	Merck
Calcium Chloride, $CaCl_2$ (ref. 1.02083.0250)	Merck
Magnesium Cloride, $MgCl_2$ (ref. 25108.295)	VWR
Sodium Bicarbonate , $NaHCO_3$ (ref. S8875)	Sigma
Glucose (ref. G8270)	Sigma
Hepes (ref. H3537)	Sigma
Bio Fluor Plus (ref. 6NE9809)	Perkin Elmer
DMSO (dimethylsulfoxyde) (ref. D2650)	Sigma

Table 13: Sofwares

SOFTWARES	SUPPLIER
GraphPad Prism ® 5.0	GraphPad Sofware Inc.
Microsoft ® Office Excell 2013	Microsoft Corporation
Microsoft ® Office Word 2013	Microsoft Corporation
Microsoft ® Office PowerPoint 2013	Microsoft Corporation
Excalibur 3.0	Thermo Fisher Scientific
Bio Rad CFX Manager 3.0	Bio-Rad Laboratories Inc.
ImageJ	National Institutes of Health
Biorad Bioplex-200 analysis sofware	Bio-Rad Laboratories Inc.
SoftMax Pro 6.2.2	Molecular Devices
EndNote web™ Basic	Thomson Reuters

ANNEXE 5:

RESUME

La présence de plus en plus importante de nanoparticules (NPs) dans les produits de la vie quotidienne, y compris dans l'alimentation, les médicaments, les cosmétiques, les textiles soulève de sérieuses inquiétudes quant à leurs potentiels effets nocifs pour la santé humaine. Les NPs de dioxyde de titane (TiO_2) sont produites à l'échelle industrielle et peuvent déjà être trouvées dans plusieurs produits commerciaux tels que les peintures, les cosmétiques ou dans les systèmes de décontamination de l'eau ou de l'air. Dans le passé, les NPs de TiO_2 étaient considérées comme inertes, mais, très récemment, l'Agence Internationale pour la Recherche sur le Cancer (IARC) les a classées comme cancérogène possible (groupe 2B) pour l'homme.

Les voies d'exposition à considérer pour les NPs de TiO_2 sont la voie cutanée (contact avec des cosmétiques) l'ingestion (utilisation du TiO_2 comme colorant alimentaire : E171) et l'inhalation (exposition des travailleurs lors de la fabrication de produits manufacturés). L'exposition des travailleurs mais également de la population générale peut donc devenir un sujet de préoccupation sachant que l'on ne possède que peu de données de biocinétique et de toxicité de ces NPs. D'après les études réalisées *in vivo*, les NPs de TiO_2 ont la capacité de franchir les barrières biologiques telle que la muqueuse intestinale et potentiellement atteindre le cerveau [1-4]. De nombreuses études *in vitro* et *in vivo* ont démontré la potentielle neuro-toxicité des NPs de TiO_2 [4-10]. Ces données suggèrent une association entre l'exposition aux NPs de TiO_2 et le développement de pathologies du système nerveux central (SNC). La barrière hémato-encéphalique (BHE), interface entre le sang et le cerveau, représente un filtre extrêmement sélectif protégeant le SNC. Malgré le rôle majeur de la BHE, très peu d'études se sont concentrées plus spécifiquement sur l'impact d'une exposition aux NPs sur cette barrière. Les résultats obtenus précédemment au laboratoire sur les conséquences d'une exposition aux NPs de TiO_2 (25 nm, anatase 75% - rutile 25% anatase) sur un modèle *in vitro* de BHE ont permis de mettre en évidence l'accumulation dans les cellules endothéliales microvasculaire de NPs de TiO_2 et l'induction d'une inflammation dont résulte une altération concentration dépendante de la perméabilité de la BHE [11].

Malgré les données montrant une translocation des NPs de TiO_2 à travers les barrières biologiques, la bio-distribution des NPs de TiO_2 au SNC et les conséquences sur les fonctions physiologiques *in vivo* de la BHE restent de nos jours encore mal caractérisées. De plus à ce jour, des facteurs de risques tels que l'âge sont très peu pris en compte dans les études de nanotoxicité[12]. En effet, au niveau cérébral, le vieillissement apparait clairement comme un facteur de vulnérabilité de part des fonctions physiologiques altérées, des capacités adaptatives réduites et un risque important de pathologie cérébrale associée. De plus, des études épidémiologiques ont mis en évidence une association entre la pollution atmosphérique aux particules fines et des effets néfastes sur la santé, en particulier chez des populations vulnérables. Les personnes âgées sont parmi les groupes les plus sensibles identifiés[13]. Chen *et al.* ont également montré l'induction d'une inflammation pulmonaire et de lésions cardiovasculaires exacerbées chez des rats âgés après exposition à des NPs de SiO_2 par

inhalation pendant un mois[14]. Face au vieillissement de la population, des facteurs comme un âge avancé doivent donc être pris en compte dans l'étude de la toxicité des NPs.

Mon projet de recherche vise à comprendre l'impact d'une exposition aux NPs de TiO_2 sur le cerveau adulte et vulnérable. Pour ce faire, il nous a fallu :1) préciser la biocinétique et la bioaccumulation du titane après une exposition des rats adultes et âgés aux NPs de TiO_2, 2) évaluer l'impact de cette biocinétique sur les modifications les propriétés structurales et de transport de la BHE, et 3) évaluer les conséquences inflammatoires au niveau cérébral.

Ce travail c'est divisé en deux parties. Tout d'abord, une étude par injection intraveneuse (IV) de NPs de TiO_2 chez le rat adulte. L'objectif était de décrire la biocinétique des NPs de TiO_2 dans le cas d'une biodisponibilité de 100%, c'est-à-dire en s'affranchissant d'un potentiel effet de translocation à travers des barrières biologiques comme celle du poumon après inhalation. Nous nous sommes concentrés tout particulièrement sur la distribution cérébrale. Cette étape devait également prouver des potentiels effets des NPs de TiO_2 distribuées par voie sanguine sur la physiologie de la BHE. La distribution se faisant uniquement *via* la circulation sanguine, la seule voie de passage vers le SNC est par translocation à travers la BHE. La physiologie de la barrière peut donc être impactée par des interactions directes entre les NPs de TiO_2 et les cellules de la BHE.

La validation d'une méthode de minéralisation et de dosage du titane par ICP-MS (spectrométrie par torche à plasma) a permis de quantifier de faibles quantités de titane dans les organes et tissus. Ces dosages réalisés par ICP-MS montrent une bioaccumulation du titane dans certains organes et en particulier dans le foie jusqu'à un an après IV. Au niveau cérébral, le titane est mis en évidence de façon significative pendant les 6 premières heures. L'analyse fine de cette dernière observation a permis de montrer une internalisation rapide du titane dans les cellules endothéliales cérébrales, une élimination au long court et l'absence de quantité significative de titane dans le parenchyme cérébral. Les fonctions de transport de la BHE *in vivo* sont évaluées grâce au suivi de la distribution de deux molécules substrats de transporteurs ABC (ATP Binding Casette) (la digoxine substrat de la P-glycoprotéine ou P-gp et la prazosine substrat de la Breast Cancer Resistance Protein ou BCRP). L'intégrité de la barrière est-elle évaluée par l'intermédiaire de la distribution de l'atenolol. Les dosages en spectrométrie de masse (LC/MS/MS) des molécules de ce cocktail dans le sang et le cerveau permettent le calcul de coefficients de partition sang/cerveau directement corrélés à l'activité des différents transporteurs ou à l'intégrité de la barrière. Les résultats montrent le maintien de l'intégrité de la BHE jusqu'à 28 jours après IV associé à une modification de l'activité BCRP au temps précoce (6h).

Malgré l'absence de titane dans le parenchyme cérébral, 28 jours après administration IV, nous notons une augmentation de l'expression transcriptionnelle de la P-gp au niveau des cellules endothéliales cérébrales ainsi que des protéines de structures et des cytokines comme l'interleukine-1β, du CXCL1 et de l'IP-10. Ces modulations suggèrent d'une part, la mise en place de mécanismes adaptatifs pour maintenir l'intégrité de la barrière et, d'autre part une inflammation neuro-vasculaire associée à une activation des cellules endothéliales cérébrales. Cette dérégulation de la physiologie de la BHE au temps tardif en absence de titane détectable

au niveau cérébral est probablement en lien avec la bioaccumulation hépatique et/ou pulmonaire associée à la sécrétion de médiateurs circulants à l'instar des cytokines/chemokines pro-inflammatoires ou de produits du métabolisme hépatique. Pour démontrer la présence de facteurs circulants, nous avons réalisé une étude *in vitro* sur le modèle de BHE disponible au laboratoire. Le modèle a été exposé aux sérums provenant des animaux contrôles et exposés recueilli 28 jours après l'exposition aux NPs de TiO_2. L'exposition dans le compartiment apical mime une distribution sanguine. Après 24 h d'exposition à ces sérums, l'intégrité de la monocouche de cellules endothéliales a été vérifiée et l'ensemble des cellules ont été récupérés pour un profilage des ARNm par RT-qPCR. Après 24 h d'exposition, l'intégrité de la monocouche n'est pas impactée confirmant ainsi le maintien de l'intégrité de la BHE observée 28 jours après l'exposition *in vivo*. Au niveau des cellules endothéliales, nous avons constaté une tendance à l'augmentation d'expression des ARNm de l'occludine, ce qui est également en accord avec les observations *in vivo*. Les ARNm de l'IL6, CXCL1 et de la GFAP sont surexprimés dans les astocytes suggérant une activation gliale. Ces observations *in vitro* permettent de consolider notre hypothèse de médiateurs circulant. Un article concernant l'étude par injection IV a été publié dans Particle and Fibre Toxicology: « Tissue biodistribution of intravenously administrated titanium dioxide nanoparticles revealed blood-brain barrier clearance and brain inflammation in rat ». (Disdier et al., Part Fibre Toxicol. 2015 Sep 4;12(1):27. doi: 10.1186/s12989-015-0102-8.).

Dans la seconde partie, nous nous sommes intéressés à l'exposition par voie inhalatoire, plus représentative de l'exposition humaine réelle. La conception de cette étude par voie inhalatoire suit les lignes directrices OCDE TG 412 pour l'exposition subaiguë. Le but est de mimer l'exposition des travailleurs: 2 périodes de 3 heures par jour, 5 jours par semaine pendant 4 semaines. La concentration choisie pour l'exposition était de 10 mg / m^3 correspondant à l'OEL française (limite d'exposition professionnelle) pour les poussières ultrafines dont celles de TiO_2. Dans la seconde partie de ce projet, nous avons exposé en parallèle des rats jeunes adultes et des rats âgés considérés comme vulnérables à un nano-aérosol de TiO_2.

Concernant l'accès au système nerveux central après inhalation, deux hypothèses sont proposées : 1) Premièrement, si les NPs de TiO_2 franchissent la barrière alvéolaire des poumons, les NPs seront distribuées par voie sanguine. Dans ce cas, la biodistribution peut présenter un profil comparable à celui observé après injection IV et la voie d'accès est une translocation à travers la BHE. Les hypothèses retenues d'impact direct et / ou indirect sur la physiologie de la BHE, comme décrit précédemment, devaient être vérifiées. 2) Plusieurs études ont évoqué une seconde voie: une translocation à partir de la muqueuse olfactive par transport axonal pour rejoindre directement le bulbe olfactif. Cette voie reste débattue, mais si elle est vérifiée, le NPs peut atteindre directement le parenchyme cérébral et induire des effets neurotoxiques.

Après exposition par voie inhalatoire, nous avons mis en évidence une biopersistence au niveau pulmonaire avec une clairance lente ainsi qu'une translocation tardive vers les tissus splénique et hépatique. Les dosages de titane dans le cerveau total n'ont pas permis de valider l'une ou l'autre des hypothèses exposées précédemment. Le profil de distribution diffère chez les rats âgés exposés au nano-aérosol de part : 1) l'observation d'une translocation significative plus

tardive (90 jours au lieu de 28 jours chez les jeunes adultes), 2) une variabilité intra-group plus importante et 3) une translocation plus importante du titane vers les organes extra-pulmonaires. Un article concernant la bio distribution après exposition par voie inhalatoire est soumis dans Particle and Fibre Toxicology : « Biopersistence and Translocation to Extrapulmonary Organs of Titanium Dioxide Nanoparticles after Subacute Inhalation Exposure to Aerosol in Adult and Elderly Rats ».

L'ensemble des expérimentations visant à caractériser l'impact au niveau cérébral a montré une forte neuro-inflammation en particulier chez les rats âgés. Cette neuro-inflammation a été caractérisée par l'augmentation de plusieurs cytokines et chémokines pro-inflammatoires dans le cortex des animaux exposés aux nano-aérosols (interleukine 1β, interferon γ ou encore fractalkine). Dans le groupe de rats âgés, cette neuro-inflammation est en plus associée à une augmentation de la perméabilité de la BHE 28 jours après la fin de la période d'exposition. Des altérations d'expressions de la Claudine 5, protéine des jonctions serrées jouant un rôle majeur dans le maintien de l'intégrité de la BHE complètent également la caractérisation de perméabilité. Ces altérations de la physiologie de la BHE ont été constatées malgré l'absence de détection de titane dans le cerveau total à ce temps de prélèvement. Au total, nos observations suggèrent une exacerbation de la neuro-inflammation chez le rat âgé en lien avec une augmentation de la perméabilité de la BHE après expositions aux NPs de TiO_2 par inhalation. L'implication de médiateurs circulants comme constaté après injection IV reste à vérifier. Un article concernant cette étude sur l'impact de l'exposition subaigüe aux aérosols de NPs de TiO_2 est rédigé pour être soumis à Particle and Fibre Toxicology : « Exacerbated Brain Inflammation and Blood Brain Barrier Disruption after Sub acute Inhalation Exposure to Titanium Dioxide Nano-aerosol in Aging Rats ».

En résumé, nos résultats ont montré que les NPs de TiO_2 sont bio-accumulées dans certains organes et tissus (principalement dans les poumons, la rate et le foie) et ne sont pas distribuées au SNC que ce soit après IV ou après inhalation. Après administration IV, une interaction directe entre NPs et cellules endothéliales microvasculaires conduit à des altérations fonctionnelles au niveau de la BHE. L'utilisation du modèle *in vitro* de BHE a permis d'approfondir la caractérisation de ces interactions directes en montrant des modifications dose-dépendante de perméabilité et des fonctions de transport. Malgré l'absence de translocation vers le SNC *in vivo*, la biopersistence du titane dans les organes périphériques est indirectement la cause de modulations de la physiologie de la BHE et d'une inflammation cérébrale. L'implication de médiateurs circulants faisant le lien entre la biopersitence de titane dans les organes périphériques et les modulations observées au niveau cérébral a été démontrée en utilisant un modèle *in vitro* de BHE. Une réponse exacerbée en terme de neuro-inflammation et de modulation de perméabilité de la BHE établi la vulnérabilité du cerveau âgés à la toxicité des NPs inhalées.

L'ensemble des résultats a démontré que l'exposition aux NPs de TiO_2 peut directement ou indirectement conduire altérations fonctionnelles de la BHE et une neuro-inflammation qui pourraient conduire à des troubles neurologiques. Par la suite, l'identification des médiateurs et la description des effets neurotoxiques pourront completer l'évaluation de l'impact de l'exposition aux NPs de TiO_2 sur le cerveau.

Références sélectionnées :

1. Wang, J.; Liu, Y.; Jiao, F.; Lao, F.; Li, W.; Gu, Y.; Li, Y.; Ge, C.; Zhou, G.; Li, B.; Zhao, Y.; Chai, Z.; Chen, C., Time-dependent translocation and potential impairment on central nervous system by intranasally instilled TiO(2) nanoparticles. *Toxicology* **2008**, *254*, 82-90.
2. Zhang, L.; Bai, R.; Li, B.; Ge, C.; Du, J.; Liu, Y.; Le Guyader, L.; Zhao, Y.; Wu, Y.; He, S.; Ma, Y.; Chen, C., Rutile TiO(2) particles exert size and surface coating dependent retention and lesions on the murine brain. *Toxicology Letters* **2011**, *207*, 73-81.
3. Ze, Y.; Zheng, L.; Zhao, X.; Gui, S.; Sang, X.; Su, J.; Guan, N.; Zhu, L.; Sheng, L.; Hu, R.; Cheng, J.; Cheng, Z.; Sun, Q.; Wang, L.; Hong, F., Molecular mechanism of titanium dioxide nanoparticles-induced oxidative injury in the brain of mice. *Chemosphere*.
4. Hu, R.; Gong, X.; Duan, Y.; Li, N.; Che, Y.; Cui, Y.; Zhou, M.; Liu, C.; Wang, H.; Hong, F., Neurotoxicological effects and the impairment of spatial recognition memory in mice caused by exposure to TiO2 nanoparticles. *Biomaterials* **2010**, *31*, 8043-8050.
5. Long, T. C.; Tajuba, J.; Sama, P.; Saleh, N.; Swartz, C.; Parker, J.; Hester, S.; Lowry, G. V.; Veronesi, B., Nanosize titanium dioxide stimulates reactive oxygen species in brain microglia and damages neurons in vitro. *Environmental Health Perspectives* **2007**, *115*, 1631-1637.
6. Liu, H.; Ma, L.; Zhao, J.; Liu, J.; Yan, J.; Ruan, J.; Hong, F., Biochemical Toxicity of Nano-anatase TiO(2) Particles in Mice. *Biological Trace Element Research* **2009**, *129*, 170-180.
7. Wang, J.; Chen, C.; Liu, Y.; Jiao, F.; Li, W.; Lao, F.; Li, Y.; Li, B.; Ge, C.; Zhou, G.; Gao, Y.; Zhao, Y.; Chai, Z., Potential neurological lesion after nasal instillation of TiO(2) nanoparticles in the anatase and rutile crystal phases. *Toxicology Letters* **2008**, *183*, 72-80.
8. Shin, J. A.; Lee, E. J.; Seo, S. M.; Kim, H. S.; Kang, J. L.; Park, E. M., Nanosized titanium dioxide enhanced inflammatory response in the septic brain of mouse. *Neuroscience* **2010**, *165*, 445-454.
9. Takeda, K.; Suzuki, K. I.; Ishihara, A.; Kubo-Irie, M.; Fujimoto, R.; Tabata, M.; Oshio, S.; Nihei, Y.; Ihara, T.; Sugamata, M., Nanoparticles Transferred from Pregnant Mice to Their Offspring Can Damage the Genital and Cranial Nerve Systems. *Journal of Health Science* **2009**, *55*, 95-102.
10. Ma, L.; Liu, J.; Li, N.; Wang, J.; Duan, Y.; Yan, J.; Liu, H.; Wang, H.; Hong, F., Oxidative stress in the brain of mice caused by translocated nanoparticulate TiO2 delivered to the abdominal cavity. *Biomaterials* **2010**, *31*, 99-105.
11. Brun, E.; Carriere, M.; Mabondzo, A., In vitro evidence of dysregulation of blood-brain barrier function after acute and repeated/long-term exposure to TiO(2) nanoparticles. *Biomaterials* **2012**, *33*, 886-896.
12. Yang, L.; Yi, Z.; Bing, Y., Nanotoxicity Overview: Nano-threat to Susceptible Populations. *International Journal of Molecular Science* **2014**, *15*, 3671-97.
13. Neupane, B.; Jerrett, M.; Burnett, R. T.; Marrie, T.; Arain, A.; Loeb, M., Long-Term Exposure to Ambient Air Pollution and Risk of Hospitalization with Community-acquired Pneumonia in Older Adults. *American Journal of Respiratory and Critical Care Medicine* **2010**, *181*, 47-53.
14. Chen, Z.; Meng, H.; Xing, G.; Yuan, H.; Zhao, F.; Liu, R.; Chang, X.; Gao, X.; Wang, T.; Jia, G.; Ye, C.; Chai, Z.; Zhao, Y., Age-Related Differences in Pulmonary and Cardiovascular Responses to SiO(2) Nanoparticle Inhalation: Nanotoxicity Has Susceptible Population. *Environmental Science & Technology* **2008**, *42*, 8985-8992